

Late Quaternary climate variability in the source region of *Homo sapiens*

Dry-wet cycles in Chew Bahir, southern Ethiopia

Inaugural-Dissertation

zur

Erlangung des Doktorgrades

der Mathematisch-Naturwissenschaftlichen Fakultät

der Universität zu Köln



vorgelegt von

Verena E. Foerster

aus Bergisch Gladbach

Köln 2014

Berichterstatter: Prof. Dr. Frank Schäbitz
(Gutachter) Prof. Dr. Olaf Bubbenzer

Vorsitzender der Prüfungskommission: Prof. Dr. Martin Melles

Tag der mündlichen Prüfung: 20. Mai 2014

Kumulative Dissertation – Vorlage und Gliederung gemäß Anhang 4 der Promotionsordnung der Mathematisch-Naturwissenschaftlichen Fakultät der Universität zu Köln vom 2. Februar 2006 (geändert durch Artikel I Absatz 10 der Ordnung zur Änderung der Promotionsordnung von 10. Mai 2012).

***'Forschung ist Bewegung,
die nie zu einem Ende kommt, per Definition.'***

*Ein schlauer Mann, der wusste wie's läuft: Der fiktive Alexander von Humboldt
in D. Buck's Verfilmung von „Die Vermessung der Welt“, 2012. 1:27:47-1:27:52.*

Acknowledgements

I would like to express my appreciation and gratitude to the many people who have helped and supported me during the last years and made this work possible.

A big *Danke* goes to you all.

Especially I want to thank my two Doktorväter Frank Schäbitz and Martin H. Trauth for their constant support, for their advise and their trust. As a ‚sandwich PhD student‘ between Köln and Potsdam I got the chance to learn from both. Thank you for offering me this unique opportunity to work with you two and get in touch with science from two different angles. I know that it was only due to their infectious enthusiasm for what they do as well as for their total support of my education that this dissertation was completed.

Olaf Bubenzer, is gratefully acknowledged for reviewing this dissertation. My appreciation goes to the reviewers of this work and the members of the commission for taking their time to evaluate the outcome of the work presented here. Karin Gotzmann is acknowledged for her uncomplicated and friendly support while guiding me through the examination regulations.

I want to express my gratitude to the German Science Foundation for making this study possible in the first place by providing the financial support to enable us to actually do science and find answers for open questions. The same applies for the priority programmes (ICDP funded) and the CRC 806.

Also, I want to thank my senior project colleagues Henry Lamb, Asfawossen Asrat and Mohammed Umer, without whom there would never had been a Chew Bahir project. Thank you for a rewarding time in the field and for providing advise and help whenever needed.

Beyond that, I thank my co-authors that greatly contributed to the shape and quality of the heart of this work: the articles that can never comprise the time, effort and passion that was invested to share our results with the scientific community in the best way possible.

Much obliged I am to my fabulous scientific A-team: Annette Hahn (U Bremen) and Annett Junginger (U Potsdam), for whose constant name mix up I honestly apologise. I am grateful for your patience for answering any such stupid question what mysterious abbreviations could possibly mean up to discussing and developing research ideas. Working with you made work fun and I am looking forward to a fruitful cooperation in the future.

Special thanks go to my colleagues associated to the various departments of the University of Cologne, and the University of Potsdam for inspiring discussions, during numerous occasions. Thank you also for the good time and the semi-scientific discussions during the more informal meetings. Especially the Arbeitsgruppe ‚Keller‘, is acknowledged, Jonathan Hense, Karsten Schitteck, Jean-Pierre Francois, Tsige Gebru-Kassa and especially my office and conference travel friend Konstantinos Panagiotopoulos. Special thanks go to Oliver Langkamp, Jonas Urban, Jan Wowrek and Diana Becker from Cologne and Stefanie Rohland, Oliver Oswald, Antje Musiol and Christina Günter from Potsdam for help and advise in the laboratories. Ralf Vogelsang introduced with a great deal of patience to archaeology and principles of the prehistoric world, which was an enjoyable and rewarding experience. Finn Viehberg and Bernd Wagner have contributed greatly to developing new train of thoughts and improving existing ones by willingly sharing their expertise, which is appreciated. *Danke*, Iris Breuer, and Werner Schuck for providing last minute rescue for financial, administrative and organisational issues more than once. Your help is not taken for granted!

In particular, I want to express my appreciation for being allowed to use the logging and scanning facilities of the Institute for Geology and Mineralogy of the University of Cologne and the help of the team of Martin Melles, Michael Weber, and Janet Rethemeyer, in particular Nicole Mantke, Volker Wennrich and Johannes Jakob. The same applies for the Geopolar Institute at the University of Bremen. Thank you, Bernd Zolitschka, Christian Ohlendorf and Sabine Stahl for the uncomplicated opportunity to scan our material. Finally, I would like to thank the initiators as well as the participants of the VW summer school 2010/2011 for a memorable time in East Africa and the lively discussions that evolved between members of the different scientific disciplines, nationalities and personalities.

My deepest gratitude goes to my friends for their help in technical, language and layout issues and last but not least their encouragement. Especially Jana Giersberg, Leonie Schütz and Sabine Benz. To my flatmates I am much indebted for their patience and sharing my enthusiasm, it is appreciated. My partner Caspar Indenhuck for his support and for making me laugh even a day before yet another paper submission. I thank Rolf and Regina Hahn for their friendly help and for providing a refuge amidst the stormy Friesian sea when deadlines were to meet and papers to be written. Last but not least I thank my family for teaching me the value of education, travelling and staying curiously marvelling at the world.

Abbreviations

AHP	African Humid Period
AMH	anatomically modern human
a.s.l.	above sea level
AMS	accelerator mass spectrometry
BP	before present
BRZ	Broadly Rifted Zone
CAB	Congo Air Boundary
CB	Chew Bahir
CRC	collaborative research center
D-O	Dansgaard-Oeschger
EARS	East African Rift System
ENSO	El Niño- Southern Oscillation
GS	grain size
H (1)	Heinrich event (1)
HSPDP	Hominin Sites and Paleolakes Drilling Project
ICDP	International Continental Scientific Drilling Program
IOD	Indian Ocean Dipole
IRD	Ice rafted debris
ITCZ	intertropical convergence zone
JJA	June to August
ka	kilo annum - 1000 years
LIA	little ice age
LGM	last glacial maximum
MAM	March to May
MAP	maximum a posteriori
MER	Main Ethiopian Rift
MIS	marine isotope stage
MWP	medieval warm period
NGRIP	North Greenland Ice Core Project
NH	Northern Hemisphere
OD	Older Dryas
ON	October to November
SST(s)	sea surface temperature
TC	total carbon
TIC	total inorganic carbon
TN	total nitrogen
TOC	total organic carbon
WAM	West African Summer Monsoon
XRD	x-ray diffraction
XRF	x-ray fluorescence
YD	Younger Dryas

	page
Acknowledgements	iii
Abbreviations	iv
Table of Contents	v
Table of Figures	viii
Tables	x
I Introduction and Objectives	001
1.1 Preface	002
1.2 Aim and objectives	004
1.2.1 Objectives and structure of the funding projects	004
1.2.2 Objectives of this study and beyond	004
1.2.3 Thesis structure	005
1.3 Setting of the study area	006
1.3.1 Geographical setting and general introduction to the study area	006
1.3.2 Magmatism, Rifting, Geology	009
1.3.3 Present climate	011
1.3.4 Vegetation cover	013
1.3.5 Chew Bahir as a potential terrestrial climate archive	015
1.4 State of the art	017
1.4.1 Climate system and forcing factors	017
1.4.2 Hypotheses on Environment-Evolution linkages	019
1.4.3 Hypotheses on Environment-Migration linkages	020
1.4.4 Socio-cultural component of mobility	021
II Climatic change recorded in the sediments of the Chew Bahir basin, southern Ethiopia, during the last 45,000 years	022
2.1 Introduction	023
2.2 Setting	025
2.2.1 Geological overview	025
2.2.2 Present-day climate	027
2.2.3 Long-term controls on East African climate	027
2.3 Methods	027
2.3.1 Core recovery	027
2.3.2 Chronology	027
2.3.3 Sedimentological investigations	028
2.4 Results	028
2.4.1 Core description	028
2.4.2 Age model and sedimentation rates	029
2.4.3 Sedimentological results	029
2.4.4 Geochemistry	030
2.4.5 Biological indicators	030
2.5 Discussion	030
2.5.1 Core chronology	030
2.5.2 Evaluation of proxies	032
2.5.3 Paleoclimatic implications for the past 45 ka	033
2.6 Conclusion	037
2.6 References	037

III Climate flickers during the last 46,000 years in the Chew Bahir basin, Southern Ethiopia	040
3.1 Introduction	041
3.2 Regional Setting	043
3.2.1 Geology and Geomorphology	043
3.2.2 Present Climate	043
3.3 Material and Methods	044
3.3.1 Field campaign	044
3.3.2 Core composition of CB-03 and CB-05	044
3.3.3 Sedimentology and Geochemistry	044
3.3.4 Rock magnetic measurements and core correlation	045
3.4 Results	045
3.4.1 Age model and core chronology	045
3.4.2 Physical parameters and mineralogy	048
3.4.3 Chemical distribution patterns	049
3.4.4 Fossil content	050
3.5 Evaluation of K as paleoclimate signal	051
3.6 Chew Bahir during a complete dry-wet cycle	053
3.7 Discussion of climatic variability recorded in Chew Bahir	054
3.6.1 Variability on orbital time scales	054
3.6.2 Variability on millennial time scales	058
3.6.3 Variability on centennial–decadal time scales	058
3.8 Conclusions and outlook	059
3.9 References	059
IV Episodes of Environmental Stability vs. Instability in Late Cenozoic Lake Records of Eastern Africa	064
4.1 Introduction	065
4.2 Detecting episodes of stability and instability in lake records	066
4.2.1 The Mid Holocene (MH) wet-dry transition in the Chew Bahir basin	066
4.2.2 The MIS 5–4 transition in the Naivasha basin	068
4.2.3 The Mid Pleistocene Transition in the Ologesailie basin	068
4.3 Examples for stability-instability in Cenozoic lake records	069
4.3.1 The Stability-Instability transition in the Mid Holocene Chew Bahir Record	069
4.3.2 The Stability-Instability transition in the Late Pleistocene Naivasha Record	070
4.3.3 The Stability-Instability transition in the Mid Pleistocene Ologesailie Record	071
4.4 Discussion	072
4.5 Conclusion	076
4.6 References	076
V Environmental Change and Human Occupation of Southern Ethiopia and Northern Kenya during the last 20,000 years	079
5.1 Introduction	080
5.2 Data and methods	082
5.2.1 Paleoclimatic reconstruction using lacustrine sedimentary records	082
5.2.2 Evidence of human occupation by radiocarbon date frequency	082
5.3 Results and Interpretation	083
5.3.1 Climatic change and phases of climatic stress	083
5.3.2 Human occupation in a changing environment	086
5.4 Discussion	088
5.4.1 Indications of climate-driven cultural change	088
5.4.2 Adaptation as a matter of timescale	089

5.5 Conclusions	089
5.6 References	089
VI Further Findings	093
6.1 Age model of the Chew Bahir transect	094
6.2 Results from CB-04 and CB-06	098
VII Synoptic Discussion	101
7.1 Chew Bahir as a suitable terrestrial climate archive	102
7.1.1 Type and character of sediment	102
7.1.2 Datable material	103
7.1.3 Development of a basic proxy-concept	104
7.1.4 Conclusions on the potential of the climate archive	104
7.2 Dry-wet shifts in East Africa	105
7.2.1 The African Humid Period	105
7.2.2 The Magnitude of the AHP	105
7.2.3 The synchronicity and internal variability of the AHP	106
7.2.4 The onset and termination of the AHP	106
7.2.5 The penultimate precession cycle	106
7.2.6 Climate oscillations on a 10 ³ timescale	106
7.3 Human-climate linkages on different time scale	107
7.3.1 Climate-evolution linkages	107
7.3.2 Climate-migration/expansion linkages	108
7.3.3 Climate-innovation linkages	108
7.4 Conclusions and Outlook	109
VIII References	110
IX Summary	116
IX Zusammenfassung	117
Appendix A	119
Appendix B	124
Chapter Contributions	125
Erklärung	127

Table of Figures - Figure captions

page

Figure 1.1 	Photos (from left to right): (1) Aerial shot of drainage towards Logipi in the almost completely desiccated Suguta Valley, northern Kenya, in 2011; (2) Chew Bahir, southern Ethiopia, site CB-03 with drought tolerant vegetation and member of the local Hammar tribe; (3) Animal tracks in the drying upper deposits in the Chew Bahir, close to the dry centre of the basin, CB-06; (4) Close-up shot of the thumbwheel-system that was used during the scientific coring campaign in 2010.	2
Figure 1.2 	The East Rift System from above: an overview over the study area that is characterised by a highly diverse landscape with highlands, plateaux, depressions and water bodies; presumed to be the source region of modern man. The sedimentary deposits of Chew Bahir (marked with arrow) could provide answers to the climatic history on a regional to global scale. Modified photo. Photocredit: Christoph Hormann, Views of the Earth, 2006 (http://earth.imagico.de/).	3
Figure 1.3 	Map shows the geographical setting of the study area, with the EARS including major faults, lakes and plateaux. Thin black lines indicate modern political borders, capital letters indicate countries. White italics show lakes, black italics point at rivers in the detail map of the Chew Bahir basin. BRZ - Broadly Rifted Zone. Shading of the map indicates elevation: light shade-lowlands, darker shade-highlands. For more detailed isohypsers refer to Figure 1.7.	6
Figure 1.4 	Chew Bahir as part of the drainage system of the southern side of the Ethiopian Plateau with overflow path to Lake Turkana and receiving drainage from Chamo-Abaya System. Figure shows cross section of the eastern branch of the EARS after Junginger and Trauth et al. (2013) with lake levels of modern and palaeo-lakes. For references and exact palaeo-lake depth refer to Junginger and Trauth (2013) and Junginger et al., (2014).	7
Figure 1.5 	The topographical setting of the Chew Bahir basin, showing the southern end of the MER to the north and the bordering rift shoulders of the Hammar Range to the West, merging into the Omo-Turkana basin and the Teltele Plateaux to the east. The overflow till to Lake Turkana is marked with an arrow. Map created with GeoMapApp3.3.9 and was a tenfold superelevated.	7
Figure 1.6 	Photos of the Chew Bahir, showing variability within the Chew Bahir basin along the margin-centre transect (A) Margin of the CB, pilot core drilling site CB-01, retrieved in Nov 2009; (B) Close to coring site CB-01, member of the Hammar people with small goat and cow flock in front of field; (C) Site CB-03, in a transitional position within the basin; looking eastwards towards the Teltele; covered with grass vegetation; (D) Site CB-03, looking westwards, with the Hammar Range in the back; (E+F) Site CB-06, in the centre of CB basin; completely vegetation-less, surface of the playa is covered by fine precipitates; drilling operation on the CB-06 site in Nov 2010; (G+H) Site CB-05, proposed ICDP deep-drilling site, eastern-most position within basin; surface deposits show deep dry-cracks, approximately 1 month after the short rainy season; (I+J, following page) cattle herd with Hammar-boy close to CB-02; (J) CB-02 with Hammar Range to the right and in the back, showing one of the extensive alluvial fans reaching far into the basin. Photos by F.Schäbitz (A); V. Foerster (B-J);	8
Figure 1.7 	Map of East Africa showing topography, rift faults and sites of lake-sediment sequences used for palaeoclimate reconstruction (white circles), the Anza-Nile Rift after Bosworth (1989) and presumed extension of mantle plume around 45 Ma (after Ebinger and Sleep, 1998). Blue circle shows the location of Chew Bahir within older and younger Rift structures. Base map modified after Trauth et al. (2005).	9
Figure 1.8 	The Chew Bahir rift located in between the Ethiopian Plateau and the Kenya rift in the BRZ that comprises several basins divided by plateaux and ridges as marked in the map: A) Chew Bahir basin; B) Omo canyon; C) Maze basin, D) Bala rift, E) Gofa basin and range F) Usno basin G) Omo basin, H) Kibish basin. Modified after Asrat et al., 2009, WoldeGabriel and Aronson, 1987. Figure inset shows profile of the Chew Bahir basin (A-A'), after Pik et al., (2008).	10
Figure 1.9 	Map of the Geology in the Chew Bahir catchment, simplified after Davidson, 1983; Key, 1988; Hassen et al., 1991; Awoke and Hailu, 2004).	10
Figure 1.10 	Synoptic climatology of tropical East Africa for November, January, April, and August. The distribution of precipitation reflects the seasonal migration of the Inter-tropical Convergence Zone (ITCZ) across the study region, as well as the Indian Summer (ISM) and Winter Monsoon (IWM). The rainfall data are derived from gridded gauge data (over land) and satellite measurements (over the sea). The locations of the CAB and the ITCZ are shown as dashed white lines. Pink circle marks the Chew Bahir site. Figure adapted and slightly modified from Junginger et al. (2014).	11
Figure 1.11 	Monthly migration of the moisture carrying convergent zone (ITCZ) that brings seasonal rainfall to the study area. Arrow indicates the location of Chew Bahir within this rain domain. Darker shades of green indicate the zones with highest monthly climatological precipitation amount, with contours in 50 mm/month intervals. End of October, the ITCZ follows with a lag the migration of max insolation values southwards, resulting in the onset of the dry season for most parts of Ethiopia during the following month (~Nov–Mar; left column). In Feb the ITCZ starts reversing direction and the northward migration of the convergent zone causes the 'short' rainy season in southern Ethiopia to begin in mid-March–mid-June. The northernmost position of the ITCZ marks a brief drier period around June, before the beginning of the main rainy season (~Jun–Sept) on the highlands of Ethiopia. Maps and data are based on monthly climatological precipitation (in mm/month) estimates from satellite emitted long-wave radiation from polar-orbiting satellite, using the period 1981–2010 as data base. Modified from IRI database, (last access, Jan 2014).	12
Figure 1.12 	Climate diagram of the Chew Bahir region, showing average of monthly min. and max. precipitation in mm/month and monthly mean temperatures in °C (base period 1971–2000). The values apply for the region 36.151E–38.032E, 3.761N–5.489N and were derived from IRI, accessed Jan 2014.	13
Figure 1.13 	Map of the potential vegetation of Ethiopia, differentiated into fourteen vegetation types and comprised into eight ecosystem types. Map adapted from Friis et al., 2001).	14
Figure 1.14 	Change of vegetation cover (generalised): present; mid-Holocene (full AHP conditions); reestablishment of humid vegetation cover after YD; towards the end of the last glacial. Single illustrations of vegetation cover, from Quaternary Environment Network (http://www.esd.ornl.gov/projects/qen/nerc.html). Years were converted into calendar years. Arrow indicates study area.	15
Figure 1.15 	Simplified model of the Earth's climate system including major forcing factors and environmental responses along a spatial and temporal axis. Modified after Maslin and Christensen, 2007. NAO-Northern Atlantic Oscillation, IOD-Indian Ocean Dipole, D-O-Dansgaard-Oeschger cycles.17	17
Figure 1.16 	Changes in the earth orbital parameters after Berger and Loutre, 1991 and Berger, 1992 for the last 0–5 Myr BP. X-Achses shows time in kyr (negative for the past and 0 being 1950). From the top: Eccentricity, Obliquity in degree and decimals and climatic precession. Variations in Insolation and therewith significantly the moisture availability for East Africa through time is strongly controlled by these orbital parameters with distinct periodicities: precession (19–23 kyr), obliquity (41 kyr), and eccentricity (100 kyr).	18
Figure 1.17 	Insolation variations (in Watts/m ²) at the equator for the last 50 ka BP (given in negative kilo years for the past, 0=1950) according to the computation of insolation quantities by Laskar (2004) showing equatorial spring and fall insolation in anti-phase.	19

Figure 2.1	Setting of the Chew Bahir basin. (A) Chew Bahir basin within the East African Rift System with major climatic influences. Dotted lines indicate the position of the ITCZ (Intertropical Convergence Zone) and CAB (Congo Air Boundary) during different times of the year (after Tierney et al., 2011). (B) Map of the Chew Bahir catchment with major rivers, paleo-lake outline and sites mentioned in the text. Numbers refer to available precipitation and temperature data summarized in climate diagrams between A and B (data: http://iridl.ldeo.columbia.edu/maproom/ – accessed 12.07.2011). A–A' cross-section along the core transect is provided in (C): Six sediment cores were recovered from a W–E transect through the Chew Bahir basin. Results of the pilot CB-01-2009 core discussed in this study provide paleo-climatic information for the past 45,000 years.	24
Figure 2.2	Present available geological information for the catchment of the Chew Bahir basin provided by the Omo River Project (Davidson, 1983).	26
Figure 2.3	Lithology, age-depth model and results of geochemical and physical investigations of the pilot core CB-01-2009. Numbers along the age model present sedimentation rates in mm/year. Stars – 14C ages; triangles – XRD samples; MS – Magnetic Susceptibility; LGM – Last Glacial Maximum; YD – Younger Dryas; AHP – African Human Period; G1eG5 e gaps in the record due to lost/unconsolidated sediment. 30 Figure 2.4 Results of XRF measurements against time; MS – Magnetic Susceptibility; K - Potassium; Fe - Iron; Si - Silicon; Ti - Titanium; Ca - Calcium; Sr - Strontium; AHP–African Humid Period; YD- Younger Dryas.	29
Figure 2.4	Results of XRF measurements against time; MS – Magnetic Susceptibility; K - Potassium; Fe - Iron; Si - Silicon; Ti - Titanium; Ca - Calcium; Sr - Strontium; AHP–African Humid Period; YD- Younger Dryas.	32
Figure 2.5	Comparison of the Chew Bahir potassium (K) record with other paleo-climate records. Records plotted from top to bottom are as follows: $\delta^{18}\text{O}$ data from NGRIP (North Greenland Ice Core Project members, 2004) with numbers referring to DO-events; terrestrial dust input to the tropical east Atlantic (deMenocal et al., 2000; note reverse scale); $\delta^{18}\text{O}$ data from Hulu (Wang et al., 2001) and Dongge caves (Dykoski et al., 2005; note reverse scale); $\delta^{15}\text{N}$ data as proxy for denitrification and productivity in the Arabian Sea in the Gulf of Oman 18 °N (Altabet et al., 2002); Chew Bahir potassium (K) record (note reverse scale); Lake Tanganyika δD leafwax as proxy for precipitation variability (Tierney et al., 2008; note reverse scale); SST (sea surface temperature) record from the eastern Pacific (Martínez et al., 2003) and insolation variations (Berger and Loutre, 1991). Dotted lines indicate time slices discussed in the text. Gray bars refer to Heinrich events, Younger Dryas and H1–H5. The red squares show ^{14}C dates along the Chew Bahir record.	34
Figure 2.6	Comparison of onset and termination of East African lake levels from lake Nakuru (Richardson and Dussinger, 1986), lake Ziway-Shala (Gillespie et al., 1983), and Lake Turkana (Johnson et al., 1991; Brown and Fuller, 2008) with the aeolian dust record to Mt. Kilimanjaro (Thompson et al., 2002) due to enhanced aridity, hydrological proxy data from Lake Challa from δD leafwax (Tierney et al., 2011), the oxygen-isotope records from Dongge cave (Dykoski et al., 2005), and the paleo-ENSO record from Laguna Pallcacocha, southern Ecuador (Moy et al., 2002). AHP–African Humid Period; YD- Younger Dryas; dark gray bars indicate dry episodes; light gray bars indicative for humid episodes.	36
Figure 3.1	Setting of the Chew Bahir site. (A) Chew Bahir basin within the East African Rift System with major climatic influences. Dotted lines indicate the position of the ITCZ (Intertropical Convergence Zone) and CAB (Congo Air Boundary) during different times of the year (after Tierney et al., 2011). (B) Map of the Chew Bahir catchment with major rivers, paleo-lake outline, overflow direction and sites mentioned in the text. Numbers refer to available precipitation and temperature data summarized in the climate diagrams (data: IRI, accessed Oct. 2013). (C): Center of CB basin, site of CB-05 and planned deep drilling location within the HSDPD project (2013–2014). (D): NW–SE transect through the Chew Bahir basin with distances between coring sites in km. (E): Setting of drilling location of the records discussed in this study, showing major input systems relevant for this study and position of sites within the basin.	42
Figure 3.2	Age model of tuned composite profiles of Chew Bahir cores CB01, 03–06. The depth in cm shows the composite depth of the model. Ages are the weighted mean of the probability density function and correspond to the last column in Table 2. (A) Radiocarbon ages per sediment core. (B) Materials used for radiocarbon dating.	46
Figure 3.3	Sediment composition of (A) CB-03 and (B) CB-05 with selected results of geochemical and physical analysis. Ages are given in calibrated kilo years before present. Ages in black refer to linearly interpolated values of the composite age-depth model. Red ages in (A) refer to radiocarbon ages from CB-03 (Table 3.2). Red and blue arrows point out prominent moisture shifts towards arid/humid conditions. Straight arrows indicate abrupt events, crooked show gradual trends. Orange (dry) and blue (wet) bars mark interpreted climate phases, referred to in the text; grey bars show arid phases that roughly coincide with high-latitude Heinrich events (H1–H4). MagSus – Magnetic Susceptibility; LGM – Last Glacial Maximum; YD – Younger Dryas; OD – Older Dryas; AHP – African Human Period.	49
Figure 3.4	Micro and macro fossils found in the Chew Bahir records CB-03 and CB-05, magnified under a binocular and a scanning electron microscope respectively. (A) The abundant gastropod <i>Melanoides tuberculata</i> from distinct horizon (M1–M5) in 520cm in CB-03 and 321cm in CB-05, both corresponding to the interval around 11–12kcalBP and 713cm in CB-03, 13.5 ka cal BP (M6). (B) Most abundant diatoms in the assemblage from Chew Bahir (from the top): <i>Cyclotella</i> , <i>Aulacoseira</i> (detail shot of frustule end that forms long chains), <i>Cyclostephanos</i> ; occurrences coincide with AHP lake phase (C) Fishbones, found in a distinct correlating layer in both records; 14.2 ka BP (F2), 15.2 ka BP (F1 + F4) and 32.7 ka BP (F3).	50
Figure 3.5	Variations of Ca normalized elements with Ca normalized Si. Data are split into high and low-K groups and represent six characteristic depth intervals indicated by the different colors. Blue points generally denote the low-K group, whereas red dots denote the high-K group. Also shown are linear regression trends for both groups. As indicated by the different linear correlation trends, the geochemical signal of the high-K group is controlled by a different silicate phase or assemblage as the signal of the low-K group.	52
Figure 3.6	The established indicators for aridity – potassium [K] – (note inverted scale) and humidity – chlorine [Cl] – show variations within the Chew Bahir basin itself. Variability comprises magnitude and proxy specific reaction towards climatic signals. Aridity proxy K reacts more sensitively towards moister increase, humidity dependent Cl– responses sensitively to induced dry conditions. Age control along the Chew Bahir record is shown by grey squares (radiocarbon ages) and red triangles (CB correlation tie points). CB records are compared to NH summer (July) insolation variations (Laskar et al., 2004) and precession cycle (Berger and Loutre, 1991).	55
Figure 3.6	Comparison of the Chew Bahir potassium (K) record with other paleo-climate records and insolation variation controlled by orbital configuration. Records plotted from top to bottom are as follows: $\delta^{18}\text{O}$ data from NGRIP (North Greenland Ice Core Project members, 2004) with numbers referring to DO- events; $\delta^{15}\text{N}$ data as proxy for denitrification and productivity in the Arabian Sea in the Gulf of Oman 18 °N (Altabet et al., 2002); Chew Bahir potassium (K) record from cores CB-01 (paleo-lake shore), CB-03 (intermediate), CB-05 (paleo-lake center), (note reverse scale); Insolation variations for spring and fall from the equator (Laskar, 2004). Dotted lines indicate dry-wet-dry cycle AHP. Age control along the Chew Bahir record is shown by grey squares (radiocarbon ages) and red triangles (CB correlation tie points).	57
Figure 4.1	Map of Eastern Africa showing topography, faults and lake basins. Note the location of the studied sites Chew Bahir, Naivasha and Olorogaisalie (modified from Trauth et al., 2005).	66
Figure 4.2	Age models of three studied records. (A) The composite age model of the Chew Bahir basin is based on 32 AMS ^{14}C ages (Foerster et al., 2012, 2014). All radiocarbon ages were converted into calibrated ages with OxCAL using the IntCal13 calibration curves (Bronk Ramsey, 1995, 2009a,b; Reimer et al., 2013). The best estimate of the true age was obtained by calculating the weighted mean of the probability density function of the calibrated ages. (B) and (C) The age model of the Naivasha and Olorogaisalie records was calculated using a probabilistic technique for complex stratigraphic sequences simply comparing the deposition time of equally thick sediment slices from the differences of subsequent radiometric age dates and the unit deposition times (the inverse of the sedimentation rate) of the various sediment types (Trauth, 2014).	67

Figure 4.3 	Lake level records of three studied sites (blue lines) with age control points (green squares) and orbital and precessional quantities (red lines) to define episodes of relative stability and instability with pronounced dry periods (red triangles). (A) Holocene environmental record of the Chew Bahir basin created by tuning the potassium records of five cores CB01 and CB03–06 and interpolating the record to the the age model shown in Figure 4.2A. (B) Late Pleistocene lake-level record of Lake Naivasha obtained by recalibrating the record published in Trauth et al. (2001, 2003) to the new age model shown in Figure 4.2B. (C) Mid Pleistocene record of the Ologesailie basin taken from Behrensmeier et al. (2002), re-calibrated to a revised age model show in Figure 4.2C and plotted together with the earth's eccentricity cycle (solid red line) as well as its 800 kyr component (dashed red line). All orbital and precessional quantities taken from Laskar et al. (2004).	69
Figure 4.4 	Lakes have a stabilizing effect by the sheer size of the water body, which reacts very slowly to changes in the moisture budget, as lake-balance modeling suggests. If there is an abrupt increase of +25% in the 13,000 km ² large catchment today, the lake would reach two thirds of the maximum lake level of 300 yrs not before 200 yrs after the climate shift, and would stabilize at the maximum lake level only after 1,000 yrs. Gradual changes in climate would cause even longer response times of the water body (Borchardt and Trauth, 2012; Junginger and Trauth, 2013).	73
Figure 4.5 	Vegetation have a stabilizing effect on the local environment due to a positive feedback which resists particular climate changes. For example, forests recycle moisture maintaining a level of rainfall for the forest to survive (Maslin, 2004). This moisture feedback does not exist with savanna; instead the relatively dry grassland environment is maintained by recurring fires keeping trees away, similar to the activity of grazers and other factors (Jeltsch et al., 2000).	74
Figure 4.6 	Models of possible environmental response to orbital forcing. The first model suggests that there is a relatively smooth gradual transition between periods with deep lakes and periods without lakes, which may invoke Red Queen (Van Valen, 1973) or Turnover Pulse Hypotheses (Vrba, 1985) as possible causes of evolution (see below). The second and third model are threshold model, with ephemeral lakes, expanding and contracting extremely rapidly, producing the wide spread, regional-scale, rapid, and extreme environmental variability required by the Variability Selection Hypothesis of human evolution (Potts, 1998). The third model, however, is characterized by extreme variability during the transitions between full to no lake conditions, which implies variability influenced human evolution or again either high-energy wet conditions or prolonged aridity (Maslin and Christensen, 2007).	75
Figure 5.1 	Setting of the Chew Bahir basin and archaeological sites in potential refugia. Archaeological sites are indicated by coloured circles and numbers, that correspond to site names and numbers in Table 5.1, to provide complete sample ID and cultural association. The pink circle marks the site of the Chew Bahir record. Climate diagrams represent monthly temperature means in °C and precipitation in mm/month (IRI, last accessed 2/2014). Photographs from top: (1) Mochena Borago rock shelter in the SW Ethiopian highlands; (2) mudflats of the Chew Bahir basin, with the Hammar range in the background; (3) aerial shot of Lake Turkana, NE shore.	81
Figure 5.2 	Comparison of (a) the 20 ka Chew Bahir climatic record (K content as a proxy for aridity) with (b) settlement in the SW Ethiopian Highlands and around lake margins (Turkana and Ziway-Shalla lakes). Climatic events: AHP - African Humid Period (~15-5 ka BP), YD - Younger Dryas (~12.8 -11.6 ka BP), OD - Older Dryas (around 14 ka BP), H1 - Heinrich event 1 (around 16 ka BP), LGM - Last Glacial Maximum (~24-18 ka BP). During the AHP, several pronounced dry spells (grey bars) occur, modulating the wet phase; the gradual Holocene aridification (orange bar) is punctuated by arid events on a decadal timescale (Trauth et al., in press). Settlement activities in both potential refugia are indicated by radiocarbon frequency of archaeological finds, as listed in Table 5.1. Cultural innovation is indicated by first documented wavy-line pottery (pot symbol) and the introduction of pastoralism (cow symbol); red or green colors refer to SW highlands or lake margins respectively. The green star signifies culture-related evidence of occupation that is not clearly datable.	87
Figure 6.1 	The weighted mean of the probability density function was used as the point estimate of the calibrated ages.	95
Figure 6.2 	Potassium curve of the Chew Bahir transect cores used as reference curves for correlation. CB-01 is the master core. Values were standardized. Note the different depth and refer to Fig. 3.f+d+e for core correlation with the basin.	96
Figure 6.3 	Tuned potassium record of the Chew Bahir transect cores. All cores were tuned to the depth of CB-01, using tiepoints (red circles).	97
Figure 6.4 	Tuned potassium record of the Chew Bahir transect cores. All cores were tuned to the composite age model based on cal. ¹⁴ C ages (grey circles).	97
Figure 6.5 	Sediment composition of (A) CB-04 and (B) CB-06 with selected results of geochemical and physical analysis. Red and blue arrows point out prominent moisture shifts towards arid/humid conditions. Straight arrows indicate abrupt events, crooked show gradual trends. Orange (dry) and blue (wet) bars mark interpreted climate phases, referred to in the text; grey bars show arid phases that roughly coincide with high-latitude Heinrich events (H1–H4). MagSus – Magnetic Susceptibility; LGM – Last Glacial Maximum; YD – Younger Dryas; AHP – African Human Period.	99–100
Figure 7.1 	Profile through the Chew Bahir basin showing coring sites along the NW-SE transect and the dimension of the extensive sediment trap.	101
Figure 7.2 	Insolation variation, wet periods in East Africa and human evolution. The compilation of lake records is based on a large volume of literature (Olduvai, Magadi-Natron-Olgosailie, Baringo-Bogoria, Omo-Turkana-Suguta, Ethiopian Rift and Afar), as well as from our own work (Central Kenya Rift) (see Trauth et al. (2005) and references therein for details). The expected Chew Bahir record is marked as green box in the compilation. From Trauth and Schäbitz, 2012.	107

Tables - Table captions

		page
Table 2.1	Radiocarbon data from the Chew Bahir sediment core CB-01-2009.	28
Table 2.2	Results of XRD analyses	31
Table 3.1	Core locations and Core details	44
Table 3.2	Ages from CB-01, CB-03 and CB-06 for Chew Bahir transect chronology	47
Table 3.3	Proxy evaluation for dry versus wet conditions in Chew Bahir. These findings are highly site specific and a generalization, an extrapolation to other sites should be handled with care and take setting of the site into consideration; exceptions can easily be found. The lake sediment proxies are controlled by three factors bound in a complex interplay; 1. distance to and restriction of the source, 2. prevailing transport mechanism (fluvial, alluvial fan activity, aeolian), that is also heavily influenced by density and type of vegetation and 3. weathering (chemical versus mechanical) and possibly diagenetic processes.	54
Table 5.1	Radiocarbon dates from archaeological sites and attribution to cultural complex	84



Chapter I

Introduction and Objectives

An introduction to the reader,
to the why, where and how of this study



1.1 Preface

Public awareness of the debate surrounding the existence of climatic change and the extent to which anthropogenic processes have forced these changes is currently of great interest to the public. The demand to understand how climate is temporally unstable and that humankind is not only affected by a changing environment but also inherently involved in the alteration of climate system is a key, and rapidly developing, aspect of science.

The establishment of the Intergovernmental Panel on Climate Change (IPCC) (<http://www.ipcc.ch/>) in the 1980's showed an increasing awareness that climate change is of worldwide social and economic significance. The large international collaboration of scientists who now deal with the assessment of research data as part of the IPCC illustrates the seriousness of current climate change and its importance for the human population.

Already events and trends induced by climatic change threaten the livelihood of millions of people on different scales by severe floods, droughts, storms, rising sea levels, and increasing global temperatures. The 'frequency and amplitude of extreme hydrological events' is expected to increase, caused by more moisture in the atmosphere (IPCC, 2007). In East Africa, a region where most countries rely on an economy that is largely dependent on rain-fed agriculture and pastoralism and therefore moisture availability (Seleshi and Zanke, 2004; Odada et al., 2003; OCHA, 2011) an increasing intra- and inter- annual rainfall variability is having dramatic consequences. The recent catastrophic droughts of the last two decades (1995, 1987-1988, 1997, 2000 and 2011-2012) in Ethiopia, Eritrea, Somalia, the Sudan and Kenya sadly proved (e.g. Seleshi and Zanke, 2004; Camberlin, 1997) how these 'extreme hydrological

events' caused severe food shortages that cost the lives of ten thousands of people and had disastrous long-term effects on the socio-economic stability (OCHA, 2011). The opposite scenario of anomalous rainfalls triggering flooding has even caused critical conditions in large parts of East Africa (e.g. Saji et al., 1999). In an environmental assessment Odada et al. (2003) evaluate the implications of the findings of IPCC reports (1996 and 2001) for the future situation of East Africa and outline that higher temperatures would lead inevitably to increased evaporation losses. Projections within the 2001 report anticipate that by 2025 many African countries (even more than already today) will experience water stress and the increase in climatic extreme events is considered as 'likely'.

It is crucial to understand natural climate variability, particularly in term of the key forcing factors, which produce varying temporal climate cycles and events. Past studies of climatic changes and deciphering of the triggering mechanisms, character, speed and foremost, the impact of these variations on the palaeoenvironment, and specifically the habitat of our ancestors, is now a focus of research. The reconstruction of past climatic change provides a framework for models, frequency patterns and feedback mechanisms, which, in turn, serve as a base to predict possible future developments and trends of climate change, and to distinguish the man-made control in these patterns.

The significance of understanding how humans previously dealt with a changing environment has developed since identifying the world is transforming on an uncertain scale. Questions including how could they survive in a changing world arise, as well as how they adapted to a changing environment and then, how and why they left their original habitat. To answer these

questions a multi- and interdisciplinary science should be used, which will need a temporally continuous and high-resolution database. The environmental key component to answer the outlined questions can be found for instance in sedimentary archives that might have potentially recorded the information on climatic conditions at a point in the past. The vastly developing scientific discipline of palaeolimnology around the deciphering and suitable interpretation of proxies contained in such sediment cores has shown that qualitative suitable cores and careful interpretation can give valuable indications on past climatic changes (Bradley, 1999; Last and Smol, 2002; Cohen, 2003). And this is the point where plastic tubes filled with ancient 'mud' such as the ones used in this study from Chew Bahir in southern Ethiopia become a relevant contribution to the debate about climate change in past present and future. A palaeoclimate reconstruction based on sediment core analysis taken from the tropics can be used to contribute to the understanding of concepts about climatic change on a global scale and then in a second step shed light on the impact of climatic change on humans in the past.

In this thesis, the environmental evolution with an emphasis on East African dry-wet shifts, is addressed by presenting the results, analyses and interpretation of sediment cores from Chew Bahir, Southern Ethiopia, nearly reaching back to the beginning of MIS 3. The site is situated amidst the East African Rift (Fig 1.2) in what is southern Ethiopia today and close to the present Kenyan border; amidst an area that is now broadly understood to represent the source region of *Homo sapiens* (e.g. Richter et al., 2012) and the crucible (if not the cradle) of humankind (Asrat et al., 2009; Trauth and Schäbitz, 2012). Consequently this opens up potential discussion fields concerning the palaeoclimatic context of key developments in human history. The scientific basis for a reliable interpretation of the climatic data at hand in a broader context is laid, allowing then hypotheses on climatic change on a global to regional scale during the last two interglacial-glacial cycles to be tested. Furthermore, potential applications and extrapolations of the data are discussed, in terms of their use in overlapping relevant fields of research and in terms of a wider spatio-temporal contexts.

◀ Figure 1.1 | Previous page, photos from left to right: (1) Aerial shot of drainage towards Logipi in the almost completely desiccated Suguta Valley, northern Kenya, in 2011; (2) Chew Bahir, southern Ethiopia, site CB-03 with drought tolerant vegetation and member of the local Hammar tribe; (3) Animal tracks in the drying upper deposits in the Chew Bahir, close to the dry centre of the basin, CB-06; (4) Close-up shot of the thumbwheelsystem that was used during the scientific coring campaign in 2010. Photos by V. Foerster

Figure 1.2 | The East Rift System from above: an overview over the study area that is characterised by a highly diverse landscape with highlands, plateaux, depressions and water bodies; presumed to be the source region of modern man. The sedimentary deposits of Chew Bahir (marked with arrow) could provide answers to the climatic history on a regional to global scale. Modified photo. Photocredit: Christoph Hormann, Views of the Earth, 2006 (<http://earth.imagico.de/>).



1.2 Aim and objectives

The main aim of this thesis is an accurate, continuous reconstruction of climatic history in the area in question, which has been found to be the source region of modern man. In order to achieve this a comprehensive understanding of the underlying climate archive, including its internal system dynamics and the driving mechanisms involved, is crucial.

More specifically, the focus of this work is to reconstruct past East African Late-Quaternary climate changes, in particular dry-wet alternations, from the uppermost lacustrine deposits in the Chew Bahir basin, southern Ethiopia. Subsequently, these findings are related to events in human evolution and migration, and used to extrapolate results for longer timescales and a broader spatial context.

1.2.1 Objectives and structure of the funding projects

The objectives of this thesis are closely interconnected with the initial research question of the projects that initiated and funded or co-funded the Chew Bahir project. The Chew Bahir pilot project entitled: 'Climate-vegetation feedbacks during the African Humid Period in the southern Ethiopian Rift' was designed as a prerequisite for the follow-up planned deep drilling initiative 'A Half-Million Year Climate Record from the Southern Ethiopian Rift, Crucible of Human Evolution' within the framework of the larger 'Hominid Sites and Paleolakes Drilling Project' (HSPDP) project. HSPDP aims to understand the palaeoenvironmental context of Human Evolution (<http://hspdp.asu.edu/>) and involves scientific drilling at four additional sites in East Africa, which all have lacustrine sedimentary records close to globally-significant fossil hominin sites.

The potential of the lacustrine deposits as a reliable source of proxy data to reconstruct the climatic and environmental history was assessed during the initial Chew Bahir pilot project (2010-2013). The aim of this pilot project was to provide answers about the characteristics of the youngest dry-wet-dry cycle (the so-called African Humid Period, ~15–5 ka BP*). After establishing a fundamental understanding of sedimentation processes and intra-basin dynamics, and proving the Chew Bahir basin to be a reliable site for scientific drilling far beyond the initially focussed timeframe of the pilot study, the deep drilling project was granted (2013-2015) and Chew Bahir became one of the key sites within the HSPDP. The sedimentation rates in-

ferred from the pilot phase suggest that a 400 m deep sediment core could cover at least to 500+ ka BP, possibly even to 750+ ka BP. Therefore such a core could enable the tackling of major research questions related to the suggested human-climate link in the timeframe of human evolution, dispersal and innovation.

From the beginning, the Chew Bahir project has formed an integral part of the A3 cluster within the Collaborative Research Centre (CRC) 806: 'Our Way to Europe: Culture-Environment Interaction and Human Mobility in the Late Quaternary' (www.sfb806.uni-koeln.de). The CRC 806 focuses on testing models and evaluating the triggering factors of expansion and mobility in early human societies, including environmental drivers, and follows a broad interdisciplinary approach. Together with a number of other Ethiopian lakes following a N-S and an E-W transect across altitudinal and biogeographical regimes in Ethiopia, the A3 project aims to retrieve important information about the role of climate and environmental factors which played a role in the dispersal of early modern humans to Europe and Asia from the African source region. The A3 source-region project focuses on the last 200,000 years, back to the assumed emergence of *Homo sapiens sapiens*.

1.2.2 Objectives of this study and beyond

From the project's initial motivation and subsequent work, which has developed from this, three major research objectives have been derived which are the basis of this study, and will serve as guidelines through this work. Each of these key aims are subdivided into more specified targets and use the data available. The available data determined the options and limitations of what could be tested and answered throughout this thesis. The sub-objectives of this research are to determine:

1. The potential of a terrestrial climate archive in the source region of modern man
 - From mud and grains to curves and concepts (or vice versa)**
 - / Determine the type and character of the deposits in the Chew Bahir basin
 - / Test for datable material and define the sedimentation rates and their variations within the basin
 - / Establish a basic proxy toolbox and a fundamental concept of weathering, transportation and sedimentation processes from source to sink
 - / Interpret the lacustrine record: decipher the climatic history in the source region of modern man

*all age indications in this thesis are given in calibrated ages before present (BP = 1950) unless explicitly noted otherwise; ka/kyr- kilo annum = 1000 years

2. The sensitivity of the sediment records to orbital driven climatic change and other climate events Understand dry-wet cycles in East Africa (e.g. AHP)

- / Test hypotheses about the timing, magnitude, synchronicity and internal variability of the AHP
- / Focus on the transition in and out of the orbital forced moisture variability, especially the possible abruptness
- / Outline short-term climate events on millennial to centennial time scale and attribute these to possible triggering mechanisms

3. Human-climate linkages on different time scales (evolution, migration, innovation) Impact of climate and climatic change on humans through time

- / Could climatic variability have had implications for the emergence of archaic and modern humans (climate \leftrightarrow evolution)?
- / Is there a relation between climate events and phases of human migration (climate \leftrightarrow migration)?
- / Which climatic scenario drove expansion of human populations (climate determined push-and-pull factors)?
- / Did climatic change on centennial and millennial timescales spur technological, economic and social innovations (climate \leftrightarrow innovation)?
- / Could the SW Ethiopian highlands have been an ecological and hydrological refuge area during times of climatic aggravation (e.g. hyper-arid intervals) (refugium theory)?
- / Are there thresholds for climatic determined boundary conditions (climate \leftrightarrow resources) that mark the limitations of human decision-making (climate \leftrightarrow human agency)?

1.2.3 Thesis structure

Chapter I i.a. Introduces the reader to the study area in a broad context, including the topographic, geological, climatological and vegetational background of East Africa and then of Chew Bahir more specifically. A brief overview is given concerning the fundamental basics of overlapping study fields which are thematised within this thesis. Chapter II and III provide an introduction to the newly investigated climate archive of Chew Bahir and give initial results on the potential of the cored de-

posits, which are in close proximity to the anthropological key-site of the oldest known anatomically modern humans (AMH). The location is of specific interest as it lies close to one of the hot spots of human evolution and source area of dispersal beyond the African continent. Chapter II is based on the multi-proxy results from the 18.8 m pilot core that was retrieved during the initial field-campaign in 2009. This pilot study, within the scope of the CRC 806, was in search of a reliable site for a record to cover the last 200 ka BP as the timeframe of the emergence of the AMH. The CB-01 record shows that the basin reacted sensitively towards regional and global climatic fluctuations on millennial to centennial timescales, and has recorded the last 45 ka of the highly variable East African climatic history. The emphasis of this chapter is on the AHP and compares the expression of this dry-wet cycle along an East African profile. In Chapter III these fundamental findings and the paleoenvironmental reconstruction of the pilot core are presented, including the integration of results from two further cores which were obtained (CB-03 and CB-05, 10-11 m long) during an ICDP field campaign in 2010, as part of a transect across the Chew Bahir basin. This chapter includes the development of a composite age model for all cores. On the basis of the entire geochemical, geophysical and biological dataset, the transect core sites are compared and a basic proxy concept is developed, integrating gained knowledge about intra-basin dynamics. The record provides valuable insight about insolation-controlled but non-linear dry-wet cycles back to ~46 ka BP. Furthermore, possibly high-latitude controlled climate events on millennial to centennial time scales, such as D-O cycles or H-events modulate the climatic history as well as centennial to decadal climate excursions. Chapter IV deals with the application of reconstructed phases of environmental stability and instability in a broader spatio-temporal context. Using three examples from the southern Kenya Rift, Central Kenya Rift and the Chew Bahir basin in the southern Ethiopian Rift, hypotheses on the implications of the change from stable to instable environmental conditions on three different timescales are discussed. Subsequently, the possible role of different scaled climatic transition for African hominin speciation, dispersal and cultural innovation is evaluated. Chapter V focusses on an interdisciplinary case study, matching 20 ka of the Chew Bahir climatic history, including the Mid-Holocene aridification and short-term drought events, with the settlement activity in hypothesised refugia. Here, two possible ecological and hydrological refuge areas in the moister SW Ethiopian Highlands and along the lake margins of Lake Turkana and the MER Lakes are compared to the synthesis of hypothesised climatic stress conditions, testing the

concept of climatically determined migration.

The emergence of cultural innovations in terms of adaptation to a changing environment is then interpreted using the climatic history from Chew Bahir. Additionally, social concepts and other factors driving human decision-making are also evaluated. Chapter VI is comprised of yet unpublished results regarding the correlation of the Chew Bahir transect cores, including basics concepts about tie points, thus providing essential information on the development and role of the age model. Furthermore, it presents the lithology and the established proxy data against depth of CB-04 and CB-06, as well as processed line-scan photographs of the Chew Bahir transect cores (Appendix), showing the visual output of the heterogenous deposits. Finally, Chapter VII discusses and synthesises the outcome of the previous chapters using the objectives of this work.

1.3 Setting of the study area

1.3.1 Geographical setting and general introduction to the study area

Chew Bahir is currently an extensive area of saline mudflats in the fault bounded depression of the Chew Bahir basin ($\sim 05^{\circ}22'N-04^{\circ}10'N$, $-36^{\circ}50'E-37^{\circ}05'E$), and is part of the active continental rift zone of the East African Rift System (EARS, Fig. 1.3, 1.7). It lies at $\sim 480-520$ m a.s.l. between the elevated Ethiopian Plateau and East African Plateau (Fig. 1.4 and Fig. 1.2)*. The basin, 70 km long (N-S) and 30 km wide (E-W) is located in a 250–300 km broadly rifted transition zone (Woldegabriel and Aronson, 1987; Bosworth, 1987), between the Omo-Turkana Basin to the west, already part of the Kenyan Rift, and the southern part of the Main Ethiopian Rift (MER). The Hammar Range, composed of Precambrian metamorphic rocks, forms Chew

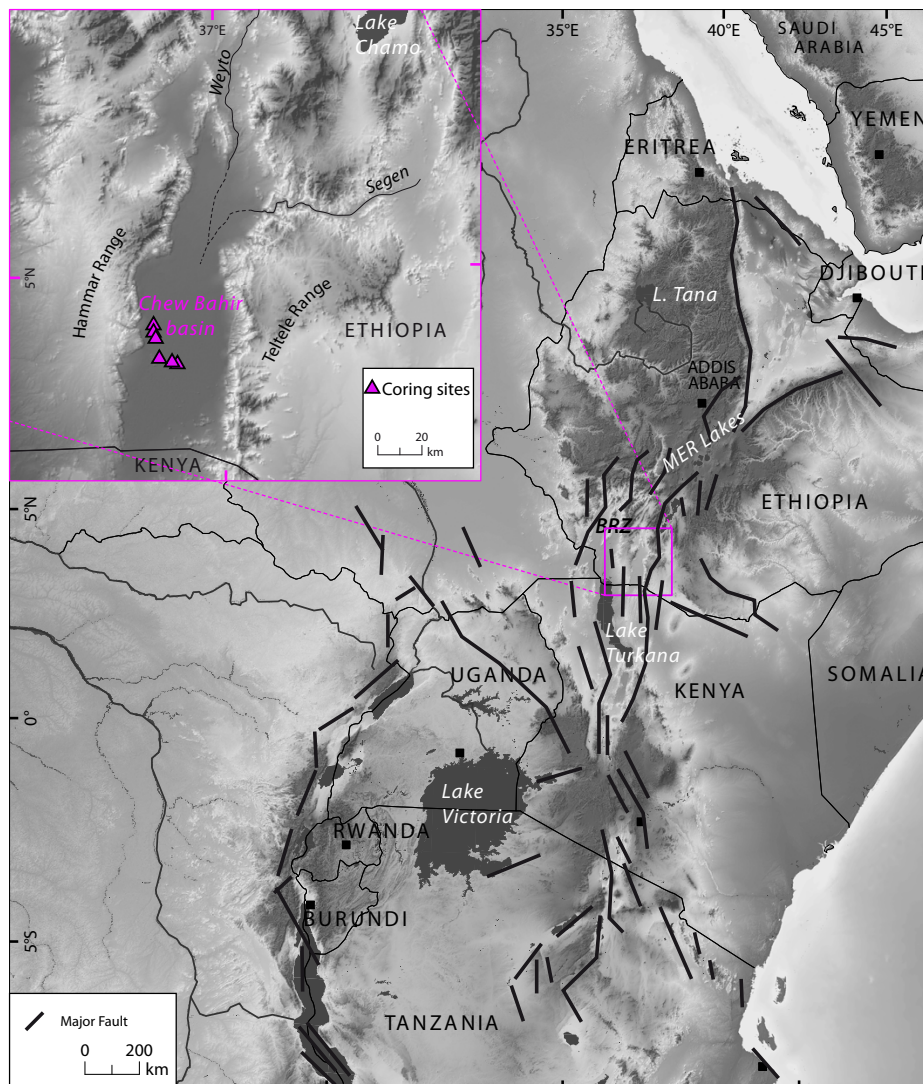


Figure 1.3 | Map shows the geographical setting of the study area, with the EARS including major faults, lakes and plateaux. Thin black lines indicate modern political borders, capital letters indicate countries. White italics show lakes, black italics point at rivers in the detail map of the Chew Bahir basin. BRZ - Broadly Rifted Zone. Shading of the map indicates elevation: light shade-lowlands, darker shade-highlands. For more detailed isohyps refer to Figure 1.7.

Bahir's margin to the west and divides the Chew Bahir basin from the Omo-Turkana basin. To the east, Chew Bahir is bounded by the higher eastern escarpment of the Teltele-Konso range, where exposures of Miocene basalts and trachytic centres are found. To the north is the narrower Weyto basin, bounded by the south-western (Gofa) highlands to the west and the Gamo-Chencha horst to the east (Fig. 1.8).

Hydrologically, Chew Bahir is part of a lake-river system of closed drainage basins (Mathisen and Vondra, 1983) along the EARS and is the southerly end-point for drainage from the Abaya-Chamo lake system (Fig. 1.4). Lake Chamo, ~220 km northeasterly of Chew Bahir, is believed to have drained into paleo-lake Chew Bahir during highstands, possibly even as a steady overflow through gaps and small divides via the Segen river (Mathisen and Vondra, 1983; Wood and Talling, 1988). To the south, the basin extends into the Kenya Rift and has an overflow sill at ~50 m (Foerster et al., 2012) that connected Paleo-Lake Chew Bahir with the terminal lake of this drainage system, Lake Turkana, via discontinuous overflow events during pronounced humid phases in the past. Lake Turkana was also the terminal lake of the drainage system from the Kenyan Rift Lakes, in the East African Plateau (Junginger et al., 2014; Fig.1.4). Turkana would then fill to produce an extensive Mega-lake until an overflow level to the White Nile was reached (Wood and Talling, 1988). The perennial Weyto and Segen (otherwise also known as Sagan) rivers are the main sources of fluvial inwash from the 32,400 km² surface catchment, which comprises part of the precipitation rich 2500–4000 m-high SW Ethiopian highlands; and the Weyto and the Konso area. Today, the rivers' influence is mainly restricted to the northern part of the basin (Davidson, 1983) and tied to the rainy season. Extensive alluvial fans run into the basin from the eastern and western flanks, contributing to the sedimentary deposition from the rift shoulders and form the outer margin of the basin sediment infill.

'Chew', means 'salt' in Amharic, a good description for

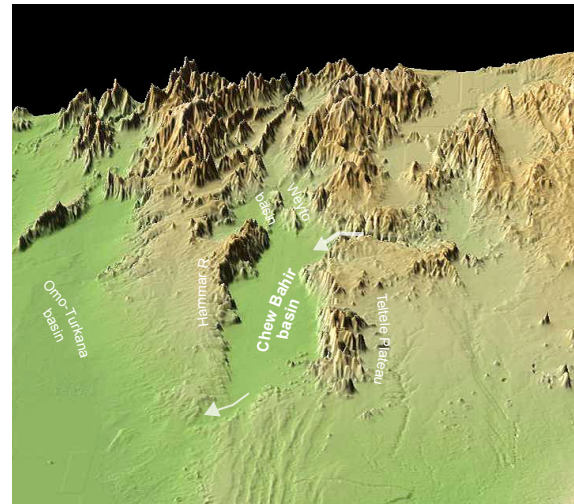


Figure 1.5 | The topographical setting of the Chew Bahir basin, showing the southern end of the MER to the north and the bordering rift shoulders of the Hammar Range to the West, merging into the Omo-Turkana basin and the Teltele Plateaux to the east. The overflow till to Lake Turkana is marked with an arrow. Map created with GeoMapApp3.3.9 and was a tenfold superelevated.

the overall appearance of the playa today. The basin is a dried out paleo-lake, which fills up to a shallow water-level after the rainy season in some areas. Due to the high evaporation/precipitation ratio, deep dry cracks (up to 5 cm; see Fig. 1.6h) and fine precipitates appear in the central parts of the playa during the dry season. Some areas, visible from satellite images, are vegetated (Fig. 1.6a–d; Fig. 3.1e) and used by the local Hammar tribe for cultivation of small maizefields and pastureland for subsistence cattle and goat herding. Due to the extensive nature of Chew Bahir there are considerable variations in surface appearance within the basin, which are mainly controlled by the availability of moisture influx (see Fig. 1.6a–j). This is also expressed in vegetation cover which varies from margin to centre, from a narrow but dense shrub belt on top of the alluvial fans to open shrub cover with tussock grass sods, xerophytic and halophytic plants, to sparsely grassed patches to no vegetation at all.

The basin sensitively reacts to moisture fluctuations with variations in lake fill, from an extensive fresh water

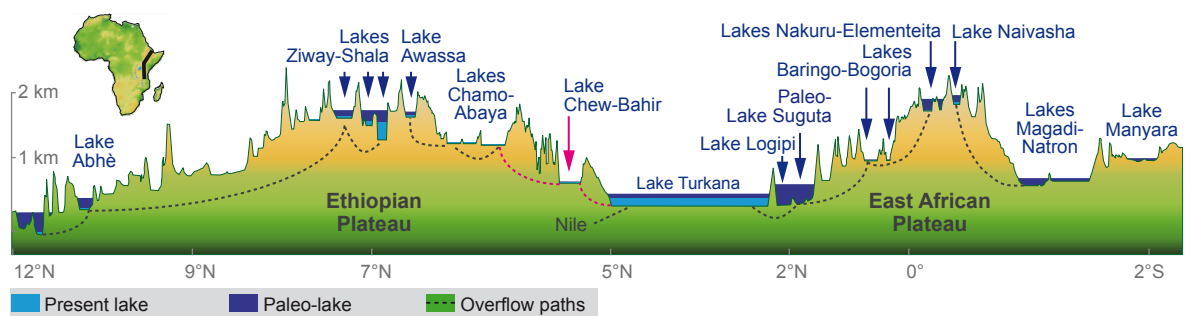


Figure 1.4 | Chew Bahir as part of the drainage system of the southern side of the Ethiopian Plateau with overflow path to Lake Turkana and receiving drainage from Chamo-Abaya System. Figure shows cross section of the eastern branch of the EARS after Junginger and Trauth et al. (2013) with lake levels of modern and palaeo-lakes. For references and exact palaeo-lake depth refer to Junginger and Trauth (2013) and Junginger et al., (2014).

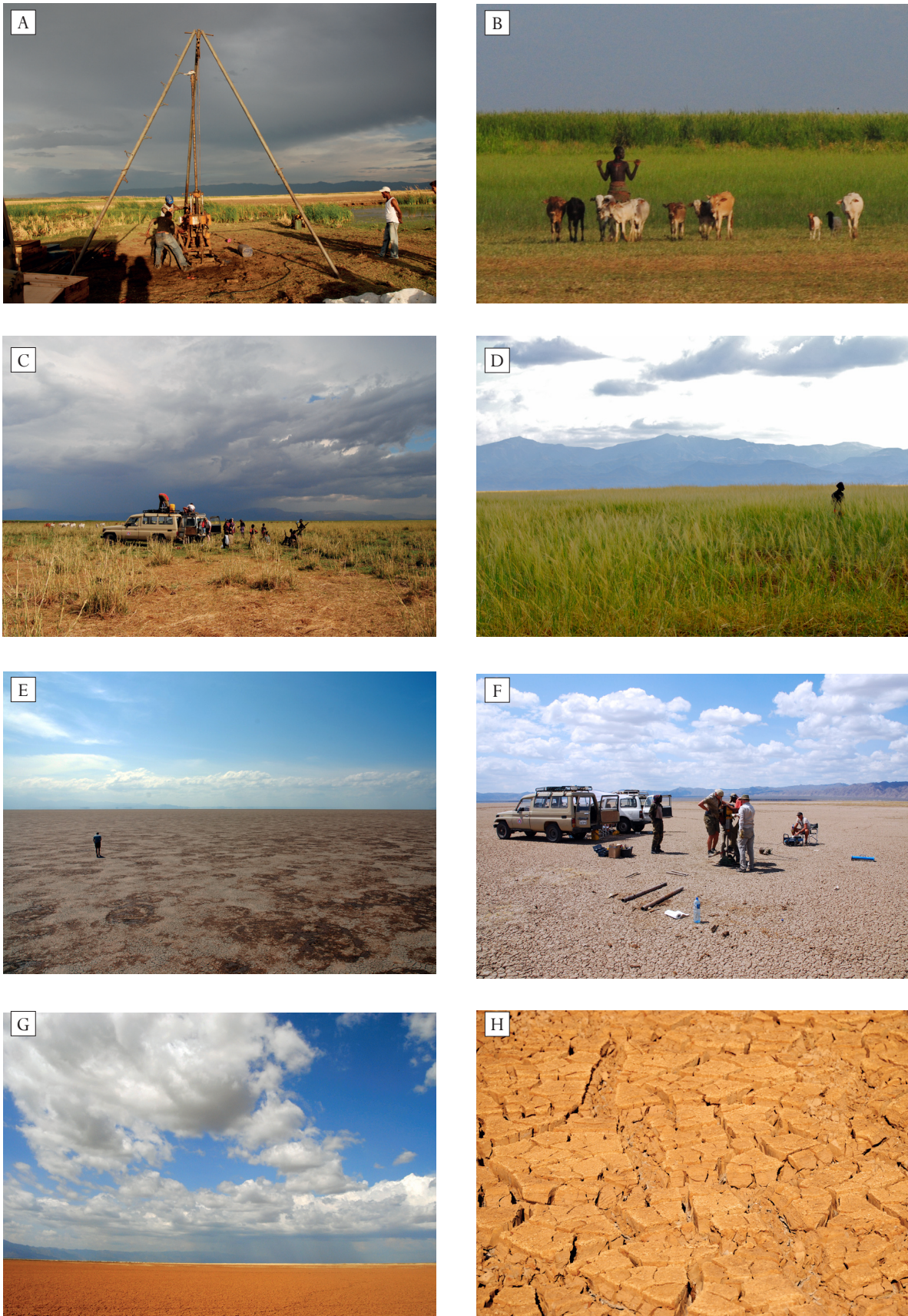


Figure 1.6 | Photos of the Chew Bahir, showing variability within the Chew Bahir basin along the margin-centre transect (A) Margin of the CB, pilot core drilling site CB-01, retrieved in Nov 2009; (B) Close to coring site CB-01, member of the Hammar people with small goat and cow flock in front of field; (C) Site CB-03, in a transitional position within the basin; looking eastwards towards the Teltele; covered with grass vegetation; (D) Site CB-03, looking westwards, with the Hammar Range in the back; (E+F) Site CB-06, in the centre of CB basin; completely vegetation-less, surface of the playa is covered by fine precipitates; drilling operation on the CB-06 site in Nov 2010; (G+H) Site CB-05, proposed ICDP deep-drilling site, eastern-most position within basin; surface deposits show deep dry-cracks, approximately 1 month after the short rainy season; (I+J, following page) cattle herd with Hammar-boy close to CB-02; (J) CB-02 with Hammar Range to the right and in the back, showing one of the extensive alluvial fans reaching far into the basin. Photos by F.Schäbitz (A); V. Foerster (B-J);



lake to a saline mudflat. The Chew Bahir, though dried out today, is known to have been filled by water until recently; maps from the seventies of the last century (e.g. Shiferaw et al., 1972-1974) still show a partially water covered basin in the south western area following the outlines of the once larger palaeolake. The lake formerly known as Lake Stefanie, after the Belgian Princess, was described by Cavendish in 1889 as “the water of the lake we always found drinkable, although salt[i]er near the south end” (Cavendish, 1889, p.377), which most likely caused by the fresh water influx from the north and high evaporation. Since then, Chew Bahir has experienced decreasing water levels accompanied by an increase in salinity and alkalinity, until complete desiccation occurred (Grove et al., 1975; Friis et al., 2001).

* The following chapters II and III will provide additional implementations, maps and tables in the setting chapters respectively

1.3.2 Magmatism, Rifting, Geology

Africa has been subject to rifting processes since the Precambrian. Consequently, many of the younger rifts and magmatism in East Africa follow these ancient pre-existing structures and trends in the basement (Shakleton, 1996; Ebinger and Sleep, 1998; Macdonald et al., 2001; Bosworth, 1989). The thermal history of the lithosphere peaked when the lithospheric plates came close to a standstill. As a result the hypothesised underlying mantle plume(s) is thought to have had a prolonged influence on the African lithosphere and upwelling mantle plumes could have penetrated the overlying crust (Bosworth, 1989; Ebinger et al., 2000; Pik et al., 2008). The magmatic history of the EARS is associated with an anomalously hot mantle beneath the rift zone, as it is today, which may have been connected to the presence of one (Ebinger and Sleep, 1998) or more mantle plumes, thought to be responsible for Cenozoic magmatism (George et al., 1998; Ebinger et al., 2000; Trauth et al., 2007). The asynchronous progress of volcanism and faulting may even be an indicator for a migrating mantle plume (Macdonald et al., 2001).



The cretaceous Anza-Nile rifts (160-60 Ma) (Ebinger et al., 2000; Fig. 1.3.2) predated the general onset of Cenozoic Rifting (Chorowicz, 2005), which characterised the formation of the EARS. Initial volcanism started ~ 45 Ma with eruptions of huge volumes of vulcanite. Volcanism preceded faulting and uplift, the latter reaching a maximum at the Plio-Pleistocene interval. The (Ethiopian) uplift shoulders were consequently placed over older topography (Sepulchre et al., 2006; Ebinger et al., 2000; Benvenuti et al., 2002). Volcanism and faulting started in the Eastern branch of the EARS, in the Main Ethiopian Rift and the adjacent plateau from ~ 45 to 33 Ma, and then proceeded diachronically from north to south, forming the Main Kenyan Rift ~ 33-25 Ma and southern Kenyan and Tanzanian Rift from ~ 15-8 Ma. This development led to a ~6000-km-long uplifted area, predominantly trending from north to south, bordered by uplift shoulders and peaks between 1500 and 5100 m (Sepulchre et al., 2006; Chorowicz, 2005). At present, the EARS is ~ 100 km wide (Ebin-

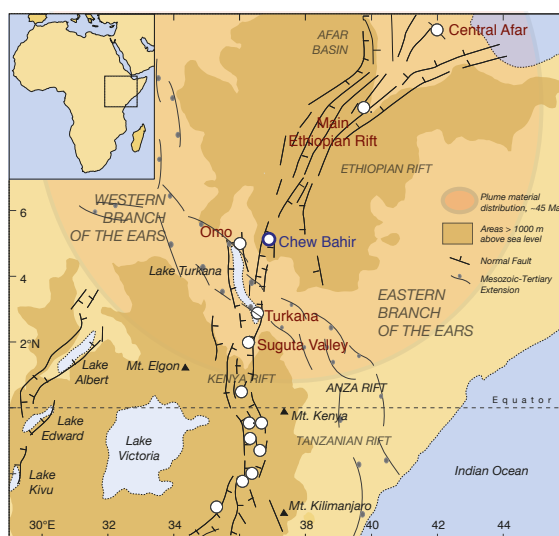


Figure 1.7 | Map of East Africa showing topography, rift faults and sites of lake-sediment sequences used for palaeoclimate reconstruction (white circles), the Anza-Nile Rift after Bosworth (1989) and presumed extension of mantle plume around 45 Ma (after Ebinger and Sleep, 1998). Blue circle shows the location of Chew Bahir within older and younger Rift structures. Base map modified after Trauth et al. (2005).

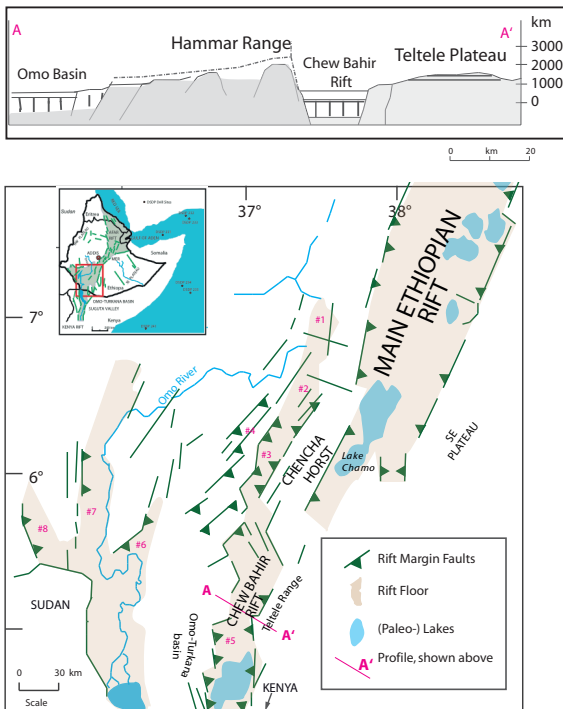


Figure 1.8 | The Chew Bahir rift located in between the Ethiopian Plateau and the Kenya rift in the BRZ that comprises several basins divided by plateaux and ridges as marked in the map: 5) Chew Bahir basin; 1) Omo canyon; 2) Maze basin, 3) Bala rift, 4) Gofa basin and range 6) Usno basin 7) Omo basin, 8) Kibish. Modified after Asrat et al. (2009), WoldeGabriel and Aronson, (1987). Figure inset shows profile of the Chew Bahir basin (A-A'), after Pik et al., (2008).

ger et al. 2000), with deformation within a relatively narrow topographic trough except for the overlapping zone between the MER and the Kenyan Rift.

This broad region of rifting is distributed over a zone up to 300 km-wide, which is thought to have formed when rifting migrated eastward along the pre-rifting structures of the Anza Rift (Ebinger et al., 2000). Alternatively, it has been suggested that the structure represents an extinct or 'failed' rift (WoldeGabriel and Aronson, 1987). The term Broadly Rifted Zone (BRZ) was coined by Davidson and Rex (1980) and later adopted by Ebinger et al., (2000) to describe this anomalously formed topographic depression between the two uplifted domes (Pik et al., 2008). During the last ~20 Ma, extensional faulting created a zig-zag fault pattern with depressions, comparable to a basin and range topography, ranging from basal 500 m asl. to 4000 m high peaks and ranges (WoldeGabriel and Aronson, 1987; Ebinger et al., 2000; Chorowicz, 2005; Pik, 2008; Corti, 2009).

The tectonic and magmatic evolution of the southern Ethiopian Rift is closely linked, however, to primary flood basalt volcanism and eruptions of rhyolites and phonolites which are thought to predate the onset of the main rifting phase at ~ 20–15 Ma (Ebinger et al., 2000; Pik et al., 2008). As shown in Fig. 1.9 and Fig.

3.1b, the geology of the Chew Bahir catchment and basin is characterised by exposed Precambrian metamorphic rocks, which form the basement and are partially covered by largely Oligocene to Quaternary volcanics. These metamorphic rocks to the west consist of a gneiss complex, interlayered with granulite and amphibolite facies (Figure 2.2). The Cenozoic southern Ethiopian rift volcanism and associated extensive pre-rift Eo-Oligocene flood basalt volcanism is evident in the Amaro and Gamo basalts in the Gofa province to the north and the Oligocene Fejej basalts which are partially exposed along the Hammar Range (WoldeGabriel and Aronson, 1987; Davidson, 1983; Ebinger et al., 2000; Pik et al., 2008). Rifting is thought to have dismantled the volcanic plateau (Pik et al., 2008) at a later phase. The Eastern plateau, the Teltele plateau, is covered by a Miocene flood basalt sequence, named Teltele basalts which are dated to ~20 Ma. The Kumbi rhyolitic tuffs and lavas, thought to be from the Jibisa Ring complex at the Ethiopian-Kenyan Border, are dated to ~ 14 Ma and cap the volcanic sequence from the Teltele basalts in large parts towards the southern margin of the Chew Bahir basin (Ebinger et al., 2000). The expression of younger volcanism in the Chew Bahir area is confined to Pliocene basaltic flows and is found to be centred on the northern part of the Chew

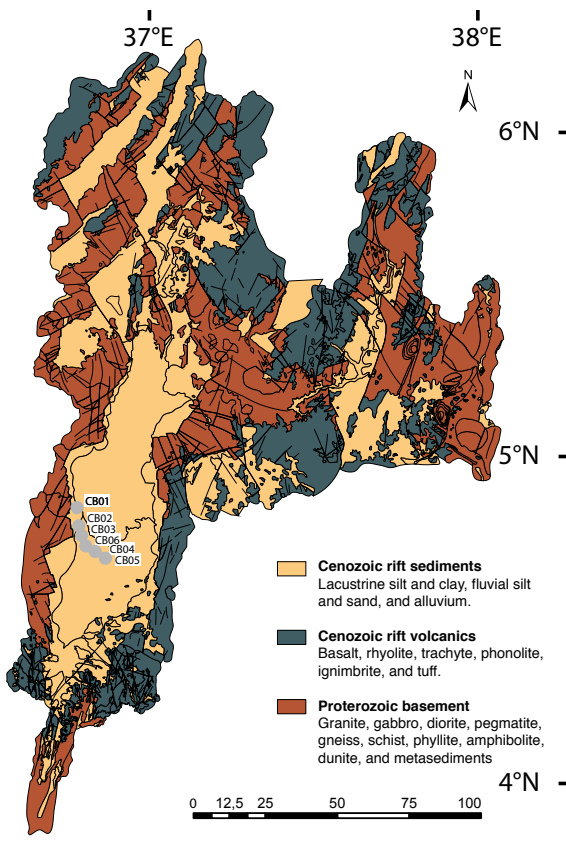


Figure 1.9 | Map of the Geology in the Chew Bahir catchment, simplified after Davidson, 1983; Key, 1988; Hassen et al., 1991; Awoke and Hailu, 2004).

Bahir, partially covering the Moiti Tuff blanket (3.9 Ma) on the northern basin floor (Asrat et al., 2009). Small cinder cones, from ~ 3.2 Ma, are locally confined to the southern end of the Chew Bahir basin (Ebinger et al., 2000). The basin itself is filled with Miocene to Quaternary deposits (Pik et al., 2008), which are thought to be largely undisturbed as rifting processes declined after the formation of the Chew Bahir rift. The sedimentary deposits in the basin reach at least ~2.5 km depth (Woldegabriel et al., 2005), potentially to a depth of ~5 km, as suggested by airborne gravity and seismic reflection data (Asrat et al., 2009). Based on tephrochronological correlations with the Afar, the Omo-Turkana basins and cores from the Indian Ocean, these Chew Bahir deposits are expected to contain several wide spread, and well dated, marker tuffs as the Moiti (3.9 Ma), Wargalo (>3.6 Ma), and SHT (3.4 Ma) Marker tuff (Asrat et al., 2009 and references within). The Konso silver tuff from the 90 km distant Konso area, dated at 154 ka BP, represents an important chronological marker and is expected to be clearly detectable in the upper part of the Chew Bahir deposits.

1.3.3 Present climate

Due to the highly diverse topography of East Africa, various meso- and micro climates are created that are modulated by altitude and position within the atmospheric circulation and monsoonal systems, which control the distribution of precipitation over East Africa (e.g. Nicholson, 1996; Barker and Gasse, 2003; Seleshi and Zanke, 2004; Diro et al., 2009; Segele et al., 2009). North of the equator a broad zonal precipitation pattern is found which is however pronouncedly broken by the rain-shadow effect of the EARS, thus causing a moisture deficit (Larrasoña et al., 2013). On the meso- to micro-scale the large water bodies of the Rift lake systems contribute to the availability of moisture and vegetation cover supports the storage of moisture (Ni-

cholson, 1996).

Intra-annual temperature variations are less than a few degrees Celsius (in Chew Bahir < 3°C; Fig. 1.12) due to the relative position to the equator. Therefore seasonality is largely determined by moisture availability. Mean temperatures follow steep elevation gradients between the fresher highlands and hotter lowlands (Gasse et al., 2000). Rainfall seasonality is driven by the migration of the Intertropical Convergence Zone (ITCZ) between 15° S (January) and 15° N (July) (Benevenuti et al., 2002; Barker and Gasse, 2003; Segele et al., 2009). The zone of maximum rainfall, the tropical rainbelt, follows the zenithal position of the sun (maximal insolation) with a 4-6 week time lag (Nicholson, 1996), which results in a bimodal rainfall pattern with increasing proximity to the equator (Fig. 1.11 and 1.12). With increasing distance to the equator, the two rainy seasons merge to a single precipitation-rich interval in summer and a drought season in winter. Figure 1.11 and 1.10 demonstrate the precipitation distribution throughout the year and show how latitudinal belts are modified by topography and ocean-land dynamics. As well as the amount of insolation, the conditions of the sea surface (i.a. temperature) in the surrounding oceans and the pressure gradient between land and ocean masses play a pivotal part in heat and moisture transport (Barker and Gasse, 2003). The ocean-land pressure gradient develops due to the differential heat capacity of landmass and ocean (Kutzbach and Street-Perrott, 1985; Kutzbach and Otto-Bliesner, 1982). Monsoonal moisture influx comes from the West African Monsoon (WAM) with westerly and southwesterly airflows as indicated in Figure 1.10. The moist airmasses of the WAM convect moisture from the Atlantic ocean and recycle humidity that is from the dense tropical vegetation over the Congo basin. The monsoonal influence reach as far eastwards as the Rift, where they converge with Indian Ocean air masses and form a highly unstable north-south trend-

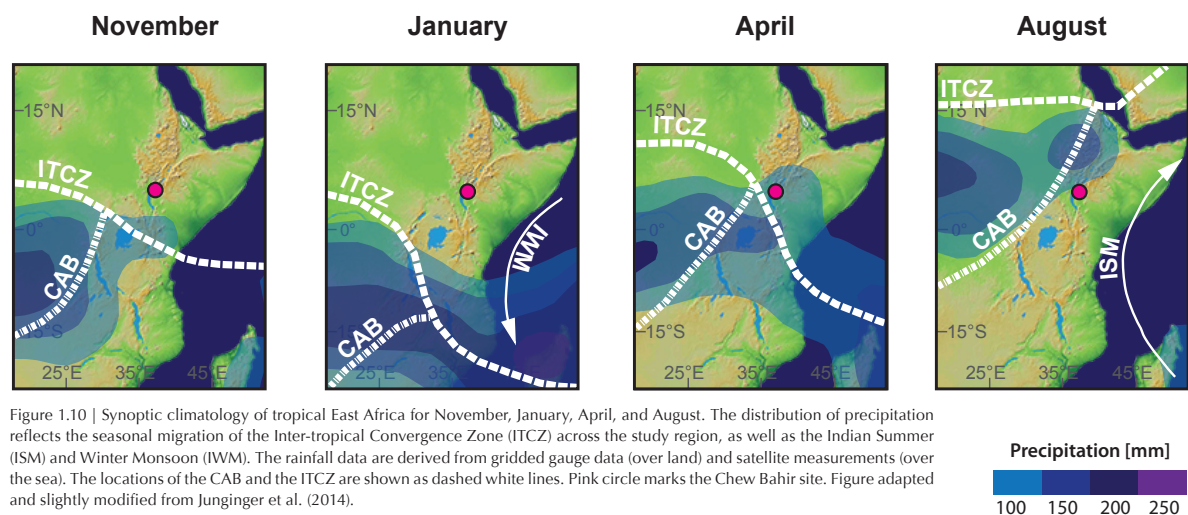
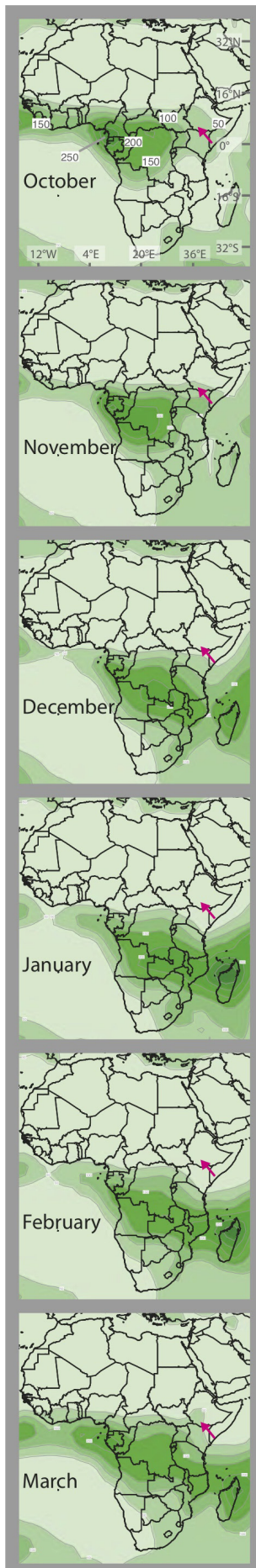


Figure 1.10 | Synoptic climatology of tropical East Africa for November, January, April, and August. The distribution of precipitation reflects the seasonal migration of the Inter-tropical Convergence Zone (ITCZ) across the study region, as well as the Indian Summer (ISM) and Winter Monsoon (WWM). The rainfall data are derived from gridded gauge data (over land) and satellite measurements (over the sea). The locations of the CAB and the ITCZ are shown as dashed white lines. Pink circle marks the Chew Bahir site. Figure adapted and slightly modified from Junginger et al. (2014).



ing convergence zone over East Africa (Fig. 1.10 and Fig. 3.1a), known as the Congo Air boundary (CAB; Nicholson, 1996; Tierney et al., 2011; Costa et al., 2014; Junginger and Trauth., 2014). The NE and SE monsoon air flows; the modern Indian Summer Monsoon and (ISM) and Indian Winter Monsoon (IWM), on the other hand, are dry over East Africa (Nicholson, 1996). The ISM transports moist air away from Africa towards the pressure low over India in NH summer. The IWM coming from the large continental landmass during boreal winter is generally too cold to advect moisture over the Indian ocean (Fig.1.10) (Nicholson, 1996).

The CAB, is considered an unstable air convergence zone and is known to have been subdued to major lateral shifts, causing significant variability in moisture influx. Furthermore, the displacement of the ITCZ (Gasse, 2000) and associated with it this convergence zone [CAB], has caused major climatic changes in the past (e.g. Junginger et al., 2014). Specifically regarding the areas towards the marginal zones affected by the tropical rainbelt, a shift of the ITCZ could mean a drastic transformation from receiving rain to close to no precipitation at all and vice versa ('Green Sahara' theory; e.g. Larrasoña et al., 2013). For the equatorial tropical climate regime, it is rather the amount of moisture carried by the ITCZ (than its migration pass) that modulated palaeoclimatic conditions.

Evapotranspiration in Ethiopia exceeds the measured mean annual rainfall for areas of Eastern Africa below 1,700 m, and for most lowlands within the MER a water deficit can be observed (Gasse and Street, 1978). For the MER, the mean annual rainfall varies between 1200 mm at the rift margins (1,400 mm on Mount Badda on the South Eastern Plateau) and the rift basins and lowlands. Conditions are drier with

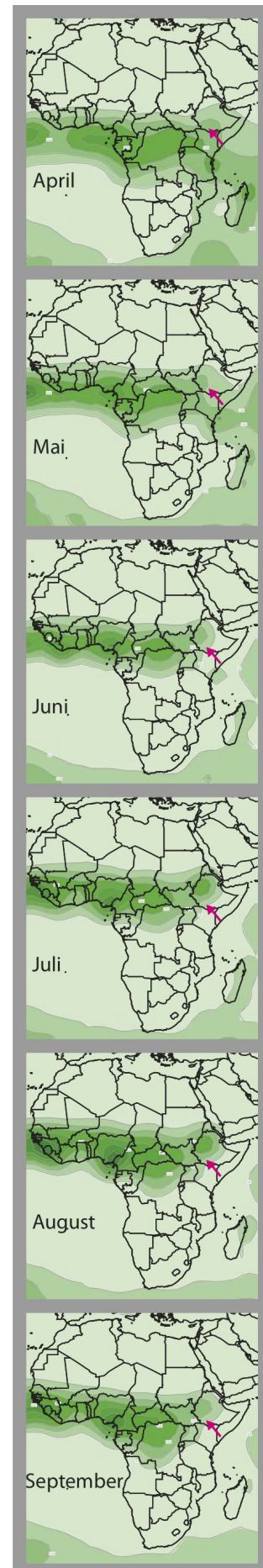


Figure 1.11 | Monthly migration of the moisture carrying convergent zone (ITCZ) that brings seasonal rainfall to the study area. Arrow indicates the location of Chew Bahir within this rain domain. Darker shades of green indicate the zones with highest monthly climatological precipitation amount, with contours in 50 mm/month intervals. End of October, the ITCZ follows with a lag the migration of max insolation values southwards, resulting in the onset of the dry season for most parts of Ethiopia during the following month (~Nov–Mar; left column). In Feb the ITCZ starts reversing direction and the northward migration of the convergent zone causes the 'short' rainy season in southern Ethiopia to begin in mid-March–mid-June. The northernmost position of the ITCZ marks a brief drier period around June, before the beginning of the main rainy season (~Jun–Sept) on the highlands of Ethiopia. Maps and data are based on monthly climatological precipitation (in mm/month) estimates from satellite emitted long-wave radiation from polar-orbiting satellite, using the period 1981–2010 as data base. Modified from IRI database, (last access, Jan 2014).

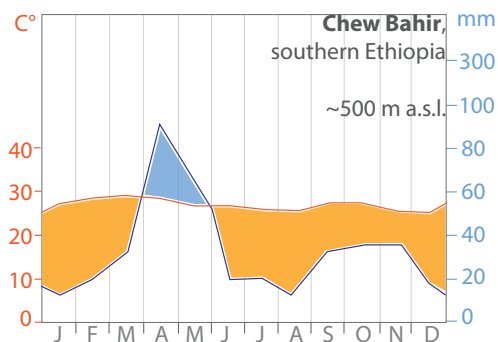


Figure 1.12| Climate diagram of the Chew Bahir region, showing average of monthly min. and max. precipitation in mm/month and monthly mean temperatures in °C (base period 1971–2000). The values apply for the region 36.151E–38.032E, 3.761N–5.489N and were derived from IRI, accessed Jan 2014.

700 mm towards the central part of the basin and even less rain was measured southwards around lakes Abiyata and Langano. Mean annual temperature at Ziway (1,640 m) is 19°C. For Dubti (Afar, 380 m) a mean annual temperature of 29 °C has been recorded and, in comparison to the MER, a clear decreased precipitation of 300 mm/a has been measured (Gasse and Street, 1978; Benevenuti et al., 2002). To the other side of the Ethiopian dome, the southern Ethiopian lowlands receive less than 500 mm/a precipitation and mean temperature is found to be ~ 25 °C (IRI, 2014), as shown in the climate diagram from the Chew Bahir area. A bimodal precipitation cycle is also evident (Fig. 1.12) in the precipitation distribution: with the longer ‘Kiremet’ rainy season in spring and shorter ‘Belg’ rainy season in fall, framing a short, variable drier interval in June–July. In NH winter, between October and mid-March, a relative stable dry phase follows under ‘normal’ conditions, with the intertropical rainbelt migrating towards the Tropic of Capricorn (Fig. 1.11).

Inter-annual rainfall variability in East Africa on a sub-decadal time-scale is strongly quasi-periodic and is mainly created by variations in SSTs in the Indian and/or Atlantic Oceans, which are associated with the El Niño/Southern Oscillation (ENSO) and Indian Ocean Dipole (IOD; Trauth et al., 2003; Nicholson, 1996; Abram et al., 2007) phenomena. The IOD (Saji et al., 1999; Abram et al., 2007; 2008) is caused by sea surface temperature anomalies in the Indian Ocean (for positive IOD phases: warmer SSTs in the western basin and cooler SSTs in the eastern Indian Ocean, off Sumatra). An equatorial surface wind and precipitation pattern reversal caused by this SST dipole may be associated with these observed positive rainfall anomalies for East Africa (and drought conditions over Indonesia) (Saji et al., 1999). For negative IOD phases, the opposed SST oscillation can trigger severe droughts over East Africa (and excessive rainfalls over Indonesia). The El Niño/Southern Oscillation (ENSO) is known to affect the rainfall in East

Africa, in particular it changes the ‘Belg’ rains (e.g. Nicholson, 1996; 2001), supposedly independently from the occurrence of IOD via teleconnection (Saji et al., 1999). The interconnectivity between ENSO and IOD (and possibly even the Indian monsoon system) and a possible relationship between both phenomena is still highly debated (Saji et al., 1999; Moy et al., 2002; Annamalai et al., 2005; Segele and Lamb 2005; Wang and Wang, 2014).

These ocean temperature oscillations are correlated with severe out-of-season droughts and floods over East Africa with an averaged periodicity of 3–7 years (Segele et al., 2009), depending on the season they occur in and on the magnitude of the prevailing event. The last inter-annual flooding anomaly linked with oceanic variability, in Chew Bahir, occurred in 2009/2010 during the pilot drilling campaign and persevered during the winter dry season, causing out of season precipitation (www.bom.gov.au/climate/enso/enlist/). The next El Niño event could be expected in late 2014 with a current 3-in-4 likelihood (Ludescher et al., 2014), potentially causing droughts over SE and southern lowlands of Ethiopia. Inter-annual climate variations on longer time-scales (10¹–10⁴ years) and their hypothesised triggering mechanisms are discussed in detail in Chapters II and III.

1.3.4 Vegetation cover

Vegetation cover follows the climatic zonation determined by rainfall distribution and along altitudinal belts (Fig. 1.13). Therewith the vegetation types in Ethiopia range from montane forests on the high mountains with partly tall forest trees, open canopy woodland with acacias, savannah vegetation with few trees, to large areas with grassland, distributed on the plateaus (Grove et al., 1975; Fig. 1.13 and Fig. 1.14a).

According to a recent mapping and classification project by Friis et al. (2001), the potential natural vegetation of Ethiopia can be differentiated into fourteen vegetation types and sub-types as depicted in Figure 1.13 and into eight generalised ecosystem types, determined by altitude and precipitation, into the following (after Friis et al., 2001, 251 pp. and the Institute of Biodiversity Conservation <http://www.biodiv.be/ethiopia/biodiversity/ecosystems-ethiopia>, last access Feb 2014):

1. The Afroalpine and Subafroalpine Ecosystem. This ecosystem is characteristically found in the higher altitudes (3200+ m), along chains of mountains, slopes and mountaintops, with the subafroalpine system between 3200 and 3500 m a.s.l. and the Afroalpine vegetation

between 3500 and 4620 m altitude. The vegetation cover comprises the striking giant *Lobelia rhynchopetalum*, which is endemic to this ecosystem, as well as evergreen shrubs and heathers and perennial herbs.

2. Dry Evergreen Montane Forest and grassland complex. This ecosystem is complex as it comprises several sub-types and successions of vegetation types, mainly in the Ethiopian highlands between 1600 and 3300 m. This ecosystem ranges from Afromontane dry evergreen forests to extensive grasslands. The first is dominated by *Juniperus procera* and *Olea europaea* and *Podocarpus falcatus*. This typical vegetation cover is followed by Acacia-dominated wooded grasslands and Afromontane woodlands covering large regions on the plateaux. The montane grassland ecosystem is determined by the occurrence of 30-80 cm high perennial grasses and species of *Cyperaceae*. Furthermore, sub-shrubs and perennial herbs, bulbuous and rhizomatous plants.

3. Moist Evergreen Montane Forest. This ecosystem consists of mainly evergreen 30-40 m high trees, comprising of a mostly closed strata of the humid forest, which includes large *Podocarpus*, medium-sized trees, large shrubs and localised mountain bamboo, as well

as epiphytes, scadoxus and ferns and small occurrences of mosses. Their distribution is confined to the precipitation-rich southwestern areas of the Ethiopian Highlands, between 1500 and 2600 m a.s.l., and the southeastern plateau on the southern slope of the Bale mountains. Transitional rainforest (TRF) also occurs in this ecosystem though restricted to lower altitudes like on western escarpment (1500-500 m a.s.l.).

4. Acacia-Commiphora Woodland. This ecosystem is determined by drought resistant trees and shrubs with either deciduous or leathery drought persistent leaves, which are found in large areas of the country at elevations between 900 and 1900 m (see map). The trees and shrubs can form a closed stratum comprising different species of *Acacias*, *Belanites* and *Commiphoras*. Characteristic shrubs and sub-shrubs are *Acalypha*, *Barleria*, *Aerva* and various succulents and *Aloe* species. The density of the canopy varies from a closed to open woodland, to single scattered trees with dominant grassland < 1m high.

5. Combretum-Terminalia Woodland. This ecosystem is characterised by small to moderate-sized trees with large deciduous leaves identified as bushwillows *Combretum* or the *Terminalia* and *Lannea*. Moreover, the lowland bamboo *Oxytenanthera abyssinica* is abundant in river valleys. Herbs such as *Justecia spp.*, *Barleria*, *Eulophia*, *Chlorophytum* and grasses including species such as *Cymbopogon*, *Hyparrhenia*, *Echinochla*, *Sorghum*, *Pennisetum* make up the ground level vegetation layer. Whether the grasses occur dominantly is controlled by the rainy season. This ecosystem can be found at altitudes between 500-1900 m a.s.l., as shown in Figure 1.13, and is interpreted to be closely tied to the influence of fires.

6. Low-land Semi-evergreen Forest. This ecosystem is restricted to the lowlands with sandy soils between 450 and 650 m altitude. The vegetation cover is characterised by semi-deciduous trees between 15-20 m tall that form a mostly open canopy. *Baphia abyssinica* is the most common tree.

7. Desert and Semi-desert Scrubland. Due to decreasing and seasonally dependent moisture availability in this zone, the ecosystem is characterised by pronouncedly drought tolerant species including xerophytic *Acacia sp.*, deciduous shrubs, few evergreen shrubs and succulents (e.g. *Euphorbia*, *Aloe*), and xeromorphic adapted grasses (e.g. *Dactyloctenium aegyptium*, *Panicum turgidum*). The vegetation type is common in the hot and dry lowlands such as Chew Bahir, the Afar and the delta of the Omo river. The grass vegetation is tied

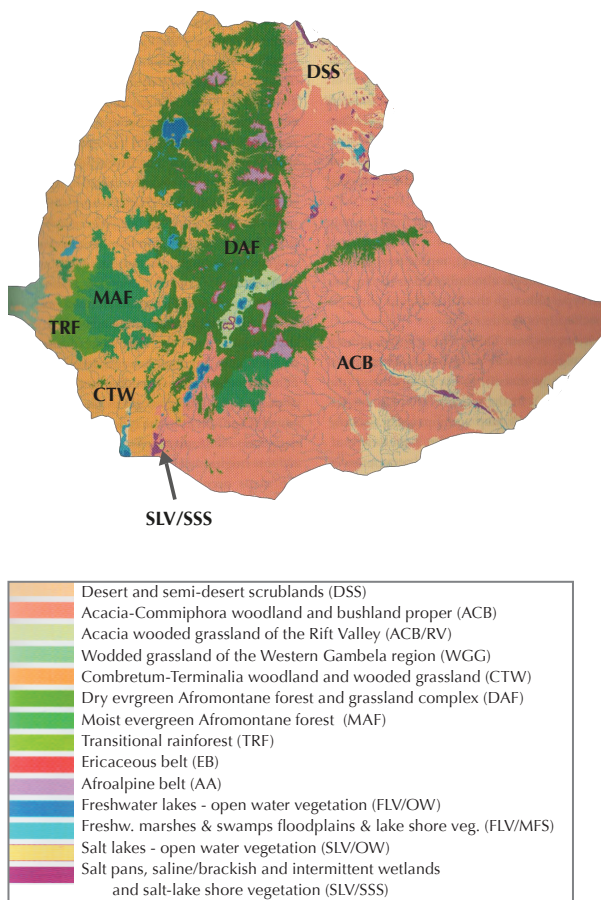


Figure 1.13 | Map of the potential vegetation of Ethiopia, differentiated into fourteen vegetation types and comprised into eight ecosystem types. Map adapted from Friis et al., 2001).

to the moisture availability during the rainy season. Anthropogenic land-use is pastoral and agro-pastoral. This eco-zone is prone to erosion by wind and water as the vegetation cover is not continuous and largely seasonal. The desert zone occurs in the NE Tigray and northern part of the Afar, the semi-desert in several parts in the north, west and north-east.

8. Aquatic Ecosystem. This ecosystem is characterised by the occurrence of inland water bodies. These include large fresh water lakes and rivers, as well as reservoirs, swamps and wetlands. Some of these only contain water during a few months of the year. The vegetation types associated with the water body depend on the quality (fresh vs. saltwater) and availability of water. Consequently, there is a wide range of characteristic species in this ecosystem, from *Celtis africana*, *Mimusops kummel* and *Tamarindus indica* along rivers to sedges and grasses along lakeshores or in the surrounding of swamps.

The Chew Bahir catchment lies within the transition zone from an open wood- and grassland in the Combretum-Terminalia woodland and wooded grassland (CTW) in the northwest to an acacia-dominated woodland (Acacia-Commiphora woodland and bushland proper) zone in the southeast. The tectonic depression of the Chew Bahir itself is marked as the zone with episodic occurrence of intermittent saline/brackish wetland vegetation and salt-lake shore vegetation (SLV and SSS), comprised of drought- and salt-tolerant shrubs, grasses and succulents, as described above.

Due to the traditional cultivation of land, based on the use of fire for clearing and fertilisation, the anthropogenic influence on natural vegetation cover is evident

and deeply rooted in the Ethiopian culture (Soromessa et al., 2004). It is assumed that the occurrence of large grasslands is a human-derived vegetation type and was induced by human settlement and cultivation activities (White, 1983).

Palaeoclimatic changes in precipitation have caused considerable changes, and, as a consequence, vegetation zones have migrated and transformed. The vegetation types and ecosystems described here represent the current conditions, determined by the present climatic conditions. During periods of increased humidity, vegetation types that are commonly found in the precipitation richer zones today could have expanded to the today drier lowlands (and vice versa). This shift in vegetation is documented exemplary in palynological studies focussed on the Holocene (Umer and Bonnefille, 1998; Umer et al., 2007) and demonstrated by the comparison to the modelled vegetation cover during the arid LGM, throughout the AHP and present (Fig.1.14).

1.2.5 Chew Bahir as a potential terrestrial climate archive

As shown in the previous sub-chapters, Chew Bahir is located in a major transition zone, topographically, climatically and biogeographically, and thus is thought to represent a suitable site to study the complex interrelationship between climate and humans and their variations through time. However, the potential and value of CB as a terrestrial archive to answer fundamental interdisciplinary research questions is determined by following key factors:

- a) The suitability and reliability of the sedimentary deposits to provide the climatic history. This comprises both type and quality of the lacustrine material,

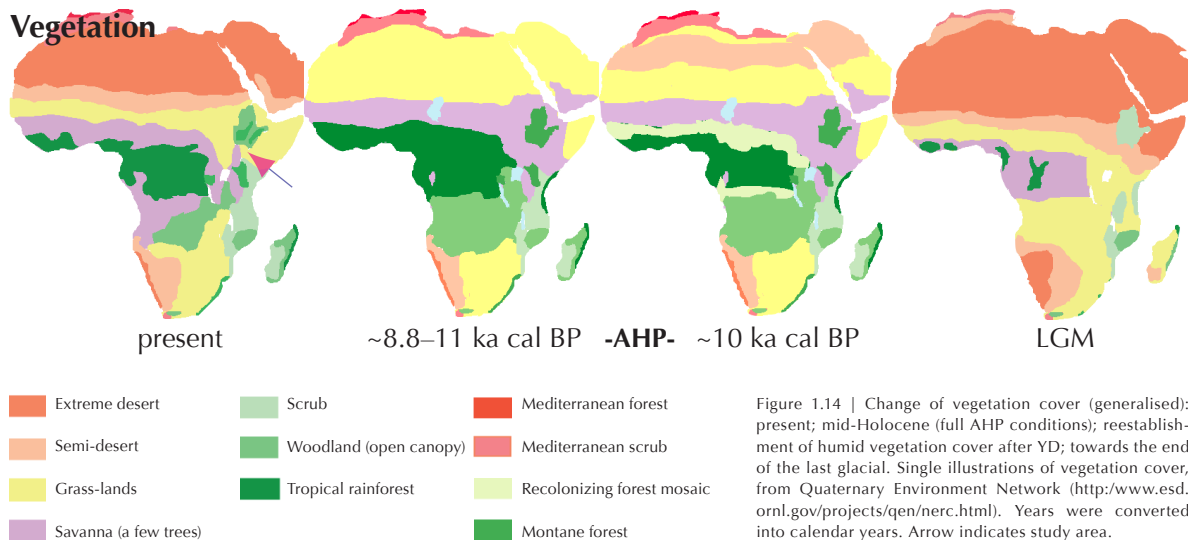


Figure 1.14 | Change of vegetation cover (generalised): present; mid-Holocene (full AHP conditions); reestablishment of humid vegetation cover after YD; towards the end of the last glacial. Single illustrations of vegetation cover, from Quaternary Environment Network (<http://www.esd.ornl.gov/projects/qen/nerc.html>). Years were converted into calendar years. Arrow indicates study area.

as well as their sensitivity towards climatic signals. This is to be tested and discussed within this thesis.

b) The type and age of the basin to hold the environmental information available that reach back far enough in time to answer research questions related to the evolution of mammalian (including hominin) taxa. This includes the extent to which sedimentary infill is disturbed by tectonic processes and its depth, the former needing to be nearly negligible and the latter deep enough to allow a continuous sedimentation process. As shown in the previous subchapter 1.3.2, the age of the basin (Miocene) and the fact that the area was relatively unaffected by Plio-Pleistocene rifting and uplift processes (Ebinger et al., 2000; Pik et al., 2008) result in this naturally bound basin being a large sediment trap. As a consequence, a continuous and largely undisturbed sediment sequence is expected which extends back as far as coring permits and technical limitations allow. The timeframe of a sediment core is determined by the sedimentation rates. These have been tested for the uppermost deposits within this study and imply that the target-timeframe of at least 500 ka BP can be easily reached (Chapter II and III). Until now a ~5 km deep infill of deposits have been presumed, based on seismic reflection surveys and airborne gravity by commercial Oil and Petroleum company surveys (Asrat et al., 2009). Though planned, no seismic survey within the framework of the project has been conducted yet to confirm this. This study covers the paleoenvironmental history to MIS 3 with < 60 ka BP, and therefore addresses questions related to more recent developments and innovations such as the development of sophisticated symbolic and cognitive behaviour (National Research Council, 2010), as well as adaptive strategies concerning hunting and pastoralism, fire and shelters.

c) The availability of archaeological records from the same or proximal region as the environmental record. Konso, Omo, Turkana and Weyto represent some of these key sites in a < 200 km radius.

Omo-Kibish and Turkana basin: The proximity to a known hotspot of human evolution or major palaeoanthropological site is a pre-requisite for testing hypothesis on climate-human linkages. As shown above, Chew Bahir is in the vicinity (separated by the Hammar Range) to the Omo valley, which contains the oldest known early modern human sites (McBrearty and Brooks, 2000; White et al., 2003; McDougall et al., 2005) and thus supports genetic studies that also suggest the East African origin of AMH (Stringer, 2003; Campbell and Tishkoff, 2010). The Omo-Turkana basin area is known for the density of archaeological sites, which document

the episodic presence and key developments of AMH (< 200 ka BP) and their antecedents (e.g. Basell, 2008; National Research Council, 2010; Blome et al., 2012).

Konso: The Konso area, situated 90 km to the NE of Chew Bahir, contains the oldest known Acheulean handaxes (~1.7 Ma), over 7000 mammalian fossils, and documents a co-existence of *Australopithecus boisei* and *Homo erectus* ~1.4-1.6 Ma (Asfaw et al., 1992; Katoh et al., 2000; Nagaoka et al., 2005; Suwa et al., 2007).

Weyto: The Weyto basin, the northern extension of the Chew Bahir basin (Fig. 1.8), contains assemblages which contain lithics and some fauna (bovids, primates, suids as well as hominid fossil) that have been attributed to the Acheulean-Middle Stone Age transition, and classic MSA based on preliminary biostratigraphic indications (A. Asrat, pers. communication, Feb 2014), suggesting the presence and activities of early Humans in the area. At present, the artifacts and fossils have not been published or dated, but could represent important data for answering key questions on this shift in human behavioural evolution.

SW Ethiopian Highlands: The catchment of Chew Bahir which cut into the adjacent SW Ethiopian Highlands are hypothesised to have been a refuge during phases of climatic aggravation (hyper-arid intervals) and therefore represent an opportunity to test the climatic determinant on hypotheses on refuge theories and bottleneck populations (Ambrose, 1998; Brandt et al., 2012). Following this refuge theory, this elevated and climatically favourable area might have served as a base for cultural and technological innovation for Hunter-gatherer groups, including Late Pleistocene and Holocene innovations and technology transfer, for instance in the context of food production (Brandt, 1986; Marshall and Hildebrand 2002; Lesur et al., 2013; see also Chapter IV and V). Also, Chew Bahir lies within the presumed **source region** of modern man (s.a.), which therewith represents the possible starting point (Richter et al., 2012b) of the dispersal of Humans beyond the limits of the African continent. This includes the testing of a possible environmental trigger for and phasing of human dispersal (e.g., Oppenheimer, 2009; Armitage et al., 2011; Campbell and Tishkoff, 2010; Scheinfeldt et al., 2010; Mellars, 2011; Richter et al., 2012b).

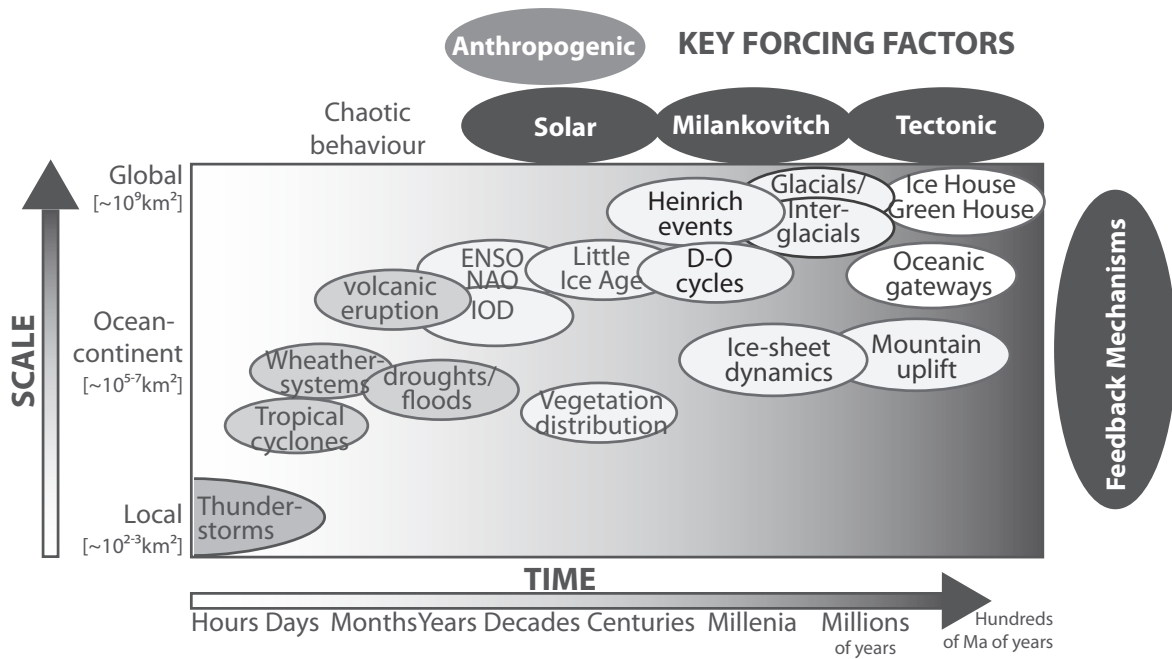


Figure 1.15 | Simplified model of the Earth's climate system including major forcing factors and environmental responses along a spatial and temporal axis. Modified after Maslin and Christensen, 2007. NAO-Northern Atlantic Oscillation, IOD-Indian Ocean Dipole, D-O-Dansgaard-Oeschger cycles.

1.4 State of the art

1.4.1 Climate system and forcing factors

Although many phases of climatic change and climate events are not currently understood fully, a general framework of the cornerstones of climate forcing factors exists (e.g. Maslin and Christensen, 2007; Kingston, 2007). Figure 1.15 demonstrates and comprises (even if strongly simplified) the complex interrelationship between internal- and external-, as well as chaotic-, drivers of the climate system. Accordingly, most of the known and described climate events can at least partly be attributed to those forcing agents along a temporal axis and with a spatial dimension ranging from local to global impact events (Figure 1.15). Overlapping forcing factors, the important role of Feedback mechanisms (e.g. climate vegetation feedbacks, as suggested by Claussen et al., 1999 or Renssen et al., 2006), are strongly responsible for non-linearity of climate change and problems in differentiation of time and scale (Maslin and Christensen, 2007) for a recorded climate event. They may complicate the interpretation, which can increase the ambiguity of results. Large parts of the discussion of the following chapters (II-IV) will concentrate on applying the known and well-studied variables of climate systems and work out the unknown, or rather hypothesised, impact agents. Even though attributing the environmental response to one or a series of overlapping forcing factors might be ambiguous, we have attempted to find patterns and regularities in the following chapters and carefully identified for instance the

last glacial/interglacial transition, the precession controlled wet cycles, H-events and D-O cycles, IOD and ENSO related events, as well as local strong rain events. Since scientific research of the last decades has been dedicated to the advancement of understanding natural climate forcing factors, a brief overview within the frame of the study area East Africa is given here:

Tectonics: East African environments are largely formed by a broad set of factors, including magmatic and tectonic activities on a timescale of millions of years (Fig. 1.15). These factors have had a significant influence on the topography and therewith on rainfall regimes, as well as the creation of various microclimates (see also chapter 1.3.3 and 1.3.2). The uplift and formation of the EARS has resulted in a general aridification trend of East Africa (Sepulchre et al., 2006). Foremost, the progressing tectonic uplift causes less zonal wind patterns and increasing elevation results in rain shadow effects. The result of this is a reduction of moisture availability for the eastern side of the uplifted areas and valleys (Maslin and Christensen, 2007).

Insolation (Solar and Milankovitch): Changes in the Earth's orbital constellation are believed to be the reason for frequent oscillations between glacial and interglacial climates, especially during the Quaternary (Kutzbach and Otto-Bliesner, 1982; Kutzbach and Street-Perrott 1985; Berger and Loutre, 1991; Laskar et al., 2004; Scholz et al., 2007). These oscillations are attributed to the specific orbital parameters obliquity, ec-

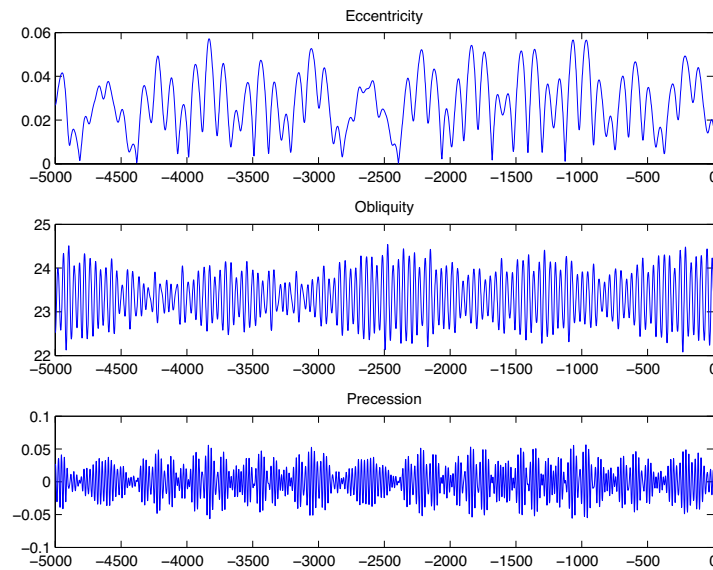


Figure 1.16 | Changes in the earth orbital parameters after Berger and Loutre, 1991 and Berger, 1992 for the last 0–5 Myr BP. X-Achses shows time in kyr (negative for the past and 0 being 1950). From the top: Eccentricity, Obliquity in degree and decimals and climatic precession. Variations in Insolation and therewith significantly the moisture availability for East Africa through time is strongly controlled by these orbital parameters with distinct periodicities: precession (19–23 kyr), obliquity (41 kyr), and eccentricity (100 kyr).

centricity and precession, which generate differences in incoming solar radiation, as they control the distance and angle of the earth towards the sun (e.g. Kingston, 2007). These orbital configurations have distinct periodicities (Fig. 1.16) and the resulting insolation from the combined effect of the overlapping periodicities for the different latitudes can be calculated back and forth in time (Fig. 1.16 and 1.17; Berger and Loutre, 1991; Berger, 1992; Laskar et al., 2004; Computation of various insolation quantities after Laskar et al., 2004: <http://www.imcce.fr/Equipes/ASD/insola/earth/online/>). The amount of insolation (usually given in Watts per m^2 ; $W m^{-2}$) is thus the result of the corresponding orbital constellation at a given time. The variations in insolation in terms of heat influx are of significant importance in the controlling of moisture availability in East Africa via the monsoonal circulation and the ITCZ. These 19–23 kyr orbitally-paced fluctuations in insolation (Kutzbach and Street-Perrott, 1985), have a great impact on moisture availability in the tropics and therefore are a major control on long-term environmental change in East Africa (Trauth et al., 2003; Gasse et al., 2008). It has been established that for the tropics precession is the most important driver of long-term climatic change, modulated by eccentricity. But the variations in obliquity predominantly impact on higher latitudes (Gasse, 2000; Barker, et al., 2004; Partridge, et al., 2004; Maslin and Christensen, 2007). The concept of half-precession cycles and their impact on the insolation-forced intertropical and equatorial climate has been suggested by Berger (1978) and Berger and Loutre (1997) and later by Trauth et al. (2003), outlining that in consequence of the geometry of the orbital precession, maximal summer

insolation follows the 19–23 kyr precessional cycles in North- and South Africa in anti-phase respectively. Whereas the equator, experiences moisture increase in a 10–11 kyr periodicity, which is accordingly half of the full precession cycle time. Along the equator increased insolation occurs then in March and September (see also chapter 3.6.1 and Fig. 3.7). Berger et al. (2006) suggest this equatorial double maximum in irradiation to produce 11-ka periods and 5.5-ka periods that are related to precession. For the late Quaternary, precession controls majorly the insolation influx in the tropics and thus plays an important role, but it is crucial to bear in mind that the amplitude of these precession cycles is controlled by variations in eccentricity (see also chapter IV; Trauth, 2003; Junginger and Trauth, 2013).

The concept of changes in solar irradiation being responsible for climatic shifts on decadal to millennial timescales is still not completely understood, but there seems to be a correlation in changes in moisture availability and perturbations in solar irradiation (Neff et al., 2001; Gupta et al., 2005; Junginger et al., 2014; Chapter III). Variations in the solar activity, measured in sunspots (Solanki et al., 2004), is hypothesised to have caused or at least contributed to significant precipitation changes in Oman (Neff et al., 2001), tropical Africa (Stager et al., 2002; Junginger et al., 2014) and Southeast Asia (Wang et al., 2005) via the weakening of summer monsoon winds, particularly during the Holocene. Bond et al., 1991 suggests solar irradiation variations are a possible triggering mechanism behind the North Atlantic cooling events (H-events), that latter expressed in East African drought conditions (chapter III).

Feedback mechanisms: Feedback mechanisms (Fig. 1.15) can amplify (positive feedback; anomaly) or buffer (negative feedback) climate forcing, and may therefore interfere with the direct cause-and-effect relationship between forcing factor and climatic response (Bradley, 1999; Maslin and Christensen, 2007; Chapter IV) that is often inferred from simplified models. In fact, all components of the climatic system are coupled, so that the entire system could be affected by changes in one of the subsystems (Bradley, 1999). An example of this is the orbital forced precession cycle, which would be expected to follow a gradual, linear increase in precipitation. Instead, abrupt climatic fluctuations have been documented through time that indicate the amplification of the onset of a linear paced wet phase by a strong feedback mechanism, as suggested for example for the case of the onset of the AHP (Charney and Stone, 1975; Claussen et al., 1999; Kutzbach and Liu, 1997; deMenocal et al., 2000). While Charney and Stone (1975) and Claussen et al. (1999) propose that the onset of humid conditions could have been amplified by vegetation cover via the change in the surface albedo, DeMenocal et al. (2000) argues that besides this vegetation-albedo feedback there must have been a coupled mechanisms with ocean temperature feedbacks to have driven the non-linear climate transition. Feedbacks can be found on any scale as indicated in Figure 1.15, e.g. Ice-albedo feedbacks play an important role for glacial-interglacial transitions and another currently heatedly discussed example are feedbacks in the carbon cycle, triggered by anthropogenic CO_2 releases (Bradley, 1999).

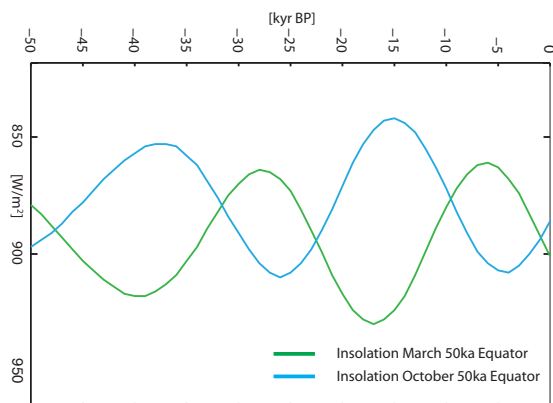


Figure 1.17 | Insolation variations (in Watts/m²) at the equator for the last 50 ka BP (given in negative kilo years for the past, 0=1950) according to the computation of insolation quantities by Laskar (2004) showing equatorial spring and fall insolation in anti-phase.

1.4.2 Hypotheses on Environment-Evolution linkages

The question which climatic scenario and environmental setting might have spurred human evolution has been controversially discussed in the past, and very different underlying triggers have been suggested (Potts, 1998; Trauth et al., 2010 and references therein; Donges, et al., 2011). There is a general consensus that *Homo sp.* evolved in Africa as numerous archaeological and hominid fossil sites in South Africa, East and Northeast Africa bear proof of the existence and intra-African movements of the antecedents of *Homo sapiens* such as the *Homo erectus*, *Homo habilis* and *Homo ergaster* and going further back in the family tree of hominin evolution, numerous finds of the genus *Australopithecus sp.* and *Ardipithecus sp.* show the broad existence and dispersal along Eastern and southern Africa through time (McBrearty and Brooks, 2000; National Research Council, 2010). The term 'Cradle of humankind' is therefore difficult to be regionally claimed and is largely a matter of definition. However, rich evidence points at East Africa as the source region of modern man (as the last steps of human evolution) implied by fossil finds (e.g. White et al., 2003) and also mitochondrial DNA reconstructions (Campbell and Tishkoff, 2010). The latter show a family tree of modern man that most likely roots in East Africa with the oldest common ancestor at about ~200 ka BP (e.g. Stringer, 2003; Tishkoff and Verrelli, 2003; Campbell and Tishkoff, 2010; Fu et al., 2013).

The discussion around the topic environment-evolution linkages seems to have as many answers as there are opinions, though most hypotheses are based somewhat on the assumption that climate, environmental change and evolution are causally linked. It is common knowledge that evolution is controlled by several mechanisms including speciation and selection, whereas natural selection is driven by environmental factors. But which are these? Though, again, there are equally many theories concerning the where (e.g. Multi-regional hypothesis), when (dating of fossils) and especially the conditions that triggered the emergence of modern man: Was it dry? Was it wet? Was it the high variability? These issues should not be neglected when discussing the variable environment in East Africa, and its implications for humans on various timescales.

Already Darwin hypothesised was aware of the role of the environment in the emergence of Bipedality (1871). The *Savanna Hypothesis* by Raimond Dart (1925, 1953) is largely based on the assumption that the shift towards a drier environment, between forest and African dry savannah in Mio-Pliocene, gave a crucial evolutionary

push. Other approaches, such as the *Aquatic Ape Hypothesis*, brought forward by Alistair Hardy (1977) and of all Elaine Morgan (1977) see the adaptation to an aquatic-determined habitat as a main driver, but these have been largely discarded today, mostly because of the single causality of a water dominant habitat as the trigger to have promoted the evolution of bipedalism is too weak. The *Aridity Hypothesis* (Peter deMenocal, 1995, 2004) instead emphasises the role of arid conditions in Africa with the intensification of high-latitude glacial cycles, based on the Sahara dust record by deMenocal. According to this record, the emergence of the genus *Homo* as well the earliest stone tools coincide with the major shift to arid conditions around 2.8 Ma, 1.7 Ma and 1.0 Ma (deMenocal, 2004). Also, the *Turnover Pulse Hypothesis* by Elisabeth Vrba (1985) sees human evolutionary changes occurring when climate shifted to a new state. Though first concentrated on the study of the smooth gradual faunal species change with the increasingly arid conditions around 2.5 Ma, this theory was later on applied to hominin evolution. Vrba proposed that the speciation of mammalian faunas from forest gazelles to foremost savannah grazer species types, such as bovids, was correlated with a major climatic shift and suggested that this transition would consequently have altered hominin interactions with mammals (Ruddiman, 2008).

The *Bottleneck Hypothesis* assumes that the population must have been reduced to 10,000 individuals or less in one (in East Africa) or multiple refugia (over Africa) with < 4,300 in each (Lahr and Foley, 1998) to account for the degree of genetic similarity that has been identified by genetic studies (e.g. Campbell and Tishkoff, 2003). A population bottleneck is caused by the dramatic change in living conditions, which leads to the reduction in population size such as during the LGM as suggested by Fu et al., (2013), or by climatic change induced by the 'volcanic winter', as proposed by Ambrose (1998). Brandt et al. (2012) assume the SW Ethiopian Highlands to have been an area highly likely to have served for such bottleneck populations as refugia and source for population radiation during times of climatic aggravation.

The *Variability Selection Hypothesis* by Rick Potts (1998) suggests that not one state or the other, but the extreme and inconsistent variability in climate conditions during longer intervals, had a decisive impact on evolutionary processes that eventually lead to the origin of *Homo sapiens* by enhancing the adaptive variability. This approach was later revisited and modified by Maslin and Christensen (2007) and then termed the *Pulsed Climate Variability Hypothesis* (Trauth et al., 2010) as

it takes the pronounced wet pulses, driven by precessional insolation variations into account. Lately the *Hypothesis of amplifier lakes* came up (Trauth et al., 2010), that represents a further specification of the last two hypothesis, as it also comprises the concept of a highly variable, diverse and changing environment as a motor for evolution, but extends the concept to include the particularities of the EARS with its amplifier lakes (Olaka et al., 2010), natural selection within such an environment and considers the role of speciation in this highly diverse setting. This discussion on potentially involved mechanisms and the most likely environmental setting that has correlated with major evolutionary shifts is taken on and intensified on the base of concrete examples on different timescales in Chapter IV.

1.4.3 Hypotheses on Environment-Migration linkages

Though genetic (mtDNA) and fossil evidence points to East Africa as the source region of modern man and therefore supports the *Out of Africa II* or *Black Eve theory* (Ambrose, 1998), there are various different schools of thought on when and how the *Homo sp.* migrated out of Africa (OOA*). The theory that seems to have found most supporters is modern humans (*Homo sapiens*) evolved out of Africa and then migrated to various parts of the world (Ambrose, 1998; Stringer, 2003; Oppenheimer, 2009; Armitage et al., 2011). The one model proposing different OOA events argues for different periods of migration with each leading to radiation of a different *Homo sp.* The theory which argues for one major OOA event suggests that modern humans moved out of Eastern Africa (probably somewhere in Ethiopia) at ca. ~100–60 ka BP along several possible dispersal corridors (for instance the strait of Bab el Mandeb and the Nile valley (Brandt et al., 2012) into Europe (~40 ka BP) and into East Asia (~70 ka BP) via the middle east and eventually into Australia (~50 ka BP) and to both Americas (Oppenheimer, 2009; Mellars, 2011). To understand and date the way from the African source region to Europe is the central theme of the CRC 806.

A critical point is the environmental condition that prevailed during the expansion OOA or even during migration within Africa. While unfavourable environmental conditions (usually associated with pronounced arid intervals in Africa) are suggested to have pushed early humans to escape their unsuitable habitat (deMenocal, 1995, Carto et al., 2009), the other side however, questions how humans might have crossed the harsh conditions in the drought scenario in the Sahara. It is suggested that pulses of wetter conditions (induced by a general wetter climate as for instance during the

Eemian) were necessary to allow a crossing of the otherwise ecologically critical zone in large parts of the Northeast Africa (Castañeda et al., 2009). The survival of populations in the Sahara desert must have therefore been highly dependent on the availability of enough moisture to provide food and energy for the migration of a population large enough to migrate through the Sahara and out of Africa. The concept of corridors of early human migration has been adapted by the CRC 806 (e.g. Richter et al., 2012a) and is recently intensified in terms of investigating possible bridges and barriers and as a feature that is channelling mobility. Migration within East Africa towards and out of retreat areas in the highlands around lake margins and rivers might have been also pushed partly by climatic change, though a broad set of other determinants needs to be taken into account to avoid the artificial construction of causalities (Basell, 2008; chapter V this thesis).

*The term 'Out of Africa' might be misleading as it falsely implies rather an exodus than an expansion or dispersal of the population beyond the African continent. However, this expression will be used as it has become an established constituent in the terminology.

1.4.4 Socio-cultural component of mobility

Human-environment interactions are not only difficult to understand and even more difficult to reconstruct, due to the complex climatic system (as shown above) which is a major aspect of this interplay. The interrelationship is so complex because causality is often inferred between climatic change and human reaction (evolution, migration, adaptation), although it is not a simple cause-and effect relationship (Widlok et al., 2012) as often portrayed by natural scientists.

The term 'human agency', though operating only within certain natural boundaries, may suggest that human mobility is not entirely determined by climatic change but decidedly influenced by a broad set of anthropogenic factors. In fact, empirical studies on mobility patterns of hunter-gatherers responses to environmental change demonstrate that a broad range of factors plays an important role in decision making. Among these are forms of aversion (conflicts, risks) and attraction (resources of food, water, social relations). Additionally, mobility itself is just one of several possible responses to environmental change, with alternative forms being changes in social networks, diet change or reproductive control as Widlok et al. (2012) conclude. Hence, human decision making within certain limitations involves social aspects such as cultural elements and traditions as well as possible conflicts and personal relationships (Dobres and Robb, 2000).



Chapter II

Climatic change recorded in the sediments of the Chew Bahir basin, southern Ethiopia, during the last 45,000 years

Verena Foerster, Annett Junginger, Oliver Langkamp, Tsige Gebru, Asfawossen Asrat, Mohammed Umer, Henry Lamb, Volker Wennrich, Janet Rethemeyer, Norbert Nowaczyk, Martin H. Trauth, Frank Schaebitz

Quaternary International 274, 25–37, 2012.

Special Issue

*‘Temporal and spatial corridors of *Homo sapiens sapiens* population dynamics during the Late Pleistocene and Early Holocene’*

Climatic change recorded in the sediments of the Chew Bahir basin, southern Ethiopia, during the last 45,000 years

Foerster, V.^{a*}, Junginger, A.^b, Langkamp, O.^a, Gebru, T.^a, Asrat, A.^c, Umer, M.[†], Lamb, H.^d, Wennrich, V.^e, Rethemeyer, J.^e, Nowaczyk, N.^f, Trauth, M.H.^b, Schäbitz, F.^a

^a University of Cologne, Seminar for Geography and Education; Gronewaldstrasse 2; 50931 Cologne; Germany

^b University of Potsdam, Institute of Earth and Environmental Science; Germany

^c Addis Ababa University, Department of Earth Sciences; P. O. Box 1176, Addis Ababa, Ethiopia

^d Aberystwyth University, Institute of Geography and Earth Sciences, Aberystwyth SY23 3DB, U.K.

^e University of Cologne, Institute of Geology and Mineralogy; Zùlpicher Str. 49A; 50674 Cologne; Germany

^f Helmholtz-Zentrum Potsdam, Deutsches GeoForschungsZentrum – GFZ, 14473 Potsdam; Germany

* corresponding author

† deceased

Abstract

East African paleoenvironments are highly variable, marked by extreme fluctuations in moisture availability, which has far-reaching implications for the origin, evolution and dispersal of *Homo sapiens* in and beyond the region. This paper presents results from a pilot core from the Chew Bahir basin in southern Ethiopia that records the climatic history of the past 45 ka, with emphasis on the African Humid Period (AHP, ~15–5 ka calBP). Geochemical, physical and biological indicators show that Chew Bahir responded to climatic fluctuations on millennial to centennial time-scales, and to the precessional cycle, since the Last Glacial Maximum. Potassium content of the sediment appears to be a reliable proxy for aridity, showing that Chew Bahir reacted to the insolation-controlled humidity increase of the AHP with a remarkably abrupt onset and a gradual termination, framing a sharply defined arid phase (~12.8–11.6 ka cal BP) corresponding to the Younger Dryas chronozone. The Chew Bahir record correlates well with low- and high-latitude paleoclimate records, demonstrating that the site responded to regional and global climate changes.

Keywords: Ethiopia, Chew Bahir, climatic fluctuations, human migration, African Humid Period, Younger Dryas, potassium

2.1 Introduction

Numerous hypotheses claim that there is a link between climate change and human evolution, since climate change provides the necessary environmental pressure for natural selection and population expansion. Various ideas have been put forward about the causes of evolutionary change in the source region of anatomically modern humans (AMH), including climatic variability causing resource stress (Potts, 1998), and adaptation to a gradual shift to a drier environment (Vrba, 1985). Current evidence points to East Africa as the origin of modern humans and thus supports the Out of Africa II or Mitochondrial Eve theory (Stringer, 2003). Much paleontological and paleoanthropological research is focused on the Ethiopian Rift and the Afar, because the oldest known *Homo sapiens* fossils, dated ~200 ka were found in the Lower Omo Valley (McDougall et al., 2005; Carto et al., 2009), and at Herto, in the Afar (White et al., 2003).

Current debate concerns whether the shift towards hyper-arid climate conditions during Heinrich event 9 (H9; 105 ka), resulting in limited resources and water availability, compelled AMH to expand beyond Africa. Environmental changes linked to orbitally-driven dry-wet alternations are thought to have favored evolutionary innovation (Behrensmeier, 2006; Trauth et al., 2010), and forced the expansion of *H. sapiens* into SW Asia in several intervals at around 100 ka (Ambrose, 1998; Oppenheimer, 2009; Armitage et al., 2011). Whether dry conditions were the driving factor (Carto et al., 2009), plus lowered sea level opening a corridor into SW Asia, or whether it was the onset of wet conditions between ~120 and 110 ka that allowed dispersal into the Arabian coastal desert (Castañeda et al., 2009), is much debated. To understand the cause – effect relationships among climate, environment and human evolution in East Africa, it is of key importance

to reconstruct the timing and mechanisms of past environmental changes.

The magnitude, timing, spatial expression and causes of wet-dry cycles in East Africa are not well understood. The most recent of these wet episodes, the African Humid Period (AHP, ~15–5 ka), demonstrates the central problem of contradictory data about the timing of these phases (deMenocal et al., 2000; Kröpelin et al., 2008). Using marine records from the northwest African coast, deMenocal et al. (2000) claim an abrupt onset and termination of the AHP, whereas Kröpelin et al. (2008) found a gradual climatic transition at the end of the AHP recorded in lacustrine sediments in the Sahara desert. Each scenario has rather different implications about the pace of human expansion through green corridors of the Sahara. The magnitude of these climate shifts is also important, determining whether

they would have allowed relatively moist refugia during dry intervals. The southwestern Ethiopian highlands and the adjacent Chew Bahir and Turkana basins might have formed refugia for human populations during past arid phases (Ambrose, 1998; Hildebrand et al., 2010; Joordens et al., 2011), hosting small but culturally diverse populations of hunter-gatherers, and favoring the development of new food-gathering technologies and cultural skills. If wet phases like the AHP did not occur synchronously in various locations, they could have created refugia for humans and other biota, thus having a major influence on the spatial distribution, size, and movement of human populations. Chew Bahir lies in a possible migration corridor between retreat areas and therefore represents an ideal natural laboratory to study environmental history in the source region of modern humans.

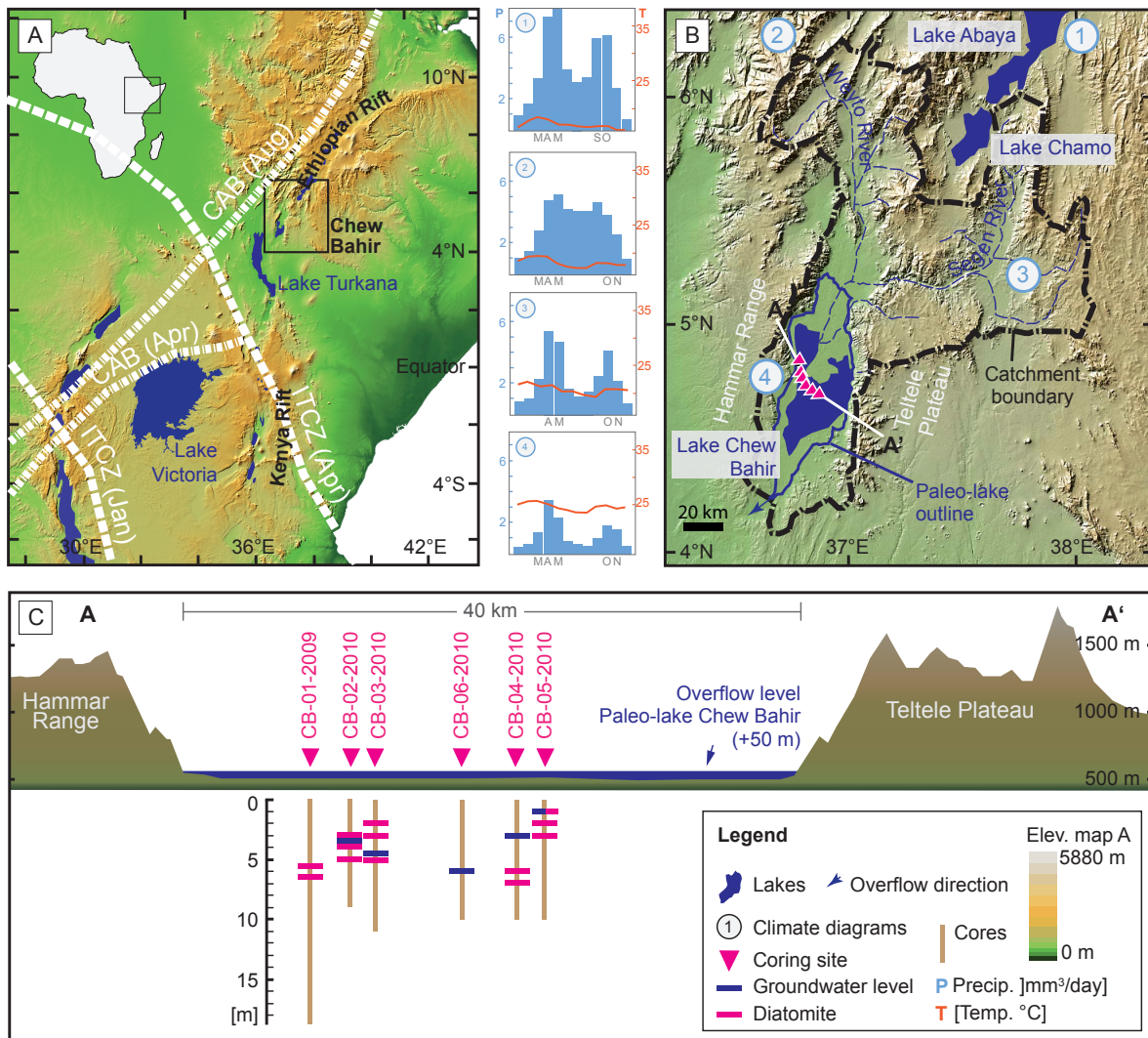


Figure 2.1 | Setting of the Chew Bahir basin. (A) Chew Bahir basin within the East African Rift System with major climatic influences. Dotted lines indicate the position of the ITCZ (Intertropical Convergence Zone) and CAB (Congo Air Boundary) during different times of the year (after Tierney et al., 2011). (B) Map of the Chew Bahir catchment with major rivers, paleo-lake outline and sites mentioned in the text. Numbers refer to available precipitation and temperature data summarized in climate diagrams between A and B (data: <http://iridl.ldeo.columbia.edu/maproom/> – accessed 12.07.2011). A–A' cross-section along the core transect is provided in (C): Six sediment cores were recovered from a W–E transect through the Chew Bahir basin. Results of the pilot CB-01-2009 core discussed in this study provide paleo-climatic information for the past 45,000 years.

This paper presents results from analysis of a pilot lacustrine sediment core obtained from the Chew Bahir basin in southern Ethiopia (Fig. 2.1). The core covers paleoenvironmental changes of the past 45 ka years. The data provide valuable insights into the timing, magnitude, synchronicity and internal variability of the most recent, and hence best-studied wet episode, the AHP. This new record of climate change will provide a basis for better understanding the complex interplay between paleoenvironmental changes and the evolution and the dispersal of our ancestors.

2.2 Setting

2.2.1 Geological overview

The Chew Bahir basin lies in a 300 km wide rift zone, between the Omo-Turkana basin to the west and the southern sector of the Main Ethiopian Rift (MER) to the east (Fig. 2.1a). The MER splits into two branches south of the Lake Abaya-Chamo basin, separated by the Amaro horst. The eastern branch forms the southernmost sector of the MER. In the western sector, rift faulting dies out at the southern shore of Lake Chamo close to the Konso uplands, but resumes farther west in the Chew Bahir basin. The Chew Bahir basin extends south to the Kenyan Rift and forms the northernmost part of the broadly rifted zone that was formed when rifting migrated eastward along pre-rift structures of the Anza Rift (Ebinger et al., 2000; Corti, 2009).

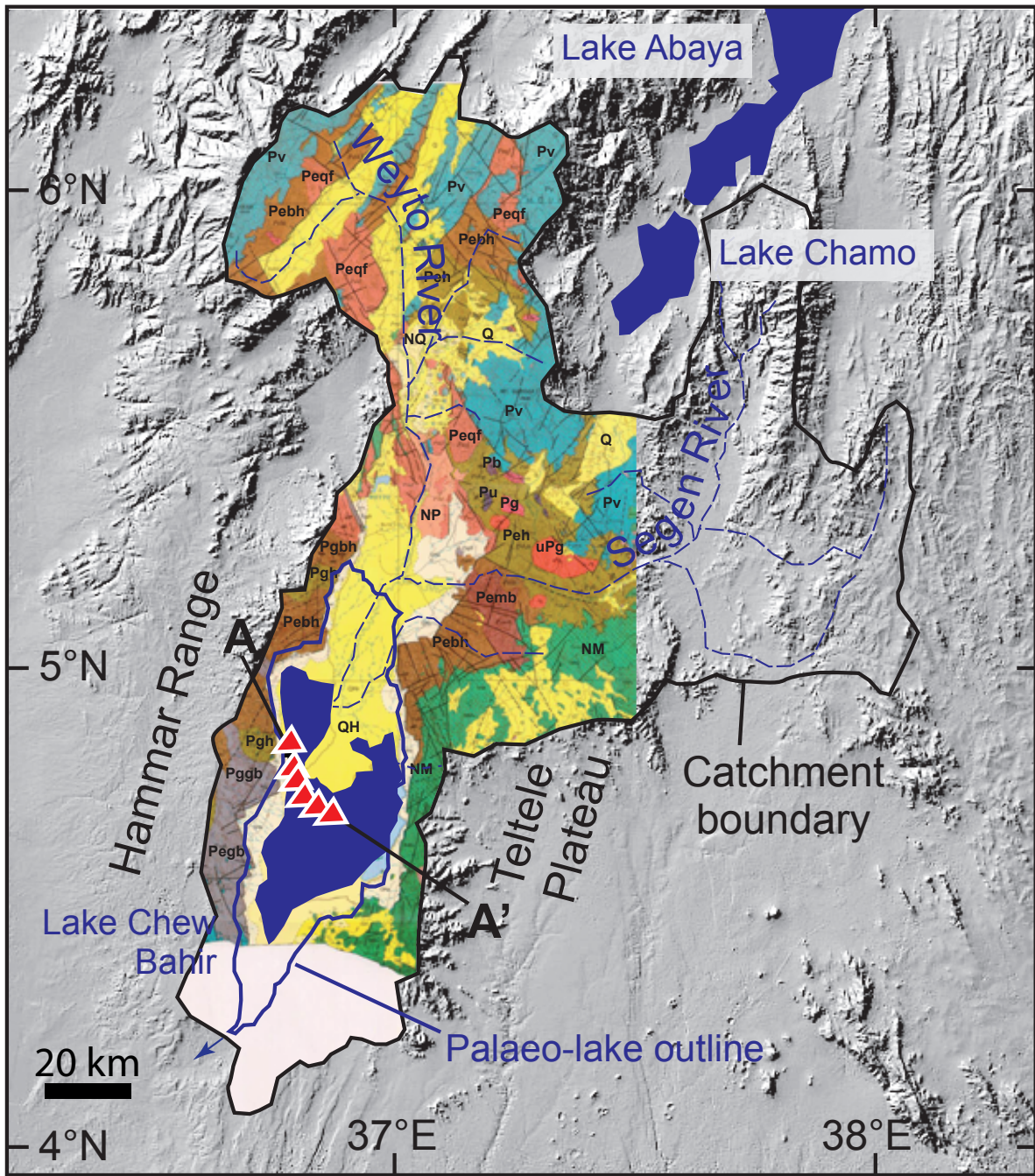
The western boundary of Chew Bahir basin, the Hammar range, consists of Precambrian basement with mainly undivided gneisses („Pebh“ and „Pegh“ in Fig. 2.2). This comprises feldspar-biotite-muscovite and hornblende gneisses dominating the Hammar range geology, migmatitic in part, with minor metasedimentary gneiss (Pegb), quartzo-feldspathic gneiss, amphibolite and granitoid orthogneiss, layered biotite-quartz-feldspar gneiss, locally with muscovite, garnet, sillimanite, minor interlayered amphibolitic quartzose inclusions (Davidson, 1983). In addition, Precambrian layered mafic gneiss (Pegh) and amphibolite or equivalent granulite facies (Pgh) occur in the Hammar range as well as north of the basin.

The higher eastern boundary of the Chew Bahir basin, the escarpment of the Teltele-Konso range, exposes Miocene basalts and trachytic centers (unit „NM“ in Fig. 2.2). Miocene basaltic lava flows with subordinate rhyolite-trachyte and felsic tuff intercalations prevail in the eastern part of the catchment. Oligocene basalt flows with subordinate rhyolites, trachytes, tuffs and ignimbrites (unit „Pv“ in Fig. 2.2) cover the Precambrian basement units in the northeastern, northern and northwestern parts of the catchment (Figs. 2.1b and 2.2;

Moore and Davidson, 1978; Davidson et al., 1983). The tectonically-formed basin provides a sedimentary archive that extends beyond the Quaternary as the basin emerged during older phases of rifting. The total sediment infill of the basin is ~5 km thick, according to airborne gravity and seismic reflection data (Asrat et al., 2009). A detailed spatial and temporal quantification of uplift and denudation along the Hammar and Teltele ranges adjoining the Chew Bahir basin showed that rifting has been continuous since its initiation in the Miocene, while Plio-Pleistocene rifting and uplift was not significant in this part of the East African Rift (Ebinger et al., 2000; Pik et al., 2008). It was further suggested that direct evidence of denudation is inconsistent with the hypothesis that massive Plio-Pleistocene rifting and associated uplift occurred in this part of the East African Rift and could have triggered recent aridification. Other studies (e.g., Ebinger et al., 2000) also suggested similar ages and processes of rifting for this basin. In short, recent tectonic uplift had little influence on the short-term climatic variations.

Today, Chew Bahir is a 30 x 70 km saline mudflat that episodically fills to a shallow lake during the rainy season, with water and sediment input by the perennial Weyto and Segen rivers, which have a ~2000 km² catchment (Fig. 2.1b; 4.1–6.3 °N; 36.5–38.1 °E; Davidson, 1983). Their influence is now limited to the northern part of the basin, where the rivers have formed a delta. Secondary, contributions to the sediment influx are alluvial fans draining from the Hammar Range to the west and the Teltele Plateau to the east. Small drainage networks at the border faults, and the strong rainfall seasonality, make sediment and water influx highly episodic, because runoff is mainly from intense rainfall events in the wet seasons, and from occasional orographic rainstorms.

Eolian input, mainly of silt, may be important, especially during dry periods, and can be regarded as a fourth sediment source. Eolian activity may also cause erosion and thus hiatuses in the sedimentary record. Winds transport material from surrounding regions, and redeposit silts within the Chew Bahir basin itself. Minor sources of sediment are volcanic materials, deposited either as pyroclastic airfall deposits, or as reworked tephra. No volcanic centers are exposed within the Chew Bahir basin. Tephrochronological correlations between the Indian Ocean, the Middle Awash and the Omo-Turkana basin represent explosive volcanic events that affected the entire region. Five dated marker tuffs are of interest, especially the Konso Silver Tuff dated to 154±7 ka, which lies within the timeframe of *Homo sapiens* presence in the area (Clark et al., 2003; Brown and Fuller, 2008; Asrat et al., 2009).



Legend

- Q; QH; NQ Holocene (QH), Plio-Pleistocene (NQ) and Pleistocene-Holocene (Q) undivided fluvialite, alluvial, and lacustrine sediments
- QH_i Holocene (QH_i)
- NP Pliocene undivided sediments
- NM Miocene basalt, rhyolite, trachyte, phonolithe, ignimbrite
- Pv Oligocene basalt, rhyolite, trachyte, tuff, ignimbrite
- uPg Late precambrian post-tectonic granite, granodiorite, minor syenite
- Pggb; Pegb Precambrian granulite facies (Pggb) or metasedimentary gneiss (Pegb): layered biotite-quartz-feldspar gneiss, locally with muscovite, garnet, sillimanite, minor interlayered amphibolitic quartzose, pyritic, graphitic, and calc-silicate gneisses, and marble
- Peh; Pgh Precambrian (Pegh) layered mafic gneiss, and amphibolite or equivalent granulite facies (Pgh) including two-pyroxene granulite
- Pebh; Pegh Precambrian undivided gneiss (Pebh): includes predominantly biotite and hornblende gneiss, migmatitic in part, with minor metasedimentary gneiss, quartzo-feldspathic gneiss, amphibolite and granitoid orthogneiss or equivalent Granulite facies (Pegh) including hyperstene-bearing rocks
- Peqf; Pyqf Precambrian leucocratic biotite-quartz-feldspar gneiss (Peqf) or equivalent granulite facies (Pyqf) including magnetite-quartz-feldspar granulite
- Pemb Precambrian muscovite-biotite granitoid gneiss and migmatite
- Pg Precambrian syn-tectonic granite, granodiorite, minor syenite
- Pb; Pu Precambrian gabbro (Pb) and periodotite, bronzitite, minor dunite, associated layered norite and gabbro, secondary diorite, serpentinite and talc schist (Pu)

Figure 2.2 | Present available geological information for the catchment of the Chew Bahir basin provided by the Omo River Project (Davidson, 1983).

2.2.2 Present-day climate

The climate of East Africa is characterized by strong rainfall seasonality, which results from the annual migration of the Intertropical Convergence Zone (ITCZ) between 10° North and South, following the zenithal position of the sun (Fig. 2.1a; Nicholson, 1996). Because of this migration, bimodal rains dominate the northeast – the „Belg“ rains from March to May, and the longer „Kiremet“ rains from June to September. In the highlands northwest of Chew Bahir, rainfall is unimodal with one wet season from March to November (Fig. 2.1b; Segele and Lamb, 2005; Williams and Funk, 2011). Chew Bahir lies in a transition zone between the influences of tropical equatorial and summer monsoonal climates, and between two major systems that bring precipitation from the Indian and Atlantic Oceans.

The northernmost position of the ITCZ in July–August allows a southwestern humid air stream with recycled eastern Atlantic moisture to reach parts of East Africa via the Congo basin (Fig. 2.1a; Nicholson, 1996; Camberlin, 1997). This unstable flow from the Atlantic converges with drier air from the Indian Ocean along a northeast-southwest trending convergence zone known as the Congo Air Boundary (CAB). During periods with an intensified Indian Summer Monsoon (ISM), the CAB is thought to bring wet spells even farther east to equatorial East Africa in July and August (Camberlin, 1997; Okoola, 1999; Junginger, 2011). Camberlin (1997) showed that an anomalous deep low over western India enhances the east-west pressure gradient between Africa and India, which results in increased westerly winds from the Congo basin causing the CAB to shift even further eastwards. Thus, the CAB plays a major role in inter-annual moisture variability (Camberlin and Philippon, 2002). Other mechanisms responsible for inter-annual variability are linked to sea surface temperature (SST) anomalies such as the Indian Ocean Dipole (IOD) and El Niño/Southern Oscillation (ENSO) (Diro et al., 2010).

Due to the marked topography of the southern side of the Ethiopian dome, the local climate varies significantly with elevation. A pronounced precipitation, temperature and evaporation gradient lies between the higher areas in the north and the lower basin in the south as well as between the rift valley and the adjacent plateaus. This results in a variety of microclimates, with high rainfall on the cooler highlands draining into the hotter and drier lowlands. The combination of climatology and closed basin morphology allows Chew Bahir to be classified as an amplifier lake, characteristic of the eastern branch of the African Rift (Olaka et al., 2010; Trauth et al., 2010). Those lakes are known to react highly sensitively to

even moderate climate changes and thus are potent sites for climate reconstruction.

2.2.3 Long-term controls on East African climate

Long-term variations of climate are controlled by Milankovitch precessional cycles (19–23 ka), regulating moisture availability in East Africa (Kutzbach and Street-Perrott, 1985); orbitally-forced radiation maxima coincide with increased humidity (Trauth et al., 2003). The most recent of these orbitally controlled dry-wet cycles included the African Humid Period (AHP; ~15–5 ka), which affected large parts of East Africa, as shown by elevated lake-levels at numerous sites (Barker et al., 2004). However, these lacustrine climatic records also show that climate does not respond linearly to precessional insolation change. The transitions are often characterized by an abruptness that can be explained by mechanisms such as climate-biosphere feedbacks functioning as strong amplifiers of basically moderate trends (Renssen et al., 2006; Castañeda et al., 2009). Apart from orbitally-forced variability, centennial-scale variations such as Dansgaard-Oeschger cycles, Heinrich events and the Younger Dryas (YD) have also influenced low-latitude climate, although the sign, magnitude and phasing of their impact is debated (Partridge et al., 2004; Brown et al., 2007; Carto et al., 2009; Chase et al., 2011; Stager et al., 2011). Furthermore, Atlantic and Indian Ocean SST changes, related to the thermohaline circulation, are considered to have a strong influence on African climate (Gasse and Van Campo, 1994; deMenocal et al., 2000; Trauth et al., 2010).

2.3 Methods

2.3.1 Core recovery

The pilot sediment core CB-01-2009 was recovered in December 2009 from the now-dry western margin of the Chew Bahir basin (N 04°50'6; E 36°46'8) close to the distal margin of the Weyto-Segen delta, and near an alluvial fan extending eastwards from the Hammar range (Fig. 2.1b, c). A rotary single tube drill provided by Addis Geosystems Ltd was used for the entire core. The sediment record covers the uppermost 18.86 m of the deposits with a recovery rate of 81 %. Coring consisted of 19 drives without overlap. In addition, five short cores (9–11 m length) were drilled with a vibro-corer along a NW-SE transect across the basin (Fig. 2.1b, c) during a second field campaign in November 2010 and are currently under investigation.

2.3.2 Chronology

Age control is provided by six AMS radiocarbon ages (Table 2.1). One organic bulk sample was taken in the

field and sent to Beta Analytic Inc. in Florida for dating. Five dates were obtained from picked shells and shell fragments of *M. tuberculata*, which were pre-treated and converted to AMS graphite cathodes at Cologne (Rethemeyer et al., in press; Wacker et al., submitted) and measured with the MICADAS AMS at ETH Zürich. The conventional ages were calibrated using the OxCal v4.1.7 calibration software (Bronk Ramsey, 2010; calibration curve: IntCal09, Reimer et al., 2009). To date, no information about a possible reservoir effect on the ages of the carbonate material is available.

2.3.3 Sedimentological investigations

Core sections were split lengthwise, and the archive halves wrapped in clingfilm to prevent desiccation, and stored in a dark cold storage room. Magnetic susceptibility (MS) was logged to detect variations in grain size, in the flux of magnetic mineral particles from soils and rocks, and volcanic ash layers. Magnetic susceptibility was obtained every 1 mm using a 2nd generation split-core logger (scl-2.3) designed at the Helmholtz Centre Potsdam GFZ. Magnetic susceptibility was measured with a Bartington MS2E spot-reading sensor attached to a MS2 control unit. Element content of the sediment core was determined by X-ray fluorescence (XRF) with an Itrax[®] core scanner using a Molybdenum (Mo) tube as radiation source. The prepared core halves were scanned at 0.5 cm resolution and a tube voltage of 30 kV, current of 30 mA and scanning time of 20 seconds.

After the non-destructive measurements, the working half was subsampled at 2 cm intervals. To avoid contamination, 0.5 cm of the core surface was first ground for mineral, carbon and nitrogen analysis. Sediment color was defined using a Munsell soil color chart. Grainsize and composition was determined by a semi quantitative finger-test, differentiating crudely between finer and coarser material in five increments (clay, silty clay, silt, sandy silt, sandy gravel; simplified in Fig. 2.3). Also the mineral content was determined semi quantitatively, by X-ray diffraction (XRD) analysis of finely

ground bulk samples, without further treatment or adding a standard indicator, using a Siemens D5000 diffractometer and EVA for phase identification.

The biogeochemical indicators Total Nitrogen (TN) and Total Carbon (TC) have been analyzed along the core in a ~32 cm resolution. TC has been differentiated into Total Inorganic Carbon (TIC) and Total Organic Carbon (TOC) and TOC/TN ratios have been calculated to distinguish between terrestrial and aquatic carbon sources. However, with very low TN values (ranging from 0.01 to 0.04 wt%) as well as a low TOC content (variations between 0.1 and 0.3 wt%), neither the values nor the variability of the ratios are significant enough and are therefore excluded from further discussion (Meyers, 2003).

Smear slide analyses were conducted on the non-ground half of subsamples along the entire core at ~30 cm intervals and in selected sections at higher resolution to gain initial insight about sediment composition and possible biological indicators, such as pollen, diatoms, ostracods and charcoal. For diatom identification, selected samples were treated with KOH and examined under an electron microscope. For semi-quantitative analyses following the principles of Gasse (1986), light microscopy was used, complemented with a polarizer.

2.4 Results

2.4.1 Core description

The pilot core CB-01-2009 was drilled to 18.86 m depth without replicate coring so that due to a 19 % core loss the recovered material comprises 15.36 m in total. Five gaps interrupt the profile (Fig. 2.3; G1–G5), because of unconsolidated sediments (G1) and material that was not completely recovered (mostly sand) or lost due to technical limits (G2–G5). The topmost section (G1; 0–130 cm) of the core has been subjected to soil formation expressed in unconsolidated sediment. The hiatuses as well as the unconsolidated section were unavailable for continuous geophysical and chemical

Lab-Nr.	Depth [cm]	Radiocarbon age [yrs BP]	Calibrated age [cal yrs BP]	2-sigma Probability	Material	$\delta^{13}\text{C}$ [‰]	^{14}C conc. [pMC]	Pretreatment
Col 1093.1.1	153	1236 ± 27	1133 ± 60	56.10%	M	-1.4 ± 0.0	85.47	H ₂ SO ₄
Col 1094.1.2	299	3077 ± 27	3301 ± 70	92.80%	M	1.7 ± 0.0	68.18	H ₂ SO ₄
Beta 271307	735	11790 ± 60	13625 ± 150	95.40%	B	-22.6	N.N.	acid washes
Col 1095.1.1	976	31085 ± 185	35674 ± 630	95.40%	M	0.8 ± 0.0	2.09	H ₂ SO ₄
Col 1096.1.2*	1278	35508 ± 581	40473 ± 1280	95.40%	M	10.1 ± 0.1	1.20	H ₂ SO ₄
Col 1097.1.1	1746	40293 ± 545	44188 ± 920	95.40%	M	-0.9 ± 0.0	0.66	H ₂ SO ₄

(*) The sample was measured only one time in the AMS. M - Mollusc shells, B - Bulk.

Table 2.1 | Radiocarbon data from the Chew Bahir sediment core CB-01-2009.

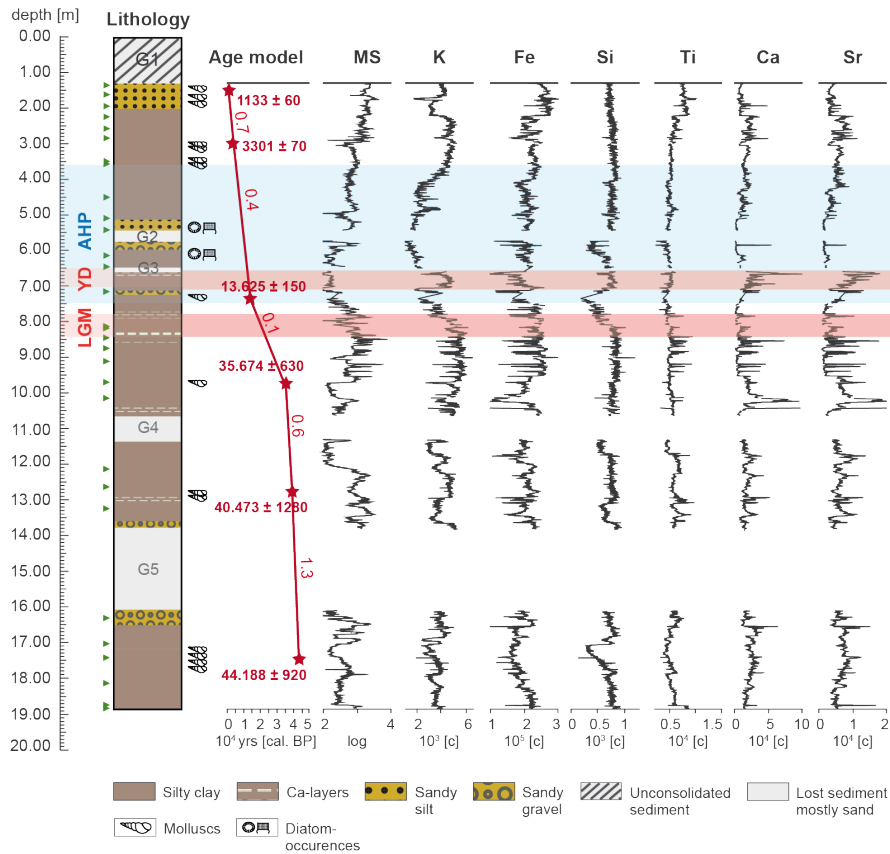


Figure 2.3 | Lithology, age-depth model and results of geochemical and physical investigations of the pilot core CB-01-2009. Numbers along the age model present sedimentation rates in mm/year. Stars – ^{14}C ages; triangles – XRD samples; MS – Magnetic Susceptibility; LGM – Last Glacial Maximum; YD – Younger Dryas; AHP – African Human Period; G1-G5 - gaps in the record due to lost/unconsolidated sediment.

measurements and therefore did not provide data. The lithology of the rest of the core comprises lacustrine un-laminated silty clays, which are intercalated with sandy layers and coarse detrital fragments. In the lowermost section, prominent carbonate layers mark parts of the lacustrine sequence. Up to six horizons with abundant gastropods *Melanoides tuberculata* occur in different matrixes from silty clay to sandy gravel.

2.4.2 Age model and sedimentation rates

The radiocarbon ages of biogenic carbonates and one bulk sediment sample (Table 2.1) are consistent with their depths, showing no reversals. Both linear model and cubic spline models were calculated from the radiocarbon ages, but these show only minor statistical deviations for the intervals of higher sedimentation rate between 150 and 300 cm and between 1280 and 1750 cm. The estimated sedimentation rate for the interval between 45 and 40 ka is relatively high with a time-averaged value of 1.3 mm/a.

After 40 ka, sedimentation rates decreased first to 0.6 mm/a (between ~40 and 35 ka) and then to only 0.1 mm/a between 35 and 13 ka. Towards the present, the sedimentation rate increases again in two steps, first

slowly with values of 0.4 mm/a between 13 to 3 ka and 0.7 mm/a between 3 and 1 ka, reaching 1.3 mm/a during the last 1,000 years (Fig. 2.3).

The mean sedimentation rate for the last 45 ka is ~0.7 mm/a. Stratigraphic changes in core sediment composition and grain size almost certainly reflect additional, short-term variations in sedimentation rate that are not apparent from interpolation between dated levels.

2.4.3 Sedimentological results

As the uppermost section has been subjected to soil formation, all scanning and logging results start at 130 cm depth (Fig. 2.3). The sediment color changes from green-gray shades at the base to brown, green-brown, gray-brown and light brown towards the top. The MS log shows generally higher values within coarser layers such as sandy silts and gravels. Some higher values in the silty clays may be attributed to non-detectable grain size variations due to the semi-quantitative method used. Higher MS fluctuations are observed between the base of the core and ~8 m depth; low values follow with lowest variability to ~6 m depth, followed by gradually increasing values, but still with very low internal variability.

Initial XRD results show that mineral assemblages vary along the core. A mixture of potassium feldspars and potassium-sodium feldspars are main constituents of the spectrum, in particular orthoclase and some sanidine, as well as plagioclase (albite and anorthite). Other mineral phases are illite, analcime, epidote, magnesiohornblende and calcite. From the smectite family, montmorillonite is present in the deposits. Quartz is also an important component of the mineral assemblage (Tab. 2.2).

2.4.4 Geochemistry

The Itrax core scanner provided the element contents for 16 elements, but only 6 of these show a clear paleoenvironmental signal (Fig. 2.3). All other elements record either a mixed signal with multiple partly anti-correlated or phase shifted signals, or their record does not differ significantly from random noise.

Potassium (K) shows marked variation with noticeably abrupt transitions. Its variance changes throughout the core, in a pattern similar to that of MS, with higher short-time amplitudes in the middle and towards the base of the core, far exceeding the amplitudes in the upper 800 cm. Mean values by contrast, show larger variations in the upper half of the core. The K content is generally higher at the middle of the core but shows from 8 m upwards a rather abrupt change to lower values, gradually returning to an elevated value level at around 4 m, while framing a pronounced short-term fluctuation between 6.50 m and 7.10 m. Iron (Fe) is high throughout the core with some marked variations between 10 and 8 m, and less extreme variations between 14 and 12 m. Abrupt transitions towards more stable conditions with less variability are apparent in the rest of the core. The Fe distribution along the record largely correlates with the K values, except the long-term mean value decrease described for the K curve between 8 and 4 m, where the Fe concentration on the contrary remains high. Silica (Si) largely follows the K curve but exhibits a generally lower variability and with gradual rather than abrupt transitions. The titanium (Ti) curve varies with a low magnitude and has generally lower amplitude short-term variations than the other elements. Calcium (Ca) values follow the macroscopically observed calcite layers and layers with greater snail abundances. Ca content varies around a constant mean, but short-term variations are present throughout the core. Highest variability occurs between 10.5–8.5 m, 7.5–6.5 m and 3–2 m. The strontium (Sr) curve parallels the Ca curve, but with generally lower values. Interestingly, most Ca and Sr peaks show distinct anti-correlations with K and Fe, particularly at 10.4 m, 10.2 m or at 8.5 m and around 7.20 m, 2.2 m and 2.85 m.

2.4.5 Biological indicators

Smear slide analyses revealed the occurrence of ostracods, charred plant remains and diatoms that are not present throughout the whole core but occur in discrete layers. The sediments do not contain detectable numbers of pollen or spores. Smear slide analyses show a gradual increase in diatom abundance towards a diatom-rich layer between ~6.20 and ~5.45 m dominated by *Aulacoseira* and *Cyclotella*, but the low absolute numbers and poor species diversity do not allow quantitative estimation of past ecologic conditions in the lake. No indicators for saline conditions were found in the core suggesting that the diatoms only occurred during freshwater episodes. Fragments and complete shells of the gastropod *Melanoides tuberculata* occur in six layers ranging from a few cm to more than 0.5 m thickness towards the base of the core. The lowermost and largest mollusc layer, from ~17.90 to 12.70 m, is followed by abundant well-preserved shells at 13.10–12.80 m and 9.80–9.75 m. At ~3.90–3.00 m and 2.00–1.52 m several single shells in a clayey matrix and dense fragmented mollusc layers have been identified.

2.5 Discussion

2.5.1 Core chronology

The age model may be rather limited with six radiocarbon dates, but the sedimentation rates were very linear with two change points and no reversals; therefore given ages might lack high precision, but are reliable. Some very striking well-studied climate events – in particular the Younger Dryas (YD) – occur exactly where they are expected to be (Figs. 2.4 and 2.5). Furthermore, this study is not attempting to determine higher frequency climate variations that would require a high-resolution age model. So, according to the age model for the core, CB-01 records climate history spanning from ~44 ka to 1.0 ka, including the Last Glacial Maximum (18–23 ka), the African Humid Period (5–15 ka) and ending with the onset of the Medieval Warm Period (700–1,000 BP / 950–1,250 AD).

Some of the metasedimentary gneisses contain minor intercalated marble units (Davidson, 1983; Fig. 2.2), and the latter could be possible source of ¹⁴C-depleted runoff. The area has no young volcanoes and few hot springs, representing other possible sources for ¹⁴C depleted water. The interpretation (below) suggests that the maximum paleo-lake depth was less than 50 m during highstands over the past 45 ka, enabling constant water circulation and thus preventing enrichment with old ¹⁴C in the deeper parts. Consequently, these factors may have reduced the chances of old ¹⁴C-depleted C entering the basin. Further investigations, such as paral-

Table 2.2 | Results of XRD analyses

Family	Mineral	Chemical formula	Sample label	Depth [cm]	Abundance code: ++ abundant +- major occurrences -+ minor occurrences -- no occurrences	Occurrences and result relevant properties
Potassium Feldspar	Orthoclase	$KAlSi_3O_8$	CB-01-2009-3b-132	132	+-	Gneiss and granitic intrusions: Si as main component. Major constituent of biotite-quartz-feldspar gneisses forming the Hammar range, Source of K and Si. Common in rhyolites and trachytes, mainly Teltete range. Na-rich end-member of plagioclase; common alteration product of granitic gneisses. Ca-rich end-member of plagioclase; commonly available in granitic gneisses. Weathering product of micas and feldspars; micas such as biotite and muscovites are common in the granites and granitic gneisses of the Hammar range. Source of K. Weathered product of biotite micas. Evaporite: calcite precipitate. Primary mineral in and alkaline igneous rocks; zeolites can be of sedimentary origin. Usually alteration of feldspar, micas, pyroxene, amphibole, garnets in gneisses during low-grade retrograde metamorphism. Common constituent of mafic gneiss.
Potassium-Sodium Feldspar	Sandine	$(K,Na)(Si,Al)_2O_8$	CB-01-2009-3b-164	163	+-	
Feldspar (Plagioclase)	Albite	$NaAlSi_3O_8$	CB-01-2009-4a-190	195	++	
Feldspar (Plagioclase)	Anorthite	$CaAl_2Si_2O_8$	CB-01-2009-4a-222	225	++	
Illite (Clay mineral)	Illite	$K_{0.65}Al_{2.0} [Al_{0.35}Si_{3.65}O_{10}](OH)_2$	CB-01-2009-4a-254	259	++	
Smectite (Clay mineral)	Montmorillonite	$(Na,Ca)_{0.33}(Al,Mg)_2 Si_4O_{10}(OH)_2 \cdot nH_2O$	CB-01-2009-4c-284	287	+-	
Carbonate	Calcite	$CaCO_3$	CB-01-2009-5a-312	318	+-	
Zeolite	Analcime	$NaAlSi_2O_7 \cdot H_2O$	CB-01-2009-5a-344	349	+-	
Sorosilicate	Epidote	$Ca_2(Fe,Al)(Al,Fe)OH(SiO_4)_2(Si_2O_7)$	CB-01-2009-6a-468	451	+-	
Amphibole	Magnesianhornblende	$Ca_2(Mg, Fe, Al)_5(Al, Si)_8O_{22}(OH)_2$	CB-01-2009-6b-532	514	+-	
			CB-01-2009-7a-562	544	+-	
			CB-01-2009-7b-656	616	+-	
			CB-01-2009-8a-698	648	++	
			CB-01-2009-8c-772	719	+-	
			CB-01-2009-9-868	813	+-	
			CB-01-2009-9-874	818	+-	
			CB-01-2009-10-910	844	+-	
			CB-01-2009-10-942	876	+-	
			CB-01-2009-10-973	907	+-	
			CB-01-2009-11a-1064	970	+-	
			CB-01-2009-13a-1268	1148	+-	
			CB-01-2009-13a-1332	1212	+-	
			CB-01-2009-14a-1386	1263	+-	
			CB-01-2009-15a-1476	1326	+-	
			CB-01-2009-15b-1572	1416	+-	
			CB-01-2009-17c-1922	1635	+-	
			CB-01-2009-18a-1996	1705	+-	
			CB-01-2009-18b-2034	1741	+-	
			CB-01-2009-19a-2128	1815	+-	
			CB-01-2009-19b-2194	1879	+-	
			CB-01-2009-19b-2204	1886	+-	

lel dating of charcoal and biogenic carbonate will shed light on the reliability of the radiocarbon chronology.

The inferred dry-wet-dry cycles are also expressed in the distinct changes of the sedimentation rate. Especially with the onset of the last humid period 15 ka ago, the sedimentation rate increased significantly by a factor of six to seven between the two dated levels of 35 and 13 ka calBP. Correspondingly, higher sedimentation rates occurred from 45 ka to 35 ka, though interrupted by a large hiatus, which prevents distinguishing whether there was one single continuous humid period or more. Thus, wetter conditions coincide with increased deposition, which is explained by enhanced fluvial input and connected to a more continuous deposition of generally finer material. The position of the coring site within this flat basin does not make fluvial erosion and redistribution during lake conditions very likely. However, postulated dry phases indicated by coarser input during strong rain events via the alluvial fan may have also led to a certain amount of fluvial erosion at the coring site, which could not be specified further. If at all, the fluvial erosion is incorporated in the hiatuses G2 to G5.

2.5.2 Evaluation of proxies

The lacustrine sediments of core CB-01-2009 reflect a highly variable environment during the Late Quaternary. The geochemical results concur with physical and biological indicators. The most conspicuous paleoenvironmental indicator is potassium, interpreted as a proxy for aridity in the Chew Bahir catchment. Under generally arid conditions with sparse vegetation cover, the gneisses (e.g. the potassium-rich orthoclase feldspar-biotite-muscovite-gneisses) as well as two-mica granites with conspicuous orthoclase phases constituting the Hammar range are eroded more easily, and then washed into the basin via alluvial fans. These events are expressed by sharp increases of K in the record, reflecting the onset of dry conditions on millennial or even centennial timescales. Increased sediment supply from the alluvial fans of Hammar range during dry conditions into a shallow or even dried out lake also is reflected by coarser material (like sandy silt and sandy gravel; Fig. 3), which is washed in during strong rain events. The K in the record can be attributed exclusively to terrigenous and allochthonous input; and once deposited, no further processes change or enrich the amount of K.

The XRD results show the occurrence of the potassium-rich mineral illite $[(K,H_3O)(Al,Mg,Fe)_2(Si,Al)_4O_{10}[(OH)_2,(H_2O)]$, throughout the stratigraphy, and other potassium-rich minerals, orthoclase (potassium feldspar; $KAlSi_3O_8$), and sanidine $[(K,Na)(Si,Al)_4O_8]$, which occur in the top 30 cm and at 8.44–12.63 depth. Illites

are commonly associated with alteration products of micas (biotites and muscovites), and in this case, illites could be alteration products of the feldspathic and micaceous gneisses and granites, which are the dominant rock units forming the Hammar range. The illite content largely correlates with phases of high K values (Tab. 2.2). Quartz, which generally is less sensitive to alteration than feldspars and micas, appears especially in the upper levels of the core, almost unaltered. This also suggests a scenario with increased alluvial fan or eolian activity.

Alluvial fans usually become active during occasional short but intense rainfall events instead of evenly distributed rainfall. Moreover, the deposits that are washed in by the Weyto and Segen River from the north of the catchment are rather unlikely to reach the elevated marginal position of CB-01 in a dried out playa scenario or when water level of paleolake Chew Bahir was very shallow. During wet phases, however, with a higher lake water levels and denser vegetation cover in the catchment area, evenly distributed rains result in the more-or-less continuous discharge of all rivers, transporting more diverse and generally finer material. This also includes Fe- and Ti-rich material input from the basalts constituting the eastern and northeastern ridges surrounding the basin. This input firstly dilutes the al-

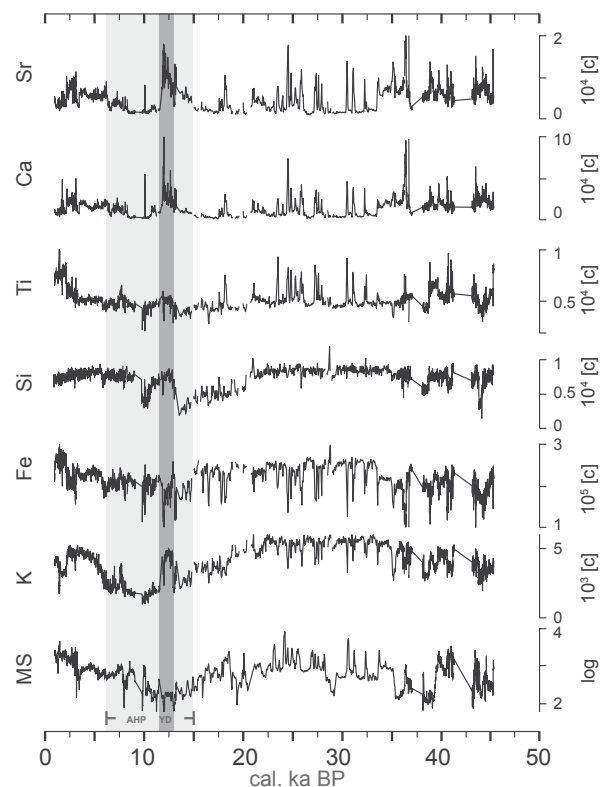


Figure 2.4 | Results of XRF measurements against time; MS – Magnetic Susceptibility; K - Potassium; Fe - Iron; Si - Silicon; Ti - Titanium; Ca - Calcium; Sr - Strontium; AHP–African Humid Period; YD- Younger Dryas.

readily decreased potassium input via the alluvial fan from the Hammar range and secondly mixes in an array of sediments from the entire catchment. Thus, the K record potentially provides a clear aridity signal, as the provenance and transport mechanisms of the element are rather constrained. In support of this dry/wet interpretation, magnetic susceptibility largely parallels the potassium record, despite very coarse layers, where MS is reduced, such as around 7 m. Here, K shows an abrupt return to high values, whereas MS remains low. Richardson and Richardson (1972) employed feldspars and associated elements as indicators for more arid phases and reduced lake levels in the Naivasha basin in central Kenya, arguing that these minerals have been transported to the deposition area by small streams that in turn were associated with larger grain sizes. The Si distribution along the record largely parallels the potassium record from the base up to ~5.5 m depth, which corresponds to the mid-AHP. This can be explained by a similar provenance as K, because mostly Si – as a quartz (SiO₂) phase – forms a major component of all the quartzo-feldspathic gneisses and the associated micaceous granites of the Hammar range, and during dry intervals Si is subjected to the same transport mechanism. However, during long wetter periods such as the AHP, the lake system stabilizes and biogenic production (e.g., silica rich diatom frustules, see also Fig. 2.3) increases the amount of Si in the sediment autochthonously. As the XRF results for Si do not differentiate between terrigenous and biogenic Si, the comparison to Ti was used to distinguish between both processes, as the Ti input is exclusively terrigenous. However, Si can be found in most other minerals, as is also clear from Table 2.2. Iron (Fe) is another allochthonous component that shows a very similar pattern to Si and especially to K in the lowermost parts of the profile up to 7.8 m depth. As iron is highly redox sensitive, post-sedimentary processes have overprinted the iron signal in the sediment, so iron values differ considerably from potassium, especially during the AHP.

Comparing Fe, K and Si results, it becomes apparent that these elements seem to react very similarly, except during the long wet phases where these three elements show major divergences in trend (Figs. 2.3 and 2.4). This has to be attributed to the far more diverse processes (e.g., biogenic production of silica and post-sedimentary reduction of iron) and a more versatile provenance of Fe and Si than K. Whereas K originates mainly from the Hammar range, Fe (found in illite and magnesiohornblende) and Si (mainly from quartz but also common in most felsic minerals) may additionally come from other sources. Iron can be attributed to major Fe-containing mineral phases such as augite,

olivine, and hornblende, and to accessory phases such as titanomagnetite from the northeastern and eastern ridges of the catchment (Fig. 2.2).

Ca and Sr are strongly correlated, indicating a common source and/or transport mechanism. Both elements are present in feldspathic gneisses, granulites and basalts of the catchment area, and are thought to have entered the lake in solution. The cycle of Sr is primarily driven by co-precipitation with authigenic calcite, due to similar ionic radiuses of Ca and Sr, during algal photosynthetic or evaporative precipitation (Stabel, 1987). Additionally, isolated carbonate layers (Fig. 2.3) throughout the lower part of the core indicate phases of high evaporation that coincide with increased XRF Ca counts (Fig. 2.4). Therefore, peaks in the Ca record appear at pronounced dry spells, hinting at evaporation. Moreover, enhanced bio-productivity as a second masking process overprints the Ca signal. The onset of heavy rainfalls after drought, bringing nutrients into the lake basin resulted in the increase of the bio-productivity of an existing lake. During these scenarios, Ca and Sr values are high, while K shows a clear anti correlation. This most likely reflects irregular short-term humid events during a period of generally reduced humidity, but still providing enough moisture to sustain at least a shallow lake. The gastropod *Melanoides tuberculata* occurs in a wide range of fresh and brackish water habitats throughout Africa (Pointier et al., 1992; Leng et al., 1999). Its littoral habitat is mostly associated with aquatic and subaquatic plants in up to 2 m water depth, providing the snails with protection from wave action, as well as food and egg laying sites (Leng et al., 1999). Some authors report that *Melanoides tuberculata* may live within fine-grained sediment at greater water depths (10–15 m) where they can form high population densities (Pointier et al., 1992). Occurrences of these snail shells in combination with the other proxies indicate water level lowering. These molluscs always appear at the postulated transition zones, indicated by the geochemical proxies for lower water levels and larger grain sizes. Therefore, it seems that these snail shells represent lake levels not deeper than 10 m.

2.5.3 Paleoclimatic implications for the past 45 ka

The high-resolution K record for the past 45 ka correlates (Fig. 2.5) with the δD leaf wax record from Lake Tanganyika (Tierney et al., 2008), marine dust records from the Atlantic coast of West Africa (deMenocal et al., 2000) and the Arabian Sea (Altabet et al., 2002), the stable isotope records from Hulu/Dongge Cave in southeast Asia (Wang et al., 2001) and with Greenland ice cores (NGRIP; North Greenland Ice Core Project

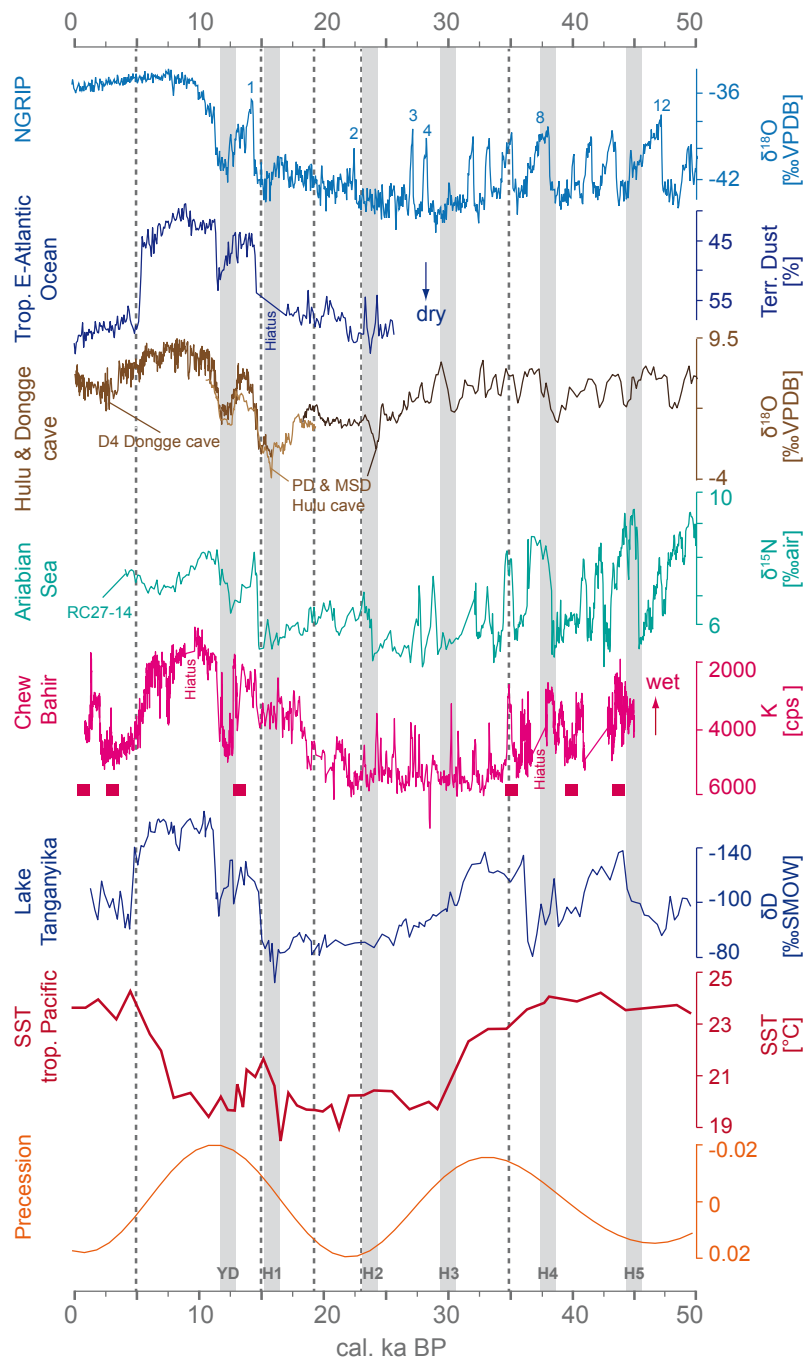


Figure 2.5 | Comparison of the Chew Bahir potassium (K) record with other paleoclimate records. Records plotted from top to bottom are as follows: $\delta^{18}\text{O}$ data from NGRIP (North Greenland Ice Core Project members, 2004) with numbers referring to DO-events; terrestrial dust input to the tropical east Atlantic (deMenocal et al., 2000; note reverse scale); $\delta^{18}\text{O}$ data from Hulu (Wang et al., 2001) and Dongge caves (Dykoski et al., 2005; note reverse scale); $\delta^{15}\text{N}$ data as proxy for denitrification and productivity in the Arabian Sea in the Gulf of Oman 18°N (Altabet et al., 2002); Chew Bahir potassium (K) record (note reverse scale); Lake Tanganyika δD leafwax as proxy for precipitation variability (Tierney et al., 2008; note reverse scale); SST (sea surface temperature) record from the eastern Pacific (Martínez et al., 2003) and insolation variations (Berger and Loutre, 1991). Dotted lines indicate time slices discussed in the text. Gray bars refer to Heinrich events, Younger Dryas and H1–H5. The red squares show ^{14}C dates along the Chew Bahir record.

members, 2004). Assuming that high values of K reflect aridity, the interval 45–35 ka is characterized by intermediate moisture conditions interrupted by drier periods every ~1,000 years. Comparable conditions were also observed in records from Lake Abhé in north Ethiopia (Gasse and Street, 1978) and Lake Tanganyika (Tierney et al., 2008). The two hiatuses in the Chew Bahir record are mostly due to lost sandy material, possibly

indicating arid episodes with coarse material transported via the alluvial fan. The arid episode around 37 ka could possibly coincide with the H4 event, which is reported to have caused widespread aridity in East Africa and Asia (Wang et al., 2001; Tierney et al., 2008). The long-term transition to greater humidity from around 35 ka on follows declines in the sea surface temperatures (SST) of the tropical East Pacific leading to generally

drier tropical climate during the Last Glacial Maximum (LGM, 18–23 ka; Gasse, 2000; Martínez et al., 2003). A strong temporal relationship between SST cooling of 2–4 °C in the eastern equatorial Pacific and ice sheet growth has been reported leading into a more La Niña like SST field (Clark et al., 2009). According to a model of the response of the NINO3 index, this cooling may have been caused by changes in the low-latitude precession-related insolation (Clement et al., 1999).

Between 35 and 23 ka, even more pronounced aridity dominated the climate in tropical East Africa with short-term shifts towards humidity indicated by distinct single negative peaks in the K record. In contrast to the time prior to 35 ka, the short-term fluctuations within the overall changes follow a generally decreasing trend. However, the amplitudes of these short-term fluctuations during the LGM far exceed all short-term fluctuations of the past 20 ka. The pattern of these strong short-term variations resembles Dansgaard-Oeschger cycles, and the dry episodes could possibly be interpreted as Heinrich events by tentative correlation with the NGRIP ice core. An African-Asian influence is suggested by correlations with records from Lake Tanganyika, the Arabian Sea and the Hulu/Dongge records (Fig. 2.5). However, the age model with merely six ages and increasing error bars down-core is not sufficiently precise to correlate dry-wet-dry excursions towards the core base with Dansgaard-Oeschger cycles.

From 23 ka to 5 ka, K values seem to follow the precession-forced increase in insolation. The time interval between 23 and 19 ka corresponds to the high-latitude LGM, which coincided with pronounced aridity in many parts of tropical Africa and elsewhere in the tropics (Gasse et al., 2008), well reflected by the K record of the Chew Bahir basin. The cooling of the equatorial Atlantic during the LGM reduced moisture transport to the Congo basin via the usually humid Congo air stream, producing higher aridity in the central parts of Africa. Since Chew Bahir lies at the foot of the Ethiopian plateau, it is occasionally influenced by the humid Congo air masses at the present day. Hence, it is possible that what is seen in the K record is the result of a combination of both mechanisms: the insolation forced moisture shifts and the migration of the CAB.

Increased insolation, on the contrary, results in greater humidity at Chew Bahir after 19 ka. However, despite gradual insolation change, the return to more humid conditions occurs in abrupt steps of increasing amplitude at 19–15 ka, 14.5–12.8 ka, and 11.5 ka. Such a stepwise increase in precipitation is also described in various paleoclimatic records from Africa north of

8–9 °S (Gasse et al., 2008). The AHP (15 to 5 ka) is the result of the precessional increase in Northern Hemisphere insolation during low eccentricity (deMenocal et al., 2000; Barker et al., 2004; Garcin et al., 2009). The humid Congo air stream may have again become more influential with the onset of the AHP 15 ka ago as suggested by a recent study from the Suguta Valley, just south of the Chew Bahir basin (Junginger, 2011). Extreme humidity in northern Ethiopia is thought to be the result of an eastward shift of the CAB due to a deepening of the atmospheric low over India causing an enhanced pressure gradient between India and Asia (Hailemichael et al., 2002). The combination of rising SSTs providing more moisture and additional continuous moisture availability during the present dry season via the CAB may have caused the pronounced humid episode in the Chew Bahir basin.

According to the age model, a rapid shift towards extreme arid conditions is indicated by increased K values around 12.8 ka, before returning to wet conditions at 11.6 ka, as reflected by a steep decrease of K. This dramatic arid event within the orbitally-controlled humid interval correlates with the high-latitude Younger Dryas event (YD, 12.8–11.6 ka) that coincides with arid conditions everywhere in Africa north of 10 °S (Barker et al., 2004; Gasse et al., 2008; Tierney et al., 2011). The K data indicate a short-term return to humid conditions around 11.8 ka ago in Chew Bahir, but the final return to full humid conditions started abruptly around 11.6 ka, within about 200 years. This rapid termination of the YD is also documented in other East African paleoclimatic records, such as the onset of ice accumulation on Mt. Kilimanjaro with the tentative age of 11.65 ka (Thompson et al., 2002) and rapid regressions of lakes Nakuru (Richardson and Dussinger, 1986), Suguta (Junginger, 2011), Abiyata (Chalié and Gasse, 2002) and Ziway-Shala (Gillespie et al., 1983) (Fig. 2.5). It is also suggested in various studies from West Africa (e.g., deMenocal et al., 2000; Shanahan et al., 2006) and Asia (e.g., Wang et al., 2001; Yuan et al., 2004).

Having returned to maximum humid conditions after the YD, multiple fluctuations in the K, Ca and Sr records indicate a series of brief drier intervals around 10.8–10.5 ka, 9.8–9.1 ka (hiatus due to unconsolidated sands), followed by a gradual decrease of moisture between 8.0 and 7.5 ka and an abrupt major drought event around 7 ka (Fig. 2.6). Most of these events have been described as abrupt phases of maximum aridity during the AHP throughout East Africa from various archives including dust events in the Kilimanjaro ice record (Thompson et al., 2002), lake-level variations, and changes in diatom assemblages (Telford and Lamb,

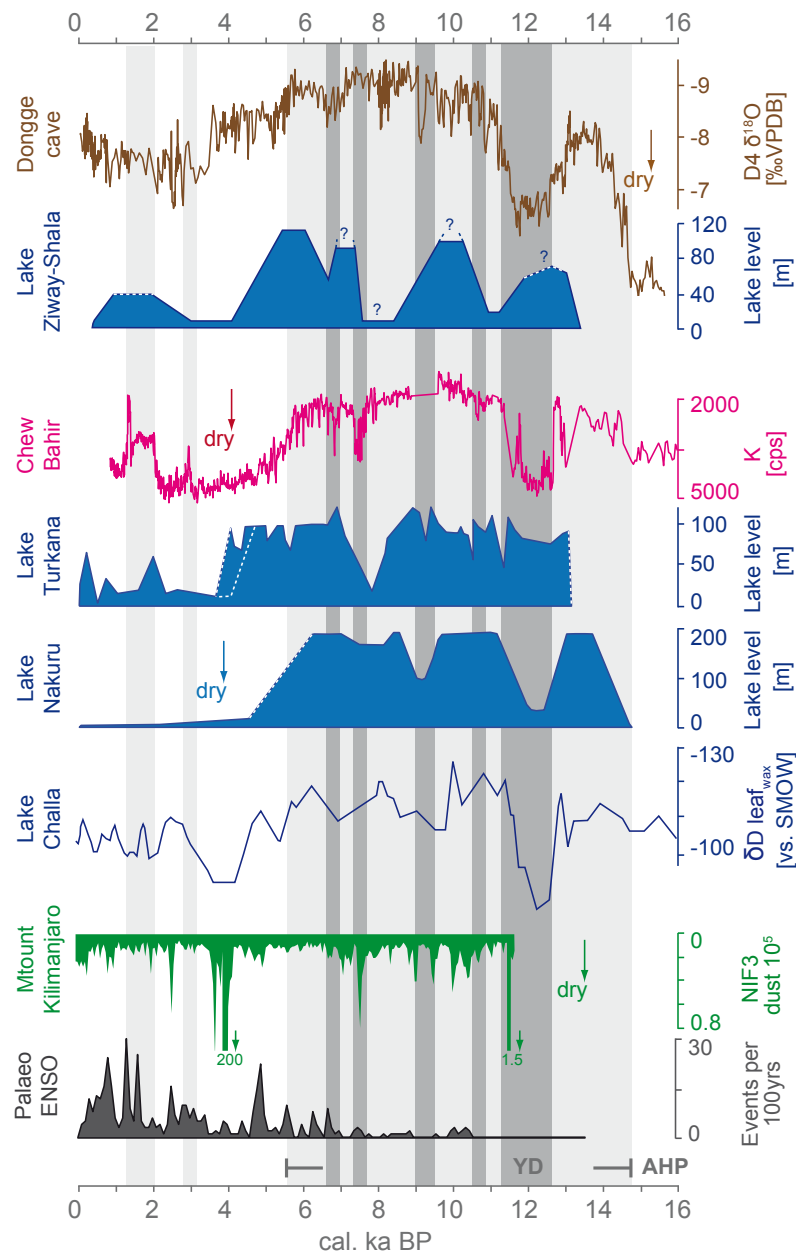


Figure 2.6 | Comparison of onset and termination of East African lake levels from lake Nakuru (Richardson and Dussinger, 1986), lake Ziway-Shala (Gillespie et al., 1983), and Lake Turkana (Johnson et al., 1991; Brown and Fuller, 2008) with the aeolian dust record to Mt. Kilimanjaro (Thompson et al., 2002) due to enhanced aridity, hydrological proxy data from Lake Challa from δD leafwax (Tierney et al., 2011), the oxygen-isotope records from Dongge cave (Dykoski et al., 2005), and the paleo-ENSO record from Laguna Pallcacocha, southern Ecuador (Moy et al., 2002). AHP–African Humid Period; YD– Younger Dryas; dark gray bars indicate dry episodes; light gray bars indicative for humid episodes.

1999; Gasse, 2000; Guo et al., 2000; Chalié and Gasse, 2002). The termination of the AHP in the Chew Bahir basin according to the K record started around 6 ka ago and continued for 1,000 years until full arid conditions were reached at 5 ka. This gradual climate change contrasts with the abrupt termination of the AHP recorded in marine archives (deMenocal et al., 2000; Renssen et al., 2006; Garcin et al., 2009). These records and climate modelling results indicate a more abrupt decline of the AHP between 5 and 4.5 ka (deMenocal et al., 2000; Morrill et al., 2003). An equally large body of evidence points to a gradual trend towards aridity since ~7.8 ka (Fleitmann et al., 2003; Gupta et al.,

2005; Wang et al., 2005; Asrat et al., 2007; Baker et al., 2010; Junginger, 2011). A highly nonlinear response of paleoclimate records implies that the abruptness of the termination of the AHP has been amplified considerably by feedback mechanisms as suggested by Clausen et al. (1999). DeMenocal et al. (2000) differentiate between two feedback mechanisms that could have amplified such a transition: coupled vegetation-albedo feedback and ocean surface temperature-moisture feedback. Comparisons of lake level records located in the vicinity of Chew Bahir show large differences in the timing and abruptness of the AHP termination (Fig. 2.6). These differences are almost certainly due to local hy-

drological factors related to the topography of the lake basins and their catchments.

Following the termination of the AHP at 5 ka, arid conditions re-established and remained relatively stable until 2 ka, with one short abrupt excursion towards more humid conditions around 3 ka. A longer humid interval began abruptly in two steps around 2 ka, and remained humid until 1.5 ka before terminating abruptly at 1.3 ka. The combined increase of Fe and Ti in the record hints at constant fluvial input as the dominant input system for that time. Dry conditions on a millennial scale are a common feature of tropical African paleo-climate archives such as that around 4 ka at Ziway-Shala (Gillespie et al., 1983) or Lake Turkana (Johnson et al., 1991; Fig. 2.6). The presence of a millennial-scale drought in the stalagmite records of southeast Asia (Wang et al., 2001) as well as marked aridity in Ethiopian speleothem records for these periods (Asrat et al., 2007; Baker et al., 2010), underlines the regional expression of this dry event. Possible mechanisms for such humidity shifts, out of phase with precessional forcing, may be related to an enhanced higher-frequency ENSO (El Niño/Southern Oscillation) causing more stable humid conditions (Fig. 2.6). Such enhanced periodicities in ENSO anomalies were observed for the 3–2.5 ka, 1.6 ka and 1.3 ka (Moy et al., 2002).

2.6 Conclusion

The sediment record from the Chew Bahir basin contains a number of valuable climate proxies that provide high resolution climate reconstructions for the past 45 ka, showing a distinct pattern of changing environmental conditions during the Late Quaternary in southern Ethiopia. These climate changes can be correlated to well-known wet-dry cycles for tropical east Africa (e.g., LGM, AHP, YD), and hint to a valuable age model even if it is based only upon six data points to date. The Chew Bahir basin has been proven to be a suitable climate archive with well datable deposits without age reversals that give valuable insight into a highly variable environment. The sediment record comprises a number of meaningful proxies, foremost K, which enabled high resolution reconstructions of the climate variability in the region since 45 ka, based on the analysis of geochemical, physical and biological indicators. Sediment types have been analyzed and indicate that input mechanisms and provenances do vary and are clearly controlled by climate changes and can therefore help to understand regional shifts in moisture availability. With six to seven fold increased sedimentation rates during humid phases, Chew Bahir reacts very sensitively towards even moderate climate changes and clearly reflects short-term variations

on millennial timescales, like the latest one known as the Younger Dryas. Precession-forced long-term variations, such as the AHP, are expressed in the Chew Bahir basin, and appear to be synchronous with changes in Lake Malawi, Lake Tanganyika, West African marine cores, and the Hulu/Dongge Caves. This wet phase in Chew Bahir is marked by a stepwise, rather abrupt onset and a gradual termination.

Longer core records, to ~150 m depth, from the basin thus will offer the possibility of reconstructing the paleoenvironmental history since the origin of *Homo sapiens* 200,000 years ago. Consequently, the site has great potential to shed light on the setting of evolution and dispersal of AMH, although only 45 ka at present. Further detailed analysis of a transect of cores through the basin will provide a better understanding of localized sedimentation in the lake and the mechanisms and processes behind the climate variations derived from these findings can be made evident from the sedimentary archive. It should also be possible to correlate the Chew Bahir results with archeological findings in the region (Brandt et al., this volume), testing models of the

Acknowledgments

We are grateful to Addis Ababa University for support in making the field campaigns possible, and to Addis Geosystems Ltd for providing drilling equipment. Nina Bösche (University of Potsdam) assisted with satellite image processing, and Frederik von Reumont and Andreas Bolten helped with cartography. We would like to thank Martin Wessels and two anonymous reviewers whose comments greatly improved the manuscript. This project is affiliated to the CRC 806, which financially supported the first field campaign. The Chew Bahir Project is a contribution to the International Continental Scientific Drilling Program (ICDP), part of the ICDP-HSPDP initiative organized by A. Cohen. We thank the German Science Foundation (DFG) for funding all these projects.

2.7 References

- Alemayehu, T., 2006. Groundwater occurrence in Ethiopia. Ph.D. Thesis, Addis Ababa University, Ethiopia.
- Altabet, M.A., Higginson, M.J., Murray, D.W., 2002. The effect of millennial-scale changes in Arabian Sea denitrification on atmospheric CO₂. *Nature* 415, 159–162.
- Ambrose, S.H., 1998. Late Pleistocene human population bottlenecks, volcanic winter, and the differentiation of modern humans. *Journal of Human Evolution* 35, 115–118.
- Armitage, S.J., Jasim, S.A., Marks, A.E., Parker, A.G., Usik, V.I., Uerpmann, H.-P., 2011. Evidence for an early expansion of modern humans into Arabia. *Science*, 331, 453–457.
- Asrat, A., Baker, A., Umer, M., Moss, J., Leng, M., Van Calsteren, P., Smith, C., 2007. A high-resolution multi-proxy stalagmite record from Mechara, Southeastern Ethiopia: Palaeohydrologi-

- cal implications for speleothem palaeoclimate reconstruction. *Journal of Quaternary Science* 22, 53–63.
- Asrat, A., Bates, R., Berger, G., Beyene, Y., Brandt, S., DeGusta, D., Duller, G., Ebinger, C., Endale, T., Hart, W.K., Hildebrand, E., Katoh, S., Kidane, T., Lamb, H., Leng, M., Lezine, A.-M., Marshall, M., Morgan, L., Pearce, N., Prave, T., Renne, P., Schäbitz, F., Strecker, M., Suwa, G., Tadesse, K., Tadesse, T., Trauth, M., Umer, M., Vogelsang, R., White, T., WoldeGabriel, G., Zeleke, A., 2009. The Chew Bahir Drilling Project: a Plio-Pleistocene climate record from the southern Ethiopian Rift, a crucible of human evolution. Proposal for the ICDP-HSPDP (Hominin Sites and Palaeolakes Drilling Project), pp. 1–8.
- Baker, A., Asrat, A., Leng, M., Thomas, L., Fairchild, I.J., Widmann, M., Dong, B., Van Calsteren, P., Bryant, C., 2010. Decadal-scale rainfall variability in Ethiopia recorded in an annually laminated, Holocene-age, stalagmite. *The Holocene* 20, 827–836.
- Barker, P.A., Talbot, M.R., Street-Perrott, F.A., Marret, F., Scourse, J., Odada, E.O., 2004. Late Quaternary variability in intertropical Africa. In: Battarbee, R.W., Gasse, F., Stickley, C.E. (Eds.), *Past climate variability through Europe and Africa*. Springer, Dordrecht, pp. 117–138.
- Behrensmeier, A.K., 2006. Climate change and human evolution. *Science* 311, 476–478.
- Berger, A., Loutre, M.-F., 1991. Insolation values for the climate of the last 10 million years. *Quaternary Science Reviews* 10, 297–317.
- Brandt, S.A., Fisher, E.C., Hildebrand, E.A., Vogelsang, R., Ambrose, S.H., Lesur, J., Wang, H., this issue. Early MIS 3 occupation of Mochena Borago Rockshelter, Southwest Ethiopian Highlands: Implications for Late Pleistocene archaeology, paleoenvironments and modern human dispersal.
- Bronk Ramsey, 2010. (OxCalv4.1.7calibration software) <http://c14.arch.ox.ac.uk/embed.php?File=index.html> (accessed 05.05.2011).
- Brown, E.T., Fuller, C.H., 2008. Stratigraphy and tephra of the Kibish Formation, southwestern Ethiopia. *Journal of Human Evolution* 55, 366–403.
- Brown, E.T., Johnson, T., Scholz, C., Cohen, A., King, J., 2007. Abrupt change in tropical African climate linked to the bipolar seesaw over the past 55,000 years. *Geophysical Research Letters* 34, L20702, 1–5.
- Camberlin, P., 1997. Rainfall anomalies in the source region of the Nile and their connection with the Indian summer monsoon. *Journal of Climate* 10, 1380–1392.
- Camberlin, P., Philippon, N., 2002. The east African March-May rainy season: associated atmospheric dynamics and predictability over the 1968–97 period. *Journal of Climate* 15, 1002–1019.
- Carto, S.L., Weaver, A.J., Hetherington, R., Lam, Y., Wiebe, E.C., 2009. Out of Africa and into an ice age: on the role of global climate change in the late Pleistocene migration of early modern humans out of Africa. *Journal of Human Evolution* 56, 139–151.
- Castañeda, I.S., Mulitza, S., Schefuss, E., Lopes de Santos, R.A., Damsté, J.S.S., Schouten, S., 2009. Wet phases in the Sahara/Sahel region and human migration patterns in North Africa. *PNAS (Proceedings of the National Academy of Sciences)* 106, 20159–22016.
- Chalié, F., Gasse, F., 2002. Late Glacial-Holocene diatom record of water chemistry and lake level change from the tropical East African Rift Lake Abiyata (Ethiopia). *Palaeogeography, Palaeoclimatology, Palaeoecology* 187, 259–283.
- Chase, B., Quick, L., Meadows, M., Scott, L., Thomas, D., Reimer, P., 2011. Late glacial interhemispheric climate dynamics revealed in South African hyrax middens. *Geology* 39, 19–22.
- Clark, J., Beyene, Y., WoldeGabriel, G., Hart, W.K., Renne, P., Gilbert, E., Defleur, A., Suwa, G., Katoh, S., Ludwig, K.R., Boisserie, J.-R., Asfaw, B., White, T.D., 2003. Stratigraphic, chronological and behavioural contexts of Pleistocene *Homo sapiens* from Middle Awash, Ethiopia. *Nature* 423, 747–752.
- Clark, P.U., Dyke, A.S., Shakun, J.D., Carlson, A.E., Clark, J., Wohlfarth, B., Mitrovica, J.X., Hostetler, S.W., McCabe, A.M., 2009. The Last Glacial Maximum. *Science* 325, 710–714.
- Claussen, M., Kubatzki, C., Brovkin, V., Ganopolski, A., Hoelzmann, P., Pachur, H.J., 1999. Simulation of an abrupt change in Saharan vegetation in the mid-Holocene. *Geophysical Research Letters* 26, 2037–2040.
- Clement, A.C., Seager, R., Cane, M.A., 1999. Orbital controls on the El Niño/Southern Oscillation and the tropical climate. *Paleoceanography* 14, 441–456.
- Corti, G., 2009. Continental rift evolution: From rift initiation to incipient break-up in the Main Ethiopian Rift, East Africa. *Earth-Science Reviews* 96, 1–53.
- Davidson, A., 1983. The Omo River project: Reconnaissance geology and geochemistry of parts of Ilubabor, Kefa, Gemu Gofa and Sidamo. *Ethiopian Institute of Geological Surveys Bulletin* 2, 1–89.
- deMenocal, P., Ortiz, J., Guilderson, T., Adkins, J., Sarnthein, M., Baker, L., Yarusinsky, M., 2000. Abrupt onset and termination of the African Humid Period: rapid climate responses to gradual insolation forcing. *Quaternary Science Reviews* 19, 347–361.
- Diro, G.T., Grimes, D.I.F., Black, E., 2010. Teleconnections between Ethiopian summer rainfall and sea surface temperature; part I: Observation and modeling. *Climate Dynamics*. doi: 10.1007/s00382-010-0837-8
- Dykoski, C.A., Edwards, R.L., Cheng, H., Yuan, D., Cai, Y., Zhang, M., Lin, Y., Qing, J., An, Z., Revenaugh, J., 2005. A high-resolution, absolute dated Holocene and deglacial Asian monsoon record from Dongge Cave, China. *Earth Planetary Science Letters* 233, 71–86.
- Ebinger, C.J., Yemane, T., Harding, D., Tesfaye, S., Kelley, S., Rex, D., 2000. Rift deflection, migration, and propagation: Linkage of the Ethiopian and Eastern rifts, Africa. *Geological Society of America Bulletin* 112, 163–176.
- Fleitmann, D., Burns, S.J., Mudelsee, M., Neff, U., Kramers, J., Mangini, A., Matter, A., 2003. Holocene forcing of the Indian monsoon recorded in a stalagmite from Southern Oman. *Science* 300, 1737–1739.
- Garcin, Y., Junginger, A., Melnick, D., Olago, D., Strecker, M., Trauth, M.H., 2009. Late Pleistocene-Holocene rise and collapse of the Lake Suguta, northern Kenya Rift. *Quaternary Science Reviews* 28, 911–925.
- Gasse, F., 1986. East African diatoms – taxonomy, ecological distribution. J. Cramer in der Gebrüder Bornträger Verlagsbuchhandlung, Berlin, Stuttgart.
- Gasse, F., 2000. Hydrological changes in the African tropics since the Last Glacial Maximum. *Quaternary Science Reviews* 19, 189–211.
- Gasse, F., Street, F.A., 1978. Late Quaternary lake level fluctuations and environments of the northern Rift Valley and Afar region (Ethiopia and Djibouti). *Palaeogeography, Palaeoclimatology, Palaeoecology* 25, 145–150.
- Gasse, F., Van Campo, E., 1994. Abrupt post-glacial climate events in West Asia and North Africa monsoon domains. *Earth and Planetary Science Letters* 126, 435–456.
- Gasse, F., Chalié, F., Vincens, A., Williams, M.A.J., Williamson, D., 2008. Climatic patterns in equatorial and southern Africa from 30,000 to 10,000 years ago reconstructed from terrestrial and near-shore proxy data. *Quaternary Science Reviews* 27, 2316–2340.
- Gillespie, R., Street-Perrott, F.A., Switsur, R., 1983. Post-glacial arid episodes in Ethiopia have implications for climate prediction. *Nature* 306, 680–683.
- Guo, Z., Petit-Maire, N., Kröpelin, S., 2000. Holocene non-orbital climatic events in present-day arid areas of northern Africa and China. *Global and Planetary Change* 26, 97–103.
- Gupta, A.K., Das, M., Anderson, D.M., 2005. Solar influence on the Indian summer monsoon during the Holocene. *Geophysical Research Letters* 32, L17703, doi:10.1029/2005GL022685
- Hailemichael, M., Aronson, J.L., Savin, S., Tevesz, M.J.S., Carter, J.G., 2002. $\delta^{18}\text{O}$ in mollusk shells from Pliocene Lake Hadar and modern Ethiopian lakes: implications for history of the Ethiopian monsoon. *Palaeogeography, Palaeoclimatology, Palaeoecology* 186, 81–99.
- Hildebrand, E.A., Brandt, S.A., Lesur-Gebremariam, J., 2010. The Holocene archaeology of Southwest Ethiopia: New insights from the Kafa Archaeological Project. *African Archaeological Review* 27 (2), 55–289.
- Johnson, T.C., Halfman, J.D., Showers, W.J., 1991. Paleoclimate of the past 4000 years at Lake Turkana, Kenya, based on the isotopic composition of authigenic calcite. *Palaeogeography, Palaeoclimatology, Palaeoecology* 85, 189–198.
- Joordens, J.C.A., Vonhof, H.B., Feibel, C.S., Lourens, L.J., Dupont-Nivet, G., Van der Lubbe, H.J.L., Sier, M., Davies, G.R., Kroon, D., 2011. An astronomically-tuned climate framework for hominins in the Turkana Basin. *Earth and Planetary Science Letters* 307, 1–8.
- Junginger, A., 2011. East African climate variability on different time scales: The Suguta Valley in the African-Asian monsoon do-

- main. Ph.D. Thesis, University of Potsdam, Germany. <http://opus.kobv.de/ubp/volltexte/2011/5683/>
- Kröpelin, S., Verschuren, D., Lézine, A.-M., Eggermont, H., Cocquyt, C., Francus, P., Cazet, J.-P., Fagot, M., Rumes, B., Russell, J.M., Darius, F., Conley, D.J., Schuster, M., von Suchodoletz, H., Engstrom, D.R., 2008. Climate-driven ecosystem succession in the Sahara: The past 6000 years. *Science* 320, 765–768.
- Kutzbach, J.E., Street-Perrott, F.A., 1985. Milankovitch forcing of fluctuations in the level of tropical lakes from 18 to 0 kyr BP. *Nature Geoscience* 317, 130–134.
- Leng, M.J., Lamb, A.L., Lamb, H.F., Telford, R.J., 1999. Palaeoclimatic implications of isotopic data from modern and early Holocene shells of the freshwater snail *Melanoides tuberculata*, from lakes in the Ethiopian Rift Valley. *Journal of Paleolimnology* 21, 97–106.
- Lundberg, J., 1990. U-series dating of carbonates by mass spectrometry with examples of speleothem, coral and shell. Ph.D. Thesis, McMaster University, Hamilton, ON.
- Martínez, I., Keigwin, L., Barrows, T.T., Yokoyama, Y., Southon, J., 2003. La Niña-like conditions in the eastern equatorial Pacific and a stronger Choco jet in the northern Andes during the last glaciation. *Paleoceanography* 18, 1033–1033.
- McDougall, I., Brown, F.H., Fleagle, J.G., 2005. Stratigraphic placement and age of modern humans from Kibish, Ethiopia. *Nature* 433, 733–736.
- Meyers, P.A., 2003. Applications of organic geochemistry to paleolimnological reconstructions: a summary of examples from the Laurentian Great Lakes. *Organic Geochemistry* 34, 261–289.
- Moore, J.M., Davidson, A., 1978. Rift structure in southern Ethiopia. *Tectonophysics* 46, 159–173.
- Morrill, C., Overpeck, J.T., Cole, J.E., 2003. A synthesis of abrupt changes in the Asian summer monsoon since the last deglaciation. *Holocene* 13, 465–476.
- Moy, C.M., Seltzer, G.O., Rodbell, D.T., Anderson, D.M., 2002. Variability of El Niño/Southern Oscillation activity at millennial timescales during the Holocene epoch. *Nature* 420, 162–165.
- Nicholson, S.E., 1996. A review of climate dynamics and climate variability in eastern Africa. In: Johnson, T.C., Odada, E.O. (Eds.), *The limnology, climatology and paleoclimatology of the East African lakes*. Gordon & Breach, Amsterdam, pp. 25–56.
- North Greenland Ice Core Project members, 2004. High-resolution record of northern hemisphere climate extending into the last interglacial period. *Nature* 431, 147–151.
- Okoola, R., 1999. A diagnostic study of the Eastern African monsoon circulation during the northern hemisphere spring season. *International Journal of Climatology* 19, 143–168.
- Olaka, L.A., Odada, E.O., Trauth, M.H., Olago, D.O., 2010. The sensitivity of East African rift lakes to climate fluctuations. *Journal of Paleolimnology* 44, 629–644.
- Oppenheimer, S., 2009. The great arc of dispersal of modern humans: Africa to Australia. *Quaternary International* 202, 2–13.
- Partridge, T.C., Lowe, J., Barker, P., Hoelzmann, P., Magri, D., Saarnisto, M., Vandenberghe, J., Street-Perrott, F., Gasse, F., 2004. Climate variability in Europe and Africa: A PAGES-PEP III Time Stream II Synthesis. Springer, Dordrecht.
- Peck, S.B., 1986. Bacterial deposition of iron and manganese oxides in North American caves. *National Speleological Society* 48, 26–30.
- Pik, R., Marty, B., Carignan, J., Yirgu, G., Ayalew, T., 2008. Timing of East African Rift development in southern Ethiopia: Implication for mantle plume activity and evolution of topography. *Geology* 36, 167–170.
- Pointier, J.P., Delay, B., Toffart, J.L., Lefevre, M., Romero-Alvarez, R., 1992. Life history traits of three morphs of *Melanoides tuberculata* (Gastropoda: Thiaridae), an invading snail in the French West Indies. *Journal of Molluscan Studies* 58, 415–423.
- Potts, R., 1998. Environmental hypotheses of hominin evolution. *Yearbook of Physical Anthropology* 41, 93–136.
- Reimer, P.J., Baillie, M.G.L., Bard, E., Bayliss, A., Beck, J.W., Blackwell, P.G., Bronk Ramsey, C., Buck, C.E., Burr, G.S., Edwards, R.L., Friedrich, M., Grootes, P.M., Guilderson, T.P., Hajdas, I., Heaton, T.J., Hogg, A.G., Hughen, K.A., Kaiser, K.F., Kromer, B., McCormac, F.G., Manning, S.W., Reimer, R.W., Richards, D.A., Southon, J.R., Talamo, S., Turney, C.S.M., van der Plicht, J., Weyhenmeyer, C.E., 2009. INTCAL09 and MARINE09 radiocarbon age calibration curves, 0–50,000 years cal BP. *Radiocarbon* 51, 1111–1150.
- Renssen, H., Brovkin, V., Fichefet, T., Goosse, H., 2006. Simulation of the Holocene climate evolution in Northern Africa: The termination of the African Humid Period. *Quaternary International* 150, 95–102.
- Rethemeyer, J., Dewald, A., Fülöp, R., Hajdas, I., Höfle, S., Patt, U., Stapper, B., Wacker, L., in press. Sample preparation facilities for ¹⁴C analysis at the new Cologne AMS centre. *Nuclear Instruments and Methods in Physics Research B*.
- Richardson, J.L., Dussinger, R.A., 1986. Paleolimnology of mid-elevation lakes in the Kenya Rift Valley. *Hydrobiologia* 143, 167–174.
- Richardson, J.L., Richardson, A.E., 1972. History of an African Rift lake and its climatic implications. *Ecological Monographs* 42, 499–534.
- Segele, Z.T., Lamb, P.J., 2005. Characterization and variability of Kiremt rainy season over Ethiopia. *Meteorology and Atmospheric Physics* 89, 153–180.
- Shanahan, T.M., Overpeck, J.T., Wheeler, C.W., Beck, J.W., Pigati, J.S., Talbot, M.R., Scholz, C.A., Peck, J., King, J.W., 2006. Paleoclimatic variations in West Africa from a record of late Pleistocene and Holocene lake level stands of Lake Bosumtwi, Ghana. *Palaeogeography, Palaeoclimatology, Palaeoecology* 242, 287–302.
- Stabel, H.H., 1987. Coupling of strontium and calcium cycles in Lake Constance. *Hydrobiologia* 176–177, 323–329.
- Stager, J., Ryves, D., Chase, B., Pausata, F., 2011. Catastrophic drought in the Afro-Asian monsoon region during Heinrich Event 1. *Science* 331, 1299–1302.
- Stringer, C., 2003. Out of Ethiopia. *Nature* 423, 692–695.
- Telford, R.J., Lamb, H.F., 1999. Groundwater-mediated response to Holocene climatic change recorded by the diatom stratigraphy of an Ethiopian crater lake. *Quaternary Research* 52, 63–75.
- Thompson, L.G., Mosley-Thompson, E., Davis, M.E., Henderson, K.A., Brecher, H.H., Zagorodnov, V.S., Mashiotta, T.A., Lin, P.-N., Mikhailenko, V.N., Hardy, D.R., Beer, J., 2002. Kilimanjaro ice core records: Evidence of Holocene climate change in tropical Africa. *Science* 298, 589–593.
- Tierney, J.E., Russell, J.M., Huang, Y., Sinninghe Damsté, J.S., Hopmans, E.C., Cohen, A., 2008. Northern hemisphere controls on tropical Southeast African climate during the past 60,000 years. *Science* 322, 252–255.
- Tierney, J.E., Russell, J.M., Sinninghe Damsté, J.S., Huang, Y., Verschuren, D., 2011. Late Quaternary behavior of the East African monsoon and the importance of the Congo Air Boundary. *QSR* 30, 798–807.
- Trauth, M.H., Deino, A.L., Bergner, A.G.N., Strecker, M.R., 2003. East African climate change and orbital forcing during the last 175 kyr BP. *Earth and Planetary Science Letters* 206, 297–313.
- Trauth, M.H., Maslin, M.A., Deino, A.L., Junginger, A., Lesoloyia, M., Odada, E.O., Olago, D.O., Olaka, L.A., Strecker, M.R., Tiedemann, R., 2010. Human evolution in a variable environment: The amplifier lakes of Eastern Africa. *QSR* 29, 2981–2988.
- Vrba, E.S., 1985. Environment and evolution: alternative causes of the temporal distribution of evolutionary events. *South African Journal of Sciences* 81, 229–236.
- Wacker, L., Fülöp, R., Hajdas, I., Molnár, M., Rethemeyer, J., submitted. A novel approach to process carbonate samples for radiocarbon measurement. *Nuclear Instruments and Methods in Physics Research B*.
- Wang, Y.J., Cheng, H., Edwards, R.L., An, Z.S., Wu, J.Y., Shen, C.-C., Dorale, J.A., 2001. A high-resolution absolute-dated late Pleistocene monsoon record from Hulu Cave, China. *Science* 294, 2345–2348.
- Wang, Y.J., Cheng, H., Edwards, R.L., He, Y., Kong, X., An, Z., Wu, J., Kelly, M.J., Dykoski, C.A., Li, X., 2005. The Holocene Asian monsoon: Links to solar changes and North Atlantic climate. *Science* 308, 854–857.
- White, T.D., Asfaw, B., DeGusta, D., Gilbert, H., Richards, G.D., Suwa, G., Howell, F.C., 2003. Pleistocene *Homo sapiens* from Middle Awash, Ethiopia. *Nature* 423, 742–747.
- Williams, A.P., Funk, C., 2011. A westward extension of the warm pool leads to a westward extension of the Walker circulation, drying eastern Africa. *Climate Dynamics*. doi: 10.1007/s00382-010-0984-y
- Yuan, D., Cheng, H., Edwards, R.L., Dykoski, C.A., Kelly, M.J., Zhang, M., Qing, J., Lin, Y., Wang, Y., Wu, J., Dorale, J.A., An, Z., Cai, Y., 2004. Timing, duration, and transitions of the Last Interglacial Asian Monsoon. *Science* 304, 575–578.



Chapter III*

Climate flickers during the last 46,000 years in the Chew Bahir basin, Southern Ethiopia

Verena Foerster, Annett Junginger, Nicole A. Stroncik, Asfawossen Asrat,
Henry F. Lamb, Michael Weber, Ute Frank, Maxwell C. Brown,
Frank Schaebitz, Martin H. Trauth

submitted to *Palaeogeography, Palaeoclimatology, Palaeoecology*

* In the first version of the dissertation that was submitted in March 2014 this part publication was comprised: Foerster, V., Junginger, A., Asrat, A., Umer, M., Lamb, H.F., Weber, M., Rethemeyer, J., Frank, U., Brown, M.C., Trauth, M.H., Schaebitz, F., (in review). 46, 000 years of alternating wet and dry phases on decadal to orbital timescales in the cradle of modern humans: the Chew Bahir project, southern Ethiopia. *Climate of the Past, Discussions* 10, doi:10.5194/cpd-10-1-2014, 1–48.

Climate flickers during the last 46,000 years in the Chew Bahir basin, Southern Ethiopia

V. Foerster^{1*}, A. Junginger², N. A. Stroncik¹, A. Asrat³, H. F. Lamb⁴, M. Weber⁵, U. Frank⁶, M.C. Brown⁶, F. Schaebitz⁷, M.H. Trauth¹

¹ University of Potsdam, Institute of Earth and Environmental Science; Karl-Liebknechtstrasse 24–25; D-14476 Golm

² University of Tübingen, Department of Earth Sciences; Hölderlin Str. 12; D-72074 Tübingen

³ Addis Ababa University, School of Earth Sciences; P. O. Box 1176, Addis Ababa, Ethiopia

⁴ Aberystwyth University, Institute of Geography and Earth Sciences, Aberystwyth SY23 3DB, U.K.

⁵ University of Cologne, Institute of Geology and Mineralogy; Zülpicher Str. 49A; D-50674 Cologne

⁶ Helmholtz-Zentrum Potsdam, Deutsches GeoForschungsZentrum – GFZ, D-14473 Potsdam

⁷ University of Cologne, Seminar for Geography and Education; Gronewaldstrasse 2; D-50931 Cologne

* corresponding author

Abstract

Rapid changes in environmental conditions are considered to be an important driver for human evolution, cultural and technological innovation, and expansion out of Africa. However, the nature of these environmental changes, their amplitude and correlation with steps in human evolution is the subject of current debates. Here we present a high-resolution (~3–12 yrs) and well-dated (32 AMS ¹⁴C ages) lake-sediment record of the last 46,000 years from the Chew Bahir basin in the southern Ethiopian Rift. The record was obtained from six cores along a NW-SE transect across the basin, which has been selected as the drilling location within the ICDP Hominin Sites and Paleolakes Drilling Project (HSPDP). Multi-proxy data and the comparison between the transect coring sites provide initial insight into intra-basin dynamics and major mechanisms controlling the sedimentation of the proxies that was used to develop a basic proxy concept for Chew Bahir for the last two wet-dry cycles. Our record suggests that the environmental response to orbitally induced insolation variation is nonlinear, probably due to complex biophysical feedbacks on climate, as several transitions observed in our data are either faster or some slower compared to changes in the forcing. On the other hand, however, they are relatively slow at time scales of human life, allowing people living in the area to adapt to a changing environment. In the view of the quality of the Chew Bahir environmental record, the basin seems to be a perfect site for the anticipated deep drilling project.

Keywords: Wet-dry cycle; precession; nonlinear feedback; potassium; African Humid Period; Ethiopia

3.1 Introduction

The cradle of humankind is today widely agreed to be located in the climatically and topographically diverse East African Rift System (EARS) that provided a highly variable environment to enable and push the evolution of mammals (Tishkoff and Verrelli, 2003; Trauth et al., 2010). One of the oldest known fossils of anatomically modern humans (AMH), dated to 195 ka BP was found in the Omo Region in the southwestern part of Ethiopia (Day, 1969; McDougall et al., 2005). From here, modern humans may have dispersed into Asia and Europe to populate the world (Stringer et al., 2003; Oppenheimer, 2009).

Determining the nature, character, and pace of a changing environment of early humans is crucial to understanding the factors that influenced human evolution (Vrba, 1985; Potts, 1998; Maslin and Trauth, 2009) and dispersal, including cultural and technological innovations (Hildebrand and Grillo, 2012; Vogelsang and Keding, 2013). The timing and synchronicity of the dry-wet cycles that have significantly modulated the East African climate is of particular interest, as they would also have had important implications for human adaptation and survival in refugia (Ambrose, 1998; Hildebrand et

al., 2010; Foerster et al., *subm.*) or might have pushed the dispersal beyond Africa during major droughts (Carto et al., 2009) or enabled migration along possible green corridors (Castañeda et al., 2009).

However, understanding the complex mechanisms driving climate shifts is a challenging task considering the uncertainties in reconstruction and attribution to the possible driving mechanisms. Numerous recent studies (e.g. Mulitza et al., 2008; Verschuren et al., 2000; Tierney et al., 2011; Junginger and Trauth, 2013) show that the system is far more complex than assumed years ago. For instance, the timing and abruptness of the transition and internal variability of the youngest and therefore best-studied dry-wet cycle, the so-called African Humid Period (AHP, 15-5 ka BP) has been debated for decades (e.g. deMenocal et al., 2000; Kröpelin et al., 2008; Foerster et al., 2012; Tierney and deMenocal,

2013; Junginger et al., 2014). For Lake Turkana, located southwest of the Chew Bahir basin, three possible styles for the transition out of the AHP have been proposed (Johnson et al., 1991; Brown and Fuller, 2008; Garcin et al., 2012). The discussion on the relative abruptness of the termination of the AHP, however, seems to be semantic in nature, and based on discontinuous records with gaps during the drier phases, dating uncertainties, site or proxy-specific responses to climate change or comparing marine and terrestrial archives.

Therefore, we try to avoid the term abrupt in our discussion of the Chew Bahir (CB) record and instead discuss the rate of change in climate relative to the forcing or to the lifetime of humans. The Chew Bahir basin in the southern Ethiopian Rift is an ideal place to study the close interplay of humans and climate, as this is the area where early humans lived (Cohen et al., 2009). The

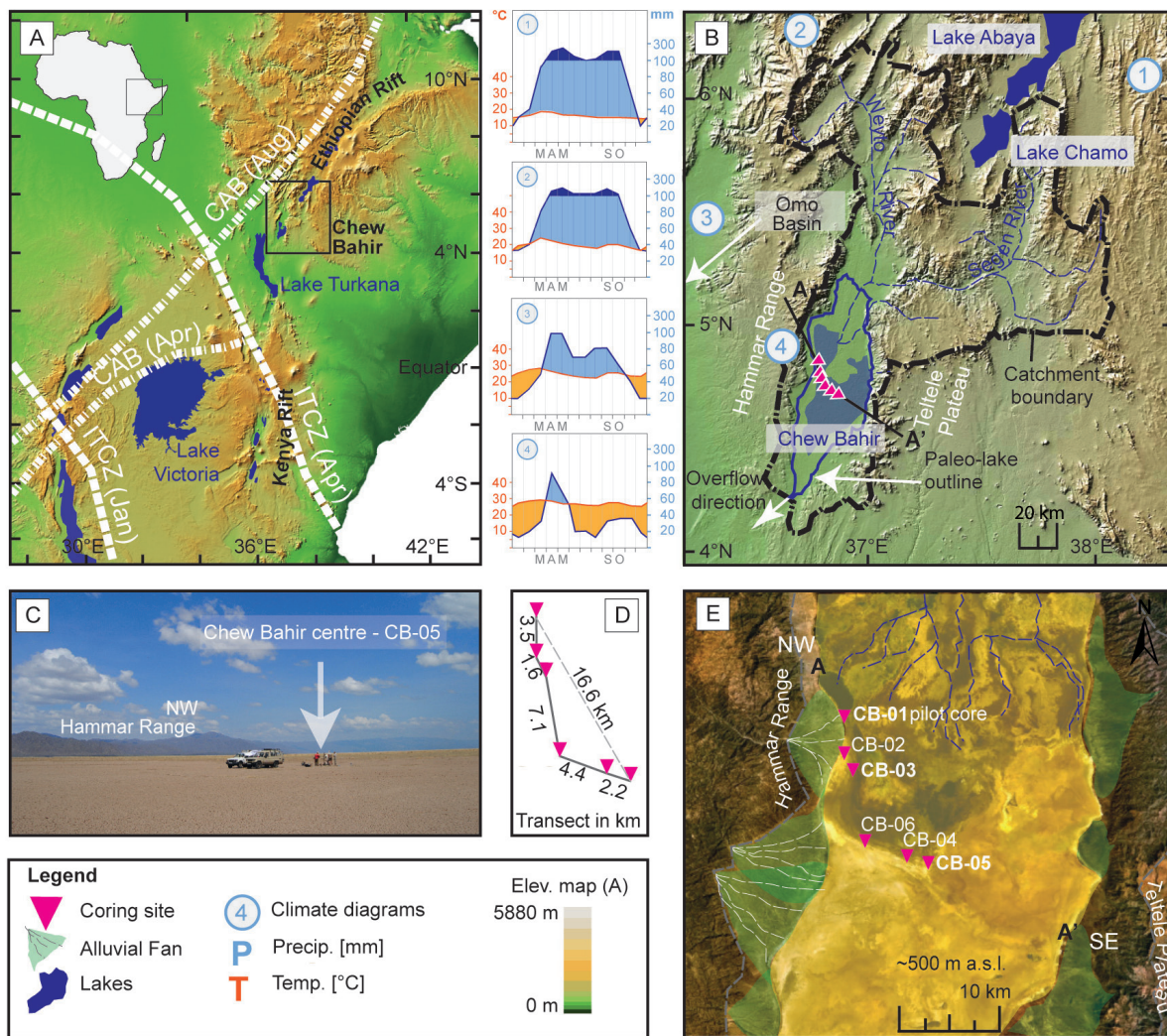


Figure 3.1 | Setting of the Chew Bahir site. (A) Chew Bahir basin within the East African Rift System with major climatic influences. Dotted lines indicate the position of the ITCZ (Intertropical Convergence Zone) and CAB (Congo Air Boundary) during different times of the year (after Tierney et al., 2011). (B) Map of the Chew Bahir catchment with major rivers, paleo-lake outline, overflow direction and sites mentioned in the text. Numbers refer to available precipitation and temperature data summarized in the climate diagrams (data: IRI, accessed Oct. 2013). (C): Center of CB basin, site of CB-05 and planned deep drilling location within the HSDPD project (2013–2014). (D): NW–SE transect through the Chew Bahir basin with distances between coring sites in km. (E): Setting of drilling location of the records discussed in this study, showing major input systems relevant for this study and position of sites within the basin.

environmental record that is presented here spans the last two orbitally driven dry-wet cycles while taking proxy and site specificity of signals as well as dynamics within the basin itself into account. These results constitute preliminary data for the Hominin Sites and Paleolake Drilling Project (HSPDP; Cohen et al., 2009) that tackles exactly this issue of understanding the paleoclimatic context of human evolution through scientific drilling. The interpretation of our records, in particular on short time scales, is preliminary and hypothetical since the processes linking climate with the proxies that were employed are not yet fully understood and require in depth research within the HSPDP project.

3.2 Regional Setting

3.2.1 Geology and Geomorphology

Chew Bahir (4.1–6.3°N; 36.5–38.1°E), today a 30 x 70 km² saline mudflat in a tectonically bounded basin in southern Ethiopia is situated in a biogeographically highly sensitive transition zone between the southern sector of the Main Ethiopian Rift (MER) to the north-east and the Omo-Turkana basin to the west (Fig. 3.1a). This ~250 km wide broadly rifted zone (BRZ, Ebinger et al., 2000; Woldegabriel and Aronson, 1987) is characterized by small fault bounded depressions, providing an archive for sedimentary deposits beyond the Quaternary as the basin and range landscape was formed during older phases of the rifting process (Ebinger et al., 2000; Corti, 2009). The sediments (Fig. 3.1b) in the catchment comprise lacustrine silt and clay, fluvial silt and sand, and alluvium. The Chew Bahir basin is bounded by the Hammar range to the west, composed of Precambrian basement, mainly undivided gneisses, and the higher escarpment of the Teltele Plateau, exposing Miocene basalts and trachytic centers to the East (Fig. 3.1b). Its northern sector is formed by the narrower Weyto basin bounded by the southwestern (Gofa) highlands to the west and the Gamo-Chencha horst to the east. In the northern, northwestern and northeastern part of the catchment Oligocene basalt flows with subordinate rhyolite, trachyte, tuffs and ignimbrites are the dominant lithology. To the south, the Chew Bahir basin extends to the broadly rifted zone that lies between the Ethiopian and Kenyan uplifted domes (Woldegabriel and Aronson, 1987; Pik et al., 2008; Corti, 2009).

The perennial rivers Weyto and Segen wash in deposits from the ~32,400 km² catchment, though their influence today is limited to the northern part of the basin by forming a delta further into the basin (Fig. 3.1 e) (Foerster et al., 2012). Today the basin is merely episodically covered by a few centimeters of water immediately after the rainy season, mostly due to an overflow of the

Weyto into the basin. In addition, Chew Bahir receives deposits via the extensive alluvial fans off the escarpment flanks: the Hammar Range to the west and the Teltele Plateau to the east. However, the small drainage networks at the border faults and the strong seasonality in rainfall make this sediment and water influx highly episodic, because the runoff is closely connected to strong rainfall events during the two rainy seasons and occasional orographic rains. During humid phases Chew Bahir represented the southernmost end point of the drainage system of the Ethiopian Rift Lakes (Junginger and Trauth, 2013; Junginger et al., 2014), and is known to have an overflow level ~50 m above the present basin floor into Lake Turkana (Fig. 3.1b; Foerster et al., 2012). The basin has sensitively reacted in the past to the drastic moisture fluctuations with a variable lake filling: from an extensive fresh water lake to a saline mudflat.

3.2.2 Present Climate

East Africa's climate is governed by moisture availability driven by strong rainfall seasonality, closely tied to the annual latitudinal migration of the Intertropical Convergence Zone (ITCZ) between 15°N in July and 15°S in January. The ITCZ follows maximum insolation values of the overhead sun with a four to six week time lag (Nicholson, 1996) (Fig. 3.1), and thus, creates a largely zonal rainfall pattern. The seasonal migration of the ITCZ attracts moisture through large-scale advection from the Indian Ocean (Levin et al., 2009) resulting in a bimodal annual climatic cycle, with "long rains" from March to May and "short rains" in October-November in the equator regions and only one rainy season at the northern and southern migration margins (Nicholson, 1996). The south-westerly humid Congo air stream delivers additional rainfall to the western parts of equatorial East Africa and Northwestern Ethiopia roughly between July to September, when the ITCZ has reached its northernmost position (known as the "September rains" in some areas of Kenya and „Kiremt“ in Ethiopia; Nicholson, 1996; Camberlin, 1997; Segele and Lamb, 2005). Moisture delivered by the Congo air stream is sourced from the Atlantic Ocean and associated with the West African summer monsoon (WAM). It is in part recycled from vegetation to the atmosphere during its transit across the Congo basin (Nicholson, 1996). This unstable flow from the Atlantic converges with drier air masses from the Indian Ocean along a north-south trending zone known as the Congo Air Boundary (CAB). Due to diverse topography of EARS and the relative position to the equator, temperatures vary only slightly, merely across elevation gradients. Various microclimates (Fig. 3.1) with a pronounced evaporation/precipitation gradient are thus created also for the

Chew Bahir catchment with generally cooler highlands receiving most rainfall that runs off into the hotter and drier lowlands (Gasse, 2000; Seleshi and Zanke, 2004). Figure 3.1 demonstrates that even adjacent to the catchment of Chew Bahir rainfall is highly dependent on elevation and position towards the influence of ITCZ and Congo Air Boundary (CAB).

3.3 Material and Methods

3.3.1 Field campaign

Five short cores (CB-02 to CB-06) of 9–11 m in length were retrieved with a percussion corer in November 2010 along a NW-SE transect through the now desiccated floor of the Chew Bahir basin (Tab. 3.1 and Fig. 3.1b, 3.1d and 3.1e). Supplemented by the 18.86 m long pilot core CB-01 drilled in 2009 (Foerster et al., 2012), the six cores cover a marginal area from extensive alluvial fans off the Hammar range in the west (CB-01 and CB-02), and eastwards through an intermediate area influenced by fluvial, lacustrine and alluvial fan run-off (CB-03) towards the center of the basin (CB-05, CB-06, CB-04). Coring at each site was continuous without overlap. Each drive measured 100 cm, controlled by the equivalent length of the drilling rods. 1 m plastic liners with an inside diameter of 4.8 cm were used to retain the core sections. Core catcher material was analyzed in the field for material composition, grain size and color. The overall core recovery ranges from 97 to 99.5%, with minor core loss due to unconsolidated material at the top (Fig. 3.3). The cores were directly sealed at the site and shipped by airfreight to the University of Cologne, where they were stored in a cool and dark place before further analysis.

3.3.2 Core composition of CB-03 & CB-05

The total length of the CB-03 (Fig. 3.3a) profile is 11.0 m and comprises 10.8 m of sediment due to coring without a replicate and a 98% recovery rate (Tab. 3.1). No gaps occur, the only core loss being of the uppermost section, which has been subjected to soil formation and

was in a rather unconsolidated form (0–20 cm). CB-05 (Fig. 3.3b) covers the uppermost 10 m of the deposits, comprising 9.62 m of sediment, as CB-05 is interrupted by one gap at 4.00–4.08 m, supposedly caused by high water content when coring through the groundwater level and 30 cm core loss from the soil horizon at the top of the core. Hiati in the records cannot be excluded but are not obvious. The composition of the cores is uniform, consisting of lacustrine silts and clays, intercalated by layers of coarse-grained silts and sands and evaporitic carbonate layers (Figs. 3.3a+b). In addition to this general composition, we found several thick layers with fish bones, some horizons rich in molluscs, and several units that show a matrix of fine clays partly disturbed by distinctive tooth shaped illuvations (Figs. 3.3a+b). For the comparative approach of this study we restricted our analysis to CB-05 as representative core for the central area as it provides the most continuous record back to +46 ka BP and CB-03 from the intermediate basin area, while CB-03 provides ~3 yr resolution during the AHP. We interpret those cores together with the previously described pilot core CB-01 (Foerster et al., 2012) from the western margin of the basin.

3.3.3 Sedimentology and Geochemistry

All core sections were split lengthwise with a manual core splitter, then described, scanned and later subsampled at 1–2 cm intervals largely following the established principles of Ohlendorf et al. (2011). Samples were freeze-dried to guarantee adequate storage of the samples to preserve them for future analysis and facilitate fine grinding without compromising the mineral structure. Smear slides were prepared in ~30 cm intervals to provide a first insight into the composition, microfossil occurrences (diatoms, pollen, charcoal), volcanic glasses and accomplish scanning results so that sections with prioritized interest could be identified for further analysis. Elemental composition of the cores was determined at 500- μ m resolution with an Itrax X-ray fluorescence (XRF) core scanner (Cox Analytical Systems) using a Chromium (Cr) tube as radiation

Position within basin	Core ID	Latitude N	Longitude E	Length (m)	Total depth (m SB)	Cored in (year)	Recovery rate (%)
Margin	CB-01-2009	04°50.6'	36°46.8'	22	18.86	Dec 2009	81
Margin	CB-02-2010	04°48.7'	36°46.2'	10	9	Nov 2010	97
Intermediate	CB-03-2010	04°47.9'	36°47.2'	11	11	Nov 2010	98
Centre	CB-04-2010	04°43.3'	36°50.2'	10	10	Nov 2010	99.5
Centre	CB-05-2010	04°42.8'	36°51.3'	10	10	Nov 2010	97
Centre	CB-06-2010	04°44.1'	36°47.9'	10	10	Nov 2010	98.8

Table 3.1 | Core locations and Core details

source, a tube voltage of 30 kV, a current of 30 mA and, an exposure time of 20 s. For comparison with the pilot core, which was measured with a Mo tube, all records were standardized (mean = 0, standard = 1).

For high-resolution sediment-physical data and optical parameters the cores have been scanned in 2 cm intervals with the Geotek Mutli-Sensor Core Logger (MSCL), following the principles of Weber et al. (1997). Grain sizes were estimated semi-quantitatively by finger test, with the sediment composition subdivided into 7 fractions (clay=1 to sandy gravel=7; Fig. 3). XRD analysis with a Siemens D5000 diffractometer was applied to finely ground bulk samples from all cores. No further treatment or the addition of a standard indicator was necessary for using this semi-quantitative approach. EVA (DIFFRAC-AT) was used for phase identification. Total nitrogen (TN), total carbon (TC), and total organic carbon (TOC) contents were determined, but with distinctly low organic content ranging around 0.2 wt%, values were in general too low to be used as an environmental parameter and thus will be excluded from further discussion (Meyers, 2003).

After diatom assemblages were outlined by smear slide analyses, samples at 2–10 cm resolution were treated with hydrogen peroxide (H₂O₂, 30%) and hydrochloric acid (HCl, 37%) to remove remaining organic components and the fine sticky clays from the diatom frustules and to dissolve carbonates, respectively. After thorough washing and adding microspheres to the solution, the diatom suspension was mounted on microscope slides and fixed with Naphrax for an optimized light refraction. A light microscope complemented with a polarizer and REM pictures were used for taxa identification.

3.3.4 Rock magnetic measurements and core correlation

Rock magnetic and high-resolution susceptibility measurements on the Chew Bahir transect cores were carried out at the Helmholtz Center Potsdam–Deutsches GeoForschungsZentrum GFZ (Frank et al., 2011; Brown et al., 2012). Remanence measurements (NRM, ARM, IRM, S-ratio, HIRM) and susceptibility were used in combination with the XRF records and MSCL analyses to find the most reliable proxy set to correlate the transect cores. Eventually, the potassium record (depth) of cores CB03-06 has been tuned to the potassium record of the master core CB01, as K seems to provide the most reliable signal across all cores in the Chew Bahir basin (see chapter 3.5). We restricted the choice of tie points to <15 critical turning points and distinct peaks to restrict the error of prediction (Fig. 3.5, Fig.

3.6). The distinct event markers in the Ca record and anti-correlated trends in the Cl record were used to provide cross control.

3.3.5 Chronology

Age control is principally provided by 32 AMS ¹⁴C ages derived from biogenic carbonates (mostly the common gastropod *Melanoides tuberculata*), organic sediment, and detrital charcoal (Table 3.2, Fig. 3.2). Our best estimate of age was obtained by calculating the weighted mean of the probability density function (PDF) of each age. To get the PDF we used OxCal (Bronk Ramsey, 1995) with 1-sigma error and converted radiocarbon dates to calendar years taking all probabilities into account. Ages shown in the age-depth model in Figure 3.2 correspond to the weighted means out of this PDF. Additionally, we present radiocarbon ages in Table 3.2 with a 2-sigma error and the 2-sigma interval of ages calibrated using the IntCal13 data set (Reimer et al., 2013) within the CALIB 6.0.html calibration program (Stuiver et al., 2005) to demonstrate the maximal possible probability interval induced by the calibration. Furthermore this demonstrates that some of the outlier ages cannot be attributed to the calibration process or even the calibration program that was used. For several dates calibration resulted in multiple possible age ranges with differing probabilities (Table 3.2). No age control for the surface is available, but since large parts of the basin were covered by water until the late 60's of the last century and the inclination of the basin slopes is almost even, we anticipate that large-scale erosion in the recent past can be excluded. We thus assume an age of 1960 AD for the surface of the Chew Bahir basin. To assess a possible reservoir effect on the dated carbonates we scanned CB-03 in 20 cm intervals for sufficient charcoal particles (as terrestrial plant remains; Geyh et al., 1998) and/or shell fragments from the same horizons. The paired dating approach was not successful as charcoal is almost absent throughout the cores. Only at 204 cm depth in CB-03 was just enough material found for parallel dating of shell fragments and charcoal. Parallel bulk/shell sampling was also used as an alternative approach to determine a possible reservoir effect in the carbonate material.

3.4 Results

3.4.1 Age model and core chronology

The composite age-depth model (Fig. 3.2) is based on 32 calibrated AMS ¹⁴C dates (Table 3.2), including six ages from the published pilot core CB01 (Foerster et al., 2012; Trauth et al., in press). A closer look at the age model reveals a number of outliers that are either too young or too old to fit the estimated age and to be in

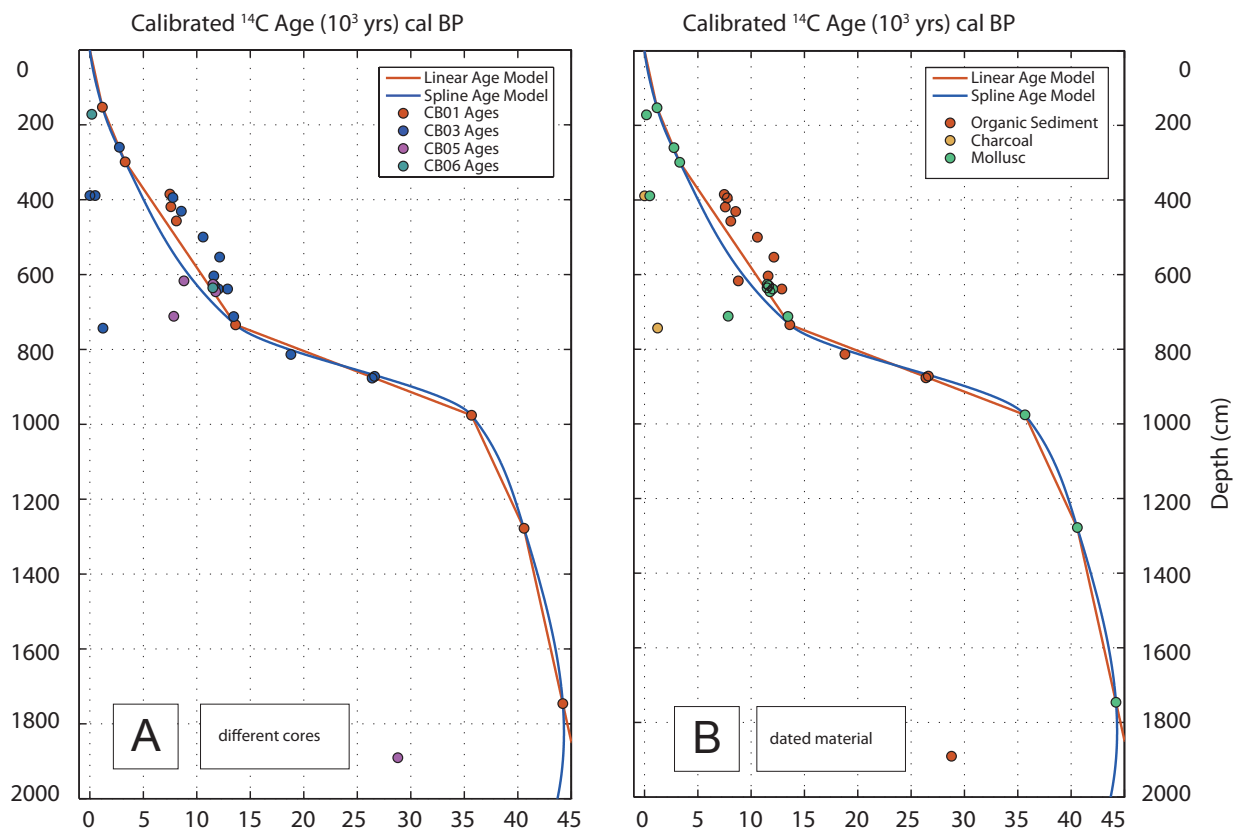


Figure 3.2 | Age model of tuned composite profiles of Chew Bahir cores CB01, 03–06. The depth in cm shows the composite depth of the model. Ages are the weighted mean of the probability density function and correspond to the last column in Table 2. (A) Radiocarbon ages per sediment core. (B) Materials used for radiocarbon dating.

line with the other age determinations. As described in great detail by others (Björck and Wohlfarth, 2001; Cohen, 2003; Felton et al., 2007; Kliem et al., 2013) there may be several explanations. For deviations on smaller timescales (up to a few centuries), a reservoir effect (old carbon effect) or a plateau effect in calibration could be taken into consideration. Much larger offsets however, can be caused by remobilization of dated material prior to deposition, redistribution within the basin, stratigraphical mixing caused by bioturbation, infills of dry cracks, or sample contamination with modern carbon during coring or later in the lab.

The Chew Bahir ages have not been corrected for a possible reservoir effect, where ages derived from biogenic carbonates would be slightly older if they had been compromised by fossil carbon as in many archives (e.g. Felton et al., 2007; Kröpelin et al., 2008, SOM; Junginger et al., 2014). However, this seems not the case for the Chew Bahir samples, though a reservoir effect could be neither determined nor ruled out as there were too few pair dated samples (charcoal and carbonates) and those few we could pair date are all clear outliers. The three most prominent anomalously young dates from CB-03 (Beta 329853, Beta 329854 parallel dating at 389 cm composite depth and Beta

329855 at 743 cm composite depth in Figure 3.2) have most likely entered the record via ground water circulation. Given the extreme scarcity of picked particles in the sample and rather small particle size, the dated material is extremely mobile. The few other closely together dated samples (organic bulk and carbonates) do however not suggest a tendency towards carbonates being consistently older compared to organic samples as Figure 3.2b shows. Whereas the dated carbonates (COL 1235) from the reworked section in CB-05 are significantly older than the organic sediment sample COL1632 from the same horizon, the pair dated samples from CB-03 show the opposite tendency, with the mollusc being younger than the bulk material.

Following, the ages that are not in line with the reliable age determinations are attributed to possible reasons that might have caused the offset, from bottom to top of the composite depth of the age model in Figure 3.2. COL 1631 from CB-05 (1890 cm composite depth in Fig. 3.2) is very likely to have been compromised by modern carbon after coring and shows the maximal offset of ~20 ka. The two apparently anomalously young Holocene ages from CB-05 (COL1632 and COL1830) at 617 cm and 711 cm composite depth may have been subject to reworking or stratigraphical mixing during the AHP lake phase

Sample ID	Core	Depth [cm]	Material	$\delta^{13}\text{C}$	^{14}C age ^b			Cal. Age Range BP ^c		Area ^d	WM ^f
				[‰]	[years BP]		[yrs cal BP]		[%]	[yrs cal BP]	
COL 1093 ^a	CB-01	153	mollusc	-1.4	1,236	± 54	1,075 / 1,192	59.3	1,174		
							1,196 / 1,262	40.7			
COL 1094 ^a	CB-01	299	mollusc	1.7	3,077	± 54	3,238 / 3,365	97.3	3,300		
							3,219 / 3,230	2.7			
Beta 347311	CB-01	384-386	organic sediment	-16.0	6,580	± 60	7,429 / 7,514	88.6	7,480		
							7,539 / 7,561	11.4			
Beta 347312	CB-01	418-420	organic sediment	-15.6	6,700	± 60	7,507 / 7,616	100.0	7,564		
Beta 347313	CB-01	456-458	organic sediment	-16.6	7,270	± 80	8,007 / 8,173	100.0	8,089		
Beta 271307 ^a	CB-01	734-735	organic sediment	-22.6	11,790	± 120	13,446 / 13,795	100.0	13,629		
COL 1095 ^a	CB-01	976	mollusc	0.8	31,085	± 370	35,049 / 36,295	100.0	35,674		
COL 1096 ^a	CB-01	1278	mollusc	10.1	35,508	± 1162	39,131 / 41,675	100.0	40,575		
COL 1097 ^a	CB-01	1746	mollusc	-0.9	40,293	± 1090	43,233 / 45,048	100.0	44,209		
COL 1227	CB-03	126.5	mollusc fragments	-7.5	2,641	± 46	2,741 / 2,781	100.0	2,758		
Beta 329853	CB-03	203-204	fossilized charcoal ^e	NA	modern		NA / NA	NA	0		
Beta 329854	CB-03	203-204	mollusc ^e fragments ^e	-3.1	450	± 60	490 / 530	100.0	504		
Beta 347314	CB-03	210-212	organic sediment	-17.8	6,930	± 80	7,675 / 7,847	100.0	7,759		
Beta 347315	CB-03	256-258	organic sediment	-18.0	7,770	± 60	8,509 / 8,599	84.1	8,545		
							8,455 / 8,501	15.9			
Beta 347316	CB-03	344-346	organic sediment	-17.2	9,360	± 100	10,481 / 10,713	94.9	10,582		
							10,426 / 10,466	5.1			
Beta 347317	CB-03	412-414	organic sediment	-16.9	10,310	± 80	11,978 / 12,225	81.6	12,135		
							12,257 / 12,381	18.4			
Beta 347318	CB-03	476-478	organic sediment	-19.5	10,060	± 80	11,391 / 11,811	98.8	11,588		
							11,355 / 11,374	1.2			
COL 1228	CB-03	509.5	mollusc	-7.2	10,079	± 60	11,591 / 11,812	72.0	11,638		
							11,404 / 11,583	28.0			
COL 1231	CB-03	521.3	mollusc ^e	-12.0	10,268	± 82	11,821 / 12,154	97.9	12,028		
							12,189 / 12,214	1.4			
							12,299 / 12,302	0.1			
							12,357 / 12,370	0.6			
COL 1630	CB-03	521-522	organic sediment ^e	-24.5	11,002	± 108	12,693 / 13,081	100.0	12,876		
COL 1831	CB-03	712-713	mollusc fragments	-7.2	11,588	± 148	13,276 / 13,645	100.0	13,443		
Beta 329855	CB-03	762-764	fossilized charcoal	-25.8	1,280	± 60	1,171 / 1,288	99.0	1,222		
							1,150 / 1,160	1.0			
COL1234	CB-03	936-937	organic sediment	-2.9	15,647	± 118	18,634 / 18,942	100.0	18,793		
COL 1233	CB-03	1086-1087	organic sediment ^e	-1.7	22,155	± 226	26,123 / 27,070	97.9	26,606		
							27,304 / 27,466	2.1			
COL 1631	CB-03	1090-1091.5	organic sediment ^e	-14.4	21,939	± 360	25,811 / 26,942	100.0	26,383		
COL 1235	CB-05	321	mollusc fragments ^e	-10.0	10,016	± 78	11,312 / 11,712	100.0	11,505		
COL 1632	CB-05	321-322	organic sediment ^e	-5.7	7,935	± 90	8,633 / 8,983	100.0	8,797		
COL 1829	CB-05	340	mollusc	-7.8	10,138	± 134	11,592 / 12,041	87.7	11,769		
	CB-05						11,462 / 11,568	8.5			
	CB-05						11,404 / 11,459	3.9			
COL 1830	CB-05	405	mollusc fragments	-2.7	7,015	± 106	7,722 / 7,952	100.0	7,847		
COL 1633	CB-05	990-991	organic sediment	-21.8	23,921	± 426	28,202 / 29,353	100.0	28,782		
COL 1828	CB-06	40.5	mollusc	-0.4	213	± 78	137 / 224	49.5	185		
							255 / 316	32.4			
							0 / 32	15.6			
								100.0			
COL 1832	CB-06	233	mollusc fragments	-6.1	9,994	± 134	11,252 / 11,752		11,493		

^a Previously published in Foerster et al. (2012).

^b Radiocarbon age with 2-sigma errors.

^c 2-sigma range of calibrated radiocarbon ages. All conventional radiocarbon ages were converted to calendar years using the IntCal13 data set (Reimer et al., 2013).

^d Relative area under the probability distribution curve.

^e Parallel dating of biogenic carbonate and organic material and fossilized charcoal, to determine possible reservoir effect.

^f Weighted mean of the probability density function of the calibrated age (1-sigma) as the best age estimate; using OxCal available online at <https://c14.arch.ox.ac.uk/oxcal> to calculate the probability density function of all calibrated ages. Ages in this column correspond to data shown in the age-depth model in Figure 2.

Table 3.2 | Ages from CB-01, CB-03 and CB-06 for Chew Bahir transect chronology

as suggested by the rather noisy proxy records and sedimentological structure in parts of the Holocene deposits of CB-05 that indicate that the material has been heavily reworked. A series of radiocarbon ages derived from organic sediment between 650 and 300 cm composite depth are slightly but consistently too old. These three ages from CB-01 (Beta 347311–347313) and five ages from CB-03 (Beta 347314–347318) are slightly offset by ~100 cm compared with the African Humid Period (15–5 kyr, ~750–400 cm composite depth) suggesting temporary storage and remobilization of organic matter in the densely vegetated catchment during a wetter climate (Fig. 3.2b). Several ages, all derived from the distinct gastropod horizon (see also section 4.5) deposited briefly after the YD, show a temporal offset (<500 yr) towards being slightly too old (COL 1228, 1231, 1630, 1235, 1832; note the several too old mollusc ages with green symbols around 11–12 ka BP in Fig. 3.2). These five ages though, are dated to a time interval within the termination phase of the YD when a shallow lake (<10 m) provided a suitable habitat for *M. tuberculata*. Assuming however, that the radiocarbon dates themselves are reliable, redeposition within a rapidly re-establishing lake as cause for the offset seems most likely. Therefore we treat all ages from this layer as a reliable biological age control point, strongly supporting our correlation, but have to refrain from including them in the age model as the original depth cannot be attributed due to redeposition.

The most reliable age model for our ages from the Chew Bahir records is a conservative composite age-depth model using a linear interpolation technique (Trauth et al., in press). We prefer a linear over a spline model as abrupt variations between low or high sedimentation rates, even episodes without deposition, may actually exist in rift environments, but are smoothed out by splines and age modeling techniques introducing an arbitrary chosen memory (e.g., Bronk Ramsey, 2008, 2009; Blaauw and Christen, 2011; Trauth, 2014). However, we used linear and cubic spline interpolation techniques while tuning the individual records but we have found no significant difference in the final result. Finally, the CB proxy records were interpolated upon the composite age model, also using a linear interpolation technique.

The composite age-depth model shows a two-time change in the sedimentation rate (Fig. 3.2). The changes in the sedimentation rates are governed by the dry-wet variations, as higher sedimentation is coinciding with wet phases, whereas aridity is expressed in significantly lower sedimentation per year. The composite age model shows clearly that two wet episodes with

five to six-fold sedimentation rates bracket an episode of a drier climate during the last glacial maximum with sedimentation rates of ~0.1 mm yr⁻¹. The sedimentation rates vary not only through time, but also within the basin from the shore to the paleo-lake center: The highest mean sedimentation rate was identified for the pilot core (CB-01) at the margin of the basin with ~0.7 mm yr⁻¹, whereas for CB-05, 16.2 km southeast into the center of the mudflat, we deduct a mean of ~0.2 mm yr⁻¹. Intermediate values apply for CB-03 with ~0.4 mm yr⁻¹. There is therefore a clear decrease of sedimentation rate towards the basin center, which naturally affects the duration and resolution of the records. Extrapolating the sedimentation rate linearly, CB-03 has a maximum age of ~26.5 ka cal BP at 11 m depth. CB-05 covers a maximum of ~46 ka cal years of sediment history in 10 m sediment depth.

According to the core chronology, the sedimentary records span climate history from ~46 ka to ~300 yrs BP and thus cover the expression of global climate events in southern Ethiopia, including the timing and character of the Last Glacial Maximum (LGM, 23–18 ka BP), the African Humid Period (AHP, 15–5 ka), the Younger and the Older Dryas (YD, 12.8–11.6 ka BP and OD, around 14 ka BP) and towards the top of the records the Medieval warm period (MWP, 700–1,000 BP).

3.4.2 Physical parameters and mineralogy

The magnetic susceptibility (MS) logs show a distinct signature that probably could indicate rather large climate transitions than small scale changes as a correlation between grain sizes is not significant amongst the cores. Grain-size variations show a correlation between coarser material and drier intervals especially towards the onset of arid conditions. The products of prevailing physical weathering during aridity may have been transported into the basin in highly episodic but strong rainfall events. Furthermore, up to 5 mm big Ca-rich precipitates occur during dry intervals that were probably formed during intervals with strongly increased evaporation.

The qualitative XRD measurements on selected samples show the overall composition of the material and changes in the mineral assemblages of different sections (for full account of mineral assemblages and their attributed provenance see Foerster et al., 2012). The sediment contains calcite, analcime, smectite, illite, sanidine, albite, anorthite, orthoclase, muscovite, and quartz. There are variations in the proportions of the different mineral phases. Generally, the most characteristic sets are composed of analcime, calcite, illite and quartz or of smectite, and illite. XRD results show that mineral assemblages vary significantly more along the core than across the core transect.

3.4.3 Chemical distribution patterns

The X-ray fluorescence (XRF) scans provide data on the elemental content of 26 to 47 elements, depending on the setting of the core scanner. Here we only represent the results of the elements silica (Si), titanium (Ti), iron (Fe), calcium (Ca), potassium (K), chlorine (Cl) and strontium (Sr), because those elements provide for a catchment area consisting almost entirely of silicate-composed rocks the best framework for determination of the controlling mechanism of the geochemical signal. As Figure 3.3a and 3.3b show, the K records of CB-03 and CB-05 show distinct variations and trends

and strontium (Sr), because those elements provide for a catchment area consisting almost entirely of silicate-composed rocks the best framework for determination of the controlling mechanism of the geochemical signal. As Figure 3.3a and 3.3b show, the K records of CB-03 and CB-05 show distinct variations and trends

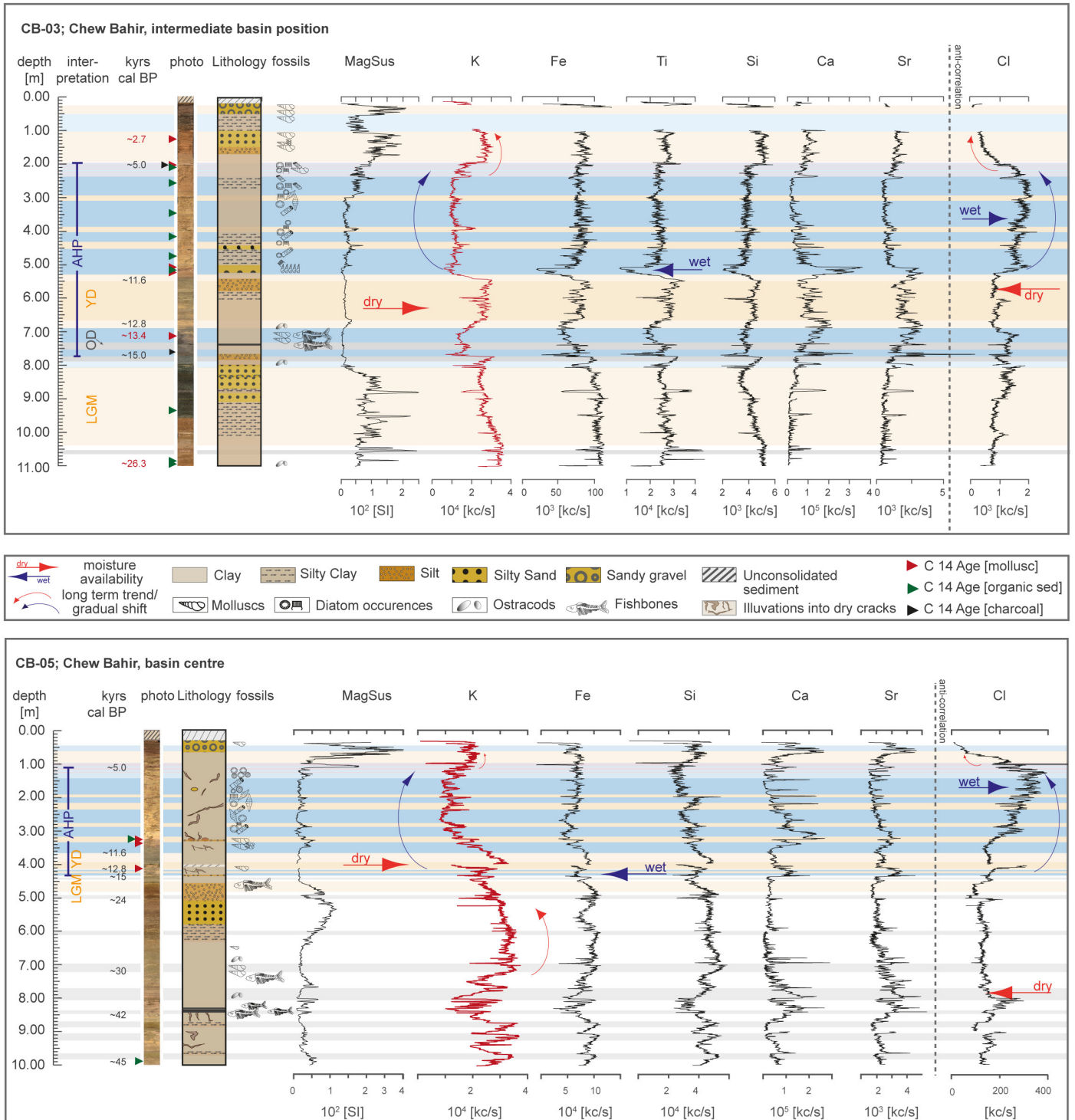


Figure 3.3 | Sediment composition of (A) CB-03 and (B) CB-05 with selected results of geochemical and physical analysis. Ages are given in calibrated kilo years before present. Ages in black refer to linearly interpolated values of the composite age-depth model. Red ages in (A) refer to radiocarbon ages from CB-03 (Table 3.2). Red and blue arrows point out prominent moisture shifts towards arid/humid conditions. Straight arrows indicate abrupt events, crooked show gradual trends. Orange (dry) and blue (wet) bars mark interpreted climate phases, referred to in the text; grey bars show arid phases that roughly coincide with high-latitude Heinrich events (H1–H4). MagSus – Magnetic Susceptibility; LGM – Last Glacial Maximum; YD – Younger Dryas; OD – Older Dryas; AHP – African Human Period.

between K-highs and -lows throughout the record, especially at 7.78 m in CB-03 (~15 ka; onset of the AHP) and 5.48 m in CB-03 (~11.8 ka; return to full humid conditions after YD). Furthermore, several short-term events expressed in sharp peaks in the K record modulate the long-term trends. Si, Ti, and Fe basically mirror the behavior of K even though the amplitudes of their signal vary compared to the K signal. The Ca signal largely follows, even though obscured by some distinct peaks not shown in the other elements (e.g. around 5 m in CB-03), the distribution signal observed in the other elements. However, below a certain depth (about 8 m in CB-03) Ca seems to be anti-correlated with Si, Ti, Fe, and K. Interestingly, the Sr signal almost exactly mirrors the Ca signal (Fig. 3.3). In contrast, the Cl signal is generally clearly anti-correlated to the signals shown by Si, Ti, Fe, and K (Fig. 3.3).

3.4.4 Fossil content

Freshwater diatoms, fish bones and some shells of the gastropod *Melanoides tuberculata* indicate lake episodes with fluctuating water levels throughout the whole record (Fig. 3.4). The gastropod *Melanoides tuberculata*, a very common and well-studied gastropod in African lakes, occurs as intact shells and shell fragments in several sections in all cores (see simplified column 'fossil' in Fig. 3.3). This mollusc species is found in high abundance during phases that are interpreted as

climatic transition zones with a shallow water cover as for example in two horizons that frame the extremely dry YD. Supporting this interpretation *Melanoides tuberculata* has been established as a strong indicator for the presence of a shallow lake, as it prefers a littoral habitat with aquatic and subaquatic plants (Pointier et al., 1992; Leng et al., 1999) in up to 2 m water depth with a tolerance to max. 10-15 m water cover. Fish bones are found episodically in a clayey matrix throughout the cores (Fig. 3.3), but are also deposited densely in some sharply defined layers that seem to correlate with a receding lake (e.g. end of the pre-YD lake phase and the pre-H1 lake phase recorded in 4.32–4.39 m in CB-05, correlating with fossilized fish remains in CB-03 at 7.38 m and 7.68 m). Diatoms (Fig. 3.3, Fig. 3.4) in both cores are restricted to the horizon that can roughly be attributed to the AHP lake phase (CB-03: 1.90–5.10 m; CB-05: 1.12–3.10 m; Fig. 3.3), with slightly changing taxa spectra within that layer. The spectrum comprises both, centric and pennate species, with a clear dominance of the genera *Aulacoseira* and *Cyclotellus*. Furthermore, species of the genera *Nitzschia*, *Synedra*, *Cymbella*, *Cyclotella* and *Achnanthes* could be identified, with the more habitat specific species restricted to the stable fresh water lake phase. *Aulacoseira* with a broader alkalinity and salinity tolerance occur almost throughout the entire section with diatoms and show dominance during shallow lake phases. The YD interval

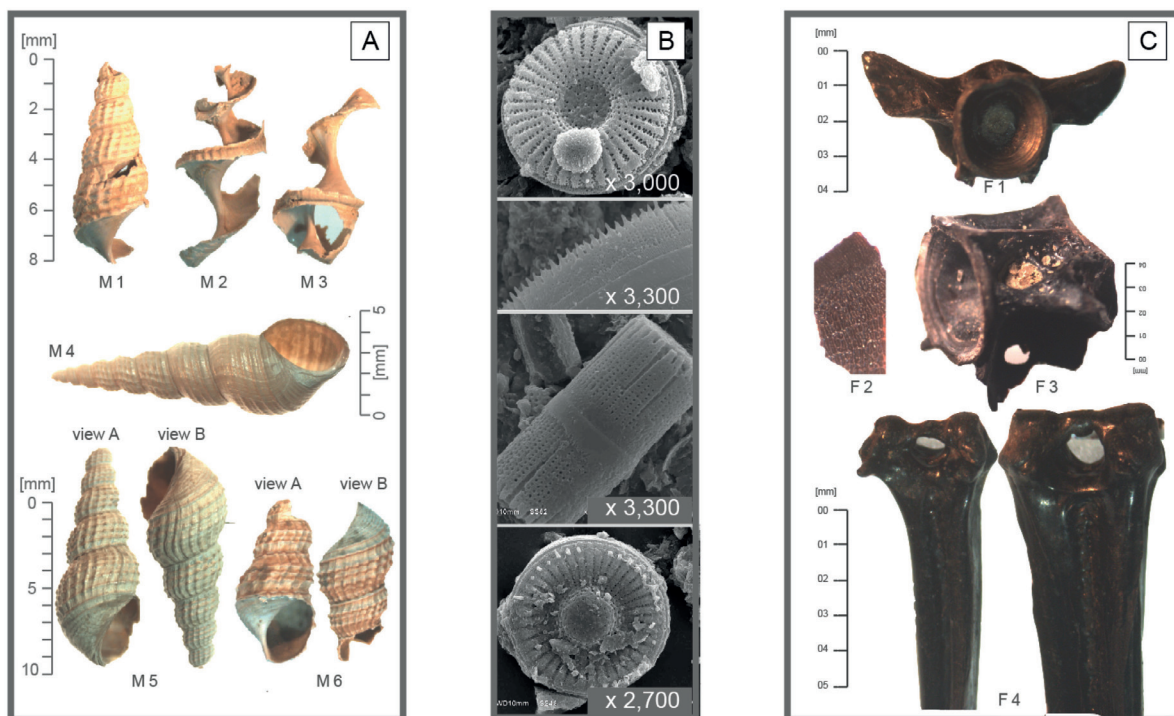


Figure 3.4 | Micro and macro fossils found in the Chew Bahir records CB-03 and CB-05, magnified under a binocular and a scanning electron microscope respectively. (A) The abundant gastropod *Melanoides tuberculata* from distinct horizon (M1–M5) in 520cm in CB-03 and 321cm in CB-05, both corresponding to the interval around 11–12kcalBP and 713cm in CB-03, 13.5 ka cal BP (M6). (B) Most abundant diatoms in the assemblage from Chew Bahir (from the top): *Cyclotella*, *Aulacoseira* (detail shot of frustule end that forms long chains), *Cyclotellus*; occurrences coincide with AHP lake phase (C) Fishbones, found in a distinct correlating layer in both records; 14.2 ka BP (F2), 15.2 ka BP (F1 + F4) and 32.7 ka BP (F3).

that caused the paleo-lake CB to regress to shallow and presumably highly saline and alkaline pools, is marked by a sharp decline of preserved frustules, expressed in the disappearance of diatom occurrences at the margin of the basin and the reduction to very few *Aulacoseira* frustules/ no diatoms at all in that section. After the YD, with the reestablishment of a freshwater lake, diatoms are quickly found again in great abundance and an increased variety of species for the entire AHP phase. This is also expressed in the Si curve reflecting the increase of biogenic silica in the lake by the autogenic production of silica rich frustules (Fig. 3.3).

3.5 Evaluation of K as paleoclimate signal

In the following we are going to show, that the K signal obtained with the XRF core scanner can be used to decipher paleoclimate changes that are related to significant variations in precipitation rates and thus to trace dry and humid phases. We will use an approach that is independent of the ideas that were developed during the pilot phase and that were based on results from CB-01 (Foerster et al., 2012). Why the K signal? As explained above and shown in Figure 3.3, all of the measured elements show systematic and correlating variations with core depth and thus with time. The K signal shows however, compared to the signal of the other elements, the best signal to noise ratio. As the objective is here to derive a reliable, fast and easy to measure paleoclimate proxy, we focused in our evaluation of the geochemical signal as possible tracer on K. The cause for the difference in signal clarity between the various elements is most likely a combination of two different effects: (1) the signal amplitude of a specific element itself and (2) the analytical specifics of the XRF scanning method.

The carrier mineral in which a chemical element is residing, controls the geochemical signal of a sediment record. This might seem a trivial statement but is easily and often forgotten looking at geochemical patterns only. In turn, the minerals composing a sediment record are influenced by a number of different factors, such as e.g. the type of rocks prevailing in the catchment area, the transport distance and mechanism, water chemistry, diagenetic processes and last but not least, due to its control on air temperature and precipitation rate and thus on the weathering process, the climate. However, all these factors are recorded differently by the chemical elements. E.g. if we have a clay dominated sediment record of alternating sequences that are composed of illite and smectite, the variations observed in Si, Al, Fe, and Ti are going to be much more subtle and harder to

detect than the changes that are observed in K. This is because the K content of illite is much larger than the K content of smectite, whereas the difference in Si, Al, Fe, and Ti content between illite and smectite is not that large (e.g. Deer et al., 2013).

Superimposed on this specific amplitude variation of each of the different elements are the specifics of the analytical method used. XRF is a well-established analytical technique for estimating the composition of geologic materials (e.g. Ramsey et al., 1995; Jenkins, 1999; De Vries and Vrebos, 2002). The principle of XRF analysis is based on excitation of electrons by incident X-ray-radiation. Ejection of electrons from inner atomic shells creates vacancies, which are filled by electrons falling back from the outer shells, emitting energy as a pulse of secondary X-ray-radiation. Emitted fluorescence energy and wavelength spectra are characteristic for specific elements, which allows an estimate of their relative abundances in the scanned material.

However, the fluorescence process is inefficient, resulting in a secondary radiation much weaker than the radiation of the incident beam. In addition, the secondary radiation from lighter elements is of relatively low energy, has low penetrating power, and is easily adsorbed. Thus, the K signal is also going to be clearer because of the physical specifics involved in the analytical process, since K is a heavier element than e.g. Si or Al. Furthermore, the measuring geometry of the XRF scanning method is, compared to quantitative XRF conducted on glass or pressed powder discs, poorly constrained. This is caused by inhomogeneity of the sample (e.g. variable water content and grain-size distribution), irregularities of the split core surface, and in some setups, spatial variations in thickness of an adhesive pore-water film forming directly below a protective foil covering the core surface. Accordingly, an additional noise level is added to the geochemical signal. Taking all these aspects into account, the best approach for establishing a paleoclimate proxy (that is based on the geochemical signal derived from the inorganic part of the sediment record) is, to focus on the element with the clearest analytical signal and determine the processes controlling it.

After establishing a down-core record for K (in counts per unit time and unit area) we looked at the ratios of counts in order to determine the actual controls of the K variations. Several authors have pointed to the advantage of using ratios of element intensities instead of the intensities of single elements (e.g. Pälke et al., 2001;

Croudace et al., 2006; Richter et al., 2006; Calvert and Pedersen, 2007). The benefit of comparing element ratios versus single elements is based on the unit-sum constraint on proportions, which can be invoked to explain the insensitivity of ratios to dilution effects. Let us envision a sediment sequence composed of the elements A, B, and C. Because the sum of these elements equals unity, selective addition or removal of element

C will affect the concentrations of both, A and B. This shows that part of the interaction that is observed in a geochemical record is an artefact of the constant-sum constraint on concentrations. If we now consider that A and B are merely of interest for the sediment system that is investigated in our example, we would regard C as noise only. This noise can be eliminated easily by evaluating the ratio of A/B or B/A, because these ratios

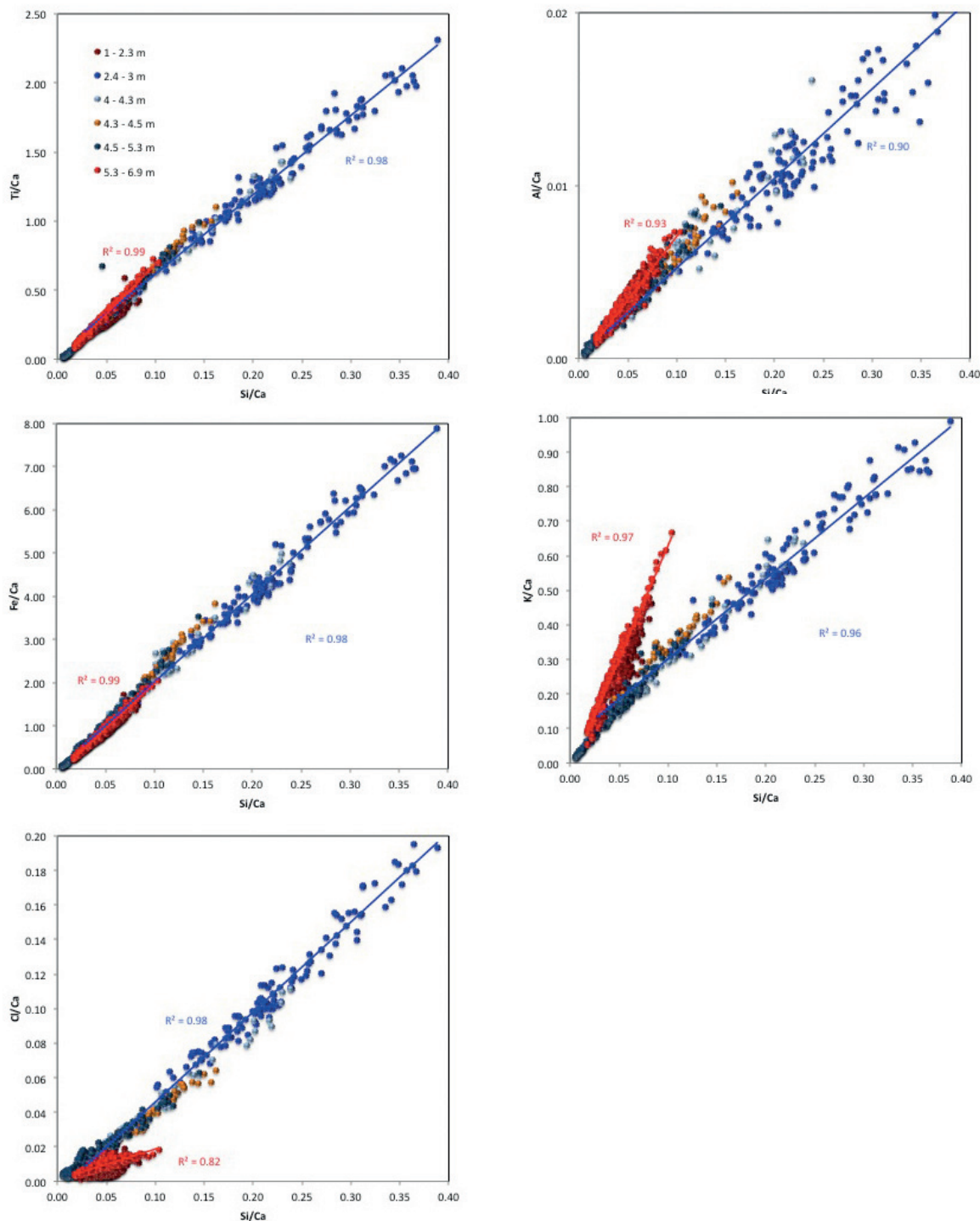


Figure 3.5 | Variations of Ca normalized elements with Ca normalized Si. Data are split into high and low-K groups and represent six characteristic depth intervals indicated by the different colors. Blue points generally denote the low-K group, whereas red dots denote the high-K group. Also shown are linear regression trends for both groups. As indicated by the different linear correlation trends, the geochemical signal of the high-K group is controlled by a different silicate phase or assemblage as the signal of the low-K group.

are fully independent of C. That way the part of the element-interaction being an artefact of the constant-sum constraint can be eliminated and the “true” interactions emerging from underlying physical and/or chemical properties of the system can be determined.

Often, the geochemical elements are normalized to Al_2O_3 . This is originally derived from the study of chemical weathering degrees of sub-aerial rock sequences and is based on the fact that Al_2O_3 behaves as a relatively immobile element during chemical weathering (e.g. see review by Bahlburg and Dobrzinski, 2011). However, for a sediment record deposited in an intercontinental basin with a relatively heterogeneous rock record in the catchment area and with a variably existing lake, the normalization of the bulk geochemical signal to Al_2O_3 does not seem useful for the assessment of the controlling mechanism of that signal, since such a complex system is not exclusively influenced by the degree of chemical weathering. This is verified by the preliminary XRD data obtained from the sediments. Basically, the obtained sediments can be split in two main groups – group one dominated by the assemblage analcime, calcite, illite and feldspar and group two dominated by smectite. As no calcite bearing rocks are exposed in the catchment area and the calcite is accompanied by analcime (a Na-rich zeolite precipitating only under highly alkaline water conditions e.g. Hay, 1966; Mees et al., 2005; Hay and Kyser, 2011), the geochemical signal that is observed in the Chew Bahir sediment records must be partly controlled by the formation of endogenic phases precipitated from the lake water. The carbonate influence on the geochemical signal is also indicated by the excellent correlation of Sr and Ca shown in Figure 3.3. This is caused by the fact that Sr^{2+} exchanges for Ca^{2+} in the crystal lattice of inorganic calcite. Thus we normalized the elements discussed in this study to Ca. In Figure 3.5 plots of Ti/Ca, Al/Ca, Fe/Ca, K/Ca, and Cl/Ca versus Si/Ca are shown; the data are split into high-K (red dots) and low-K (blue dots) groups with depth. Generally, all these elements show a positive correlation with Si converging at the point of origin, showing that in the first instance the geochemical signal of the obtained sediments is controlled by a binary mixture of carbonates and silicates. In addition, it becomes obvious that (1) the high-K group plots along a different binary mixing trend than the low-K group and (2) that the high-K group is characterized by a lower maximum Si/Ca ratio than the low-K group. The different mixing trends indicate that two compositionally fundamental different silicates or silicate assemblages, mixing with the carbonate, control the sediment geochemistry. The silicate or silicate assemblage forming the high-K group, are characterized by significantly higher K and a slightly

higher Ti, Al, and Fe content but lower Cl content than the low-K group. This would be consistent with the indications derived from the preliminary XRD data that the high-K group is dominated by illite as silicate phase, whereas the low-K group is dominated by smectite. The difference in the maximum Si/Ca ratio observed between the two groups, indicates that the carbonate content in the high-K group must be significantly higher than in the low-K group.

Even though we are not able to formulate a detailed model of the processes controlling the geochemical signal with the existing data, the systematics discussed above clearly indicate that the K signal is controlled by two significantly different silicates or silicate assemblages, varying systematically with depth and thus time. In addition, the fact that the high-K group is also characterized by a much higher authigenic carbonate content than the low-K group indicates that the high K signal is characteristic for a much drier climate than the low-K group. The precipitation of significant amounts of calcite in conjunction with analcime occurrences would have required a fundamental change in lake water chemistry to significantly more alkaline conditions and this in turn must have been caused by a significant decrease of precipitation rates.

3.6 Chew Bahir during a complete dry-wet cycle

Table 3.3 shows a simplified conceptual model of the responses of the Chew Bahir basin to wet and dry conditions. During arid phases in Chew Bahir (Table 3.3), we postulate a desiccated or strongly regressed lake, framed by a higher lithogenic fraction, and a lower biogenic productivity, high K counts as explained above, and activation of alluvial fans transporting weathering products of the metamorph gneisses from the constrained source in the western part of the catchment (i.e., the Hammar Range, Fig. 3.1) and lesser dilution. During wet phases, we postulate a freshwater lake with max. 50 m water level, finer grain deposits, freshwater diatom occurrences, high Cl and low K. For humid phases we can assume a dense vegetation cover on the slopes of the rift flanks and the whole catchment area, strongly restricting the erosion of weathered products into the basin via the alluvial fans. The main input system is fluvial, with the major provenance of deposits being northern, northeastern and northwestern catchment, depending on the magnitude of humidity. Sharp Ca peaks mark the onset of wet conditions, while their terminations (and onsets) are mostly accompanied by rich mollusc occurrences that require shallow-water habitats (max.10–15 m).

Comparing the climate records CB01, CB03 and CB05 from Chew Bahir (Fig. 3.6), derived from different proxies and from different sites in the same archive, it becomes apparent that the deposits have largely recorded the same climatic events, though with differing expressions. We postulate that minor lead or lags in the responses and the abruptness of the shifts are enhanced by proxy specificity, whereas the magnitude of the climate signal recorded in the CB deposits are site specific. The proxies could be controlled by three major factors bound in a complex interplay: distance to and restriction of the source (provenance), prevailing erosion and transport mechanism (fluvial, alluvial fan activity, aeolian) that is heavily influenced by density and type of vegetation and weathering (chemical versus mechanical) and possibly diagenetic processes.

Comparing the same dry-wet alternations (e.g. the onset of the AHP) in between the cores in Figure 3.6, makes clear that each coring site although just a few km apart and all belonging to the same sedimentary archive in the same catchment, still show remarkable site specific expressions. We assume the shifting dominance of the transport, erosional and possibly authigenic mechanisms to be responsible for that. Whereas CB-01 at the marginal area of the basin has a 2–3 fold resolution, is controlled by less processes and has a restricted provenance, CB-05 in the middle of the paleo-lake Chew Bahir has been subdued to redistribution processes in the former lake as both, the sedimentary composition and the partially overprinted elemental record during lake-phases indicate. Moreover, differences in between

the records as shown in Figure 3.6 can partly be attributed to the choice and strict limitation of the employed tie points that were used to tune the records to CB-01 (chapter 3.3.4). Aligning the records would be therefore more or less a matter of inserting indefinitely more tie points, to level out the differences in sedimentation rates, deposition processes and material, but is not the aim of this work designed in transect. Instead, all cores show the major dry-wet cycles and mostly the short-term climate events that are discussed in the following chapter. By integrating the results from all three areas in the basin in the following discussion, we essay to provide cross control to avoid misinterpretation of one bore site-specific disturbance in the deposits as an actual climate event.

3.7 Discussion of climatic variability recorded in Chew Bahir

The Chew Bahir records provide insights into the velocity and character of wet-dry-wet transitions over the past 46,000 years in the source region of AMH on different time scales. Three different modes were identified showing variability on precessional, millennial as well as decadal time scales, all characterized by different rates of change, some of which may have affected humans living in the area.

3.7.1 Variability on orbital time scales

On long-term times scales (10^4 yrs), the environmental record of the Chew Bahir covers the last two precessional cycles, including the African Humid Period

DRY arid phases in Chew Bahir	WET humid phases in Chew Bahir
<ul style="list-style-type: none"> desiccated or strongly regressed lake less and open vegetation on the slopes low sedimentation rate; possibly hiatus higher lithogenic fraction (GS), MS activation of alluvial fans (e.g. Hammar Range) high authigenic production of analcime and calcite (precipitates) dry phases often show calcite related Ca peaks high K counts 	<ul style="list-style-type: none"> freshwater lake with max 50 m water level dense vegetation cover on the slopes high sedimentation rate fine grained/lacustrine deposits: clay, fine silt fluvial input dominates (N, NE, NNW catchment) high biogenic productivity; fresh water diatoms, fish mollusc occurrences mark end/beginning of lake phase high Cl counts

Table 3.3 | Proxy evaluation for dry versus wet conditions in Chew Bahir. These findings are highly site specific and a generalization, an extrapolation to other sites should be handled with care and take setting of the site into consideration; exceptions can easily be found. The lake sediment proxies are controlled by three factors bound in a complex interplay: 1. distance to and restriction of the source, 2. prevailing transport mechanism (fluvial, alluvial fan activity, aeolian), that is also heavily influenced by density and type of vegetation and 3. weathering (chemical versus mechanical) and possibly diagenetic processes.

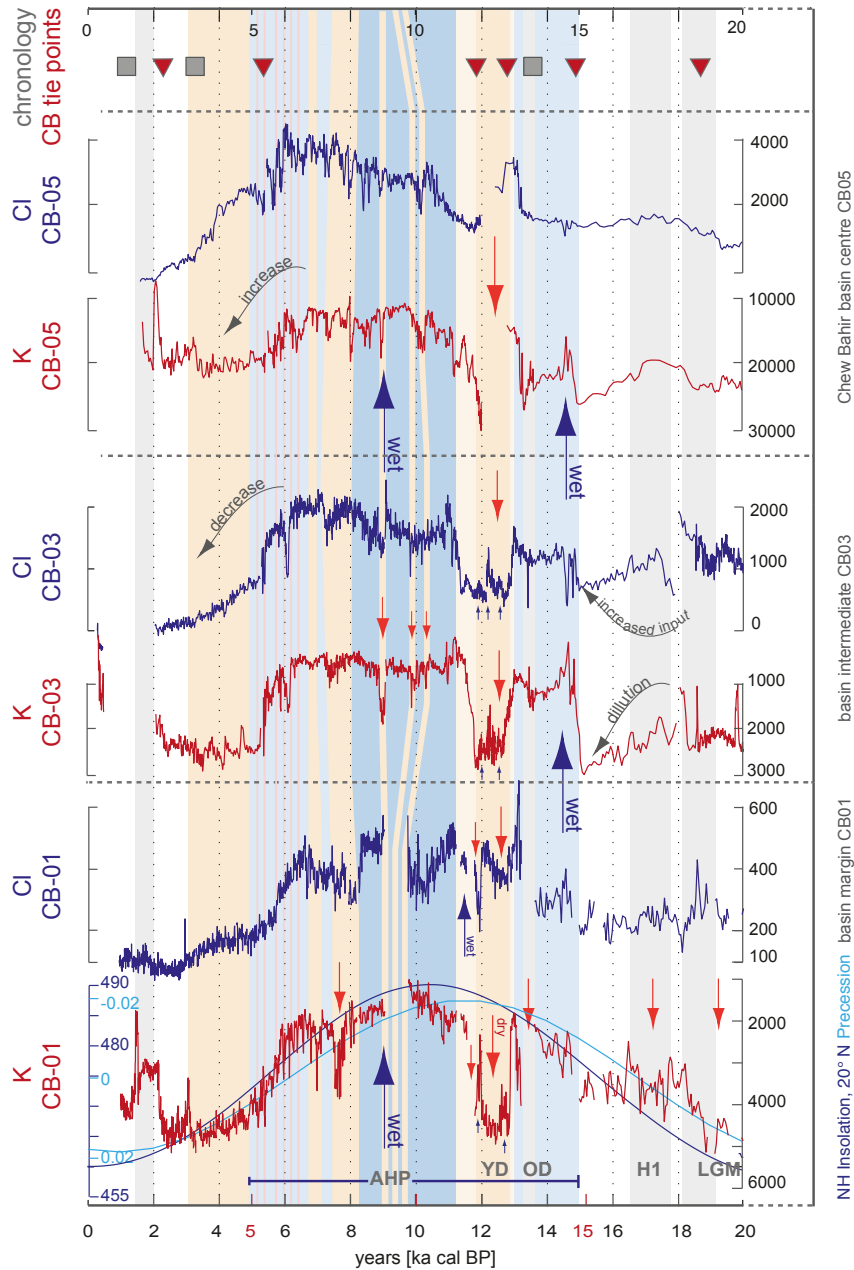


Fig. 3.6 | The established indicators for aridity – potassium [K] – (note inverted scale) and humidity – chlorine [Cl] – show variations within the Chew Bahir basin itself. Variability comprises magnitude and proxy specific reaction towards climatic signals. Aridity proxy K reacts more sensitively towards moister increase, humidity dependent Cl- responses sensitively to induced dry conditions. Age control along the Chew Bahir record is shown by grey squares (radiocarbon ages) and red triangles (CB correlation tie points). CB records are compared to NH summer (July) insolation variations (Laskar et al., 2004) and precession cycle (Berger and Loutre, 1991).

(AHP, ~15–5 ka BP), which has occurred during the last precession minimum (e.g., Gasse and Van Campo, 1994; Gasse, 2000; Trauth et al., 2001; 2003; Barker et al., 2004). This orbital configuration that is associated with higher insolation values in June–August (JJA) for the northern hemisphere (e.g., Laskar et al., 2004) has caused (a) the displacement of the ITCZ during JJA further north, bringing more moisture to regions that are usually not under the influence of the ITCZ, such as in the Sahara or Oman (e.g., Burns et al., 1998; Holzmann et al., 2000; Neff et al., 2001; Lancaster et al., 2002), (b) a stronger West African Summer Monsoon

(WAM) associated with a weakening of the African easterly jet that is responsible for the export of moisture out of Africa (e.g., Patricola and Cook, 2007) and (c) a shift of the CAB eastwards, over the highly-elevated plateaus of East Africa, therewith contributing to the synchronous character observed in the rise of lake levels in the basins of the EARS up to their overflow levels (Tierney et al., 2011; Costa et al., 2014; Junginger et al., 2014). Though, as recently shown by Junginger and Trauth (2013), the influence of the CAB during the last dry-wet cycle, has been restricted to phases with the highest Indian Summer Monsoon activity (~14.8–7.8 ka

BP) due to constraints imposed by an atmospheric pressure gradient between Asia and East Africa.

The Chew Bahir record contributes to the current debate on the relative abruptness of the onset and termination of the AHP, with the main contributors Peter deMenocal and collaborators (e.g., deMenocal, 2000; Tierney and deMenocal, 2013), supported by climate modelers such as Martin Claussen (e.g., Brovkin and Claussen, 2008), suggesting an abrupt termination of the AHP, in contrast to the findings of Stefan Kröpelin and collaborators (e.g., Kuper and Kröpelin, 2006; Kröpelin et al., 2008). In the Chew Bahir basin, the onset of the AHP occurred within less than 500 years, as indicated by the K record (Fig. 3.7), and also by the proxies Cl, Ti, Fe, Ca and fossil occurrences (Fig. 3.3, Fig. 3.6), and therefore much faster than the forcing but relatively slow at the time scale of a human life. These findings from Chew Bahir are in agreement with the records from other sites in East Africa (Gasse, 2000; Junginger et al., 2014). The character of the termination of the AHP in the Chew Bahir basin seems to be more complex, suggesting an onset of the Middle Holocene aridification at ~6.5 ka BP, reaching full arid conditions earliest at ~5 ka BP (Fig. 3.6, Fig. 3.7). Here, the rate of change seems to be generally lower than that of the forcing. Again, whether this could be called *gradual* or *abrupt* is rather a matter of the time scale in which we examine the transition.

The non-linear character and temporal offset of the AHP transitions in the EARS could have been related to a complex interplay of several factors: changes in precession, changes in the general source of moisture and boundary conditions imposed by the extent of NH ice sheets. In detail, it has been hypothesized that moisture availability towards the end of the AHP in tropical Africa was prolonged despite the decline in the NH summer insolation maximum due to a change in precession leading to a higher insolation in October–November (ON) at the equator (Marzin and Braconnot, 2009; Junginger et al., 2014). This latitudinal change in higher insolation values from maximum values during summer months for the NH to increased insolation values for ON at the equator (Fig. 3.7) was tied to a fundamental change in moisture sources. The CAB was prevented then from reaching the EARS – including Chew Bahir – by the reorganization of atmospheric pressure, but instead more moisture became available during the short rainy season in ON carried via the ITCZ (Junginger and Trauth, 2013). As explained in these studies, despite the comparatively enhanced moisture availability during the short rainy season, the provided moisture was not sufficient anymore to sustain the high lake levels in

the EARS as observed during NH summer insolation maxima. This change caused a delayed but relatively slow decline of the lakes at the termination of the AHP following ON insolation (Fig. 3.6). Moreover, the role of the dense vegetation cover that could develop during the long humid phase would have saved moisture within the system and thus might have also contributed to the delay of the precession driven aridification process.

For the equatorial insolation maximum during the long rainy season from March to May (MAM), that has occurred at ~22–16 ka BP we would theoretically expect a similar scenario as described above. The Chew Bahir climate records of CB01 and CB03 show a clear though moderate tendency towards more humid conditions slightly differing in their character but distinctly following the March–May equatorial insolation maximum (Fig. 3.6). But in contrast to the termination of the AHP, the equatorial MAM insolation – although preceding maximum JJA NH insolation – is not leading to a slow transition into the full humid conditions marking the onset of the AHP. This could be attributed to the fact that these equatorial insolation maxima in spring (MAM) coincide with the Last Glacial Maximum (LGM, 23–18 ka) that is known to have caused a reduction in moisture fluxes in the atmosphere on a global scale due to colder temperatures (Gasse, 2000). This generally low moisture availability is also reflected in numerous low-latitude sites showing a phase of pronounced aridity (e.g., Gasse, 2000; Barker et al., 2004), although the orbital parameters would predict increased rainfall. This implies that for the LGM interval, precipitation in Chew Bahir could have been controlled by high-latitude ice sheet coverage more than by the equatorial insolation alternations. Moreover, the extent of NH ice sheets most likely largely contributed to the delayed, but then relatively fast response of East African lake levels to the increase of NH summer insolation (Gasse, 2000). This approach states a threshold, assuming that a particular stage of ice cover retreat is necessary, to allow for the development of distinct atmospheric pressure gradients which in turn are steep enough for the CAB to be shifted eastwards and thus decidedly modulating the rapid establishment of deep lakes (Junginger and Trauth, 2013; Costa et al., 2014) in East Africa.

When extrapolating those three preconditions that significantly modulated the AHP to the penultimate precessional cycle (~46–23 ka) (Fig. 3.7), we would expect to see a similar expression in the records of Chew Bahir as during the last orbitally controlled wet-dry cycle, in particular for the intervals during insolation maxima at the equator in MAM and ON and NH JJA insolation maxima. Also, the age model (Fig. 3.2) seems to be

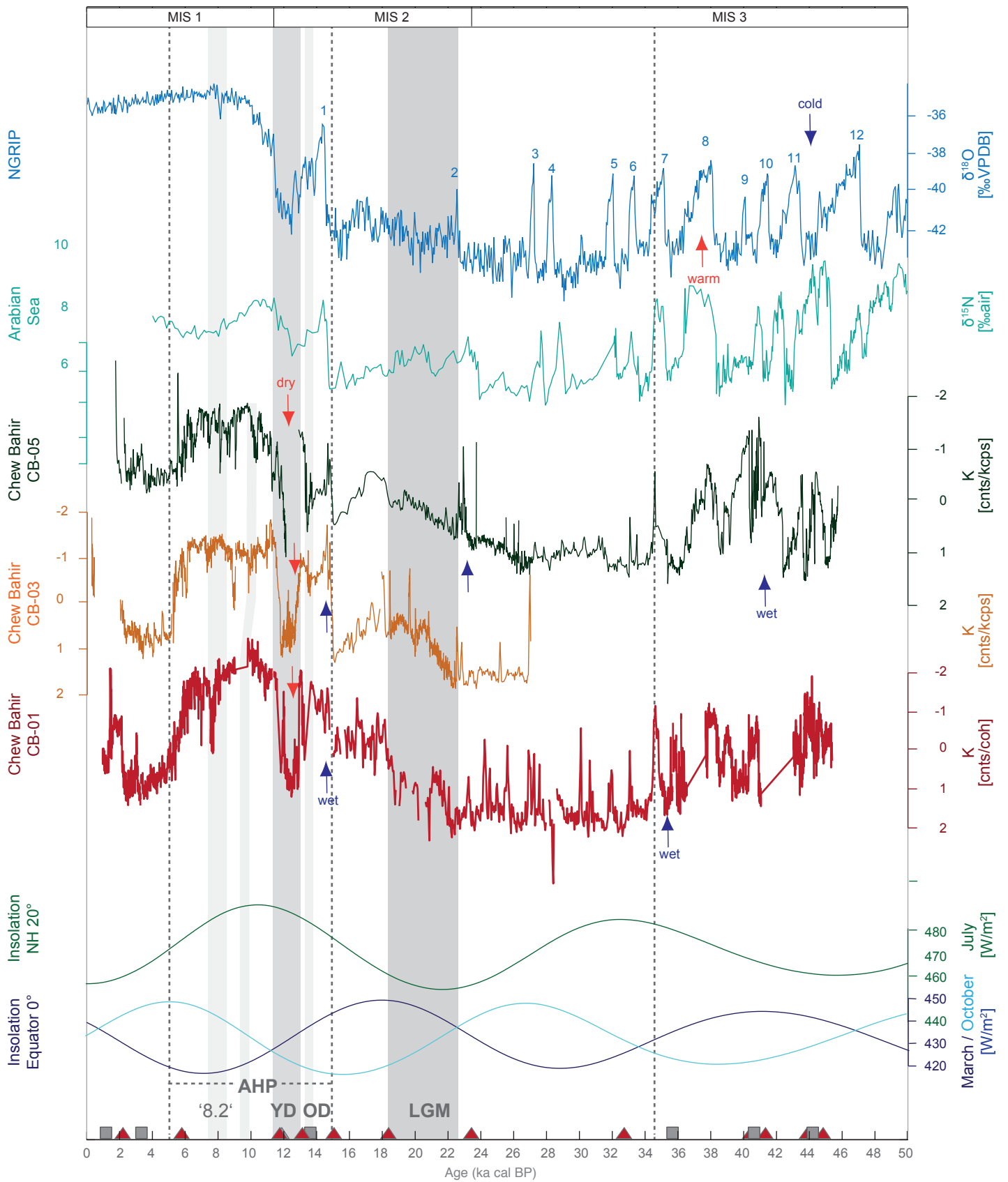


Figure 3.7 | Comparison of the Chew Bahir potassium (K) record with other paleo-climate records and insolation variation controlled by orbital configuration. Records plotted from top to bottom are as follows: $\delta^{18}\text{O}$ data from NGRIP (North Greenland Ice Core Project members, 2004) with numbers referring to DO-events; $\delta^{15}\text{N}$ data as proxy for denitrification and productivity in the Arabian Sea in the Gulf of Oman 18°N (Altabet et al., 2002); Chew Bahir potassium (K) record from cores CB-01 (paleo-lake shore), CB-03 (intermediate), CB-05 (paleo-lake center), (note reverse scale); Insolation variations for spring and fall from the equator (Laskar, 2004). Dotted lines indicate dry-wet-dry cycle AHP. Age control along the Chew Bahir record is shown by grey squares (radiocarbon ages) and red triangles (CB correlation tie points).

pointing at increased sedimentation rates between 45–35 ka BP. However, the penultimate precessional cycle could above all be characterized as a rather long dry episode, reflecting the reduced atmospheric pressure gradients and reduced moisture that heavily buffered the impact of orbital parameters on the East African climate during the last glacial (Gasse, 2000). Moreover it is crucial to bear in mind that the amplitude of these precession cycles (and therewith the insolation) is also controlled by variations in eccentricity (Trauth et al., 2003).

3.6.2 Variability on millennial time scales

Despite the climate's overall arid character during MIS 3 (our core covers ~46–23 ka BP), we observe abrupt short-term excursions from this level of aridity towards more humid conditions in southern Ethiopia, lasting between ~500–1000 years with one exception at ~42.5–40.5 ka BP that lasted ~2000 years. The timing, duration and character of some of these dry-wet shifts could possibly look similar to the high-latitude millennial-scale climate oscillations (Fig. 3.7) during the last glacial that are known as Dansgaard-Oeschger cycles (D-O) (e.g. Dansgaard et al., 1993, Braun et al., 2005), although a one-to-one correlation of the dry-wet shifts to the D-O cycles is not possible for now due to the large uncertainties of the age model prior to the LGM. These cycles, together with the Heinrich-events (H0-H6) (e.g., Heinrich, 1988; Bond and Lotti, 1995; Hemming, 2004; Jullien et al., 2007) are known to have left a global footprint that is mostly coinciding with dry spells in low-latitude Africa (e.g., Brown et al., 2007).

Whether the millennial cycles or the pronounced shifts in Chew Bahir lead or lag these high-latitude events is therefore not clear, since we refrain from pairing designated D-O cycles to the millennial dry-wet cycles that are distinct in the CB record. Therefore we cannot contribute to debate on whether possibly low-latitude forcing could be the triggering factor of these events. The most recent and rather sharply defined wet interval on a millennial time scale interrupts the mid-late Holocene dry phase between 2.2–1.3 ka BP. This excursion to humid conditions could possibly also be related to pronounced short-term changes in the solar activities (Solanki et al., 2004), despite occurring during an interglacial.

There are two similar climate events that occurred during the AHP (thus full humid conditions), but featuring with a distinctive shift towards major drought conditions a seemingly reversed character: A major

arid event around 14 ka BP in Chew Bahir resembles a synchronous decline in Lake Victoria (Stager et al., 2002) that was interpreted as the tropical African expressions of the cold European Older Dryas (OD) event otherwise sparsely documented for low-latitudes. The most prominent and sharply defined dry phase in the CB record that occurs between 12.8 ka BP and 11.6 ka BP and therewith closely coincides with the H0-event (Bond and Lotti, 2005) or Younger Dryas chronozone that is well documented to have caused extreme arid conditions in a series of sites in Africa north of 10°S (e.g. Barker et al., 2004). Also the internal variability within the YD (e.g. Liu et al., 2013), with at least two wet excursions, is distinct in our CB record (Fig. 3.7). The return to full humid conditions occurred relatively fast within ± 200 years, as indicated by the humidity sensitive K record, a freshwater diatom flora and the sensitive Ca marker peaks and is also consistent with other records in East Africa north of 10°S (Gasse, 2000; Barker et al., 2004; Junginger et al., 2014).

Aside from the underlying driving mechanisms, the question remains whether the moisture that was provided by these millennial-scale wet periods was sufficient to allow the establishment of open fresh water lakes, crucial for the survival of mammals including the AMH or whether the enhanced moisture did in fact not exceed evaporation, merely leaving small and alkaline lakes behind. Barker et al. (2004) has shown that central Kenyan lakes have remained alkaline although exceeding present day levels during moisture periods within the last glacial.

3.6.3 Variability on centennial to decadal time scales

The K record also shows clearly decadal to centennial scale short-term events punctuating the AHP by several dry intervals, such as visible at ~10.5, ~9.5 ka BP, 8.15–7.8 ka BP and ~7 ka BP (Fig. 3.7). While these events are available with no doubt, their cause is unclear. Given the decreasing signal-to-noise ratio at these time scales, in conjunction with the uncertainties of the age model, any interpretation of these events is pure speculation. However, some of these drought events may correlate -within a given error range- with records implying the weakening of the ISM (Neff et al., 2001; Gupta et al., 2005; Wang et al., 2005), increased iceberg discharges in the NH (Bond et al., 2001), reduced precipitation in West and Central Africa (Stager et al., 2002; Weldeab et al., 2007) as well as considerable regressions of several lakes in the EARS with falling lake levels of up to -120 m (e.g., Gasse, 2000; Stager et al., 2002;

Brown and Fuller, 2008; Junginger et al., 2014). These events that have been observed on a global scale have been associated with short-term changes in solar activity (Solanki et al., 2004), although the exact physical process still remains poorly understood (Gray et al., 2010).

The event between ~8.15–7.8 ka BP, however, differs from the other high-frequency drought events in the record due to its gradual drying character of over ~350 years. The gradual drying trend is also observed in other low latitude records (e.g., Fleitmann et al., 2003, Dykoski et al., 2005; Gupta et al., 2005; Weld-eab et al., 2007) and is widely assumed to predate the abrupt cooling event at 8.2 ka BP in the NH (e.g., Alley et al., 1997). Lake level reconstructions in the EARS revealed pronounced lake regressions up to almost full desiccations (Gillespie et al., 1983, Gasse, 2000; Garcin et al., 2012; Junginger et al., 2014). The relatively slow, 1,500-year long aridification trend at the end of the AHP starting at ~6.5 ka ago in southern Ethiopia is also punctuated by several minor 20–80 year long dry events as observed by Trauth et al. (in press) indicating that even gradual transitions can be influenced by short-term droughts affecting several generations of the AMH. A plausible mechanism behind these rapid excursions towards dry climate has not yet been found (Trauth et al., press).

3.8 Conclusions and outlook

The Chew Bahir transect covers the environmental history of the last 46,000 years, reflecting dry-wet cycles on timescales from ten to ten thousand years. These transitions are very diverse in their character and occur at all time scales, some of which may have affected humans living in the area. The results from this pilot study suggests that the Chew Bahir basin is an ideal site for studying climate-human interactions within the framework of the HSPDP project.

Acknowledgements

The Chew Bahir Project is part of the ICDP „Hominin Sites and Paleolakes Drilling Program Project“. It has received funding and support from the German DFG-SPP 1006 „International Continental Scientific Drilling Program“, the DFG-funded CRC 806 „Our Way to Europe“ and the DFG-SPP 1488 „Planetary Magnetism“. We thank the Addis Ababa University for continuing support in the Chew Bahir Project. We thank V. Wennrich for support with the XRF scanning procedure and advise related to the geochemical interpretation and J. Rethemeyer and her

team for the support related to radiocarbon dating. We thank J.P. Francois, J. Hense, T. Kassa, K. Panagiotopoulos and K. Schittek for fruitful discussions. We also acknowledge the dedicated lab assistance of D. Becker, J. Jacob, N. Mantke, O. Oswald, S. Rohland, J. Urban and J. Wowrek.

3.9 References

- Alley, R.B., Mayewski, A., Sowers, T., Stuiver, M., Taylor, K.C. and Clark, P.U.: Holocene climatic instability: A prominent, widespread event 8200 years ago, *Geology*, 25, 483–486, 1997.
- Altabet, M.A., Higginson, M.J. and Murray, D.W.: The effect of millennial-scale changes in Arabian Sea denitrification on atmospheric CO₂, *Nature*, 415, 159–162, 2002.
- Ambrose, S.H.: Late Pleistocene human population bottlenecks, volcanic winter, and the differentiation of modern humans, *Journal of Human Evolution*, 35, 115–118, 1998.
- Bahlburg, H. and Dobrzinski, N.: A review of the Chemical Index of Alteration (CIA) and its application to the study of Neoproterozoic glacial deposits and climate transitions, in: *The Geological Record of Neoproterozoic Glaciations*, Arnaud, E., Halverson, G. P. and Shields, G. A. (eds.), Geological Society of London, London, UK, 81–92, London, 2011.
- Barker, P.A., Talbot, M.R., Street-Perrott, F.A., Marret, F., Scourse, J. and Odada, E.O.: Late Quaternary variability in intertropical Africa, in: *Past Climate Variability through Europe and Africa*, Battarbee, R.W., Gasse, F., Stickley, C.E. (eds.), Springer, Dordrecht, Netherlands, 117–138, 2004.
- Berger, A. and Loutre, M.-F.: Insolation values for the climate of the last 10 million years, *Quaternary Science Reviews*, 10, 297–317, 1991.
- Björck, S. and Wohlfarth, B.: 14C chronostratigraphic techniques in paleolimnology, in: *Tracking Environmental Change Using Lake Sediments Volume 1: Basin Analysis, Coring, and Chronological Techniques*. Last, W. and Smol, J. (eds.), Springer, Dordrecht, Netherlands, 205–246, 2001.
- Blaauw, M. and Christen, J. A.: Flexible paleoclimate age-depth models using an autoregressive gamma process, *Bayesian Analysis*, 6, 457–474, doi:10.1214/11-BA618, 2011.
- Bond, L. and Lotti, R.: Iceberg Discharges into the North Atlantic on Millennial Time Scales During the Last Glaciation, *Science*, 267, 1005–1010, 1995.
- Bond, G., Kromer, B., Beer, J., Muscheler, R., Evans, M.N., Showers, W., Hoffmann, S., Lotti-Bond, R., Hajdas, I., Bonani, G.: Persistent Solar Influence on North Atlantic Climate During the Holocene, *Science*, 294, 2130–2136, 2001.
- Braun, H., Christl, M., Rahmstorf, S., Ganopolski, A., Mangini, A., Kubatzki, C., Roth, K., and Kromer, B.: Possible solar origin of the 1,470-year glacial climate cycle demonstrated in a coupled model, *Nature*, 438, 208–211, 2005.
- Bronk Ramsey, C.: Deposition models for chronological records, *Quaternary Sci. Rev.*, 27, 42–60, 2008.

- Bronk Ramsey, C.: Bayesian analysis of radiocarbon dates, *Radiocarbon*, 51, 337–360, 2009.
- Bronk Ramsey, C.: OxCal v4.1.7 Calibration Software, available at: <http://c14.arch.ox.ac.uk/> (last access: 19 November 2013), 2010.
- Brown, E.T. and Fuller, C.H.: Stratigraphy and tephra of the Kibish Formation, southwestern Ethiopia, *Journal of Human Evolution*, 55, 366–403, 2008.
- Brown, E.T., Johnson, T.C., Scholz, C.A., Cohen, A.S., King, J.W.: Abrupt change in tropical African climate linked to the biopolar seesaw over the past 55,000 years, *Geophysical Research Letters*, 34, L20702, 2007.
- Brown, M.C., Frank, U., Foerster, V.; Kassa, T., Nowaczyk, N., Schäbitz, F., and Korte, M.: Holocene paleomagnetic field variations recorded in lake sediments from southern Ethiopia, AGU Fall Meeting, San Francisco, USA, 3–7 December 2012, GP33B-01, 2012.
- Burnett, A.P., Soreghan, M. J., Scholz, C. A. and Brown, E. T.: Tropical East African climate change and its relation to global climate: A record from Lake Tanganyika, Tropical East Africa, over the past 90+kyr, *Palaeogeography, Palaeoclimatology, Palaeoecology*, 303, 155–167, 2011.
- Burns, S.J., Matter, A., Frank, N. and Mangini, A.: Speleothem-based paleoclimate record from northern Oman, *Geology*, 26, 499–502, 1998.
- Calvert, S.E., Pedersen, T.F.: Elemental proxies for palaeoclimatic and palaeoceanographic variability in marine sediments: interpretation and application, in: *Developments in Quaternary Research*, Hillaire, C. and de Vernal, A. (eds.), Elsevier Science, Amsterdam, Netherlands, 567–644, 2007.
- Camberlin, P.: Rainfall anomalies in the source region of the Nile and their connection with the Indian summer monsoon, *J. Climate*, 10, 1380–1392, 1997.
- Carto, S.L., Weaver, A.J., Hetherington, R., Lam, Y. and Wiebe, E.C.: Out of Africa and into an ice age: on the role of global climate change in the late Pleistocene expansion of early modern humans out of Africa, *Journal of Human Evolution*, 56, 139–151, 2009.
- Castañeda, I.S., Mulitza, S., Schefuß, E., Santos, R.A.L., Damste, J.S.S. and Schouten, S.: Wet phases in the Sahara/Sahel region and human expansion patterns in North Africa, *PNAS*, Proceedings of the National Academy of Sciences, 106, 1–5, 2009.
- Cohen, A.S.: *Paleolimnology, The History and Evolution of Lake Ecosystems*, Oxford University Press, Oxford, pp. 500, 2003.
- Cohen, A., Arrowsmith, R., Behrensmeier, A. K., Campisano, C., Feibel, C., Fisseha, S., Johnson, R., Kubsa Bedaso, Z., Lockwood, C., Mbua, E., Olago, D., Potts, R., Reed, K., Renaut, R., Tiercelin, J.-J., and Umer, M.: Understanding paleoclimate and human evolution through the hominin sites and paleolakes drilling project, *Scientific Drilling*, 8, 60–65, doi:10.2204/iodp.sd.8.10.2009, 2009.
- Corti, G.: Continental rift evolution: from rift initiation to incipient break-up in the Main Ethiopian Rift, East Africa, *Earth-Science Reviews*, 96, 1–53, 2009.
- Costa, K., Russell, J., Konecky, B. and Lamb, H.: Isotopic reconstruction of the African Humid Period and Congo Air Boundary migration at Lake Tana, Ethiopia, *Quaternary Science Reviews*, 83, 58–67, 2014.
- Croudace, I.W., Rindby, A. and Rothwell, R.G.: ITRAX: description and evaluation of a new X-ray core scanner, in: *New ways of looking at sediment cores and core data*, Rothwell, R.G., (Ed.) Geological Society Special Publication, 267, London, UK, 51–63, 2006.
- Dansgaard, W., Johnson, S.J., Clausen, H.B., Dahl-Jensen, D., Gundestrup, N.S., Hammer, C.U., Hvidberg, C.S., Steffensen, J.P., Sveinbjornsdottir, A.E., Jouzel, J. and Bond, G.: Evidence for general instability of past climate from a 250-kyr ice-core record, *Nature*, 364, 218–220, 1993.
- Day, M.H.: Omo human skeletal remains, *Nature*, 222, 1135–1138, 1969.
- deMenocal, P., Ortiz, J., Guilderson, T., Adkins, J., Sarnthein, M., Baker, L. and Yarusinsky, M.: Abrupt onset and termination of the African Humid Period: rapid climate responses to gradual insolation forcing, *Quaternary Science Reviews*, 19, 347–361, 2000.
- De Vries, J.L., Vrebos, B.A.R.: Quantification of infinitely thick specimens by XRF analysis, in: *Handbook of X-Ray Spectrometry, Second Edition*, van Grieken, R.E., Markovicz, A.A. (eds.), Marcel Dekker, New York, 341–405, 2002.
- Dykoski, C.A., Edwards, R.L., Cheng, H., Yuan, D., Cai, Y., Zhang, M., Lin, Y., Qing, J., An, Z. and Revenaugh, J.: A high-resolution, absolute dated Holocene and deglacial Asian monsoon record from Dongge Cave, China, *Earth and Planetary Science Letters*, 233, 71–86, 2005.
- Ebinger, C.J., Yemane, T., Harding, D., Tesfaye, S., Kelley, S. and Rex, D.: Rift deflection, migration, and propagation: linkage of the Ethiopian and Eastern rifts, Africa, *Geological Society of America Bulletin*, 112, 163–176, 2000.
- Felton, A.F., Russell, J.M., Cohen, A.S., Baker, M.E., Chesley, J.T., Lezzar, K.E., McGlue, M.M., Pigati, J.S., Quade, J., Stager, J.C. and Tiercelin, J.J.: Paleolimnological evidence for the onset and termination of glacial aridity from Lake Tanganyika, Tropical East Africa, *Palaeogeogr. Palaeoclimatol. Palaeoecol.*, 252, 405–423, 2007.
- Fleitmann, D., Burns, S.J., Mudelsee, M., Neff, U., Kramers, J., Mangini, A. and Matter, A.: Holocene forcing of the Indian monsoon recorded in a stalagmite from Southern Oman, *Science*, 300, 1737–1739, 2003.
- Foerster, V., Junginger, A., Langkamp, O., Gebru, T., Asrat, A., Umer, M., Lamb, H., Wennrich, V., Rethemeyer, J., Nowaczyk, N., Trauth, M.H. and Schäbitz, F.: Climatic change recorded in the sediments of the Chew Bahir basin, southern Ethiopia, during the last 45,000 years, *Quaternary International, Special Issue Collaborative Research Center*, doi.org/10.1016/j.quaint.2012.06.028, 2012.
- Foerster, V., Vogelsang, R., Junginger, A., Asrat, A., Lamb, H.F., Schaebitz, F., Trauth, M.H.: Environmental Change and Human Occupation of Southern Ethiopia and Northern Kenya during the last 20,000 years, *Quaternary Science Reviews*, submitted.
- Frank, U., Brown, M., Foerster, V., and Schäbitz, F.: Paleomagnetism of Lake Sediments, Chew Bahir, Ethiopia, AGU Fall Meeting, San Francisco, USA, 5–9 December 2011, GP43A-04, 2011.
- Garcin, Y., Melnick, D., Strecker, M.R., Olago, D. and Tiercelin, J.-J.: East African mid-Holocene wet–dry transition recorded in palaeo-shorelines of Lake Turkana, northern Kenya Rift, *Earth and Planetary Science Letters*, 331–332, 322–334, 2012.

- Gasse, F.: Hydrological changes in the African tropics since the Last Glacial Maximum, *Quaternary Science Reviews*, 19, 189–211, 2000.
- Gasse, F. and Van Campo, E.: Abrupt post-glacial climate events in West Asia and North Africa monsoon domains, *Earth and Planetary Science Letters*, 126, 435–456, 1994.
- Geyh, M.A., Schotterer, U. and Grosjean, M.: Temporal changes of the (super 14) C reservoir effect in lakes, *Radiocarbon*, 40, 921–931, 1998.
- Gillespie, R., Street-Perrott, F.A. and Switsur, R.: Post-glacial arid episodes in Ethiopia have implications for climate prediction, *Nature*, 306, 680–683, 1983.
- Govin, A., Holzwarth, U., Heslop, D., Ford Keeling, L., Zabel, M., Mulitza, S., Collins, J.A. and Chiessi, C.M.: Distribution of major elements in Atlantic surface sediments (36°N–49°S): Imprint of terrigenous input and continental weathering, *Geochem Geophys Geosyst*, 13, 1–23, 2012.
- Gray, L. J., Beer, J., Geller, M., Haigh, J.D., Lockwood, M., Matthes, K., Cubasch, U., Fleitmann, D., Harrison, G., Hood, L., Luterbacher, J., Meehl, G.A., Shindell, D., van Geel, B. and White, W.: Solar influences on climate, *Rev. Geophys.*, 48, RG4001, doi:10.1029/2009RG000282, 2010.
- Gupta, A. K., Das, M. and Anderson, D.M.: Solar influence on the Indian summer monsoon during the Holocene, *Geophys. Res. Lett.*, 32, L17703, doi:10.1029/2005GL022685, 2005.
- Hay, R. L., and Kyser, T. K.: Chemical sedimentology and paleoenvironmental history of Lake Olduvai, a Pliocene lake in northern Tanzania, *Geological Society of America Bulletin*, 113, 1505–1521, 2011.
- Hay, R. L.: Zeolites and Zeolitic Reactions in Sedimentary Rocks, *Geological Society of America Special Papers*, 85, 1–122, 1966.
- Heinrich, H.: Origin and consequences of cyclic ice rafting in the Northeast Atlantic Ocean during the past 130,000 years, *Quaternary Research*, 29, 142–152, 1988.
- Hemming, S.R.: Heinrich events: Massive late Pleistocene detritus layers of the North Atlantic and their global climate imprint, *Review of Geophysics*, 42, 1–43, 2004.
- Hildebrand, E., Brandt, S. and Lesur-Gebremariam, J.: The Holocene archaeology of Southwest Ethiopia: new insights from the Kafa archaeological project, *African Archaeological Review*, 27, 255–289, 2010.
- Hildebrand, E. and Grillo, K.: Early herders and monumental sites in eastern Africa: New radiocarbon dates, *Antiquity*, 86, 338–352, 2012.
- Hoelzmann, P., Kruse, H., Rottinger, F., 2000. Precipitation estimates for the eastern Saharan palaeomonsoon based on a water balance model of the West Nubian Palaeo-lake Basin. *Glob. Planet. Chang.* 26, 105–120.
- IRI (International Research Institute for Climate and Society), Earth Institute, Columbia University, Climate and Society Maproom: <http://iridl.ldeo.columbia.edu/maproom/>, last access: 4 October, 2013.
- Jenkins, R.: *X-Ray Fluorescence Spectroscopy*, Second Edition. Wiley & Sons, New York, 207, pp.1999.
- Jullien, E., Grousset, F., Malaizé, B., Duprat, J., Sanchez-Goni, M.F., Eynaud, F., Charlier, K., Schneider, R., Bory, A., Bout, V. and Flores, J.A.: Low-latitude “dusty events” vs. high-latitude “icy Heinrich events”, *Quaternary Research*, 68, 379–386, 2007.
- Junginger, A. and Trauth, M.H.: Hydrological constraints of paleo-Lake Suguta in the Northern Kenya Rift during the African Humid Period (15–5 ka BP), *Global and Planetary Change*, 111, 174–188, 2013.
- Junginger, A., Roller, S., Olaka, L. A., and Trauth, M. H.: The effect of solar radiation changes on water levels in paleo-Lake Suguta, Northern Kenya Rift, during late Pleistocene African Humid Period (15–5 ka BP), *Paleogeography, Paleoclimatology, Paleoecology*, 396, 1–16, 2014.
- Johnson, T.C., Halfman, J.D. and Showers, W.J.: Paleoclimate of the past 4000 years at Lake Turkana, Kenya, based on the isotopic composition of authigenic calcite, *Palaeogeography, Palaeoclimatology, Palaeoecology*, 85, 189–198, 1991.
- Kliem, P., Dirk Enters, Annette Hahn, Christian Ohlendorf, Agathe Lisé-Pronovost, Guillaume St-Onge, Stefan Wastegård, Bernd Zolitschka and the PASADO science team: Lithology, radiocarbon chronology and sedimentological interpretation of the lacustrine record from Laguna Potrok Aike, southern Patagonia, *Quaternary Science Reviews*, 71, 54–62, 2013.
- Kröpelin, S., Verschuren, D., Lézine, A.-M., Eggermont, H., Cocquyt, C., Francus, P., Cazet, J.-P., Fagot, M., Rumes, B., Russell, J. M., Darius, F., Conley, D. J., Schuster, M., von Suchodoletz, H. and Engstrom, D.R.: Climate-Driven Ecosystem Succession in the Sahara: The Past 6000 Years, *Science*, 320, 765–768, 2008.
- Lancaster, N., Kocurek, G., Singhvi, A., Pandey, V., Deynoux, M., Ghienne, J.-F. and Lô, K.: Late Pleistocene and Holocene dune activity and wind regimes in the western Sahara Desert of Mauritania, *Geology*, 30, 991–994, 2002.
- Laskar, J., Gastineau, M., Joutel, F., Robutel, P., Levrard, B. and Correia, A.: A long term numerical solution for the insolation quantities of Earth, *Astronomy and Astrophysics*, 428, 261–285, 2004.
- Leng, M.J., Lamb, A.L., Lamb, H.F. and Telford, R.J.: Palaeoclimatic implications of isotopic data from modern and early Holocene shells of the freshwater snail *Melanooides tuberculata*, from lakes in the Ethiopian Rift Valley, *Journal of Paleolimnology*, 21, 97–106, 1999.
- Levin, N. E., E. J. Zipser, and T. E. Cerling: Isotopic composition of waters from Ethiopia and Kenya: Insights into moisture sources for eastern Africa, *J. Geophys. Res.*, 114, D23306, doi:10.1029/2009JD012166, 2009.
- Liu, D., Wang, Y., Cheng, H., Kong, X. and Chen, S.: Centennial-scale Asian monsoon variability during the mid-Younger Dryas from Qingtian Cave, central China, *Quaternary Research*, 80, 199–206.
- Marzin, C. and Braconnot, P.: Variations of Indian and African monsoons induced by insolation changes at 6 and 9.5 kyr BP, *Clim. Dyn.*, 33, 215–231, 2009.
- Maslin, M.A. and Trauth, M.H.: Plio-Pleistocene East African Pulsed Climate Variability and its influence on early human evolution, in: “The First Humans - Origins of the Genus Homo”, Grine, F. E., Leakey, R.E. and Fleagle J.G. (Eds.), Springer Verlag, Dordrecht, Netherlands, *Vertebrate Paleobiology and Paleoanthropology Series*, 151–158, 2009.
- McDougall, I., Brown, F.H. and Fleagle, J.G.: Stratigraphic

- placement and age of modern humans from Kibish, Ethiopia, *Nature*, 433, 733–736, 2005.
- Mees, F., Stoops, G., Van Ranst, E., Paepe, R. and Van Overloop, E.: The nature of zeolite occurrences in deposits of the Olduvai Basin, northern Tanzania, *Clays and Clay Minerals*, 53, 659–673, 2005.
- Meyers, P.A.: Applications of organic geochemistry to paleolimnological reconstructions: a summary of examples from the Laurentian Great Lakes, *Organic Geochemistry*, 34, 261–289, 2003.
- Mulitza, S., Prange, M., Stuut, J.-B., Zabel, M., von Dobeneck, T., Itambi, A. C., Nizou, J., Schulz, M. and Wefer, G.: Sahel megadroughts triggered by glacial slowdowns of Atlantic meridional overturning, *Paleoceanography*, 23, PA4206, doi:10.1029/2008PA001637, 2008.
- Neff, U., Burns, S.J., Mangini, A., Mudelsee, M., Fleitmann, D. and Matter, A.: Strong coherence between solar variability and the monsoon in Oman between 9 and 6 kyr ago, *Nature*, 411, 290–293, 2001.
- Nicholson, S.E.: A review of climate dynamics and climate variability in eastern Africa, in: *The Limnology, Climatology and Paleoclimatology of the East African Lakes*, Johnson, T.C. and Odada, E.O. (eds.), Gordon & Breach, Amsterdam, Netherlands, 25–56, 1996.
- North Greenland Ice Core Project members: High-resolution record of northern hemisphere climate extending into the last interglacial period, *Nature*, 431, 147–151, 2004.
- Ohlendorf, C., Gebhardt, C., Hahn, A., Kliem, P., Zolitschka, B. and the PASADO science team: The PASADO core processing strategy - A proposed new protocol for sediment core treatment in multidisciplinary lake drilling projects, *Sedimentary Geology*, 239, 104–115, 2011.
- Oppenheimer, S.: The great arc of dispersal of modern humans: Africa to Australia, *Quaternary International*, 202, 2–13, 2009.
- Patricola, C.M. and Cook, K.H.: Dynamics of the West African monsoon under mid-Holocene precessional forcing: regional climate model simulations, *Journal of Climate*, 20, 694–716, 2007.
- Pälike, H., Shackleton, N.J., Röhl, U.: Astronomical forcing on late Eocene marine sediments, *Earth Planet. Sci. Lett.*, 193, 589–602, 2001.
- Pik, R., Marty, B., Carignan, J., Yirgu, G. and Ayalew, T.: Timing of East African Rift development in southern Ethiopia: Implication for mantle plume activity and evolution of topography, *Geology*, 36, 167–170, 2008.
- Pointier, J.P., Delay, B., Toffart, J.L., Lefevre, M. and Romero-Alvarez, R.: Life history traits of three morphs of *Melanoides tuberculata* (Gastropoda: Thiaridae), an invading snail in the French West Indies, *Journal of Molluscan Studies*, 58, 415–423, 1992.
- Potts, R.: Environmental Hypotheses of Hominin Evolution. *Yearbook of Physical Anthropology*, 41, 93–136, 1998.
- Ramsey, M.H., Potts, P.J., Webb, P.C., Watkins, P., Watson, J.S., Coles, B.J.: An objective assessment of analytical method precision: comparison of ICP-AES and XRF for the analysis of silicate rocks, *Chem. Geol.*, 124, 1–19, 1995.
- Reimer, P.J., Baillie, M.G.L., Bard, E., Bayliss, A., Beck, J.W., Blackwell, P.G., Bronk Ramsey, C., Buck, C.E., Burr, G.S., Edwards, R.L., Friedrich, M., Grootes, P.M., Guilderson, T.P., Hajdas, I., Heaton, T.J., Hogg, A.G., Hughen, K.A., Kaiser, K.F., Kromer, B., McCormac, F.G., Manning, S.W., Reimer, R.W., Richards, D.A., Southon, J.R., Talamo, S., Turney, C.S.M., van der Plicht, J. and Weyhenmeyer, C.E.: INTCAL13 and MARINE13 radiocarbon age calibration curves, 0–50,000 years cal BP, *Radiocarbon*, 55, 1869–1887, 2013.
- Richter, T.O., Van der Gaast, S., Koster, B., Vaars, A., Gieles, R., De Stigter, H., De Haas, H., van Weering, T.C.E.: The Avaatech XRF core scanner: technical description and applications to NE Atlantic sediments, in: *New Techniques in Sediment Core Analysis*, Rothwell, R.G. (Ed.), Special Publication, 267, Geological Society, London, 39–50, 2006.
- Segele, Z.T. and Lamb, P.J.: Characterization and variability of Kiremt rainy season over Ethiopia, *Meteorology and Atmospheric Physics*, 89, 153–180, 2005.
- Seleshi, Y. and Zanke, U.: Recent changes in rainfall and rainy days in Ethiopia, *International Journal of Climatology*, 24, 973–983, 2004.
- Solanki, S.K., Usoskin, I.G., Kromer, B., Schüssler, M. and Beer, J.: Unusual activity of the sun during recent decades compared to the previous 11,000 years, *Nature*, 431, 1084–1087, 2004.
- Stager, J.C., Mayewski, P.A. and Meeker, L.D.: Cooling cycles, Heinrich event 1, and the desiccation of Lake Victoria, *Palaeogeogr. Palaeoclimatol. Palaeoecol.*, 183, 169–178, 2002.
- Stuiver, M., Reimer, P. J., and Reimer, R. W.: CALIB 6.0.2.html, available at: <http://calib.org>, last access: 10 July 2013, 2005.
- Stringer, C.: Out of Ethiopia, *Science*, 423, 692–694, 2003.
- Tierney, J.E. and deMenocal, P.B.: Abrupt Shifts in Horn of Africa. Hydroclimate Since the Last Glacial Maximum, *Science*, 342, 843–846, doi:10.1126/science.1240411, 2013.
- Tierney, J.E., Russell, J.M., Sinninghe Damsté, J.S., Huang, Y. and Verschuren, D.: Late Quaternary behavior of the East African monsoon and the importance of the Congo Air Boundary, *Quaternary Science Reviews*, 30, 798–807, 2011.
- Tishkoff, S. and Verelli, B.: Patterns of Human Genetic Diversity: Implications for Human Evolutionary History and Disease, *Annual Review of Genomics and Human Genetics*, 4, 293–340, 2003.
- Trauth, M.H.: A new probabilistic technique to determine the best age model for complex stratigraphic sequences, *Quaternary Geochronology*, 22, 65–71, 2014.
- Trauth, M.H., Bergner, A., Foerster, V., Junginger, A., Maslin, M. and Schaebitz, F.: Episodes of Environmental Stability vs. Instability in Late Cenozoic Lake Records of Eastern Africa, *Journal of Human Evolution*, in press.
- Trauth, M.H., Deino, A.L., Bergner, A.G.N. and Strecker, M.R.: East African climate change and orbital forcing during the last 175 kyr BP, *Earth and Planetary Science Letters*, 206, 297–313, 2003.
- Trauth M.H., Deino A. and Strecker M.R.: Response of the East African climate to orbital forcing during the last interglacial (130–117 ka) and the early last glacial (117–60 ka), *Geology*, 29, 499–502, 2001.
- Trauth, M.H., Maslin, M.A., Deino, A.L., Junginger, A., Leso-

- Iloyia, M., Odada, E.O., Olago, D.O., Olaka, L.A., Strecker, M.R. and Tiedemann, R.: Human evolution in a variable environment: the amplifier lakes of Eastern Africa. *Quat. Sci. Rev.*, 29, 2981–2988, 2010.
- Verschuren D., Laird K.R. and Cumming B.F.: Rainfall and drought in equatorial east Africa during the past 1,100 years, *Nature*, 403, 410–414, 2000.
- Vogelsang, R. and Keding, B.: Climate, culture, and change: From hunters to herders in northeastern and southwestern Africa, in: *Comparative Archaeology and Paleoclimatology – Socio-cultural responses to a changing world*, Baldia, M.O., Perttula, T.K., Frink, D.S. (eds.), BAR International Series, 2456, Archaeopress, Oxford, UK, 43–62, 2013.
- Vrba, E.S.: Environment and evolution: alternative causes of the temporal distribution of evolutionary events, *South African Journal of Sciences*, 81, 229–236, 1985.
- Wang, Y., Cheng, H., Edwards, R.L., He, Y., Kong, X., An, Z., Wu, J., Kelly, M.J., Dykoski, C.A. and Li, X.: The Holocene Asian monsoon: links to solar changes and North Atlantic climate, *Science*, 308, 854–857, 2005.
- Weber, M., Niessen, F., Kuhn, G. and Wiedcke, M.: Calibration and application of marine sedimentary physical properties using multi-sensor core logger, *Marine Geology*, 136, 151–172, 1997.
- Weldeab, S., Lea, D.W., Schneider, R.R. and Andersen, N.: Centennial scale climate instabilities in a wet early Holocene West African monsoon, *Geophysical Research Letters*, 34, L24702, doi:10.1029/2007GL031898, 2007.
- Woldegabriel, G. and Aronson, J.L.: Chow Bahir rift: A “failed” rift in southern Ethiopia, *Geology*, 15, 430–433, 1987.



Chapter IV

Episodes of Environmental Stability vs. Instability in Late Cenozoic Lake Records of Eastern Africa

Martin H. Trauth, Andreas G.N. Bergner, Verena Foerster, Annett Junginger,
Mark A. Maslin, Frank Schaebitz

Journal of Human Evolution (in press)

Special Issue on 'Environmental Variability and Hominin Dispersals'

Episodes of Environmental Stability vs. Instability in Late Cenozoic Lake Records of Eastern Africa

Trauth, M. H.^{a*}, Bergner, A.G.N.^a, Foerster, V.^b, Junginger, A.^a, Maslin, M.A.^c, Schäbitz, F.^b

^a University of Potsdam, Institute of Earth and Environmental Science, Karl-Liebknecht-Str. 24-25, D-14476 Potsdam

^b University of Cologne, Seminar for Geography and Education; Germany

^c Department of Geography, University College London; UK

* corresponding author

Abstract

Episodes of environmental stability and instability may be equally important for African hominin speciation, dispersal and cultural innovation. Three examples of a change from stable to unstable environmental conditions are presented on three different time scales, (1) the Mid Holocene (MH) wet-dry transition in the Chew Bahir basin (Southern Ethiopian Rift) (between $1.1\text{--}0.4 \times 10^4$ yr), (2) the MIS 5–4 transition in the Naivasha basin (Central Kenya Rift) (between $1.6\text{--}0.5 \times 10^5$ yr), and (3) the Early Mid Pleistocene Transition (EMPT) in the Olorgesailie basin (Southern Kenya Rift) (between $1.25\text{--}0.4 \times 10^6$ yr). A probabilistic age modeling technique is used to determine the timing of these transitions, taking into account possible abrupt changes in the sedimentation rate including episodes of no deposition (hiatuses). Interestingly, the stable- unstable conditions identified in the three records are always associated with an orbitally-induced decrease of insolation: the descending portion of the 800 kyr cycle during the EMPT, declining eccentricity after the 1.15×10^5 yr maximum at the MIS 5–4 transition, and after $\sim 1.0 \times 10^4$ yr. This observation contributes to an evidence-based discussion of the possible mechanisms causing the switching between environmental stability and instability in Eastern Africa at three different orbital time scales (10^4 to 10^6 yr) during the Cenozoic. This in turn may lead to great insights into the environmental changes occurring at the same time as hominin speciation, brain expansion, dispersal out of Africa and cultural innovations and may provide key evidence to build new hypothesis regarding the causes of early human evolution.

Keywords: Paleoclimate, East Africa, Human Evolution, Lakes, Sediments

4.1 Introduction

The possible influence of environmental variability, both temporally and spatially, on human evolution and dispersal is an intensely debated topic in the scientific community (Potts et al., 1996; Trauth et al., 2005, 2007; Maslin and Christensen, 2007; Maslin and Trauth, 2009; Potts, 2013). However, evidence was found recently, that episodes of stable environmental conditions play an equally important role for human evolution, dispersal and technological innovation (e.g., Grove et al., 2013). Periods of reduced environmental variability may act as windows for growing population sizes and hominin dispersal, whereas subsequent episodes of less favorable environmental conditions, pronounced droughts or rapid shifts between wet and dry climates, cause geographic isolation of population parts into vicariance, and hence allopatric speciation and adaptation of humans (Maslin and Trauth, 2009).

The sedimentary record of Eastern African lakes is rich in examples of both environmental stability and instability in the course of climate change (e.g. Trauth et al., 2003, 2005; Foerster et al., 2012; Junginger and Trauth, 2013; Junginger et al., 2014) (Fig. 4.1). These lakes, particularly those which occur in the rift basins, are amplifiers of moderate climate change (Olaka et al., 2010; Trauth et al., 2010). As an example, the water level of the Early Holocene paleo-Lake Suguta rose to 300 m during a +25% change in precipitation during the African Humid Period (ca. $1.5\text{--}0.5 \times 10^4$ yr BP) (Garcin et al., 2009, Borchardt and Trauth, 2011; Junginger and Trauth, 2013). On the other hand, as hydrological modeling suggests, large water bodies buffer rapid shifts in climate due to their delayed response to changes in the precipitation- evaporation balance (Borchardt and Trauth, 2011). The identification and correlation of

episodes of stability vs. instability between lake basins, however, is unfortunately hampered by ambiguous interpretation of environmental indicators or proxies within the sediments (Owen et al., 2008, 2009; Trauth and Maslin, 2009). Furthermore, fluctuating sedimentation rates and hiatuses between radiometric age dates, which themselves contain errors, complicates the assessment of the actual timing of environmental stability vs. instability (e.g. Sadler, 1988; Blaauw, 2010; Schumer et al., 2011; Trauth, 2014).

This manuscript attempts to meet this challenge and presents three examples of stability vs. instability on three different time scales in lake records in Eastern Africa, **(1)** the Mid Holocene (MH) wet-dry transition in the Chew Bahir basin (Southern Ethiopian Rift) (between $1.1\text{--}0.4 \times 10^4$ yr BP), **(2)** the MIS 5–4 transition in the Naivasha basin (Central Kenya Rift) (between $1.6\text{--}0.5 \times 10^5$ yr BP), and **(3)** the Mid Pleistocene Transition (MPT) in the Ologesailie basin (Southern Kenya Rift) (between $1.25\text{--}0.4 \times 10^6$ yr BP). First, we will re-analyze the three lake records using a probabilistic technique to determine the best age model for stratigraphic sequences (Trauth, 2014). Second, we will interpolate the published lake records on the new age model and distinguish episodes of environmental stability vs. instability in the records. Third, we will put together plausible mechanisms which cause stable or unstable conditions in the course of climate change. Last, the results are discussed in the light of the importance of both stability and instability for human evolution and dispersal, providing a basis for further discussions of the influence of the environmental on early humans.

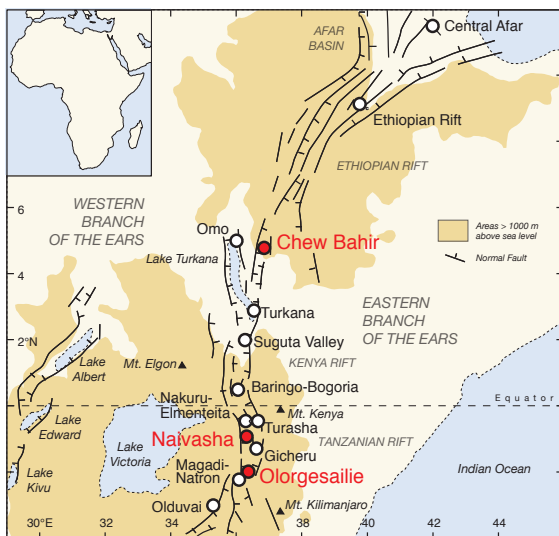


Figure 4.1 | Map of Eastern Africa showing topography, faults and lake basins. Note the location of the studied sites Chew Bahir, Naivasha and Ologesailie (modified from Trauth et al., 2005).

4.2 Detecting episodes of stability and instability in lake records

In our analysis of episodes of environmental stability and instability, we use published lake records, which include critical episodes of Eastern African climate change and human evolution, dispersal and cultural innovation. We use the amplitudes of water level changes as published, without revising or reinterpreting the proxies of lake levels and climate used by the authors of the original work. While the amplitudes have been left untouched, we have subjected all age models a critical review, because the timing and rate of climate change as well as its correlation with climate forcing is essential for our analysis. Having developed consistent age models for the four records, we defined episodes of relative stability and instability by visual inspection and correlated these with orbital forcing (Laskar et al., 2004). We have not used any more sophisticated method to determine the degree of variability for two reasons: (1) The quantitative significance of the records is not sufficient to analyze them statistically. (2) An arbitrary definition of a critical value of the variability would be necessary to separate stable from unstable episodes what we wanted to avoid.

4.2.1 The Mid Holocene (MH) wet-dry transition in the Chew Bahir basin

The Mid Holocene (MH) wet-dry transition in the **Chew Bahir basin** (Southern Ethiopian Rift) is reconstructed from five up to ~20 m long sediment cores CB01, CB03–06 collected along a ~20 km long NW–SE transect across the basin (Foerster et al., 2012, submitted). The composite age model of the sediment cores is based on 32 AMS ^{14}C ages derived from biogenic carbonate, fossilized charcoal and organic sediment, resulting in a very solid chronology for lake record spanning the last 4.5×10^4 yr BP (Foerster et al., 2012) (Fig. 4.2a). Furthermore, the Laschamp geomagnetic excursion ($\sim 4.1 \times 10^4$ yr BP, Nowaczyk et al., 2012) was identified at 9.19 m depth in CB05 that was retrieved from the centre of the basin (Foerster et al., 2014).

The proxy-climate record of the Chew Bahir basin is based on potassium (K^+) abundance, previously established as a reliable proxy for aridity in the Chew Bahir cores (Foerster et al., 2012). The potassium (K^+) record of cores CB03–06 has been tuned to the K^+ record of CB01 assuming that K^+ , as a weathering product of feldspar, feldsparthoids and mica, is transported instantaneously in solution from source to sink, and complete mixing in the water body of paleo-Lake Chew Bahir. We used linear and cubic spline interpolation techniques while tuning the individual records but we have

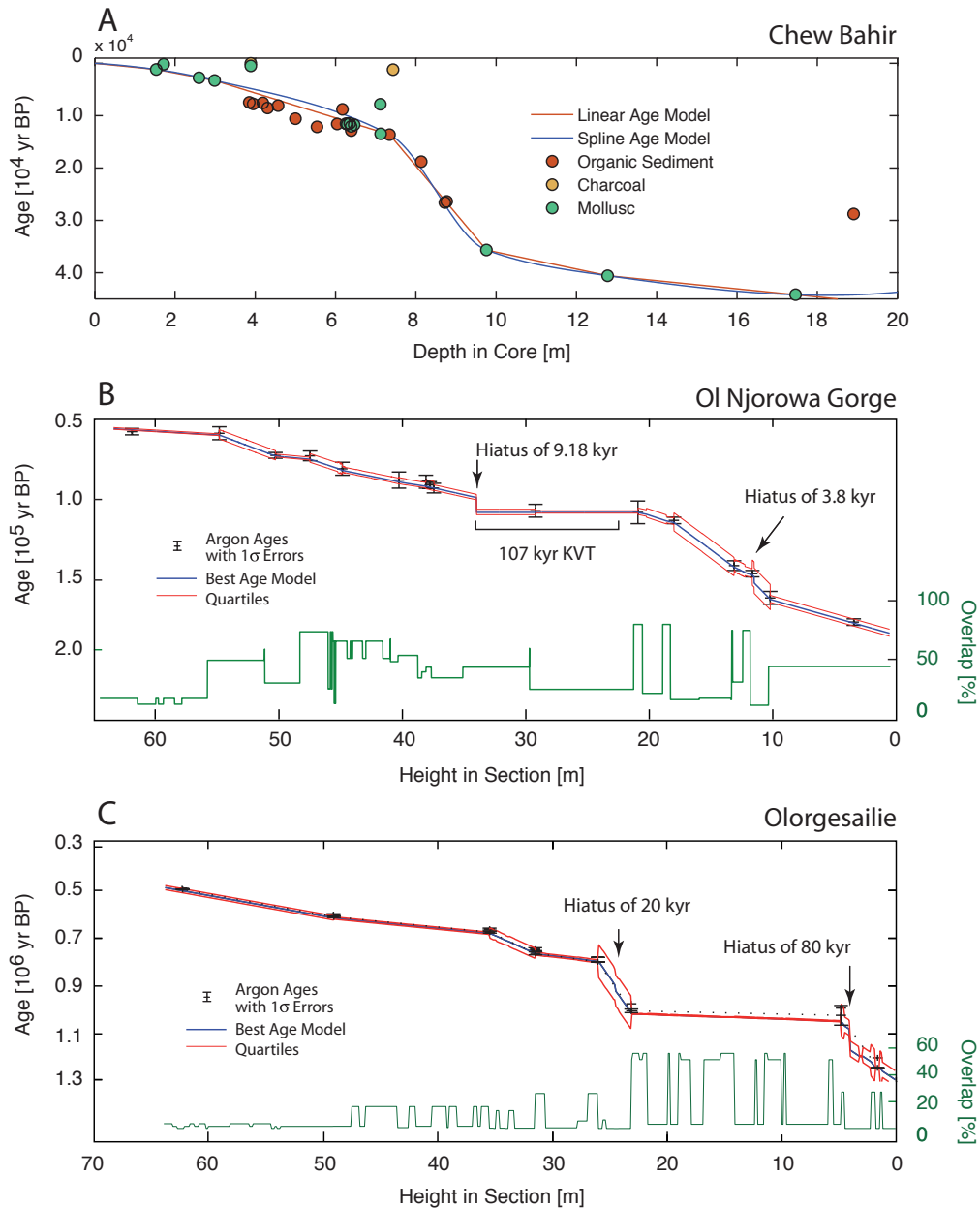


Figure 4.2 | Age models of three studied records. (A) The composite age model of the Chew Bahir basin is based on 32 AMS 14C ages (Foerster et al., 2012, submitted). All radiocarbon ages were converted into calibrated ages with OxCAL using the IntCal09 calibration curves (Bronk Ramsey, 1995). The best estimate of the true age was obtained by calculating the weighted mean of the probability density function of the calibrated ages. (B) and (C) The age model of the Naivasha and Olorgesailie records was calculated using a probabilistic technique for complex stratigraphic sequences simply comparing the deposition time of equally thick sediment slices from the differences of subsequent radiometric age dates and the unit deposition times (the inverse of the sedimentation rate) of the various sediment types (Trauth, submitted).

found no significant difference in the final result. All radiocarbon ages were converted into calibrated ages with OxCAL using the IntCal13 calibration curves (Bronk Ramsey, 1995, 2009a,b; Reimer et al., 2013). The best estimate of the true age was obtained by calculating the weighted mean of the probability density function of the calibrated ages.

The potassium, and all other proxy records, were interpolated upon the age model using a linear interpolation technique. We prefer a linear over a spline model as abrupt variations between low or high sedi-

mentation rates, even episodes without deposition, may actually exist in rift basins; these are smoothed out by splines and age modeling techniques introducing an arbitrary chosen memory (e.g., Bronk Ramsey, 2008, 2009a,b; Blaauw and Christen, 2011; Trauth, 2014). We used the K⁺ record between 1.1–0.4x10⁴ yr BP of core CB01 for our analysis of stability vs. instability because it is the most complete and detailed record of the Mid Holocene (MH) wet-dry transition in the Chew Bahir basin. Between ~0.98–0.91x10⁴ yr BP, we fill a gap in the core CB01 with the corresponding piece from the adjacent core CB03.

4.2.2 The MIS 5-4 transition in the Naivasha basin

The MIS 5-4 transition is recorded in the 60 m thick Ol Njorowa Gorge section in the southern **Naivasha basin**, which covers the interval between $\sim 1.5\text{--}0.6 \times 10^5$ yr BP (Trauth et al., 2001, 2003). The age model is based on anorthoclase and sanidine phenocryst concentrates from 16 tephra beds dated by the laser-fusion $^{40}\text{Ar}/^{39}\text{Ar}$ method (Trauth et al., 2001, 2003). The lake record has been inferred from sediment characteristics, diatoms, authigenic mineral assemblages (Trauth et al., 2001, 2003). The best age model was determined using a technique presented by Trauth (2014). In contrast to established age modeling techniques, such as intuitive definition of the age-depth relationship, calibrating the stratigraphy to insolation or orbital target curves, Monte-Carlo modeling of age distributions along sediment cores and Bayesian age-depth models (see review of Blaauw, 2010; Trauth, 2014), the approach by Trauth (2014) helps detecting abrupt variations in sedimentation rates, including the possibility of episodes of no deposition (hiatuses).

The new probabilistic technique for complex stratigraphic sequences simply compares the deposition time of equally thick sediment slices from the differences of subsequent radiometric age dates and the unit deposition times (the inverse of the sedimentation rate) of the various sediment types. First, the time difference is determined from the two $^{40}\text{Ar}/^{39}\text{Ar}$ dates and their independent Gaussian errors. Second, the time difference is again calculated from the unit deposition time of the sediment types and their Gamma-distributed dispersion (Trauth, 2014). The percentage overlap of the distributions of these two sources of information, together with the evidence from the sedimentary record, helps to find the best age model of complex sequences including abrupt variations in the rate of deposition including one or more hiatuses.

The sedimentation rates of the various types of deposits exposed in the Ol Njorowa Gorge is very different, ranging from less than a tenth of a millimeter per year for diatomite to several meters of volcanic airfall deposits within a couple of hours, followed by a longer time of no deposition (Trauth et al., 2001, 2003). Most importantly, a thick welded tuff called the Kedong Valley Tuff, $1.06 \pm 0.04 \times 10^5$ yr old, is located in the middle of the section, which is considered to be deposited within zero time on the $^{40}\text{Ar}/^{39}\text{Ar}$ time scale. The chronology is free of age reversals within the one-sigma error bars of the Argon ages. The means, however, show in fact $0.92 \pm 0.05 \times 10^5$ yr BP). Statistical age modeling requires monotonically increasing ages from top to bottom of the

section (e.g. Blaauw and Christen, 2011; Trauth, 2014). Therefore, we have edited the age of these two layers within the errors bars of the $^{40}\text{Ar}/^{39}\text{Ar}$ ages: 0.58×10^5 yr BP and 0.88×10^5 yr BP. This is quite permissible within the error bars, in particular since the modification of the ages does not affect the modeling result.

The Gamma model for the most likely unit deposition time for each sediment type (e.g. three types of materials: tephra, clastic sediments, diatomite) has two parameters, shape and scale. In the experiments described here, a Gamma model $\text{gamma}(\text{shape}, \text{scale})$ with $\text{shape}=2$ best describes the frequency distribution of unit deposition times, which is in agreement with the work of Blaauw and Christen (2011). We used a scale factor of 1.5, 2.0, and 8.0 for the three sediment types tephra, clastic sediments, and diatomite, determined in a first run of the model to adjust the Gamma parameters, corresponding to sedimentation rates of ~ 0.667 , 0.500, and 0.125 mm yr^{-1} .

4.2.3 The Early Mid Pleistocene Transition in the Olorgesailie basin

The EMPT is recorded in the 80 m thick Olorgesailie Formation in the **Olorgesailie basin**, which covers the interval between $\sim 1.25\text{--}0.49 \times 10^6$ yr BP (Deino and Potts, 1990; Behrensmeier et al., 2002; Owen et al., 2008, 2011; Decampo et al., 2010). The age model is based on seven $^{40}\text{Ar}/^{39}\text{Ar}$ ages of tephra layers, of which the oldest date (1.2×10^6 yr BP) has no error bar, and the $\sim 0.78 \times 10^6$ yr old Bruhnes-Matuyama magnetic reversal also without an error bar (Deino and Potts, 1990; Behrensmeier et al., 2002; Owen et al., 2008, 2011; Decampo et al., 2010). Again we used the new probabilistic technique for complex stratigraphic sequences by Trauth (2014) to determine the best age model of the Olorgesailie sequence. The lake record is taken from Figure 4 of Behrensmeier et al. (2002), describing three different environments, (1) fluctuating lacustrine, (2) wetland, and (3) subaerial conditions.

Behrensmeier et al. (2002) classifies the sediment layers of the Olorgesailie formation in four types of deposits: (1) sands and/or gravel, (2) subaerial exposure, (3) extensive pedogenesis, and (4) bedded diatomite. We interpret these types of deposits as (1) coarse-grained sediments, (2) and (3) fine-grained sediments of two different types, and (4) diatomite, where the precise distinction is not decisive for the outcome of the experiment. Interactive modeling yields a Gamma model for the sediment types with a shape factor of 2 and scale factors of 0.5 for coarse-grained sediments, 2 for both types of fine-grained sediments, although the model also allows for different values, and 20 for diatomite.

The corresponding sedimentation rates are 2 mm yr^{-1} for coarse-grained sediments, 0.5 mm yr^{-1} for fine-grained deposits, and 0.05 mm yr^{-1} for diatomite.

4.3 Examples for stability-instability in Cenozoic lake records

4.3.1 The Stability-Instability transition in the Mid Holocene Chew Bahir Record

Although we are interested only in the time interval between $1.1\text{--}0.4 \times 10^4 \text{ yr}$ the consistent age model for the entire core using all AMS ^{14}C ages must be calculated (Foerster et al., 2012, 2014) (Fig. 4.2A). In a first approximation, the age model based on radiocarbon dating of mixed materials suggests a linear relationship between age and depth, with a two-time change in the sedimentation rate at $\sim 9.75 \text{ m}$ and 7.35 m (Foerster et al., 2012, submitted) (Fig. 4.2A). The timing of the

transitions correlates with a change of climate in Eastern Africa. Two wet episodes before $3.5 \times 10^4 \text{ yr}$ after $\sim 1.5\text{--}0.5 \times 10^4 \text{ yr}$ (the so-called African Humid Period, between $\sim 1.5\text{--}0.5 \times 10^4 \text{ yr BP}$; e.g. Barker et al., 2004) with sedimentation rates in the order of $\sim 0.5\text{--}0.6 \text{ mm yr}^{-1}$ are bracketing an episode of a drier climate during the Last Glacial Maximum with sedimentation rates of $\sim 0.1 \text{ mm yr}^{-1}$ (Foerster et al., 2012, 2014). The sedimentation rates vary not only with time, but also from core to core along the transect of the pre-study. The mean sedimentation rate (SAR) decreases from $\sim 0.7 \text{ mm yr}^{-1}$ at the basin margin (core CB01) to $\sim 0.2 \text{ mm yr}^{-1}$ towards the centre (CB05) (Foerster et al., 2012, 2014). A closer look at the age model reveals slightly too old radiocarbon ages between 6.5 and 3.0 m composite depth, i.e. slightly delayed by $\sim 1.0 \text{ m}$ compared with the African Humid Period ($\sim 7.5\text{--}4.0 \text{ m}$ composite depth) suggesting temporary storage and remobilization of organic mat-

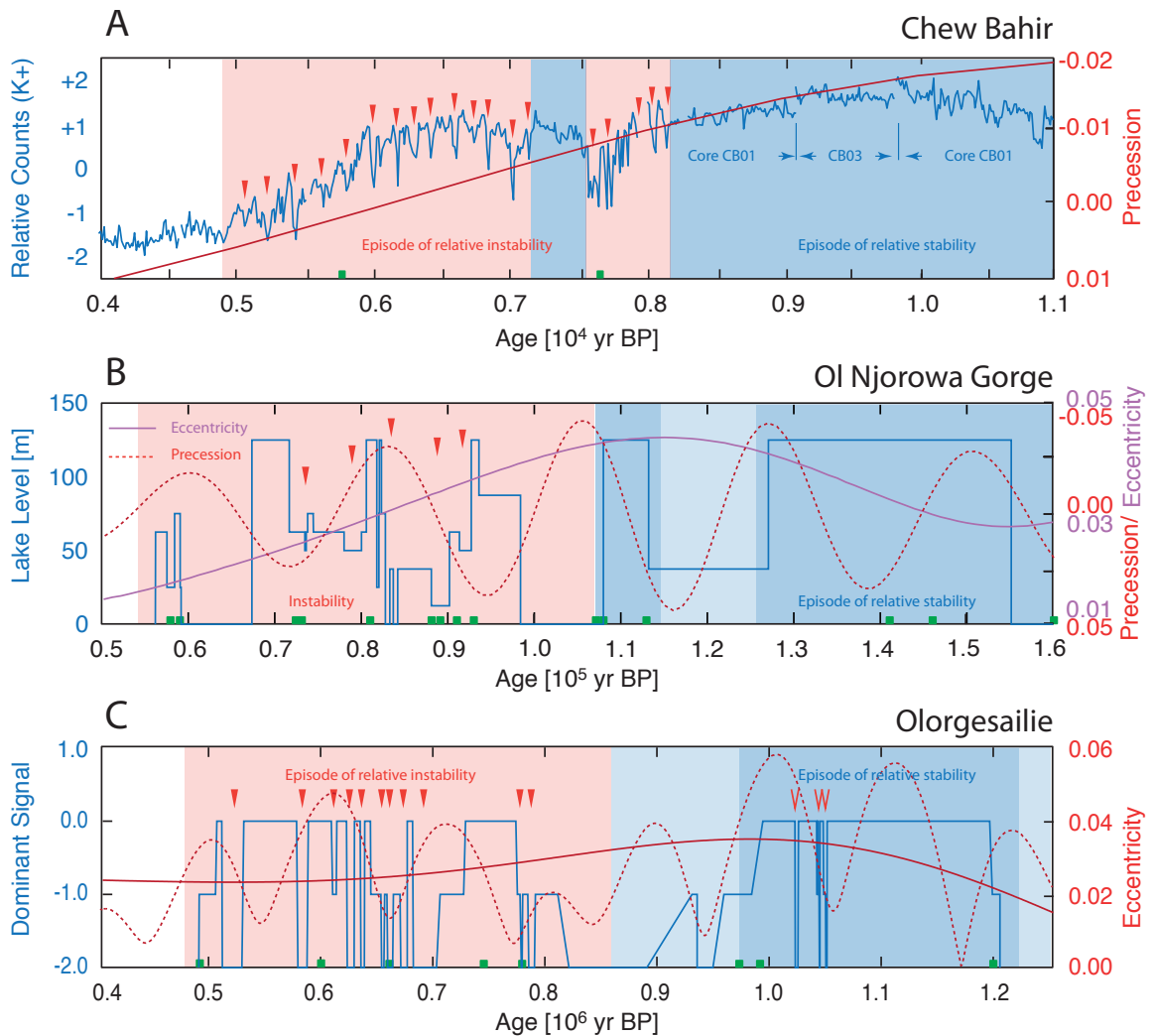


Figure 4.3 | Lake level records of three studied sites (blue lines) with age control points (green squares) and orbital and precessional quantities (red lines) to define episodes of relative stability and instability with pronounced dry periods (red triangles). (A) Holocene environmental record of the Chew Bahir basin created by tuning the potassium records of five cores CB01 and CB03–06 and interpolating the record to the age model shown in Figure 4.2A. (B) Late Pleistocene lake-level record of Lake Naivasha obtained by recalibrating the record published in Trauth et al. (2001, 2003) to the new age model shown in Figure 4.2B. (C) Mid Pleistocene record of the Olorgesailie basin taken from Behrensmeier et al. (2002), re-calibrated to a revised age model shown in Figure 4.2C and plotted together with the earth's eccentricity cycle (solid red line) as well as its 800 kyr component (dashed red line). All orbital and precessional quantities taken from Laskar et al. (2004).

ter in the densely vegetated catchment during a wetter climate (Fig. 4.2A). Three ages, younger than 0.2×10^4 yr, at ~ 7.45 and 3.9 m, are believed to be too young due to contamination of the sediment core (Foerster et al., 2012, 2014) (Fig. 4.2A).

The examination of the K^+ record between $1.1\text{--}0.4 \times 10^4$ yr reveals an episode of relative environmental stability until about 0.82×10^4 yr, before a distinctive drought event occurs at $\sim 0.815 \times 10^4$ yr (Fig. 4.3A). This drought event is the first of a series of five events, between $\sim 80\text{--}40$ yrs long and recorded by 6–2 data points in our K^+ record. This episode of relative instability, characterized by a relatively wet climate with a decrease in humidity between $\sim 0.815\text{--}0.775 \times 10^4$ yr and interrupted by the $\sim 80\text{--}40$ yrs long drought events, is followed by an interval of relative stability between $\sim 0.775\text{--}0.715 \times 10^4$ yr at a high moisture level. This wet and stable episode is again followed by a two-thousand year long interval of instability between $\sim 0.715\text{--}0.5 \times 10^4$ yr. This episode is characterized by a relatively high moisture level between $\sim 0.715\text{--}0.595 \times 10^4$ yr, before the onset of one-thousand year long drying of the region. The entire period between $\sim 0.715\text{--}0.5 \times 10^4$ yr is again characterized by at least fourteen pronounced drought events, again between $\sim 80\text{--}20$ yrs long and recorded by 7–2 data points in our K^+ record. This unstable interval is followed by relatively dry and stable climate after $\sim 0.5 \times 10^4$ yr.

In a first approximation, the K^+ record follows the earth's precession cycle during the interval from $1.1\text{--}0.4 \times 10^4$ yr, which is in agreement with the proposed link between increased humidity during the African Humid Period (AHP) and more intense heating of the northern hemisphere as a consequence of a minimum in the orbital precession (e.g., Kutzbach and Liu, 1997) (Fig. 4.3A). On closer inspection, however, the K^+ record suggests a strong nonlinear relationship between orbital forcing and climate during the Mid Holocene (MH) wet-dry transition in the Chew Bahir basin and its catchment. During the precession increased from -0.020 to zero, the climate on average between $1.1\text{--}0.4 \times 10^4$ yr remained relatively moist. However, after falling below zero, climate became unstable with pronounced dry periods recurring every 160 ± 40 yrs, which have a duration of $80\text{--}20$ yrs. The precession having increase above $+0.005$, climate returns to relative stability, but at a much lower moisture level.

4.3.2 The Stability-Instability transition in the Late Pleistocene Naivasha Record

We examine the period between $1.6\text{--}0.5 \times 10^5$ yr for which we calculate the most likely age model (Fig.

4.2B). First, we have calculated an age model based on the unit deposition times of the three types of sediments tephra, clastic sediments, and diatomite. The determination of the best age model requires the interactive adjustment of the age of the base of the section and the Gamma parameters of each sediment type. Using an age of 1.83×10^5 yr for the base of the section and the scale factors of 1.5, 2.0, and 8.0 for the three sediment types tephra, clastic sediments, and diatomite, corresponding to sedimentation rates of ~ 0.667 , 0.500 , and 0.125 mm yr⁻¹ leads to the best fit between the age model and the independent Argon ages of the section.

Second, we are comparing the unit deposition times (and their Gamma distributions) with the differences of subsequent radiometric age dates (and their Gaussian distributions). The percentage overlaps of the distributions ranges from 11 and 80%, with the lower values indicating possible abrupt changes in the sedimentation including episodes of no deposition (hiatuses) (Fig. 4.2B). Using this information we find an hiatus at 11.5 m height in the section, where we add 3.8 kyrs to the age model. At this location in the section, the percentage overlap between the two sources of evidence, the sediment types and Argon ages, is $\sim 11\%$ only. Introduce an interval of 3.8 kyr without deposition causes a perfect match between the age model and the Argon ages in this part of the section. If we examine the stratigraphic description of the 0.12 m thick unit in the profile, which includes the possible hiatus, we find a complex deposit comprising sands and silts, mixed with diatomaceous sediments, but also volcanoclastic deposits with rounded pumice lapilli and rock fragments (Trauth et al., 2001, 2003). This unit is immediately below the oldest diatomite unit, 3.30 m thick, documenting a major lacustrine interval in the Naivasha basin.

A second hiatus is possibly located at 34 m just above the Kedong Valley Tuff, $1.06 \pm 0.04 \times 10^5$ yr old, located in the middle of the section, which is considered to be deposited within zero time on the $^{40}\text{Ar}/^{39}\text{Ar}$ time scale. The best match between the age model and the Argon ages is obtained by introducing an interval of no deposition with a duration of 9.18 kyrs at the top of the tuff. Again, the examination of the stratigraphic log of the section reveals a 0.3 m thick unit of a sandy tuff overlying the heavily eroded and weathered top of the Kedong Valley Tuff, suggesting subaerial conditions after the deposition of the 10 m thick tuff in a shallow lake in the southernmost part of the Naivasha basin (Trauth et al., 2001, 2003). At this location in the section, the percentage overlap between the two sources of evidence, the sediment types and Argon ages, is $\sim 43\%$ only. The Late Pleistocene lake level re-

cord from the Naivasha basin reveals a relatively long episode of stability between $1.55\text{--}1.06 \times 10^5$ yr, which is particularly evident through a series of diatomite beds with a total thickness of ~ 4.9 m with intercalated clastic and volcanoclastic deposits (Fig. 4.3B) (Trauth et al., 2001, 2003). During this lake episode, the lake has reached water depths of up to 150 m and a size of ~ 520 km², whereas the up to 9 m deep modern lake covers ~ 180 km² only (Bergner et al., 2003). Climate variability during this interval was relatively low, as pH fluctuations between $\sim 8.0\text{--}8.5$ of the lake water inferred from diatom assemblages suggest (Bergner et al., 2004). In contrast, the episode after $\sim 1.06 \times 10^5$ yr is characterized by remarkable climate fluctuations (Trauth et al., 2001, 2003). Short freshwater phases are characterized by thin diatomite layers, unaltered volcanic glass and absence of authigenic silicates. In contrast, silicic glass with perlitic cracks, glass shards with montmorillonite rims, occasional chabazite and phillipsite represent the transition to alkaline conditions with a pH of about 9. Even higher alkalinity results in the formation of clinoptilolite, and extremely alkaline pore waters (pH > 11) lead to the precipitation of analcime (Trauth et al., 2001, 2003). The diatomite layers within this part of the section are characterized by diatom species with the preference for slightly higher alkalinities than the ones identified in the lower, thick diatomite beds (Bergner et al., 2004).

The relation between climate and orbital forcing is complex in this part of the Eastern Africa, as it seems to follow equatorial March and September insolation at times of maximum eccentricity and hence maximum amplitude of the Earth's precessional cycle, causing half precessional cycles (~ 11.5 kyr) rather than precessional (~ 23 kyr) in climate records (Berger and Loutre, 1997, 2006; Trauth et al., 2003). Furthermore, it seems the complicated topography of the East African Rift System, with horst and graben structures and extensive plateaus modulate this influence in a complicated manner (Trauth et al., 2010). The new age model of this section suggests lake highstands as the result of a wetter climate between $1.55\text{--}1.27 \times 10^5$ yr, $1.13\text{--}1.08 \times 10^5$ yr, as well as between $\sim 0.98\text{--}0.93 \times 10^5$ yr, $\sim 0.83\text{--}0.80 \times 10^5$ yr and $\sim 0.72\text{--}0.67 \times 10^5$ yr, which is slightly different from the chronology of high lake levels as published by Trauth et al. (2001, 2003). Whereas the old chronology of highstands suggest a linear correlation of the lake level with March and September insolation, the lake record according to the new age model suggests a more complex link between insolation and the hydrological budget of Lake Naivasha than previously thought. The lake highstands, however, seem to occur 5–2 kyrs after minimum or

maximum precession suggesting a causal but complex link between orbital forcing and humidity between $1.6\text{--}0.5 \times 10^5$ yr (Fig. 4.3B). One explanation would involve a shift in the relative importance of the northern hemisphere and equatorial insolation in the course of decreasing eccentricity. Between these wet episodes, the most remarkable drought events are centered at ~ 0.91 , 0.88 , 0.83 , 0.78 , and 0.73×10^5 yr, i.e. within the episode of instability after $\sim 1.06 \times 10^5$ yr (Fig. 4.3B).

4.3.3 The Stability-Instability transition in the Mid Pleistocene Ologesailie Record

The Early to Mid Pleistocene lake sediment sequence exposed in the Ologesailie basin has led to lively discussions during the last couple of yrs (Trauth and Maslin, 2009; Owen et al., 2009). In particular, there is disagreement over the duration of stable lacustrine conditions, which is documented in up to 7 m thick diatomite beds within the section. In our interpretation of the published evidence by Behrensmeyer et al. (2002), we concluded that a large, deep lake existed between $\sim 1.2\text{--}0.9 \times 10^6$ yr, whereas Owen et al. (2009) reads the same stratigraphic section as the record of a series of short (less than 0.01 Ma) lacustrine episodes, interrupted by long (more than 0.2 Ma) intervals of complex conditions including several hiatuses (Owen et al., 2009). According to the interpretation of Owen et al. (2009), only $\sim 45\%$ of the time interval between $\sim 1.25\text{--}0.49 \times 10^6$ yr is recorded in the sediments of the Ologesailie formation. On the other hand, the Ologesailie formation is the key section for the variability selection hypothesis by Potts (1996) claiming that environmental instability is a key driver of evolution.

We examine the period between $1.25\text{--}0.49 \times 10^6$ yr, for which we calculate the most likely age model (Fig. 4.2C) using the approach by Trauth (2014). First, we have calculated an age model based on the unit deposition times of the four types of sediments coarse-grained sediments, fine-grained sediments of two different types, and diatomite. The determination of the best age model requires the interactive adjustment of the age of the base of the section and the scale factors of 0.5 for coarse-grained sediments, 2 for both types of fine-grained sediments, and 20 for diatomite, corresponding to sedimentation rates of 2 mm yr⁻¹, 0.5 mm yr⁻¹, and 0.05 mm yr⁻¹ leads to the best fit between the age model and the independent argon ages of the section.

Second, we are comparing the unit deposition times (and their Gamma distributions) with the differences of subsequent radiometric age dates (and their Gaussian distributions). The percentage overlaps of the dis-

tributions ranges from close to zero and ~56%, with the lower values indicating possible abrupt changes in the sedimentation including episodes of no deposition (hiatuses) (Fig. 4.2C). Using this information we find an hiatus at 4.0 m height in the section, where we add 80 kyr to the age model. At this location in the section, the percentage overlap between the two sources of evidence, the sediment types and argon ages, is close to zero. Introducing an interval of 80 kyr without deposition causes a perfect match between the age model and the argon ages in this part of the section. A second hiatus is possibly located at 24.5 m. The best match between the age model and the argon ages is obtained by introducing an interval of no deposition with a duration of 20 kyr at the top at this level. At this location in the section, the percentage overlap between the two sources of evidence, the sediment types and argon ages, is again close to zero (Fig. 4.2C). In contrast to the interpretation of Owen et al. (2009), we believe that only ~13% of the Olorgesailie formation is without a record of environmental change.

The Early to Mid Pleistocene lake level record from the Olorgesailie basin reveals a relatively long episode of stability between 1.15–0.95 $\times 10^6$ yr, which is particularly evident through a series of up to 7 m thick diatomite beds with intercalated clastic and volcanoclastic deposits (Fig. 4.3C) (Trauth et al., 2001, 2003). Climate variability during this interval was relatively low, as pH fluctuations between ~7.5–9.5 of the lake water inferred from diatom assemblages suggest (Owen et al., 2008). This episode of remarkable stability is followed by a relatively dry episode between 0.95–0.75 $\times 10^6$ yr with predominantly subaerial conditions, before the onset of a second major lake episode between 0.75–0.49 $\times 10^6$ yr. In contrast to the first lake episode, this lacustrine phase is characterized by rapid climate fluctuations within less than a thousand yrs (Owen et al., 2008).

The Olorgesailie record nicely correlates with the Earth's eccentricity cycle modulating the amplitude of the precessional cycle (Fig. 4.3C). Both lake episodes correlate with maxima of the 400 kyr component of the eccentricity cycle, whereas the dry interval between 0.95–0.75 $\times 10^6$ yr correlates with a minimum of this cycle. Most interestingly, the greater amplitude of the maximum at ~1.0 $\times 10^6$ yr seems to correlate with more stable conditions, while the second, lower maximum at ~0.6 $\times 10^6$ yr correlates with more unstable conditions. Looking at the longer, 800 kyr component of the eccentricity cycle, the transition from stable to unstable environmental conditions occurs at the descending portion of the 800 kyr component of the earth's eccentricity cycle (Fig. 4.3C).

4.4 Discussion

Our analysis of published climate time records shows that episodes of stability and instability in the environmental conditions occur on three different orbital time scales (10^4 to 10^6 yr) during the Cenozoic.

On very long time scales of $>10^6$ yr, changes in lakes are primarily determined by tectonics, which initially creates but also destroys lake basins. However, tectonics also affects the conditions in a lake on shorter time scales, when they changed the shape and size of catchments and drainage networks (e.g. Bergner et al., 2009; Olaka et al., 2010; Trauth et al., 2010; Feibel, 2011). Furthermore, tectonics shapes the morphology of lake basins and hence the sensitivity of these lakes to changes in the precipitation/evaporation balance (Olaka et al., 2010; Trauth et al., 2010). The tectonic influence on lakes is thus the first example where long-term processes can cause stable vs. unstable conditions on time scales relevant for humans and other animals.

If the tectonic conditions for a lake are provided, it is mainly orbital cycles, which determines the hydrological budget of the lake on time scales of 10^4 to 10^5 yr (e.g., Kutzbach and Street-Perrott, 1985; Trauth et al., 2003, 2007; Kingston et al., 2007; Bergner et al., 2009; Trauth et al., 2010). The most dramatic fluctuations in humidity are caused by the 400- and 800-kyr components of the eccentricity cycle, which cause clusters of large lakes in Eastern Africa (Trauth et al., 2005, 2007). The Olorgesailie record shows that the amplitude of the 400 and 800 kyr cycle affects the relative stability of the environmental conditions, with a tendency to instability in times of low amplitude (Fig. 3C). Furthermore, the Naivasha record suggests that, during an interval of maximum eccentricity between 1.6–0.5 $\times 10^5$ yr, intervals of relative stability and instability alternate. At this time scale, it is the amplitude of the 100-kyr component of the eccentricity cycle, which controls the amplitude of the precession cycle and hence the insolation on the African continent (Kutzbach and Street-Perrott, 1985; Trauth et al., 2003; Junginger and Trauth, 2013). Again, lower amplitudes of the 100-kyr cycle causes relative instability in the environment (Trauth et al., 2003) (Fig. 4.3B).

If the orbital conditions (e.g., positive or negative precession during maximum eccentricity) result in highly variable lake levels, the hydrological budget of the lakes on the shorter time scales of $<10^3$ yr is influenced by millennium scale global climate fluctuations, such as Dansgaard-Oeschger/Heinrich events including the Younger Dryas (Brown et al., 2007; Foerster et al., 2012;

Junginger and Trauth, 2013) and solar variations (Verschuren et al., 2000; Junginger et al., 2014). Interestingly, as the Chew Bahir record of the Mid Holocene transition shows, the relation between environmental conditions and orbital forcing is highly nonlinear (Fig. 4.3A). After the precession minimum at $\sim 1.0 \times 10^4$ yr, climate remains relatively moist despite an increase of precession from -0.018 to zero, followed by an episode of remarkable instability with at last 19 intervals of extreme aridity, recurring every 160 ± 40 yrs and in durations of $80-20$ yrs. Stability is reached after $\sim 0.5 \times 10^4$ yr, when precession has increased above zero. Importantly, the overall transition from wet to dry at the termination of the AHP is relatively gradual, in contrast to the observation of deMenocal et al. (2000) and Tierney and deMenocal (2013) (Fig. 4.3A).

What are the possible mechanisms for the stabilization and destabilization of environmental conditions? On very long time scales ($>10^6$ yrs), volcano-tectonic phenomena associated with the East African Rift System (EARS) and associated plateaus can cause both stability and instability. The formation of plateaus, as an example, has contributed very effectively to stability of the environment, as it has resulted in a blockage of

moisture-bearing winds from both oceans in the West and the East and thus persistently drier conditions in Eastern Africa (Sepulchre et al., 2006; Wichura et al., 2010). On the other hand, if northern hemisphere insolation crosses a certain threshold during a precession minimum and the west-east pressure gradient increases during the July to September months, the Congo Air Boundary, currently blocked by topography, crosses the East African plateaus, bringing extra moisture from the Congo basin further to the East (Junginger and Trauth, 2013). This mechanism seems to have worked at time scales of 10^2 yrs, introducing a high level of instability if the threshold is crossed through solar variability (Junginger et al., 2014).

Rift lakes are another factor in the development of stability and instability, as they might act as amplifiers of relative moderate climate shifts on time scales of 103 yrs (so-called amplifier lakes; Street-Perrott and Harrison, 1985; Olaka et al., 2010; Trauth et al., 2010). On the other hand, they also have a stabilizing effect by the sheer size of the water body, which reacts very slowly to changes in the moisture budget (Fig. 4.4). As an example, paleo-Lake Suguta in the northern Kenya Rift was about 300 m deep and 2,200 km² large dur-

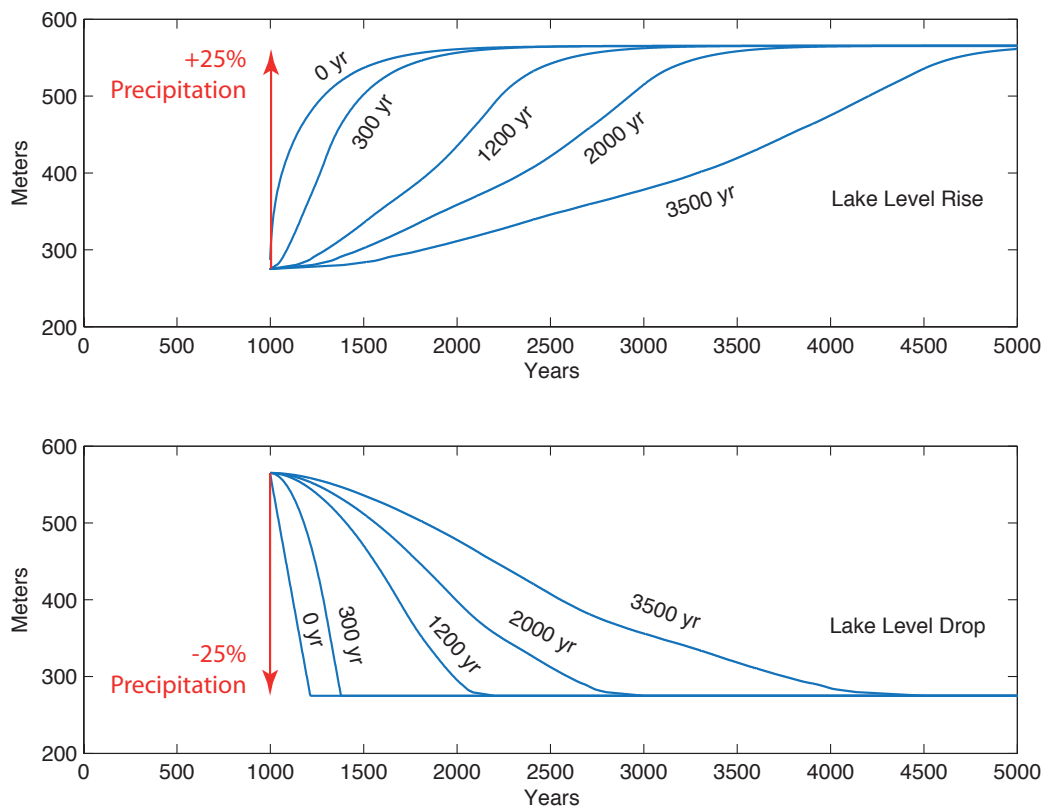


Figure 4.4 | Lakes have a stabilizing effect by the sheer size of the water body, which reacts very slowly to changes in the moisture budget, as lake-balance modeling suggests. If there is an abrupt increase of +25% in the 13,000 km² large catchment today, the lake would reach two thirds of the maximum lake level of 300 yrs not before 200 yrs after the climate shift, and would stabilize at the maximum lake level only after 1,000 yrs. Gradual changes in climate would cause even longer response times of the water body (Borchardt and Trauth, 2012; Junginger and Trauth, 2013).

ing the African Humid Period, while there is a 0.5–5 m deep, alkaline Lake Logipi today (Garcin et al., 2009). If there is an abrupt increase of precipitation of +25% in the 13,000 km² large catchment today, the lake would reach two thirds of the maximum lake level of 300 m not before 200 yrs after the climate shift, and would stabilize at the maximum lake level only after 1,000 yrs. Gradual changes in climate would cause even longer response times of the water body. Correspondingly, an abrupt or gradual decrease of precipitation results in a delayed decline of the water level of paleo-Lake Suguta (Borchardt and Trauth, 2012; Junginger and Trauth, 2013) (Fig. 4.4). In other words, large lakes smooth (or low-pass filter) rapid, low-amplitude variations of climate and therefore stabilize the environment.

An additional mechanism to stabilize local environmental conditions is the vegetation-climate feedbacks (e.g. Jeltsch et al., 2000; Maslin, 2004) (Fig. 4.5). This is because there can exist positive feedbacks which resist particular climate changes. For example if an area is covered with forest and the region starts to dry out the vegetation recycles moisture maintaining a level of rainfall for the forest to survive (Maslin, 2004). There is, however, a threshold at which this mechanism is not sufficient and forest is replaced by savanna. This moisture feedback does not exist with savanna; instead the relatively dry grassland environment is maintained by recurring fires keeping trees away, similar to the activity of grazers and other factors (Jeltsch et al., 2000). Hence, the climate must get much wetter before forest can recolonize that region. The interesting aspect here is the character of the transitions near the thresholds in this saddle-node bifurcated system response: how does the environment switch from one to the other stable

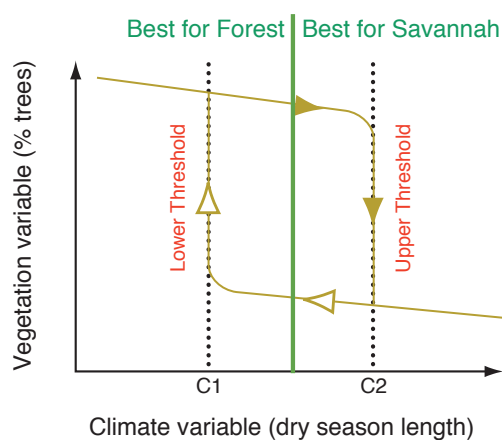


Figure 4.5 | Vegetation have a stabilizing effect on the local environment due to a positive feedback which resists particular climate changes. For example, forests recycle moisture maintaining a level of rainfall for the forest to survive (Maslin, 2004). This moisture feedback does not exist with savanna; instead the relatively dry grassland environment is maintained by recurring fires keeping trees away, similar to the activity of grazers and other factors (Jeltsch et al., 2000).

mode? Maybe this model helps explain the remarkable instability and the occurrence of extreme droughts during the Mid Holocene wet-dry transition in the Chew Bahir basin (Fig. 4.3).

The observed character of transitions between stable and unstable conditions can be compared with the theoretical models proposed by Maslin and Christensen (2007) and refined by Maslin et al. (2014) (Fig. 4.6). In their work, they present three different models of how the lakes could responded to local orbital forcing. The first model suggests that there is a relatively smooth gradual transition between periods with deep lakes and periods without lakes, which may invoke Red Queen (Van Valen, 1973) or Turnover Pulse Hypotheses (Vrba, 1985) as possible causes of evolution (see below). The second model is a threshold model with ephemeral lakes, expanding and contracting extremely rapidly, producing the wide spread, regional-scale, rapid, and extreme environmental variability required by the Variability Selection Hypothesis (Potts, 1998). The third model is characterized by extreme variability during the transitions between full to no lake conditions, which provides climate variability at a time-scale relevant to evolutionary processes. In both Models 2 and 3 human evolution could still be strongly influenced by the high-energy wet conditions or prolonged aridity (Maslin and Christensen, 2007). These models are the basis of the Pulsed Climate Variability Hypothesis (Maslin and Trauth 2009; Trauth et al., 2010) that provides a palaeoclimate framework within which to discuss the causes of early human evolution (Maslin et al., 2014). Different species or, at the very least, different emerging traits within a species could have evolved through various mechanisms including the Turnover Pulse Hypotheses, Pulsed Climate Variability Hypothesis or allopatric speciation.

Understanding how the East African climate switches from stability to instability is essential if we want to understand the effect of climate variation on human evolution. Because it is becoming apparent that different climate modes may have influenced the evolution of different species and their definitive characteristics or traits (Maslin et al., 2015). For example the statistical modeling work of Shultz and Maslin (2013) show the significant brain expansion around $1.9\text{--}1.7 \times 10^6$ yr, due to the appearance of *Homo rudolfensis*, *H. georgicus* and *H. ergaster*, was associated with the emergence of ephemeral deep water lakes in almost all the East African rift basins. Maslin et al. (2014) note that though no evidence for these large brained hominins existed before 1.9×10^6 yr this interpretation may be limited as there is a lack of cranial capacity data between 2×10^6

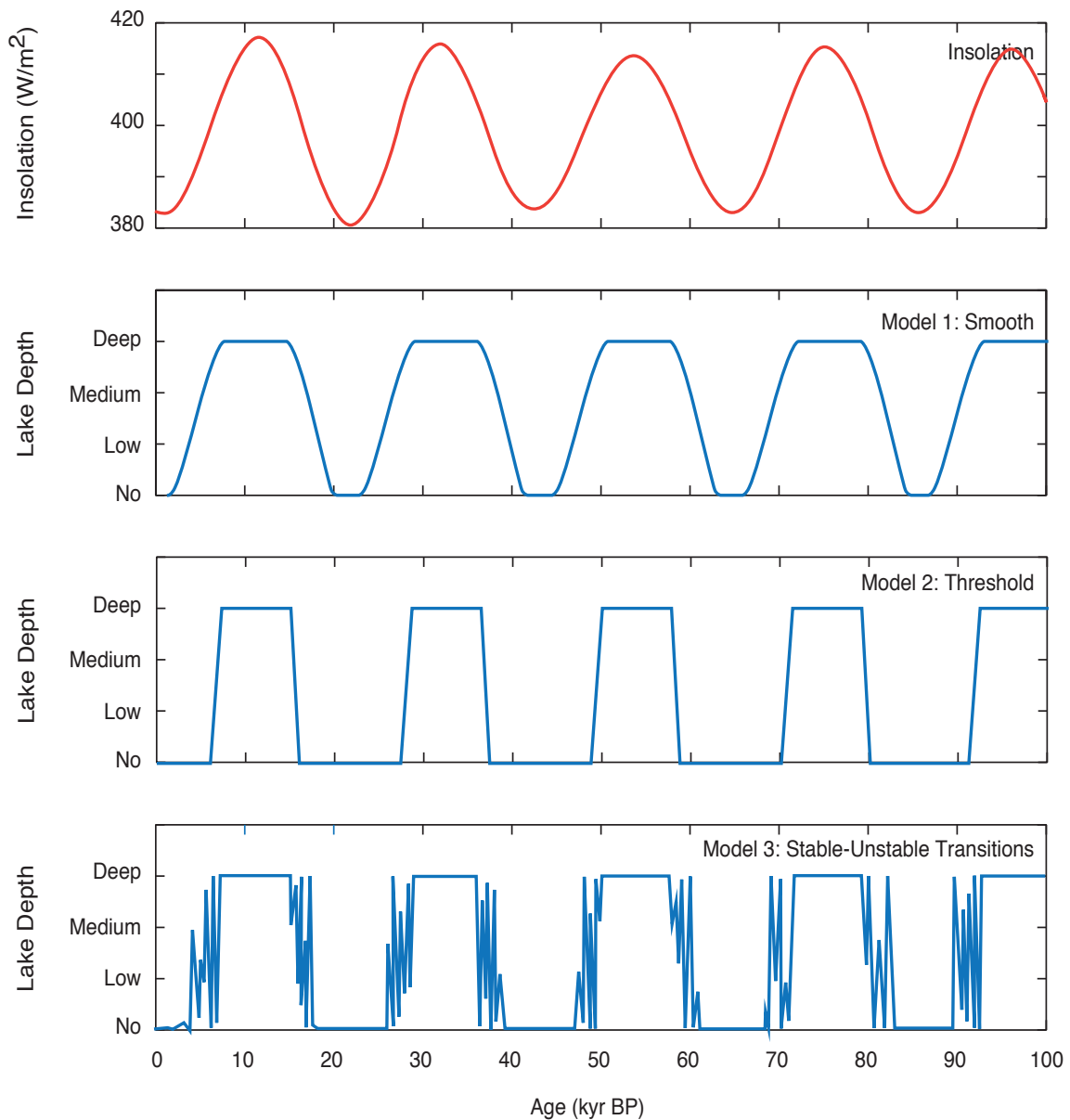


Figure 4.6 | Models of possible environmental response to orbital forcing. The first model suggests that there is a relatively smooth gradual transition between periods with deep lakes and periods without lakes, which may invoke Red Queen (Van Valen, 1973) or Turnover Pulse Hypotheses (Vrba, 1985) as possible causes of evolution (see below). The second and third model are threshold model, with ephemeral lakes, expanding and contracting extremely rapidly, producing the wide spread, regional-scale, rapid, and extreme environmental variability required by the Variability Selection Hypothesis of human evolution (Potts, 1998). The third model, however, is characterized by extreme variability during the transitions between full to no lake conditions, which implies variability influenced human evolution or again either high-energy wet conditions or prolonged aridity (Maslin and Christensen, 2007).

yr and 2.5×10^6 yr. Shultz and Maslin (2013) also found that subsequent expansion of brain capacity seems to be linked to dry stable conditions. Other characteristics that could have been forced by varying climate modes and may have been independently forced from brain expansion such as the changes in life history (shortened inter-birth intervals, delayed development), body size, shoulder morphology allowing throwing of projectiles (Roach et al., 2013), adaptation to long distance running (Bramble and Lieberman, 2004), ecological flexibility (Hopf et al., 1993) and social behaviour (Anton, 2003). At about $1.1\text{--}0.9 \times 10^6$ yr, at the stable-unstable transition during with the Early Mid Pleistocene Transi-

tion also included in the Ologesailie Formation, environmental pressure and natural selection may have contributed to the extinction of the robust Australopithecines with large teeth and small brains, whose last appearance datum is currently dated to the slightly older date of 1.2×10^6 yr. Instead, *H. ergaster* survived because they were able to adapt their stone tools to a change of the environment and hence the type of food (Potts, 2013) (Fig. 4.3A). There is also discussion whether these changing environmental conditions could have contributed to the step like increase in brain capacity between $0.8\text{--}1.0 \times 10^6$ yr and the emergence of *H. heidelbergensis* around 800 ka (Shultz et al., 2012).

The Ol Njorowa Gorge section in the Naivasha basin includes the Late Pleistocene MIS 5–4 transition, when *H. sapiens* may have been able to expand beyond the limits of Eastern Africa into southern Arabia, eventually during low water levels of the Red Sea and Persian Gulf for the first time when it was already wet in Eastern Africa at $\sim 1.25 \times 10^5$ yr (Armitage et al., 2011). Stable environmental conditions prevailed between 1.50 – 1.25×10^5 yr which may have led to an increase in the population size in Eastern Africa before the first shift towards arid conditions at $\sim 1.25 \times 10^5$ yr may have caused the first expansions of this species along this southern route into Arabia (Armitage et al., 2011) (Fig. 4.3B). The second major wave of expansion, this time through the “Nile corridor” into the Levant, occurs after $\sim 1.05 \times 10^5$ yr (Niewoehner, 2001; Rightmire, 2009; Campbell and Tishkoff, 2010; Scheinfeldt et al., 2010), when climate finally got drier and unstable, according to our lake record from the Naivasha basin (Fig. 4.3B). This interval also coincides with increased cultural differentiation, innovation in hunting and other foraging activities, including fishing tools and first obvious symbolic expression using preservable materials (Potts, 2013).

The Chew Bahir record ultimately shows in detail how the environment responds to gradual changes in insolation in a nonlinear, saddle-node bifurcation type transition (Fig. 4.3A). This high-resolution (~ 12 yrs) record may provide an important basis for discussion of the character and causes of the cultural transition from fishing to herding in the region (Ambrose, 1998; Marshall and Hildebrand, 2002; Scheinfeldt et al., 2010). The record clearly shows, that climate developed from wet and stable conditions until $\sim 0.82 \times 10^4$ yr towards dry and stable conditions after $\sim 0.5 \times 10^4$ yr. The intermediate interval between 0.82 – 0.5×10^4 yr is characterized by relatively wet conditions during most of the time, but punctuated by at least 19 events of extreme aridity, 20–80 yrs long and recurring every 160 ± 40 yrs, which may have made life difficult for humans living in the region. Drought that last for several decades may have forced people to develop new technologies for food production, as documented in the archeological record.

4.5 Conclusion

We found episodes of stability and instability in the environmental conditions at three different orbital time scales (10^4 to 10^6 yrs) during the Cenozoic. These episodes of stability and instability may correlate with important steps in hominin speciation, brain expansion, cultural and technological innovation, and dispersal out of Africa. Hence, understanding the stability and

instability of East African climate may be important if we are to increase our understanding of the key factors which may have driven human evolution.

Acknowledgements

This project was funded by grants to M.H.T. by the German Research Foundation (DFG). The work is the result of a pilot study to the Hominin Sites and Paleolakes Drilling Project (HSPDP) in the framework of the International Continental Scientific Drilling Program (ICDP). We thank the Government of Kenya and the University of Nairobi for research permits and support. We thank A. Asrat, A.K. Behrensmeyer, I. Fer, Y. Garcin, F. Jeltsch, H. Lamb, D. Melnick, E. Odada, D. Olago, L. Olaka, R.B. Owen, R. Potts, M.R. Strecker, and R. Tiedemann for inspiring discussions. We would also like to thank H. Douglas-Dufresne and P. Ilsley of WildFrontiers Kenya, and B. Simpson and J. Roberts of TropicAir Kenya for logistical support during the helicopter expeditions to the Suguta Valley in between 2007 and 2013.

4.6 References

- Ambrose, S.H., 1998. Chronology of Later Stone Age and Food Production in East Africa. *Journal of Archaeological Science*, 25, 377–392.
- Antón, S.C., 2003. Natural history of *Homo erectus*. *American Journal of Physical Anthropology*, 122, 126–170.
- Armitage, S.J., Jasim, S.A., Marks, A.E., Parker, A.G., Usik, V.I., Uerpmann, H.P., 2011. The Southern Route “Out of Africa”: Evidence for an Early Expansion of Modern Humans into Arabia. *Science*, 331, 453–456.
- Barker, P.A., Talbot, M.R., Street-Perrott, F.A., Marret, F., Scourse, J., Odada, E.O., 2004. Late Quaternary climatic variability in intertropical Africa. In: Battarbee, R.W., Gasse, F., Stickley, C.E. (Eds.), *Past Climate Variability through Europe and Africa*. Kluwer Academic Publishers, pp. 117–138.
- Berger, A., Loutre, M.F., 1997. Intertropical latitudes and precessional and half-precessional cycles. *Science*, 278, 1476–1478.
- Berger, A., Loutre, M.F., Melice, J.L., 2006. Equatorial insolation: from precession harmonics to eccentricity frequencies. *Climate of the Past*, 2, 131–136.
- Bergner, A.G.N., Trauth, M.H., Bookhagen, B., 2003. Paleoprecipitation estimates for the Lake Naivasha basin (Kenya) during the last 175 k.y. using a lake-balance model. *Global and Planetary Change*, 36, 117–135.
- Bergner, A.G.N., Trauth, M.H., 2004. Comparison of the hydrologic and hydrochemical evolution of Lake Naivasha (Kenya) during three highstands between 175 and 60 kyr. *Palaeogeography Palaeoclimatology Palaeoecology*, 215, 17–36.
- Bergner, A.G.N., Strecker, M.R., Trauth, M.H., Deino, A., Gasse, F., Blisniuk, P., Dühnforth, M., 2009. Tectonic versus climate influences on the evolution of the lakes in the Central Kenya Rift. *Quaternary Science Reviews*, 28, 2804–2816.
- Behrensmeyer, A.K., Potts, R., Deino, A., Ditchfield, P., 2002. Olorgesailie, Kenya: A million yrs in the life of a rift basin. In: Renaut, R.W., Ashley, G.M. (Eds.), *Sedimentation in Continental Rifts*, SEPM Special Publication 73, pp. 97–106.
- Blaauw, M., 2010. Methods and code for ‘classical’ age-modelling of radiocarbon sequences. *Quaternary Geochronology*, 5, 512–518.

- Blaauw, M., Christen, J.A., 2011. Flexible paleoclimate age-depth models using an autoregressive gamma process. *Bayesian Analysis* 6, 457-474.
- Borchardt, S., Trauth, M.H., 2012. Remotely-sensed evapotranspiration estimates for an improved hydrological modeling of the early Holocene mega-lake Suguta, northern Kenya Rift. *Palaeogeography, Palaeoclimatology, Palaeoecology*, 361-362, 14-20.
- Bramble, D.M., Lieberman, D.E., 2004. Endurance running and the Evolution of Homo. *Nature*, 432, 345-352.
- Bronk Ramsey, C., 1995. Radiocarbon calibration and analysis of stratigraphy: the OxCal program. *Radiocarbon* 36, 425-430.
- Bronk Ramsey, C., 2008. Deposition models for chronological records. *Quaternary Science Reviews* 27, 42-60.
- Bronk Ramsey, C., 2009a. Bayesian analysis of radiocarbon dates. *Radiocarbon*, 51, 337-360.
- Bronk Ramsey, C., 2009b. Dealing with outliers and offsets in radiocarbon dating. *Radiocarbon* 51, 1023-1045.
- Brown, E.T., Johnson, T.C., Scholz, C.A., Cohen, A.S., King, J.W., 2007. Abrupt change in tropical African climate linked to the bipolar seesaw over the past 55,000 yrs. *Geophysical Research Letters*, 34, L20702. Deino, A., Potts, R., 1990. Single-crystal ⁴⁰Ar/³⁹Ar dating of the olorgesailie formation, Southern Kenya Rift. *Journal of Geophysical Research*, 95, 8453-8470.
- Decampo, D.M., Behrensmeyer, A.K., Potts, R., Ultrafine clay minerals of the Pleistocene Ologesailie Formation, Southern Kenya Rift: Diagenesis and paleoenvironments of early hominins. *Clays and Clay Minerals*, 58, 294-310.
- Feibel, C.S., 2011. A Geological History of the Turkana Basin. *Evolutionary Anthropology*, 20, 207-216. Foerster, V., Junginger, A., Langkamp, O., Gebru, T., Asrat, A., Umer, M., Lamb, H., Wennrich, V.,
- Rethemeyer, J., Nowaczyk, N., Trauth, M.H., Schäbitz, F., 2012. Climatic change recorded in the sediments of the Chew Bahir basin, southern Ethiopia, during the last 45,000 yrs. *Quaternary International*, 274, 25-37.
- Foerster, V., Junginger, A., Asrat, A., Umer, M., Lamb, H.F., Wennrich, V., Weber, M., Rethemeyer, J., Frank, U., Brown, M.C., Trauth, M.H., Schaebitz, F., 2014. 46 000 years of alternating wet and dry phases on decadal to orbital timescales in the cradle of modern humans: the Chew Bahir project, southern Ethiopia. *Climate of the Past Discussions*, 10, 977-1023.
- Hopf, F.A., Valone, T.J., Brown, J.H., 1993. Competition theory and the structure of ecological communities. *Evolutionary Ecology*, 7, 142-154.
- Garcin, Y., Junginger, A., Melnick, D., Olago, D.O., Strecker, M.R., Trauth, M.H., 2009. Late Pleistocene- Holocene rise and collapse of the Lake Suguta, northern Kenya Rift. *Quaternary Science Reviews*, 28, 911-925.
- Grove, M., 2013. Periods of reduced environmental variability may act as windows for hominin dispersal. Society for American Archaeology, 78th Annual Meeting, Abstracts of Individual Presentations, 179.
- Jeltsch, F., Weber, G.E., Grimm, V., 2000. Ecological buffering mechanisms in savannas: A unifying theory of long-term tree-grass coexistence. *Plant Ecology*, 161, 161-171.
- Junginger, A., Trauth, M.H., 2013. Hydrological constraints of paleo-Lake Suguta in the Northern Kenya Rift during the African Humid Period (15 - 5 ka). *Global and Planetary Change*, 111, 174-188.
- Junginger, A., Roller, S., Trauth, M.H., 2014. The effect of solar irradiation changes on water levels in the paleo-Lake Suguta, Northern Kenya Rift, during the late Pleistocene African Humid Period (15-5 ka). *Palaeogeography, Palaeoclimatology, Palaeoecology*, 396, 1-16.
- Kingston, J.D., Deino, A., Hill, A., Edgar, R., 2007. Astronomically forced climate change in the Kenyan Rift Valley 2.7-2.55 Ma: implications for the evolution of early hominin ecosystems. *Journal of Human Evolution*, 53, 487-503.
- Kutzbach, J.E., Street-Perrott, F.A., 1985. Milankovitch forcing of fluctuations in the level of tropical lakes from 18 to 0 kyr. *Nature* 317, 130-134.
- Kutzbach, J.E., Liu, Z., 1997. Response of the African monsoon to orbital forcing and ocean feedbacks in the middle Holocene. *Science*, 278, 440-443.
- Laskar, J., Gastineau, M., Joutel, F., Robutel, P., Levrard, B., Correia, A., 2004. A long term numerical solution for the insolation quantities of Earth. *Astronomy and Astrophysics*, 428, 261-285.
- Marshall, F., Hildebrand, E., 2002. Cattle before crops: the beginnings of food production in Africa. *Journal of World Prehistory*, 16, 99-143.
- Maslin, M.A., 2004. Ecological versus Climatic Thresholds. *Science*, 306, 2197-2198.
- Maslin, M.A., Christensen, B., 2007. Tectonics, orbital forcing, global climate change, and human evolution in Africa: introduction to the African paleoclimate special volume. *Journal of Human Evolution*, 53, 443-464.
- Maslin, M.A., Trauth, M.H., 2009. Plio-Pleistocene Eastern African Pulsed Climate Variability and its influence on early human evolution. In: Grine, F.E., Leakey, R.E., Fleagle, J.G. (Eds.), *The First Humans—Origins of the Genus Homo*. Springer Verlag, Vertebrate Paleobiology and Paleoanthropology Series, pp. 151-158.
- Maslin, M.A., Brierley, C.M., Milner, A.M., Shultz, S., Trauth, M.H., Wilson, K.E., 2014. East African climate pulses and early human evolution, commissioned review paper. *Quaternary Science Reviews*, 101, 1-17.
- Niewoehner, W.A., 2001. Behavioral inferences from the Skhul-Qafzeh early modern human hand remains. *PNAS*, 98, 2979-2984.
- Nowaczyk, N.R., Arz, H.W., Frank, U., Kind, J., Plessen, B., 2012. Dynamics of the Laschamp geomagnetic excursion from Black Sea sediments. *Earth and Planetary Science Letters*, 351-352, 54-69.
- Olaka, L.A., Odada, E.O., Trauth, M.H., Olago, D.O., 2010. The sensitivity of East African rift lakes to climate fluctuations. *Journal of Paleolimnology*, 44, 629-644.
- Owen, R.B., Potts, R., Behrensmeyer, A.K., Ditchfield, P., 2008. Diatomaceous sediments and environmental change in the Pleistocene Ologesailie Formation, southern Kenya Rift Valley. *Palaeogeography Palaeoclimatology Palaeoecology*, 269, 17-37.
- Owen, R.B., Potts, R., Behrensmeyer, A.K., 2009. Reply to the comment on "Diatomaceous sediments and environmental change in the Pleistocene Ologesailie Formation, southern Kenya Rift Valley" by R.B. Owen, R. Potts, A.K. Behrensmeyer and P. Ditchfield. *Palaeogeography, Palaeoclimatology, Palaeoecology*, 282, 147-148.
- Owen, R.B., Renaut, R.W., Potts, R., Behrensmeyer, A.K., 2011. Geochemical trends through time and lateral variability of diatom floras in the Pleistocene Ologesailie Formation, southern Kenya Rift Valley. *Quaternary Research*, 76, 167-179.
- Potts, R., 1996. Evolution and Climate Variability. *Science*, 273, 922-923.
- Potts, R., 2013. Hominin evolution in settings of strong environmental variability. *Quaternary Science Reviews*, 73, 1-13.
- Reimer, P.J. et al., 2013. IntCal13 and Marine13 Radiocarbon Age Calibration Curves 0–50,000 Years cal BP. *Radiocarbon*, 55, 1869-1887.
- Rightmire, G.P., 2009. Middle and later Pleistocene hominins in Africa and Southwest Asia, Proceeding of the National Academic of Sciences of the United States of America, 106, 16047-16050.
- Roach, N.T., Venkadesan, N., Rainbow, M., Lieberman, D.E., 2013. Elastic energy storage in the shoulder and the evolution of high-speed throwing in Homo. *Nature*, 498, 483-487.
- Sadler, P.M., 1999. The influence of hiatuses on sediment accumulation rates. *GeoResearch Forum*, 5, 15-40.
- Scheinfeldt, L.B., Soi, S., Tishkoff, S.A., 2010. Working toward a synthesis of archaeological, linguistic, and genetic data for inferring African population history. Proceeding of the National Academic of Sciences of the United States of

- America, 107, 8931-8938.
- Schumer, R., Jerolmack, D.J., 2009. Real and apparent changes in sediment deposition rates through time. *Journal of Geophysical Research* 114, F00A06.
- Sepulchre, P., Ramstein, G., Fluteau, F., Schuster M., Tiercelin, J.J., Brunet, M., 2006. Tectonic Uplift and Eastern Africa Aridification. *Science*, 313, 1419-1423.
- Shultz, S., Nelson, E., Dunbar, R.I.M., 2012. Hominin cognitive evolution: identifying patterns and processes in the fossil and archaeological record. *Philosophical Transactions of the Royal Society B: Biological Sciences*, 367, 2130-2140.
- Shultz, S., Maslin, M., 2013. Early human speciation, brain expansion and dispersal influenced by African climate pulses, *PLoS ONE*, 8, 76750.
- Street-Perrott, F.A., Harrison, S.P., 1985. Lake levels and climate reconstruction: In: Hecht, A.D. (Ed.), *Paleoclimate Analysis and Modeling*. Wiley, New York, pp. 291-340.
- Tierney, J.E., deMenocal, P.B., 2013. Abrupt shifts in Horn of Africa hydroclimate since the last glacial maximum. *Science*, Published online at Science Express 10 October 2013
- Trauth, M.H., Deino, A., Strecker, M.R., 2001. Response of the East African climate to orbital forcing during the Last Interglacial (130-117 kyr) and the early Last Glacial (117-60 kyr). *Geology*, 29, 499-502.
- Trauth, M.H., Deino, A., Bergner, A.G.N., Strecker, M.R., 2003. Eastern African climate change and orbital forcing during the last 175 kyr. *Earth Planetary Science Letters*, 206, 297-313.
- Trauth, M.H., Maslin, M.A., Deino, A., Strecker, M.R., 2005. Late Cenozoic Moisture History of Eastern Africa. *Science*, 309, 2051-2053.
- Trauth, M.H., Maslin, M.A., Deino, A., Strecker, M.R., Bergner, A.G.N., Dühnforth, M., 2007. High- and low- latitude forcing of Plio-Pleistocene African climate and human evolution. *Journal of Human Evolution*, 53, 475-486.
- Trauth, M.H., Maslin, M.A., 2009. Comments on "Diatomaceous sediments and environmental change in the Pleistocene Ologesailie Formation, southern Kenya Rift" by R. Bernhart Owen, Richard Potts, Anna K. Behrensmeyer and Peter Ditchfield. *Palaeogeography, Palaeoclimatology, Palaeoecology*, 282, 145-146.
- Trauth, M.H., Maslin, M.A., Deino, A., Junginger, A., Lesoloyia, M., Odada, E., Olago, D.O., Olaka, L., Strecker, M.R., Tiedemann, R., 2010. Human Evolution in a Variable Environment: The Amplifier Lakes of Eastern Africa. *Quaternary Science Reviews*, 29, 2981-3348.
- Trauth, M.H., 2014. A New Probabilistic Technique to Determine the Best Age Model for Complex Stratigraphic Sequences. *Quaternary Geochronology*, 22, 65-71.
- Wichura, H., Bousquet, R., Oberhänsli, R., Strecker, M.R., Trauth, M.H., 2010. Evidence for Mid-Miocene uplift of the East African Plateau. *Geology*, 38, 543-546.



Chapter V

Environmental Change and Human Occupation of Southern Ethiopia and Northern Kenya during the last 20,000 years

Verena Foerster, Ralf Vogelsang, Annett Junginger, Asfawossen Asrat,
Henry F. Lamb, Frank Schaebitz, Martin H. Trauth

submitted to *Quaternary Science Research*

Environmental Change and Human Occupation of Southern Ethiopia and Northern Kenya during the last 20,000 years

V. Foerster^{1*}, R. Vogelsang², A. Junginger³, A. Asrat⁴, H. F. Lamb⁵, F. Schaebitz¹, M.H. Trauth³

¹ University of Cologne, Seminar for Geography and Education; Gronewaldstrasse 2; 50931 Cologne; Germany

² University of Cologne, Institute of Prehistoric Archaeology; Germany

³ University of Potsdam, Institute of Earth and Environmental Science; Germany

⁴ Addis Ababa University, School of Earth Sciences; Ethiopia

⁵ Aberystwyth University, Institute of Geography and Earth Sciences; U.K.

* corresponding author

Abstract

Debate about the impact of climate-driven environmental change on prehistoric human populations suffers from the rarity of continuous paleoenvironmental records in the vicinity of archaeological sites. Here we compare the last 20 ka of a continuous paleoclimatic record from the Chew Bahir basin, southwest Ethiopia, with the available archaeological record of human presence in the region. The paleoclimatic record suggests a complex nonlinear response of the environment to orbitally-driven insolation variations, reflected in several long-term and short-term transitions of only several years between wet and dry conditions, interpreted as favorable and unfavorable human living conditions, respectively. Correlating the patchy archaeological record in the surrounding region, postulated to include montane and lake-marginal refugia for human populations, with our record of climate change suggests a complex interplay between humans and their environment during the last 20 ka. The result may be an indication of how a dynamic environment may have impacted the adaptation and dispersal of early humans in eastern Africa.

Keywords: Refugia, climatic change; climate event; push-factor; migration; hunter-gatherer; adaptation; African Humid Period; Chew Bahir; Mid-Holocene wet-dry transition

5.1 Introduction

Climatic change is broadly considered to be one of the major drivers for human migration including the dispersal of early modern humans (Beyin, 2011a; Rosenberg et al., 2011; Richter et al. 2012) and the shift from hunter-gatherers to pastoralism (Garcin et al., 2012; Lesur et al., 2013). However, it is not clear whether climate change affected human migration (e.g. Brandt et al., 2012) and how other factors, such as human agency, might have been involved. The same issue applies to the role of climatic change for the emergence of technological and behavioral innovation (Ambrose et al., 1998; Garcin et al., 2012; Ziegler et al., 2013).

If climatic change is assumed to play an important role and the mode of climatic change could have controlled the way in which human populations responded to climatic variations, questions arise as to whether this depended on the duration and direction of transitional

states, whether short-term events or rather long-term gradual transitions were the relevant drivers, what the underlying climatic conditions to be associated with human dispersal were and whether abrupt changes to unfavorable conditions i.e. pronounced aridity (deMenocal, 1995; Carto et al., 2009) may have triggered the migration of surviving populations to more favorable locations, or whether it was the change to favorable living conditions, a humid phase, that provided sufficient resources to allow the population to grow and subsequently disperse through otherwise ecologically critical zones (e.g. Kröpelin et al., 2008; Castañeda et al., 2009) into larger geographical space over several generations. These debates are hampered by the lack of continuous high-resolution terrestrial paleoenvironmental records in Eastern Africa (Brandt et al., 2012) and the limited resources of archaeological data in the same region for the corresponding timespan (Basell, 2008; Leplongeon, 2013).

As a contribution to these debates, a continuous high-resolution lacustrine record for the past 20 ka from Chew Bahir, a deep sedimentary basin in southwest Ethiopia is presented here. The record is correlated with the available archaeological record of human occupation in the region, as a way of evaluating the impact of different climatic shifts on local terrestrial ecosystems (including human communities) at various timescales (10^1 – 10^4 yrs). The evidence of human occupation is based on the variations in radiocarbon frequency in documented archaeological sites in the nearby SW Ethiopian highlands and the adjacent lake margin of Lake Turkana and the Main Ethiopian Rift lakes (Fig. 5.1). The precipitation-rich (Fig. 5.1) highlands (Ambrose, 1998; Brandt et al., 2012; Brandt and Hildebrand, 2005) and these lake margins (Basell, 2008; Joordens et al., 2011) are hypothesized to have been a refugium and centre of innovation during times of climatic stress. The Chew Bahir, today a completely dried out saline mud-flat providing the climatic background for this correla-

tion, is situated in a biogeographically highly sensitive transition zone between the Main Ethiopian Rift and the Omo-Turkana basin where the fossils of the oldest known anatomically modern human were found (e.g. Day and Stringer, 1991; McDougall et al., 2005; 2008; Sisk and Shea, 2008).

In order to evaluate how contrasting rates of environmental change impacted settlement pattern and cultural innovation for survival and adaptation, we test the extent to which gradual and rapid climatic events in the lacustrine sedimentary record are also expressed in the archaeological record of hypothesized refugia. A period covering the last 20 ka was used because it provides both, the highest archaeological data coverage for post Middle Stone age assemblages (Basell, 2008) as well as a detailed sedimentary record of dry-wet alternation within a full precessional cycle. This is a novel and first time approach to directly link two research areas, archaeology and paleoclimatology, directly from the

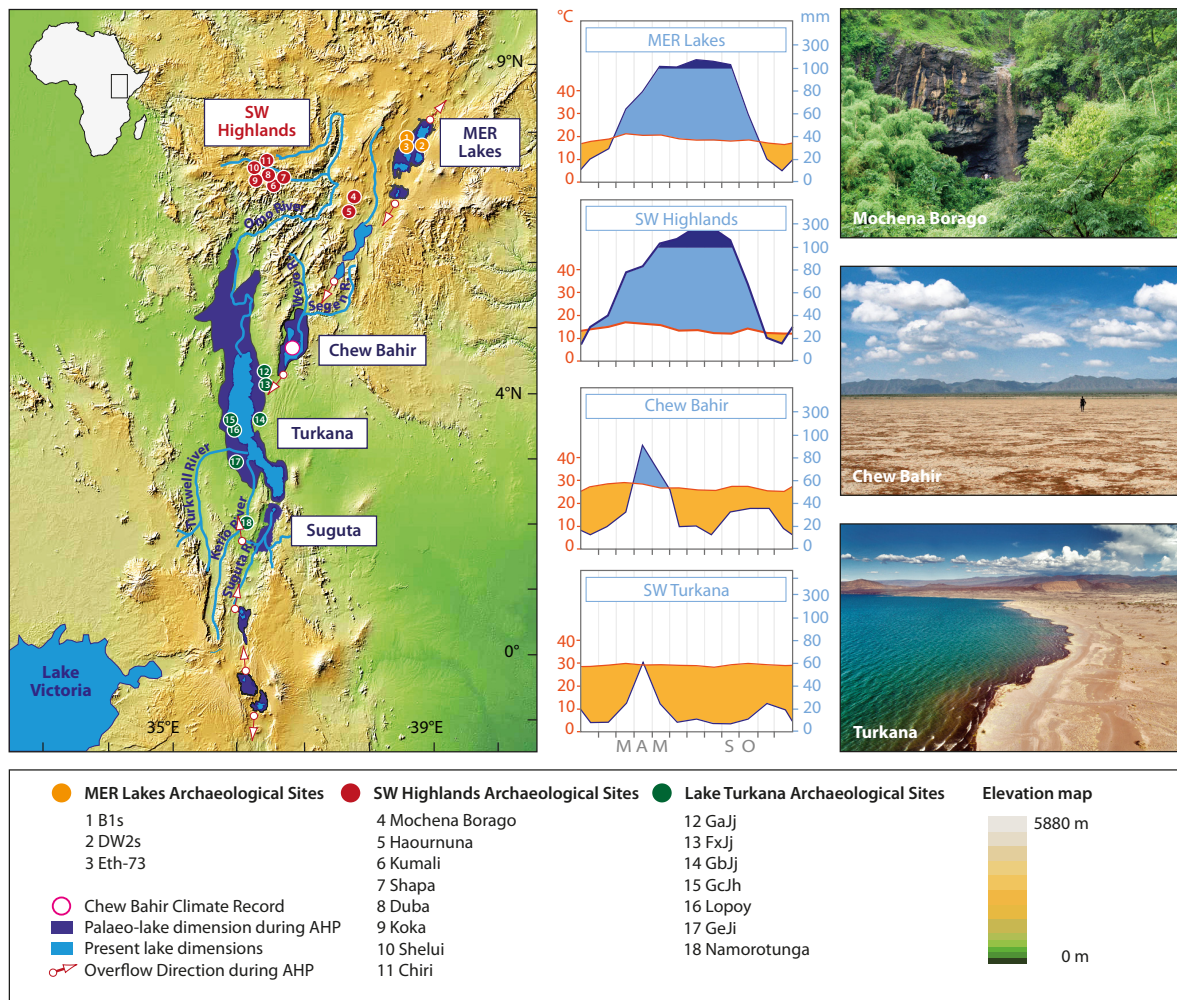


Figure 5.1 | Setting of the Chew Bahir basin and archaeological sites in potential refugia. Archaeological sites are indicated by coloured circles and numbers, that correspond to site names and numbers in Table 5.1, to provide complete sample ID and cultural association. The pink circle marks the site of the Chew Bahir record. Climate diagrams represent monthly temperature means in °C and precipitation in mm/month (IRI, last accessed 2/2014). Photographs from top: (1) Mochena Borago rock shelter in the SW Ethiopian highlands; (2) mudflats of the Chew Bahir basin, with the Hammar range in the background; (3) aerial shot of Lake Turkana, NE shore.

source area of modern humans and synthesis first hypotheses on the interrelationship of both. Due to the incompleteness of the archaeological data set, the result is of course very hypothetical but could be the starting point for in-depth studies on the subject.

5.2 Data and methods

5.2.1 Paleoclimatic reconstruction using continuous lacustrine sedimentary records

In a pilot study for the deep-drilling campaign of the ‘Hominid Sites and Paleolakes Drilling Project’ (HSPDP, <http://hspdp.asu.edu/>), six cores on a NW-SE transect across the Chew Bahir basin were collected during two consecutive drilling campaigns in 2009 and 2010. The cores were 9 to 19 m long, covered up to 60 ka (all reported ages are expressed as ka cal BP) and were analyzed for geochemical, geophysical, biological, and sedimentological parameters. The composite age model is based on 32 AMS ^{14}C ages derived from biogenic carbonate, fossilized charcoal and organic sediment (Foerster et al., 2012; Trauth et al., in press). Ages were calibrated with OxCal (Bronk Ramsey, 1995) using the IntCal13 calibration data set (Reimer et al., 2013). The weighted mean of the probability density function was used for the age model, which was constructed by linear interpolation between dated levels (Trauth et al., in press). For the interpolation of all proxy records upon the age model the most reliable results were obtained by using a linear interpolation technique. We refrained from tuning our climate record to high-latitude records or other East African records. For the paleoclimate discussion here we focus on the results of CB01 since this core has the highest temporal resolution (~3–10 years) for the past 20 ka.

The proxy-climate record (Fig. 5.2) is based on potassium (K) abundance, previously established as a reliable proxy for aridity in the Chew Bahir cores (Foerster et al., 2012). Increased influx of K occurs during dry phases, due to enhanced activity of extensive, sparsely-vegetated alluvial fans fed by the potassium-rich gneisses and granites of the adjacent Hammar Range. During arid phases, when rainfall events are rare and short-lived, K, the weathering product of feldspar, feldspar-thoids and mica with a high solubility and reactivity, is rapidly transported from the constrained source of the Hammar Range to the Chew Bahir basin. Furthermore, high occurrences of K have been shown to be linked to changes in the lake water chemistry, that in turn is controlled by variations in precipitation influx (Foerster et al., 2014). During the most arid phases, the paleolake is thought to have become completely desiccated, or at least strongly regressed with a very low biogenic

productivity (Foerster et al., 2014). With the onset of greater, more evenly distributed rainfall during humid phases, an extensive (2,000 km²) paleolake filled the basin with a maximal water depth of 50 m. Fluvial input increased and a dense vegetation cover that must be assumed for phases of increased humidity (e.g. Mohammed and Bonnefille, 1998; Dupont et al., 2000; Umer et al., 2007) on the slopes of the Rift flanks most likely constrained the influence of the alluvial fans off the Hammar Range, which represents the major source of the K-rich minerals. Other proxies support this interpretation: the diatom stratigraphy indicates that freshwater conditions prevailed during long, stable humid phases (Foerster et al., 2014). These data, taken together with lake-level reconstructions from Lake Turkana and Lake Suguta (Fig. 5.2), give an indication of the immense environmental impact of the major climatic fluctuations, especially the dry intervals that punctuate the early-mid Holocene African Humid Period (AHP).

5.2.2 Evidence of human occupation by radiocarbon date frequency

The regional and chronological distribution of archaeological sites may not be a direct indicator of settlement intensities, as it is influenced by a number of external factors. The method of using radiocarbon frequency to infer human presence and mobility has limitations generally caused by gaps during certain phases, that connote human absence in the area, but do not prove that humans were definitely not present during that time: the evidence of their presence may not have yet been recovered, or, also possible, was not preserved. The accessibility of the area has a clear influence on the research activities and therewith on the number of yet undiscovered sites and, consequently, the number of derived ages. Preservation conditions of datable organic material under changing climatic conditions contribute to the availability of radiocarbon dates, which also include the undocumented removal of finds by natural (degradation, inundation, erosion etc.) as well as anthropogenic forces.

However, keeping these caveats in mind, and considering that this is the only available approach to determine the settlement intensity in the area, the frequency of radiocarbon dates from archaeological sites nevertheless provides a valuable indication of changing settlement patterns, allowing inferences about where, when and, at best, how far humans were influenced by climatic conditions: Increased human occupation should give rise to a higher archaeological visibility. Human occupation is presented here using radiocarbon date frequency from two documented ecologically favorable zones in close proximity to our

climate record; the high-precipitation highlands and around lake margins (Figure 5.1).

Specifically, our initial archaeological dataset is comprised of 26 radiocarbon dates from the SW Ethiopian highlands (Table 5.1), predominately from two research projects; the Kaffa Archaeological Project (sites are located between 1370 and 2260 m a.s.l.; Hildebrand et al., 2010; Hildebrand and Brandt, 2010) and the excavations at Mochena Borago rock shelter (2230 m a.s.l.; Brandt et al., 2012; Gutherz et al., 2002). Due to the close proximity of these sites to the Chew Bahir catchment, climatic shifts of the highland region should be visible in the sedimentary record of the basin. Similarly, we would expect to find an expression of climatic extremes in the settlement activities of the postulated highland refugia (Fig. 5.1) for the last dry-wet cycle. A second dataset, the lake refugia dataset, comprises 31 radiocarbon dates from Lake Turkana and 6 dates from the Ziway-Shalla basin, (Table 5.1), which are hypothesized to have served as retreat areas for humans during times of climatic stress (Basell, 2008; Joordens et al., 2011). In order to ensure consistent calibrated ages, we used conventional radiocarbon ages and calibrated them using CalPal (version April 2013, Weninger and Jöris, 2008) with the IntCal13 calibration curve (Reimer et al., 2013). All ages were calibrated using the 2-sigma standard deviation. Age determinations on bone apatite were excluded because of the large uncertainties of these ages.

5.3 Results and Interpretation

5.3.1 Climatic change and phases of climatic stress

The climatic record of the Chew Bahir sediments, expressed here in the variability of the aridity proxy *K*, shows that moisture availability has been subject to dramatic fluctuations on time scales ranging from 10^4 to 10^1 years, with either relative abrupt or gradual expression (Fig. 5.2). Extreme dry conditions in the Chew Bahir basin prevailed prior to 15 ka BP and were interrupted by short-term wet-spells of 200–500 year duration (Foerster et al., 2012). From 15 ka onwards an abrupt change into full humid conditions of the 10,000 year-long African Humid Period (AHP) occurred as a late response to a precessional-controlled Northern Hemisphere (NH) insolation maximum (Foerster et al., 2012). The observed pronounced change is presumably to have forced a marked environmental transformation from unstable dry conditions to a pronounced moisture availability, which resulted in the establishment of large fresh water lakes and the development of a lush vegetation cover. Despite the high moisture availabil-

ity, several short-term drought events interrupted this humid period. For instance, between 14.2–13.5 ka, an event suggested to be related to the Older Dryas (OD, ~14 ka, Stager et al., 2002) potentially caused the return to drought conditions directly after the abrupt and pronounced onset of the AHP. Another major dry spell occurred between ~12.8–11.6 ka that correlates with the well known NH Younger Dryas cold event (YD, Foerster et al., 2012) and is expressed in Chew Bahir record as an abrupt return to aridity, comparable to drought conditions during the last glacial which were thought to cause the complete desiccation of paleolake Chew Bahir. This arid event is documented in a wide range of sites in Africa north of 10°S (e.g. Barker et al., 2004; Tierney et al., 2011; Junginger et al., 2014). The transition from the YD to the relatively stable humid climate of the early and mid-Holocene also occurred relatively fast, within ± 200 years. As the climate proxies and fossil records indicate, this rapidly changing environment culminated in the development of an extensive (2,000 km²), nutrient-rich freshwater lake, at least 50 m in depth, with abundant fish and surrounded by dense vegetation. This paleo-lake Chew Bahir overflowed into Lake Turkana during high stands (Grove et al., 1975; Junginger and Trauth, 2013).

Other arid excursions during the AHP with moisture fluctuations are observed at ~10.5, ~9.5, 8.15–7.8 and ~7 ka BP which were not thought to have resulted in a complete desiccation of the paleolake and disappearance of the surrounding vegetation. The most pronounced arid excursion, dated here to ~7.8 ka BP, would have affected the environment considerably, but would not have resulted in a complete lake regression or vegetation change, possibly allowing human populations to persist in the area, despite droughts lasting several centuries. This interpretation is supported by lake level reconstructions of nearby paleolake Turkana and paleolake Suguta (Garcin et al., 2012; Junginger et al., 2013) that also show several excursions to arid conditions during the AHP lake interval. The dry spell at ~7.8 ka BP was preceded by a gradual ~1,000 year-long gradual slight moisture reduction, which has been also observed at many low-latitude sites (e.g. Fleitmann et al., 2003, Dykoski et al., 2005; Gupta et al., 2005; Weldeab et al., 2007), and is assumed to have preceded/lead into the 8.2 ka event observed in the NH (Benson et al., 1997). In southern Ethiopia the humid conditions of the AHP gradually declined from ~6.5 ka to ~5 ka, punctuated by several 80–20 year-long dry events (Trauth et al., in press). Arid conditions have persisted since, interrupted only by a short-lived event of higher moisture availability at ~3 ka BP and a sharply defined wet phase between ~2.2–1.3 ka BP.

Table 5.1 | [page 1] Radiocarbon dates from archaeological sites and attribution to cultural complex

Site	Fig. Ref ^c	Excavation unit	Cultural complex	Sample ID	Sample material	¹⁴ C age [yrs BP] ^a	Age [cal BP] ^b	AMS Conv.	Reference
Main Ethiopian Rift (MER) Lakes									
B1s1	1	Unit XIV	Terminal Pleistocene LSA	Beta-292524	charcoal	11,480 ± 50	13,340 ± 70	AMS	Ménard, C. et al., 2014
B1s1	1	Unit VIII	Terminal Pleistocene LSA	LY-6059	charcoal	11,480 ± 60	13,330 ± 80	AMS	Ménard, C. et al., 2014
DW2s2	2	PS4	Early Holocene LSA	Beta-295898	charcoal	10,040 ± 50	11,560 ± 190	AMS	Ménard, C. et al., 2014
DW2s1	2	PS3	Early Holocene LSA	Beta-320183	charcoal	9,830 ± 50	11,250 ± 50	AMS	Ménard, C. et al., 2014
B1s4	1		Terminal Pleistocene LSA	Beta-332588	charcoal	12,040 ± 50	13,900 ± 90	AMS	Ménard, C. et al., 2014
Eth-73-3-III	3		LSA	SMU-86	charcoal	10,330 ± 90	12,190 ± 140	Conv.	Humphreys, 1978
Turkana; eastern shore									
GauJ3	12	Beach sands Unit B	Fishing settlement	Gx 5475 A	bone (fish)	4,560 ± 185	5,240 ± 280	Conv.	Owen et al., 1982; Bartheime 1985, 131
GauJ1; Nderati Wells	12		Pre-ceramic LSA	Gx 5478	?	13,040 ± 640	15,550 ± 1320	Conv.	Mgomezulu, 1981
GauJ11 ^a	12	Sand bar	Fishing settlement; (pre-pottery LSA?)	Hel-1276	shell	8,920 ± 130	9,920 ± 250	Conv.	Owen et al., 1982
GauJ11	12	Sand bar	Fishing settlement; (pre-pottery LSA?)	Hel-1277	<i>Ethiopia</i> shell	9,110 ± 130	10,250 ± 230	Conv.	Owen et al., 1982
FxJ12	13	Sand spits	Fishing settlement; (pre-pottery LSA?)	Gx-5479	shell	9,660 ± 235	11,030 ± 510	Conv.	Owen et al., 1982
FxJ12	13	Sand spits	Fishing settlement; (pre-pottery LSA?)	R1-954	shell	9,940 ± 260	11,530 ± 600	Conv.	Owen et al., 1982
GauJ2	12	Beach sands; Lower horizon	Pastoral Neolithic; (cattle bones)	P-2609	charcoal	3,970 ± 60	4,410 ± 110	Conv.	Owen et al., 1982; Bartheime, 1985
GauJ2	12	Beach sands; Lower horizon	Pastoral Neolithic; (cattle bones)	SUA-634	charcoal	4,160 ± 110	4,680 ± 180	Conv.	Owen et al., 1982; Bartheime, 1985
GauJ4; Dongodien	12	Beach sands; Unit 5C	Pastoral Neolithic; (cattle bones)	SUA-637	charcoal	3,945 ± 135	4,410 ± 290	Conv.	Owen et al., 1982; Bartheime, 1985, 181
GauJ4; Dongodien	12	Beach sands; Unit 5C	Pastoral Neolithic; (cattle bones)	SUA-637 B	humic acid	4,100 ± 125	4,550 ± 210	Conv.	Owen et al., 1982; Bartheime, 1985, 181
GauJ4; Dongodien	12	Beach sands; Unit 5C	Pastoral Neolithic; (cattle bones)	P-2610	charcoal	3,960 ± 60	4,400 ± 110	Conv.	Owen et al., 1982; Bartheime, 1985, 181
GauJ4; Dongodien	12	Beach sands; Unit 5C	Pastoral Neolithic; (cattle bones)	Beta-252053	charcoal	4,180 ± 40	4,710 ± 90	AMS	Ashley et al., 2011
GauJ4; Dongodien	12	Beach sands; Unit 5C	Pastoral Neolithic; (cattle bones)	Beta-252054	charcoal	4,240 ± 40	4,770 ± 70	AMS	Ashley et al., 2011
GauJ4; Dongodien	12	Beach sands; Unit 5C	Pastoral Neolithic; (cattle bones)	Beta-252056	charcoal	4,180 ± 40	4,710 ± 90	AMS	Ashley et al., 2011
Jarigole GbJ1	14		Pillar site; Pastoral Neolithic	AA85131	OES-bead	4,381 ± 39	4,950 ± 70	AMS	Hildebrand and Grillo, 2012
Jarigole GbJ1	14		Pillar site; Pastoral Neolithic	AA85132	OES-bead	4,251 ± 39	4,780 ± 60	AMS	Hildebrand and Grillo, 2012
Jarigole GbJ1	14		Pillar site; Pastoral Neolithic	AA85133	OES-bead	4,401 ± 39	4,970 ± 80	AMS	Hildebrand and Grillo, 2012
Jarigole GbJ1	14		Pillar site; Pastoral Neolithic	AA85134	OES-bead	4,146 ± 53	4,680 ± 110	AMS	Hildebrand and Grillo, 2012
Il Lokeride Gaj23	12		Pillar site	TO-4911	charcoal	4,180 ± 60	4,690 ± 110	AMS	Koch, 1994; Koch et al., 2002
Turkana; southern shore									
Namoratunga	18		Burial site	GX-5042-A	bone collagen	2,285 ± 165	2,320 ± 290	Conv.	Lynch and Robbins, 1979
Turkana; western shore									
Lopoy	16		LSA „Turkwell“ tradition (pottery)	UCLA 2124J	charcoal	950 ± 80	860 ± 110	Conv.	Lynch and Robbins, 1979
Lopoy	16	Hearth	LSA „Turkwell“ tradition (pottery)	UCLA 2124G	Charcoal	870 ± 80	810 ± 90	Conv.	Lynch and Robbins, 1979
Lothagam North; GeJ9	17		Pillar site	ISGS-A1491	OES-bead	4,385 ± 15	4,940 ± 60	AMS	Hildebrand and Grillo, 2012
Lothagam North; GeJ9	17		Pillar site	ISGS-A1505	OES-bead	4,165 ± 20	4,720 ± 80	AMS	Hildebrand and Grillo, 2012
Lothagam North; GeJ9	17		Pillar site	ISGS-A1492	OES-bead	4,265 ± 15	4,840 ± 20	AMS	Hildebrand and Grillo, 2012
Lothagam West; GeJ10	17		Pillar site	ISGS-A1494	charcoal	4,290 ± 20	4,850 ± 20	AMS	Hildebrand and Grillo, 2012
Kaloko; GcJh3	15		Pillar site	ISGS-A1493	OES-fragment	3,890 ± 15	4,330 ± 60	AMS	Hildebrand and Grillo, 2012
Manemanya; GcJh5	15		Pillar site	ISGS-A1504	OES-bead	4,255 ± 15	4,840 ± 20	AMS	Hildebrand and Grillo, 2012
Manemanya; GcJh5	15		Pillar site	ISGS-A1490	OES-bead	3,805 ± 15	4,190 ± 30	AMS	Hildebrand and Grillo, 2012
Kokito 01; GcJh11	15	Unit A	LSA; (pre-pottery)	ISGS-A1714	charcoal	9,785 ± 35	11,220 ± 30	AMS	Beysie, 2011b
Kokito 01; GcJh11	15	Unit A	LSA; (pre-pottery)	ISGS-A1715	charcoal	9,060 ± 30	10,220 ± 30	AMS	Beysie, 2011b

5.3.2 Human occupation in a changing environment

Although derived from a sparse archaeological dataset, the frequency distribution of radiocarbon dates over the past 20 ka contains distinct patterns of human occupation, including episodes of human settlement, interrupted by periods without such activity. The record of radiocarbon dates demonstrates that the oldest evidence for occupation is at two brief episodes between ~14.0–13.7 and ~13.4–13.2 ka BP, which comes from sites in the Ziway-Shalla basin. During the AHP high-stands this basin was a paleolake up to 120 m deep, formed by the merging of the MER lakes Abiyata, Langano, Ziway and Shalla (Gillespie et al., 1983). The interval of ~14–13.2 ka BP may coincide with the high-latitude OD climatic event (Stager et al., 2002), recorded in Chew Bahir as a ~700 year-long drier episode after the abrupt onset of the AHP. The sites where the MER artefacts were found are situated between Lake Ziway and Abiyata-Langano, which implies that during this dry episode the lake level had been reduced to a level where settlement between the lake systems was possible. As these settlement activities coincide with a short phase of drier conditions, lake regressions and deterioration of water quality, this area can also be interpreted as a (lake) refugia. Human occupation is also identified at ~13.9 ka BP in the SW Highlands. Generally, no evidence for occupation is apparent before this interval, probably because extremely dry LGM conditions could have made the area mostly uninhabitable, although it is not sure whether the SW highlands were also entirely abandoned and where humans were during this interval. In general, a strong hiatus on archaeological remains during the period between 30 to 15 ka BP exists, presumably superimposed by the prevailing dry conditions (e.g. Leplongeon, 2013). At the onset of the AHP, living conditions greatly improved enough with significantly increased moisture availability as reflected in the climate record of Chew Bahir (Fig. 5.2) and the abrupt and rapid development of large lakes (Junginger et al., 2013).

Evidence for human activity follows at the northeastern shore of paleo-Lake Turkana between ~11.5 and 9.2 ka BP. Due to the contrasting reconstructions of paleo-Lake Turkana's lake levels that are based on non-continuous and/or different proxy data sets (Johnson et al., 1991; Brown and Fuller, 2008; Garcin et al., 2012) it is not clear though whether the level of paleolake Turkana may have fluctuated repeatedly by 50 m during this interval or it may have fallen gradually by 20 m between ~10.8–10 ka BP. After the pronounced dry phase of the Younger Dryas, lasting for about 1,200 years, all rift lakes including the Chew Bahir and Lake Turkana

rapidly re-filled. Two archaeological sites at the north-eastern shore (Fxj 12 and Gaji 11) are situated almost at the highest shoreline of the paleolake, right at the river that connected Chew Bahir with Turkana during overflow. Assuming occupation along the lake shore at ~11.5–9.2, there was probably an additional third rainy season in August-September, between the regular spring and autumn rainy seasons linked to the insolation maximum at the equator. This additional rainy season would have resulted in almost continuous rainfall from April to November (Junginger and Trauth, 2013; Junginger et al., 2014). Lake-level records indicate that this extra rainy season may have been unstable, causing pronounced fluctuations in the water budget of the lakes (Junginger et al., 2014). The apparent break in the occupation record after 9.2 ka could be explained by the highly fluctuating lake levels, simply washing away all archaeological evidence. It is also possible that the lake-marginal environment was unfavorable for occupation during periods of high rainfall, when relatively dense woody vegetation would have made hunting more difficult and could have favored the spread of disease.

The evidence for human occupation in the SW highlands during the AHP is especially noteworthy: here, several short-term occupation episodes are dated to 10.5–10.2 ka, 9.5–9.3 ka, 8.0–7.8 ka and 7.0–6.5 ka. These intervals predominantly coincided (within dating limitations) with short-term events of pronounced aridity interrupting the pronounced wet phase of the AHP. The climatic events in question are found in the Chew Bahir record, and are also strongly evident in both paleolake Turkana and in paleolake Suguta, where lake regression and a rapidly changing environment would have been accompanied by marked deterioration in water quality. Paleolake Chew Bahir would have been increasingly saline and alkaline, which is likely to be comparable to Lake Turkana today (e.g. Odada et al., 2003).

The short-term changes in moisture availability during the AHP may have been driven by variations in insolation, caused by pronounced sun-spot events (Solanki, et al., 2004; Junginger et al., 2014). The solar activity variation is assumed to have caused the absence of the third rainy season in August-September as well as attenuation of the other two wet seasons, as reconstructed for many sites ranging from Lake Victoria along the Eastern Rift to Oman (e.g. Burns et al., 2008; Neff et al., 2001; Stager et al., 2002). This caused short-term episodes of pronounced aridity within a few decades, which caused unfavorable conditions for humans in large parts of the lowlands. As the radiocarbon frequency record suggests, the SW Highlands seem to

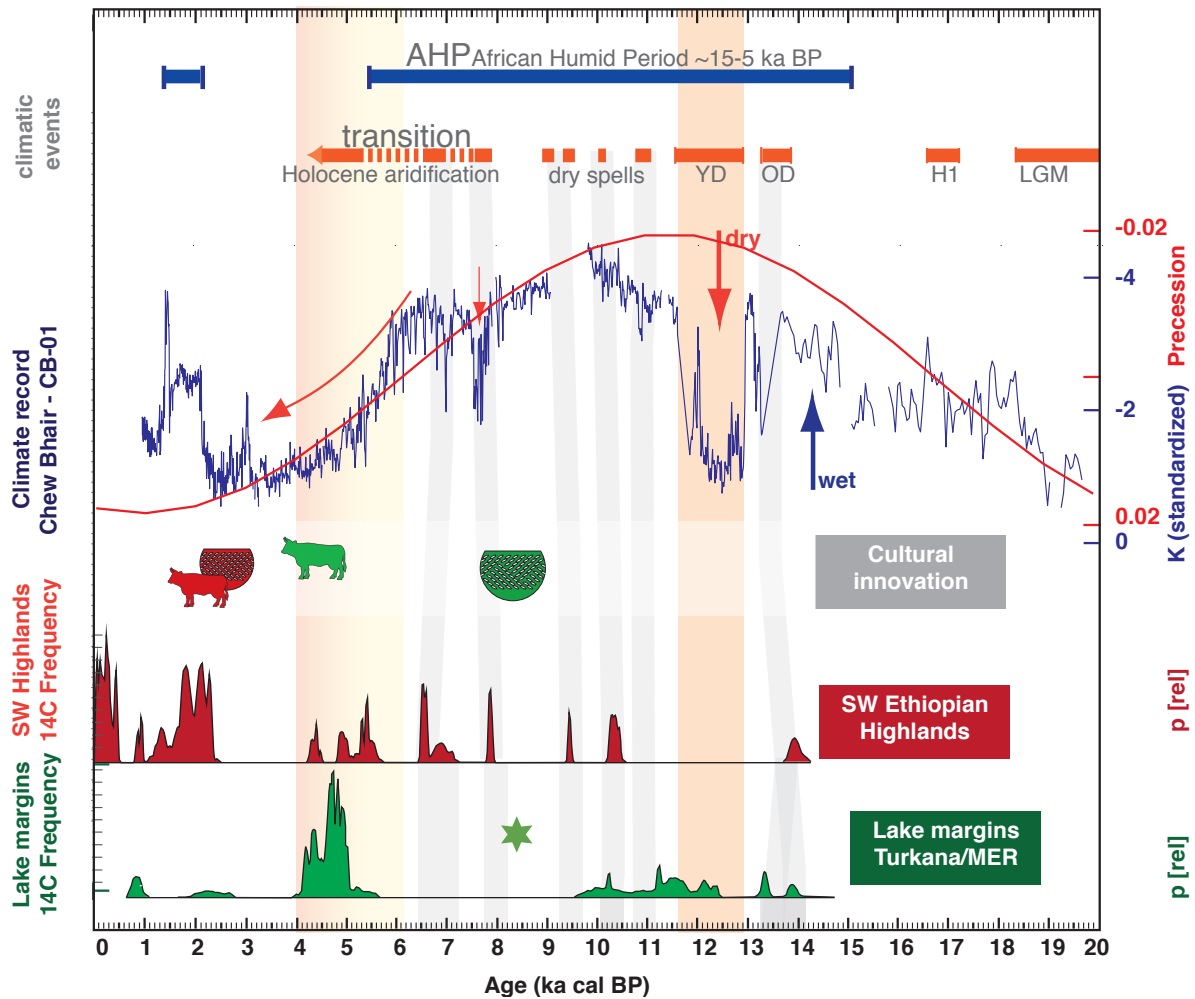


Figure 5.2 | Comparison of (a) the 20 ka Chew Bahir climatic record (K content as a proxy for aridity) with (b) settlement in the SW Ethiopian Highlands and around lake margins (Turkana and Ziway-Shalla lakes). Climatic events: AHP - African Humid Period (~15-5 ka BP), YD - Younger Dryas (~12.8 -11.6 ka BP), OD - Older Dryas (around 14 ka BP), H1 - Heinrich event 1 (around 16 ka BP), LGM - Last Glacial Maximum (~24-18 ka BP). During the AHP, several pronounced dry spells (grey bars) occur, modulating the wet phase; the gradual Holocene aridification (orange bar) is punctuated by arid events on a decadal timescale (Trauth et al., in press). Settlement activities in both potential refugia are indicated by radiocarbon frequency of archaeological finds, as listed in Table 5.1. Cultural innovation is indicated by first documented wavy-line pottery (pot symbol) and the introduction of pastoralism (cow symbol); red or green colors refer to SW highlands or lake margins respectively. The green star signifies culture-related evidence of occupation that is not clearly datable.

have served as a refugium during these climatically stressed episodes, on decadal to millennial time scales during otherwise long-term favorable conditions. Although the dates are too few for a robust interpretation and dating precision is a problem, the seemingly striking correlation of settlement episodes in the highlands with the occurrence of pronounced aridity events at least deserves further research, specifically on the locations of human occupation during more favorable climatically conditions.

Therefore, a phase, which is climatically characterized by several sharp drought events punctuating a humid phase (that otherwise would have enabled favorable living conditions over broad areas), is then reflected in the archaeological record of a hypothesized retreat area as several phases of increased settlement activity. These were most likely caused by short-term vertical

migration of mobile hunter-gatherers. We thus carefully interpret this co-occurrence of short-term aridity and occupation of the highlands as the possible result of drought working as a push-factor for a refugium-directed movement that would have otherwise been against hunter-gatherers' preference.

With the onset of the >1,500 year-long Holocene aridification trend (~6.5–5 ka), there is a striking coincidence between moisture decrease and colonization of the lake regions and the highlands. It is rather likely that this movement was even further pushed by the series of short drought events 20–80 years long, which are further described by Trauth et al. (in press, JHE). These at least 19 events of extreme aridity punctuating the gradual transition to present-day arid conditions are presumed to have had considerable effect on humans, and may have contributed to the climate-driven cultural

change presented hereafter. Between ~4.5 and 2 ka BP, extreme aridity could have ended habitation even in the two ecologically favored regions and where human populations survived is still an open question. The climate record suggests that aridity reached a level where lakes became highly saline and alkaline, rivers dried up, and the vegetation cover diminished in conditions of sparse, unevenly distributed rainfall. There is a significant discontinuity in the record of human occupation over the same interval, which could imply that movement to nearby refugia was an inadequate strategy for survival and mortality was high throughout the region, with survivors dispersed to distant regions. Renewed human occupation of both lake and montane refugia occurred only with the inferred moisture increase around ~2 ka BP, with consequent amelioration of living conditions.

5.4 Discussion

5.4.1 Indications of climate-driven cultural change

The environmental shifts recorded in the Chew Bahir sediments were likely to impact on the living conditions of prehistoric humans. One possible impact of these shifts is fluctuations of human occupation in the area, inferred from the presence or absence of archaeological data for certain periods, particularly for the period prior to 15 ka BP. Some human populations may not have survived aridity; others would have adopted novel or modified subsistence strategies. Garcin et al. (2012) interpreted the chronological synchronism of low lake levels and the emergence of pastoralism in the Turkana Lake region in a similar manner. However, a simplistic model of cause and effect between environmental parameters and human behavior is an inadequate conception of their complex interplay. Examples of economic transformations from other regions, such as northeast Africa, show that external conditions reduce the range of possible developments, while socio-cultural conditions favor particular concepts (Keding, 2009; Vogel-sang and Keding, 2013). In addition, further incalculable factors, which may be summarized under the ambiguous term of “human agency” play a determining role in the human decision making (Dobres and Robb, 2000).

Despite their proximity, cultural development in the highlands and lake-marginal areas differ considerably. At Turkana, early pottery is found at forager sites as early as ~10 ka BP. Diagnostic features of these sites are fisher-hunter-gatherer subsistence which relied heavily on aquatic resources and restricted residential mobility. This lifestyle and its diagnostic artefacts, such as wavy-line pottery and harpoons (Phillipson, 1977; Barthelme,

1985) link these sites with assemblages from the southern Sahara, which are grouped under the term “African Aqualithic” (Sutton, 1977) or “Khartoum Horizon-Style” (Hays, 1971). However, dating of the Turkana sites is problematic (see error bar that is associated with the presumed emergence of early pottery at Turkana in Fig. 5.2), because most early dates were measured on bone apatite, and were therefore considered too unreliable to be represented in our dataset (Fig. 5.2). Despite these dating problems it is commonly agreed that pottery was already produced in the area before early domesticates arrived. The diagnostic decorated sherds can be assigned to the eastern facies of the wavy line group, which is distributed over a large area in north-eastern Africa between ~11 and ~7 ka BP (Jesse, 2003, Tab. 61, Tab.62, p.283 ff.).

The beginning of herding around 4 ka BP is contemporaneous with the construction of megalithic pillar sites and with the earliest secure dates for Nderit pottery (Hildebrand and Grillo, 2012). In contrast, domesticates and pottery do not appear in combination in the southwest Ethiopian highlands until 2,000 years later (Lesur-Gebremariam, 2009, Hildebrand et al. 2010, Lesur et al., 2013). Preliminary occupation of the highlands is characterized by highly mobile unspecialized hunter-gatherer groups, which exploited a broad spectrum of resources in an opportunistic way (Lesur et al., 2007). This contrasts with the social organization of more complex hunter-gatherers, identifiable by sedentism or substantially restricted residential mobility, and a “focal exploitation of a particular resource (commonly fish)” (Kelly, 1995, 302). The lake environment of Lake Turkana may have fostered the emergence of such complex hunter-gatherer groups. Further characteristics of such groups are ownership of resources, a more formal leadership and an erosion of egalitarian ideology (Kelly, 1995, 302; Zvelebil, 1998, 8). Such attributes of a socio-economic pre-adaptation to a food producing economy might have facilitated a subsistence change in the Turkana region.

Nevertheless, the chronological difference of 2,000 years between the earliest evidence of domestic animals in the Lake Turkana region and the southwest Ethiopian highlands has implications for the refugium hypothesis. If pastoral people retreated to the highlands during arid phases, they also changed their subsistence to a hunting and gathering way of life. Alternatively, settlement activities in the highlands were exclusively by local hunter-gatherer groups until 2,000 years ago. There is ethnographic evidence for both scenarios from historical times and only more archaeological investigations can provide an answer.

5.4.2 Adaptation as a matter of timescale

An important aspect to consider is the time scale on which the climate is changing. Assuming the recorded climatic history in Chew Bahir between ~15 ka and ~5 ka BP reflects prevailing wet conditions punctuated by several pronounced dry spells (~14.2-13.5 ka BP, around ~10.5 and ~9.5 ka BP, between 8.15 and 7.8 and at ~7 ka BP), causing a rapid change of the habitat with strongly regressed and increasingly alkaline and saline lakes and a sparse vegetation cover, hunter-gatherers were forced to find expeditiously alternative subsistence strategies. Such short-term solutions may be reflected in the higher frequency of dated settlement in the highlands during arid spells, which is interpreted as vertical migration of hunter-gather groups into more favorable environments. The change from a foraging subsistence to a productive mode of economy is intrinsically tied to changes in the social structure and ideology (Vogelsang and Keding, 2013, 56ff.). Consequently it is implausible that an abrupt transition of 50 years or even less might trigger such a fundamental transformation. In contrast, the gradual and >1,500 year-long transition from wet to dry conditions that characterizes the end of the AHP in the Chew Bahir record could have fostered a socio-economic transition.

5.5 Conclusions

A 20 ka long paleoclimate record from the Chew Bahir basin in southwest Ethiopia shows both orbitally-driven long-term transitions from favorable to unfavorable living conditions, including several and short abrupt excursions towards drier or wetter episodes. The history of Chew Bahir is important in this context in providing a high resolution and continuous climate record rather than providing archaeological data which are not available for the studied timeframe (nor beyond), and is not within the scope of this study.

The comparison of prehistoric settlement activities in the surrounding potential refugia, indicated by radiocarbon dates frequency distribution with reconstructed climatic stress events from the Chew Bahir record suggests a correlation of short dry events with population movements into refugia, particularly the Southwest Ethiopian Highlands. Long-term climatic deterioration seemed to cause large-scale migrations. An adaptation to a changing environment by changing the subsistence strategy is sometimes assumed to be the beginning of herding in the Late Holocene period and can only be a long-term process and related to long-term climatic shifts.

However, the comparison of climatic and archaeological history indicates that not all climatic stress events

correlate with increased occupation of refugia. Despite all data limitations, this reminds us that external environmental factors merely reduce the range of possible developments, while socio-cultural conditions favor particular concepts. Further incalculable factors play a role and human behavior has not been entirely climatically determined. This concept of decision-making within certain environmental boundaries, the 'human agency', has a crucial influence on the final development of culture as well as on societal decisions about the timing and direction of mobility.

Acknowledgements

We thank Addis Ababa University for support in the realization of the Chew Bahir field campaign in difficult terrain. We are also grateful to our colleagues from the Universities of Cologne and Potsdam for their lab support and fruitful discussions. Most of all we are much obliged to Bernd Wagner, Finn Viehberg and Nicole Stroncik for providing valuable advice. We would also like to thank Steven Brandt, Elisabeth Hildebrand, Friederike Jesse, Birgit Keding, Josephine Lesur and Clément Menard for their constant readiness to answer our questions and their participation in discussions. This work presented here is supported by the CRC 806 and the International Continental Scientific Drilling Program (ICDP). We thank the German Science Foundation (DFG) for funding these projects.

5.6 References

- Ambrose, S.H.: Late Pleistocene human population bottlenecks, volcanic winter, and the differentiation of modern humans, *Journal of Human Evolution*, 35, 115–118, 1998.
- Ashley, G.M., Ndiema, E.K., Spencer, J.Q.G., Harris, J.W.K., and Kiura, P.W.: Paleoenvironmental Context of Archaeological Sites, Implications for Subsistence Strategies under Holocene Climate Change, Northern Kenya, *Geoarchaeology*, 26, 809–837, 2011.
- Assefa, Z., Pleurdeau, D., Duquesnoy, F., Hovers, E., Pearson, O., Asrat, A., T/Tsion, C., Man Lam, Y.: Survey and explorations of caves in southeastern Ethiopia: Middle Stone Age and Later Stone Age archaeology and Holocene rock art, *Quaternary International* dx.doi.org/10.1016/j.quaint.2013.07.132, 2013.
- Bachechi, L.: Preliminary report on the 2002 excavation of the Harurona cave deposit, in: *Wolayta: Una regione d'Etiopia*, Cavanna, C. (Ed.), *Atti Del Museo di Storia Naturale Della Maremma*, Supplemento, Grosseto, Italy, 21, 67–78, 2005.
- Barker, P.A., Talbot, M.R., Street-Perrott, F.A., Marret, F., Scourse, J. and Odada, E.O.: Late Quaternary variability in intertropical Africa, in: *Past Climate Variability through Europe and Africa*, Battarbee, R.W., Gasse, F., Stickley, C.E. (Eds.), Springer, Dordrecht, Netherlands, 117–138, 2009.

- Barthelme, J.W.: Fisher-hunters and neolithic pastoralists in East Turkana, Kenya, *British Archaeological Reports International Series 254*, Oxford, UK, 1985.
- Basell, L.S.: Middle Stone Age (MSA) site distributions in eastern Africa and their relationship to Quaternary environmental change, refugia and the evolution of *Homo sapiens*, *Quaternary Science Reviews*, 27, 2484–2498, 2008.
- Benson, L. V., Burdett, J. W., Lund, S. P., Kashgarian, M., and Mensing, S.: Nearly synchronous Northern Hemispheric climate change during the Last Glacial Termination? *Nature*, 388, 263–265.
- Berger, A. and Loutre, M.-F.: Insolation values for the climate of the last 10 million years, *Quaternary Sci. Rev.*, 10, 297–317, 1991.
- Beyin, A.: Upper Pleistocene Human Dispersals out of Africa: A Review of the Current State of the Debate, *International Journal of Evolutionary Biology*, 2011, 615094, doi:10.4061/2011/615094, 2011a.
- Beyin, A.: Recent archaeological survey and excavation around the greater Kalokol Area, west side of Lake Turkana: Preliminary findings, *Nyame Akuma*, 75, 40–50, 2011b.
- Brandt, S.A. and E.A. Hildebrand: Southwest Ethiopia as an Upper Pleistocene Refugium. Paper presented at the Workshop on the Middle Stone Age of Eastern Africa. Nairobi, Kenya and Addis Ababa, Ethiopia, July 2005, 2005.
- Brandt, S.A., Fisher, E.C., Hildebrand, E.A., Vogelsang, R., Ambrose, S.H., Lesur, J. and Wang, H.: Early MIS 3 occupation of Mochena Borago Rockshelter, Southwest Ethiopian Highlands: Implications for Late Pleistocene archaeology, paleoenvironments and modern human dispersals, *Quaternary International*, 274, 38–54, 2012.
- Bronk Ramsey, C.: Radiocarbon calibration and analysis of stratigraphy: the OxCal program, *Radiocarbon*, 36, 425–430, 1995.
- Brown, E. T. and Fuller, C. H.: Stratigraphy and tephra of the Kibish Formation, southwestern Ethiopia, *J. Hum. Evol.*, 55, 366–403, 2008.
- Brown E.T., Johnson T.C., Scholz C.A., Cohen A.S and King J.W.: Abrupt change in tropical African climate linked to the bipolar seesaw over the past 55,000 years, *Geophysical Research Letters*, 34, doi:10.1029/2007GL031240, 2007.
- Burns, S.J., Matter, A., Frank, N. and Mangini, A.: Speleothem-based paleoclimate record from northern Oman, *Geology*, 26, 499–502, 1998.
- Carto, S.L., Weaver, A.J., Hetherington, R., Lam, Y. and Wiebe, E.C.: Out of Africa and into an ice age: on the role of global climate change in the late Pleistocene expansion of early modern humans out of Africa, *Journal of Human Evolution* 56, 139–151, 2009.
- Castañeda, I.S., Mulitza, S., Schefuß, E., Santos, R.A.L., Damste, J.S.S. and Schouten, S.: Wet phases in the Sahara/Sahel region and human expansion patterns in North Africa. *Proceedings of the National Academy of Sciences* 106, 20159–2016, 2009.
- Day, M.H. and Stringer, C.B.: The Omo Kibish cranial remains and classification within the genus *Homo*, *L'Anthropologie*, 95, 573–594, 1991.
- DeMenocal, P.: Plio-Pleistocene African Climate, *Science*, 270, 53–59, 1995.
- Dobres, J. and Robb, J. (Eds.): *Agency in archaeology*, Routledge, London and New York, 2000.
- Dupont, L., Jahns, S., Marret, F., Ning, S.: Vegetation change in equatorial West Africa: time-slices for the last 150 ka, *Paleogeography, Paleoclimatology, Paleoecology*, 155, 95–122, 2000, doi:10.1016/S0031-0182(99)00095-4.
- Dykoski, C.A., Edwards, R.L., Cheng, H., Yuan, D., Cai, Y., Zhang, M., Lin, Y., Qing, J., An, Z. and Revenaugh, J.: A high-resolution, absolute dated Holocene and deglacial Asian monsoon record from Dongge Cave, China, *Earth and Planetary Science Letters*, 233, 71–86, 2005.
- Foerster, V., Junginger, A., Langkamp, O., Gebru, T., Asrat, A., Umer, M., Lamb, H., Wennrich, V., Rethemeyer, J., Nowaczyk, N., Trauth, M.H. and Schäbitz, F.: Climatic change recorded in the sediments of the Chew Bahir basin, southern Ethiopia, during the last 45,000 years, *Quaternary International, Special Issue Collaborative Research Center*, doi.org/10.1016/j.quaint.2012.06.028, 2012.
- Foerster, V., Junginger, A., Asrat, A., Lamb, H. F., Wennrich, V., Weber, M., Rethemeyer, J., Frank, U., Brown, M.C., Trauth, M.H. and Schaebitz, F.: 46 000 years of alternating wet and dry phases on decadal to orbital timescales in the cradle of modern humans: the Chew Bahir project, southern Ethiopia, *Climate of the Past Discussions*, doi:10.5194/cpd-10-1-2014, 2014.
- Fleitmann, D., Burns, S.J., Mudelsee, M., Neff, U., Kramers, J., Mangini, A. and Matter, A.: Holocene forcing of the Indian monsoon recorded in a stalagmite from Southern Oman, *Science*, 300, 1737–1739, 2003.
- Garcin, Y., Melnick, D., Strecker, M.R., Olago, D. and Tierce-lin, J.-J.: East African mid-Holocene wet–dry transition recorded in palaeo-shorelines of Lake Turkana, northern Kenya Rift, *Earth and Planetary Science Letters*, 331–332, 322–334, 2012.
- Gasse, F.: Hydrological changes in the African tropics since the Last Glacial Maximum, *Quaternary Science Reviews*, 19, 189–211, 2000.
- Gillespie, R., Street-Perrott, F.A. and Switsur, R.: Post-glacial arid episodes in Ethiopia have implications for climate prediction, *Nature*, 306, 680–683, 1983.
- Grove, A., Street, A. and Goudie, A.: Former Lake Levels and Climatic Change in the Rift Valley of Southern Ethiopia, *The Geographical Journal*, 141, 177–194, 1975.
- Gupta, A. K., Das, M. and Anderson, D.M: Solar influence on the Indian summer monsoon during the Holocene, *Geophys. Res. Lett.*, 32, L17703, doi:10.1029/2005GL022685, 2005.
- Gutherz, X., Jallot, L., Lessur, J., Pouzolles, G. and Sordoillet, D.: Les fouilles de l'abri sous-roche de Moche Borago (Soddo-Wolayta), premier bilan, *Annales d'Ethiopie*, 18, 181–190, 2002.
- Hays, T.R.: *The Sudanese Neolithic: a critical analysis*, Ph.D. thesis, Southern Methodist University, Dallas, USA, 162 pp., 1971.
- Hemming, S.R.: Heinrich events: Massive late Pleistocene detritus layers of the North Atlantic and their global climate imprint, *Review of Geophysics*, 42, 1–43, 2004.
- Hildebrand, E. and Brandt, S.: An archaeological survey of the tropical highlands of Kafa, SW Ethiopia. *Journal of*

- African Archaeology, 8, 43–63. 2010.
- Hildebrand, E., Brandt, S. and Lesur-Gebremariam, J.: The Holocene archaeology of Southwest Ethiopia: New insights from the Kafa archaeological project, *African Archaeological Review*, 27, 255–289, 2010.
- Hildebrand, E. and Grillo, K.: Early herders and monumental sites in eastern Africa: New radiocarbon dates, *Antiquity*, 86, 338–352, 2012.
- Humphreys, G.K.: A Preliminary Report of some Late Stone Age occurrences in the Lake Ziway area of the Central Ethiopian Rift Valley, *Annales d’Ethiopie*, 11, 45–66, 1978.
- IRI (International Research Institute for Climate and Society), Earth Institute, Columbia University, Climate and Society Maproom available at: <http://iridl.ldeo.columbia.edu/maproom/> (last access: 28 February), 2014.
- Jesse, F.: Rahib 80/87. Ein Wavy-Line-Fundplatz im Wadi Howar und die früheste Keramik in Nordafrika, *Africa Praehistorica*, 16, Köln, Germany, 2003.
- Joordens, J.C.A., Vonhof, H.B., Feibel, C.S., Lourens, L.J., Dupont-Nivet, G., Van der Lubbe, H.J.L., Sier, M., Davies, G.R. and Kroon, D.: An astronomically-tuned climate framework for hominins in the Turkana Basin. *Earth and Planetary Science Letters* 307, 1–8, 2011.
- Joussaume R.: Tiya. Une campagne de fouilles (1982), *Annales d’Ethiopie*, 13, 69–84, 1985.
- Joussaume, R. (Ed.): *Tuto Fela et les stèles du sud de l’Ethiopie*, Éditions Recherche sur les Civilisations, Paris, France, 2007.
- Jullien, E., Grousset, F., Malaizé, B., Duprat, J., Sanchez-Goni, M.F., Eynaud, F., Charlier, K., Schneider, R., Bory, A., Bout, V. and Flores, J.A.: Low-latitude “dusty events” vs. high-latitude “icy Heinrich events”, *Quaternary Research*, 68, 379–386, 2007.
- Junginger, A., Roller, S., Olaka, L.A. and Trauth, M.H.: The effect of solar radiation changes on water levels in paleo-Lake Suguta, Northern Kenya Rift, during late Pleistocene African Humid Period (15–5 ka BP), *Paleogeography, Paleoclimatology, Paleoecology*, 396, 1–16, 2014.
- Junginger, A. and Trauth, M. H.: Hydrological constraints of paleo-Lake Suguta in the northern Kenya Rift during the African humid period (15–5 ka BP), *Global Planet. Change*, 111, 174–188, 2013.
- Johnson, T.C., Halfman, J.D. and Showers, W.J.: Paleoclimate of the past 4000 years at Lake Turkana, Kenya, based on the isotopic composition of authigenic calcite, *Palaeogeography, Palaeoclimatology, Palaeoecology*, 85, 189–198, 1991.
- Keding, B.: *Leben und Überleben in der Wüste – Kulturwandel bei prähistorischen Gesellschaften im Spannungsfeld von Umweltänderung und Tradition*, unpublished habilitation, University of Cologne, Cologne, Germany, 914 pp., 2009.
- Kelly, R.L. (Ed.): *The Foraging Spectrum: Diversity in Hunter-Gatherer Lifeways*, Smithsonian Institution Press, Washington, USA, 1995.
- Koch, C.P.: The Jarigole Mortuary Tradition: new light on Pastoral Neolithic burial practices, Turkana Basin, northern Kenya, Biennial Conference of the Southern African Association of Archaeologists, Pietermaritzburg, South Africa, 1994.
- Koch, C.P.: Pavlish, L.A., Farquhar, R.M., Hancock, R.G.V., and R.P. Beukens: INAA of pottery from Il Lokeridede and Jarigole, Koobi Fora Region, Kenya, in: *Archaeometry 98: Proceedings of the 31st Symposium*, Budapest, edited by E. Jerem and K.T. Biro, 587–592, Oxford, Archaeopress, 2002.
- Kröpelin, S., D. Verschuren, A.-M. Lézine, H. Eggermont, C. Cocquyt, P. Francus, J.-P. Cazet, M. Fagot, B. Rumes, J. M. Russell, F. Darius, D. J. Conley, M. Schuster, H. von Suchodoletz, D. R. Engstrom: Climate-Driven Ecosystem Succession in the Sahara: The Past 6000 Years, *Science*, 320, 765–768, 2008.
- Leplongeon, A.: Microliths in the Middle and Later Stone Age of eastern Africa: New data from Porc-Epic and Goda Buticha cave sites, Ethiopia, *Quaternary International*, [dx.doi.org/10.1016/j.quaint.2013.12.002](https://doi.org/10.1016/j.quaint.2013.12.002), 2013.
- Lesur-Gebremariam, J.: Origine et diffusion de l’élevage dans la Corne de l’Afrique. Un état de la question, *Annales d’Ethiopie*, 24, 173–208, 2009.
- Lesur, J., Vigne, J.-D. and Gutherz, X.: Exploitation of wild mammals in south-west Ethiopia during the Holocene (4000 BC–500 AD): the finds from Moche Borago shelter (Wolayta), *Environmental Archaeology*, 12, 139–159, 2007.
- Lesur, J., Hildebrand, E.A., Abawa, G. and Gutherz, X.: The advent of herding in the Horn of Africa: New data from Ethiopia, Djibouti and Somaliland, *Quaternary International*, in press, [dx.doi.org/10.1016/j.quaint.2013.11.024](https://doi.org/10.1016/j.quaint.2013.11.024), 2013.
- Lynch, B.M. and Robbins, L. H.: Cushitic and Nilotic prehistory: New archaeological evidence from North-West Kenya, *The Journal of African History*, 20, 319–328, 1979.
- Ménard, C., Bon, F., Dessie, A., Bruxelles, L., Douze, K., Fauvelle-Aymar, F.-X., Khalidi, L., Lesur, J. and Mensan, R.: Late Stone Age variability in the Main Ethiopian Rift: new data from the Bulbula River, Ziway-Shala basin, *Quaternary International* 343, 53–68, 2014.
- McDougall, I., Brown, F.H. and Fleagle, J.G.: Stratigraphic placement and age of modern humans from Kibish, Ethiopia, *Nature*, 433, 733–736, 2005.
- McDougal, I., Brown, F.H. and Fleagle, J.G.: Spropels and the age of hominins Omo I and Omo II, Kibish, Ethiopia, *Journal of Human Evolution*, 55, 409–420, 2008.
- Mgomezulu, G.G.Y.: Recent archaeological research and radiocarbon dates from Eastern Africa, *The Journal of African History*, 22, 435–456, 1981.
- Mohammed, M. U. and Bonnefille, R.: A late Glacial/late Holocene pollen record from a highland peat at Tamsaa, Bale Mountains, south Ethiopia, *Global and Planetary Change*, 16–17, 121–129, 1998.
- Neff, U., Burns, S.J., Mangini, A., Mudelsee, M., Fleitmann, D. and Matter, A.: Strong coherence between solar variability and the monsoon in Oman between 9 and 6 kyr ago, *Nature*, 411, 290–293, 2001.
- Odada, E.O., Olago, D.O., Bugenyi, F., Kulindwa, K., Karimurumungu, J., West, K., Ntiba, M., Wandiga, S., Aloo-Obudho, P. and Achola, P.: Environmental assessment of the East African Rift Valley lakes, *Aquatic Sciences - Research Across Boundaries*, 65, 254–271, 2003.
- Owen, R.B. Paleolimnology and archaeology of Holocene deposits north-east of Lake Turkana, Kenya. *Nature*, 298, 523–529, 1982.

- Phillipson, D.W.: Lowasera, Azania, 12, 1–32, 1977.
- Reimer, P.J., Baillie, M.G.L., Bard, E., Bayliss, A., Beck, J.W., Blackwell, P.G., Bronk Ramsey, C., Buck, C.E., Burr, G.S., Edwards, R.L., Friedrich, M., Grootes, P.M., Guilderson, T.P., Hajdas, I., Heaton, T.J., Hogg, A.G., Hughen, K.A., Kaiser, K.F., Kromer, B., McCormac, F.G., Manning, S.W., Reimer, R.W., Richards, D.A., Southon, J.R., Talamo, S., Turney, C.S.M., van der Plicht, J. and Weyhenmeyer, C.E.: INTCAL13 and MARINE13 radiocarbon age calibration curves, 0-50,000 years cal BP, *Radiocarbon*, 55, 1869-1887, 2013.
- Richter, J., Hauck, T., Vogelsang, R., Widlok, T., Le Tensorer, J.-M. and Schmid, P.: "Contextual areas" of early Homo sapiens and their significance for human dispersal from Africa into Eurasia between 200 ka and 70 ka, *Quaternary International*, 274, 5–24, 2012.
- Rosenberg, T.M., Preusser, F., Fleitmann, D., Schwalb, A., Penkman, K., Schmid, T.W., Al-Shanti, M.A., Kadi, K. and Matter, A.: Humid periods in southern Arabia: Windows of opportunity for modern human dispersal, *Geology*, 39, 1115–1118, 2011.
- Sisk, M. L., and Shea, J. J.: Intrasite spatial variation of the Omo Kibish Middle Stone Age assemblages: Artifact re-fitting and distribution patterns, *Journal of Human Evolution*, 55, 486–500, 2008.
- Solanki, S.K., Usoskin, I.G., Kromer, B., Schüssler, M. and Beer, J.: Unusual activity of the sun during recent decades compared to the previous 11,000 years, *Nature*, 431, 1084–1087, 2004.
- Stager, J.C., Mayewski, P.A. and Meeker, L.D.: Cooling cycles, Heinrich event 1, and the desiccation of Lake Victoria, *Palaeogeogr. Palaeoclimatol. Palaeoecol.*, 183, 169–178, 2002.
- Sutton, J.E.G.: The African aqualithic, *Antiquity*, 51, 25–34, 1977.
- Tierney, J.E., Russell, J.M., Sinninghe Damsté, J.S., Huang, Y. and Verschuren, D.: Late Quaternary behavior of the East African monsoon and the importance of the Congo Air Boundary, *Quaternary Science Reviews*, 30, 798–807, 2011.
- Trauth, M.H., Bergner, A.G.N., Foerster, V., Junginger, A., Maslin, M.A., Schaebitz, F. in press, Episodes of Environmental Stability vs. Instability in Late Cenozoic Lake Records of Eastern Africa. *Journal of Human Evolution*.
- Umer, M., Lamb, H.F., Bonnefille, R., Lezine, A.M., Tiercelin, J.J., Gibert, E., Cazet, J.P. and Watrin, J.: Late Pleistocene and Holocene Vegetation History of the Bale Mountains, Ethiopia. *Quaternary Science Reviews*, 26, 2229–46, 2007, doi:10.1016/j.quascirev.2007.05.004.
- Vogelsang, R. and Keding, B.: Climate, culture, and change: From hunters to herders in northeastern and southwestern Africa, in: Baldia, M.O., Perttula, T.K., Frink, D.S. (Eds.): *Comparative Archaeology and Paleoclimatology – Socio-cultural responses to a changing world*, BAR International Series, 2456, Archaeopress, Oxford, UK, 43–62. 2013
- Weldeab, S., Lea, D.W., Schneider, R.R. and Andersen, N.: Centennial scale climate instabilities in a wet early Holocene West African monsoon, *Geophysical Research Letters*, 34, L24702, doi:10.1029/2007GL031898, 2007.
- Weninger, B. and Jöris, O., A 14C age calibration curve for the last 60 ka: the Greenland-Hulu U/Th timescale and its impact on understanding the Middle to Upper Paleolithic transition in Western Eurasia, *Journal of Human Evolution*, 55, 772–781, 2008.
- Ziegler, M., Simon, M.H., Hall, I.R., Barker, S., Stringer, C., and Zahn, R. Development of Middle Stone Age innovation linked to rapid climate change, *Nature Communications* 4, 1905, 1-7, 2013
- Zvelebil, M. 1998 – What's in a Name: The Mesolithic, the Neolithic, and Social Change at the Mesolithic Neolithic Transition, in: Edmonds, M. and Richards, C. (Eds.): *Understanding the Neolithic of North-Western Europe*, Cruithne Press, Glasgow, 1–35, 1998.



Chapter VI

Further Findings

The enigma of how to find an age-depth model
and unpublished insights into CB-04 and CB-06

6.1 Age model of the Chew Bahir transect

The development of a reliable and precise age-depth model and subsequent creation of a chronological frame is crucial to derive any palaeoclimatic meaning out of the cores (Björck and Wohlfarth, 2001; Blaauw and Heegard, 2012; Trauth, 2014), which goes beyond local deposition information (for instance, in 3.34 m core depth in CB03 a count of 80,182 of Fe per second is identified). As fittingly put by Blaauw and Heegard (2012):

„Palaeolimnology without chronology is history without dates“, (Blaauw and Heegard, 2012, p. 379).

Following it can be concluded that without a reliable age model the deposited material, which was described and analysed previously is no more than very expensive lake deposits in a plastic liner. The age-depth model, therefore, is a key pre-requisite of palaeoclimatic research and in the formation of a robust chronology (Trauth, 2014). On the other hand, this issue is the most vulnerable part of the interpretation, due to broad range of uncertainties and ambiguity, which comes with the process of age determination, calibration and interpolation, and require the choice of adequate techniques. Thus this sub-chapter is dedicated to shed light on some fundamental considerations that were made in general and with specific reference to the Chew Bahir material and ages at hand when the age-depth model (presented in chapter III), was developed.

To create a meaningful and robust age-depth model, initially age control points along the core depth are needed (^{14}C , ^{210}Pb , tie points, ^{10}Be , integration of tephrochronology; Blaauw and Heegard, 2012). Radiocarbon dating was used, as the material was still within the age limitation of radiocarbon dating. Though dating on clearly identifiable material (plant remains for example) would have been preferred, the scarcity of organic material (see ultra-low TOC values in chapter II) left us with the choice of using the biogenic carbonates of the mollusc occurrences in the cores which do not occur throughout the record or dating bulk samples. Dating the latter always runs a higher risk of being imprecise or possibly containing contaminated shares from other depths or modern material. The overall lack of charcoal particles made the approach to determine or rule out a possible reservoir effect difficult, as shown in chapter 3.4.1. Therefore, the material in the core that could be dated was dated, with all problems attached, such as risking the dating of redeposited material, contaminated material or compromised by other effects to provide additional ages. Even though we currently estimate the

reservoir effect to not have affected the water body of Chew Bahir, and the dated molluscs themselves seem not to have been contaminated by fossil radiocarbon, the results show that especially those occurring in dense layers have most likely been redeposited. The shells in a clayey matrix occurring irregularly through the core (especially the marginal core CB-01) are more reliable than the core site position points at being situated in a shallow water littoral habitat during lake phases, preferred by *M. tuberculata* and therefore points at an in situ deposition. A difficulty lay with dating the organic sediment due to the interval associated with the AHP, as outlined in the discussion (chapter 3.4.1), where a mix of temporarily stored and then remobilised organic matter in the densely vegetated catchment during the AHP must be assumed, which was later deposited in Chew Bahir together with autochthonous material. The identification of tephtras and their ages in the material would certainly contribute to additional age control points, but would also help to test the validity of the present model. Further palaeomagnetic analyses would be valuable for improving the reliability of the given model. The Laschamp event, a well-documented magnetic excursion that was dated to $40,700 \pm 950$ yrs (2-sigma) (Singer et al., 2009; Nowaczyk et al., 2012) has been distinctly identified in CB05 (~919 cm) and, with less certainty, in CB-04 and CB-06. This could provide a valuable radioisotopic tie point to support the age model, but currently the probability ranges below 20 % certainty to correctly correlate this event with CB-01, and thus the Laschamp event could eventually not be included in the age-depth model unless new results provide more certainty.

An age-depth curve needs to be chosen to finally provide a close approximation to the sedimentation history of the core. This age-depth curve provides us with both an estimate of the age-depth relationship as well as a calculated age for every centimetre in the core. Naturally, this step is based on the interpolation between a few points that again are only determined within certain boundaries of uncertainty. We are likely to see changes in sedimentation rates and abrupt changes between these that are created by interpolation although they might have been rather gradual in real sedimentation history. Vice versa, we know that these abrupt changes occur in nature (for instance abrupt onset of the AHP) and smoothing the curve could mask this. We chose for a linear interpolation. It is important to consider that the assumption of more complex models being more advanced and therefore more likely to be correct is a common fallacy. However, “...the fit produced by linear interpolation is rarely incorrect in comparison with other, more complex models” (Blaauw and Heegard,

2012, p.392). The choice of a fitting age-depth curve is highly case specific. A crucial role in determining the model is how many ages there are available, how reliable these are and whether further age control points are available. Then the sort of material that was dated and what is known about sedimentation rates in the region are of further importance for finding the best model.

Radiocarbon ages (and all other dates that come with deviations; Blaauw and Heegard, 2012) need calibration. That is a translation from radiocarbon ages into calendar years. Calibration is therefore a necessary pre-requisite for age modelling as radiocarbon ages are slightly longer and included fluctuations in comparison to a calendar year (Blaauw and Heegard, 2012). A broad variety of calibration software packages are available (e.g. OxCal, Bronk Ramsey, 1995; CALIB, Stuiver et al., 2005; Calpal, Weninger and Jöris, 2008), as downloadable versions or online, to convert the ages into calendar years with laboratory standard deviations (1 or 2). We used the latest calibration curve IntCal09 (Reimer et al., 2009), though recently IntCal13 has been published (Reimer et al., 2013). Calibration, however, generates an entire interval of possible calibrated ages and therefore adds an extra dimension of complexity (Telford et al., 2004). Passionate debate exists as to whether to use a 68% or 95% probability range. For some ages in our dataset we observed a strong bimodal distribution or, in some cases, multimodal distribution of probability, and used, in order to show the full array of possible ages, the 95% (2-sigma) confidence interval (see Table 3.2). For most models, a point estimate of the calibrated ages is needed, though that requires a decision for one age point out of the entire interval. Among the commonly used methods as the mean, intercept, mid of most probable age etc., we decided for the weighted mean point estimate of the probability density function and thus acknowledge the whole probability integral (table output of probability interval of OxCal; <https://c14.arch.ox.ac.uk/oxcal/>). Taken simply, the mean value as a point estimate is critical as the

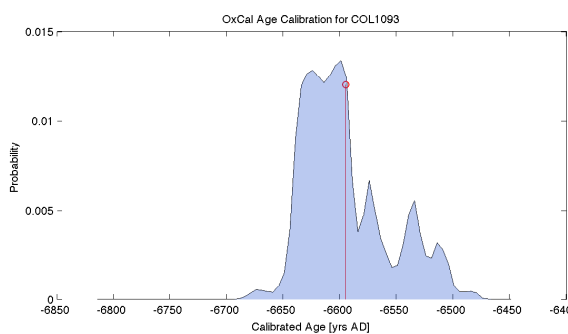


Figure 6.1 | The weighted mean of the probability density function was used as the point estimate of the calibrated ages.

mean in a bimodal distribution can easily lie where the least probability is assumed or even outside the confidence interval, in-between both peaks. In MATLAB we used a script that incorporates the entire table output, therefore including the min and max values (column 1 and column 2), (Fig. 6.1).

Other models were tested, such as the BACON model by Blaauw and Christen (2011) or McAgeDepth by Higuera et al. (2009), which integrate several a priori information (e.g. like average sedimentation rates, reservoir effect or marking beforehand certain ages as outliers) into the probabilistic age-depth model and moreover take the problem of the probability distribution into account, by integrating directly the entire calibration output into the model. Several choices can be made and in the Bayesian-based statistics, which are applied in BACON for example, the best possible approach to age-depth relationship was found through integration of some well-defined tie points, as the well-constrained YD event in East Africa, which is clearly visible in the records. Nevertheless we eventually refrained from using these tie points because (although the confidence of the data could provide a helpful mean to improve an age model) we aimed at an independent chronology. However, the tests showed that the outcome of these models could be highly manipulated by the choice of a priori information, like the number of executed iterations or the memory effects (c.f. Trauth, 2014). Furthermore, by integrating a sedimentation mean value for the entire core length, the problem was encountered that since applying an average for a period that is marked by high variability (change to 6–7 fold sedimentation per year) through time, the model presents results that infer a forced offset of the age-depth relationship for all extreme phases above (wet) or below (dry) the mean. If we compare the used linear and cubic spline through the weighted mean of the single point estimates for the limited reliable ages with the maximum a posteriori (MAP; the single iteration with the highest probability) iteration output by the BACON model, it is apparent that this advanced approach results in an age-depth curve partly running outside the 95% confidence limit, with changing kinks that imply a wildly fluctuating sedimentation rate, which is not impossible, but during a long wet phase like the AHP in that extend rather unlikely. Instead this seems to be the result of forcedly fitting the age-depth curve through all ages. The necessity to take all available information into account to find the best (that is the) age-depth model was recently also registered by Trauth (2014), after dealing with problems that were encountered in finding a suitable model for the CB record and others. Following the technique of Trauth (2014) the as-

sumed deposition time of the various sediment types is integrated into the model and therewith acknowledges the variable sedimentation conditions associated with each type and aims at the detection of hiatuses.

Correlation: In the case of the Chew Bahir transect cores, the ages were derived from different cores (Table 3.2 and Figure 3.2), several kilometres apart and each site subdued to varying sedimentation rates from basin margin to basin centre due to changing sedimentation conditions. A good example for the need of correlation in this case, is CB-06. With just one radiocarbon age, CB-06 was dependent on a core correlation within the transect cores and thus to be part of a composite age-depth model that integrates all ages that were determined from CB-01 to CB-06. The same is found to apply to the other cores for different sections. The Holocene section in CB-05, CB-04 and CB-06 are largely unconstrained, due to the lack of datable material (apart from the distinct mollusc layer that was dated and used as biological tie point) and apparent re-depositions during lacustrine phases that produced disturbed sequences. As a consequence the correlation of all cores (and attached to them the age determinations of each single core) was necessary to gain a chronology for each core and therefore a palaeoclimatic history from each core.

Tuning: To achieve this, we tuned CB-03 to CB-06, and then to the tuning target CB-01. The pilot core represents the master core with the highest resolution and the most radiocarbon ages (Fig. 3.2). The most reliable curve, the potassium curve, was used for the tuning of the transect cores, although thorough analyses on palaeomagnetic properties and the geochemical dataset, especially Cl and Ca provided the necessary cross-control for the selection of tuning points. The potassium curve was used for the tuning of the transect cores, because K, until crystallisation in the lake sediment in the form of illite, is generally easily soluble (see chapter III) and can as such be easily transported and distributed in the palaeo-lake. Magnetite, however, the main source of the magnetic susceptibility signal which is often used for correlation of duplicate cores, is transported in solid phase, which results in an uneven distribution within the palaeo-lake Chew Bahir, controlled by distance to its provenance. Hence, the (precipitation-) signal recorded by the MS-record is likely to vary considerably with the sites in the system, which are kilometres apart, as our results have proven. All potassium records were then standardised to enable comparability (mean=0 and standard=1) and converted to centimetres, as different scanners and output software resulted in different units. First, each core was plotted against their individual depth (Fig. 6.2). Then a minimum set of tuning

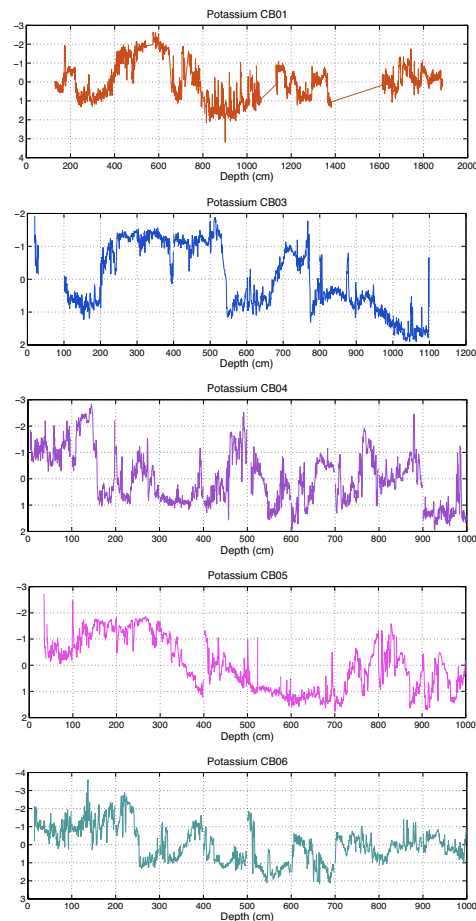


Figure 6.2 | Potassium curve of the Chew Bahir transect cores used as reference curves for correlation. CB-01 is the master core. Values were standardised. Note the different depth and refer to Fig. 3.1d-e for core correlation with the basin.

control points was defined, considering all available information at hand (Fig. 6.3). We limited the number of points to 12 crucial tie points that were defined for each of the cores, plus two more points to 'tie' loose ends within a gap in CB-05 in 400 cm and the end of the younger CB-03. We therewith followed the principles of only using the minimal possible number of tuning points to reduce the prediction error as far as possible. Muller and MacDonald (2000) argue that inferring too many points bears certain dangers, which are referred to as 'overtuning'. Anything beyond that risks slipping into something informal and is, fittingly, referred to as 'geo-phantasy' as there often is more personal interpretation and wishfulness involved than facts. For the choice of reliable tie points it was therefore important to concentrate on identifying turning points rather than concise peaks as far as possible, because turning points are less proxy-specific and avoid the issue to define a termination or beginning of a phase. Terminations are dependent on the sensitivity and response time of the proxy, turning points however remain mostly the same as Broecker and Henderson imposingly demonstrated (1998).

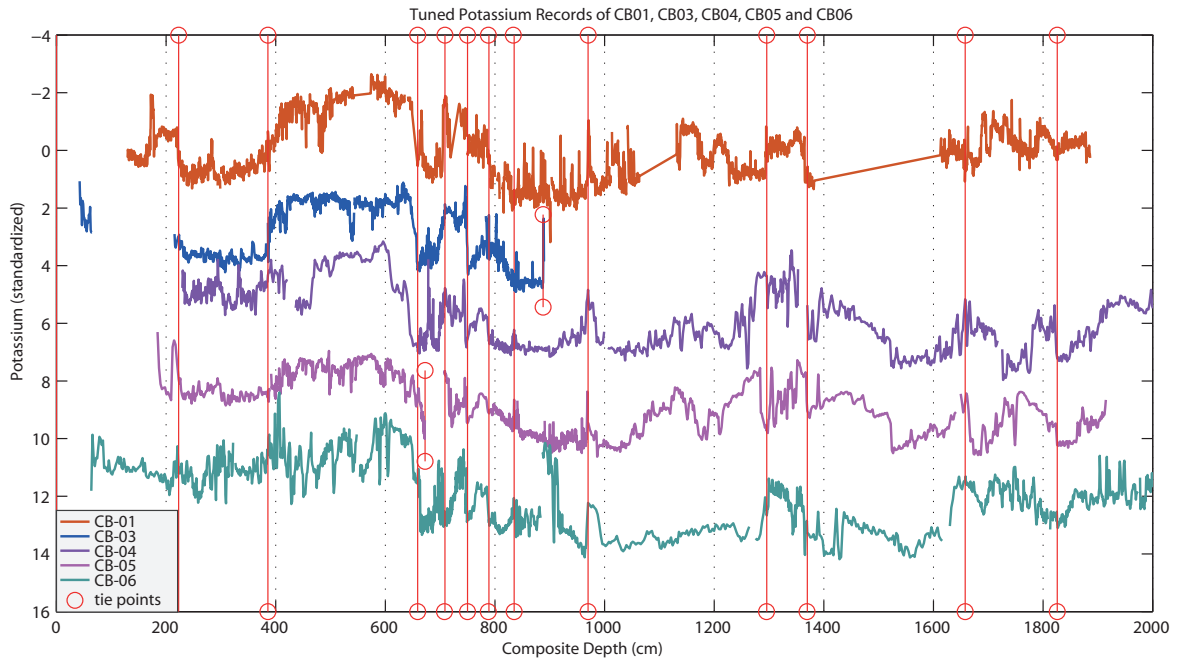


Figure 6.3 | Tuned potassium record of the Chew Bahir transect cores. All cores were tuned to the depth of CB-01, using tiepoints (red circles).

To create the most robust age model with the material from different cores and inferred ages, we then produced a linear age model based on the weighted probability functions of the six first ages from CB-01. We used a linear interpolation as well as a cubic spline, which did not affect the outcome considerably, as Figure 3.2 shows. In a final step, all data (XRF, MSCL, etc.) was interpolated to the age model (Fig. 6.4) and therewith applied the ‘golden rule of finding the simplest model which explains the data which is available (Trauth, 2014, p. 4).

„All age-depth models are wrong: but how badly?“
(Telford et al., 2004).

There is no such thing as the right or correct age model. Having that said, it is to add that age modelling itself is always based on assumptions, which are based on a few points that again represent assumptions based on probabilities. We are aware of the necessity to have a chronological frame as there is otherwise no climatic history. Hence, the choice of a suitable model for the

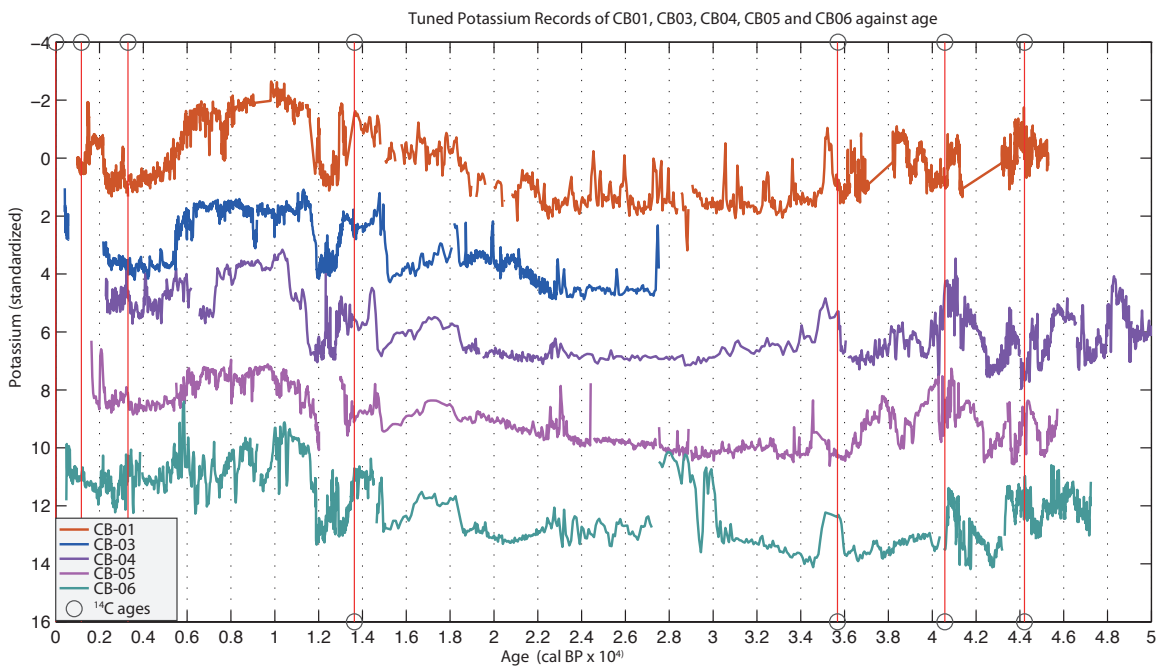
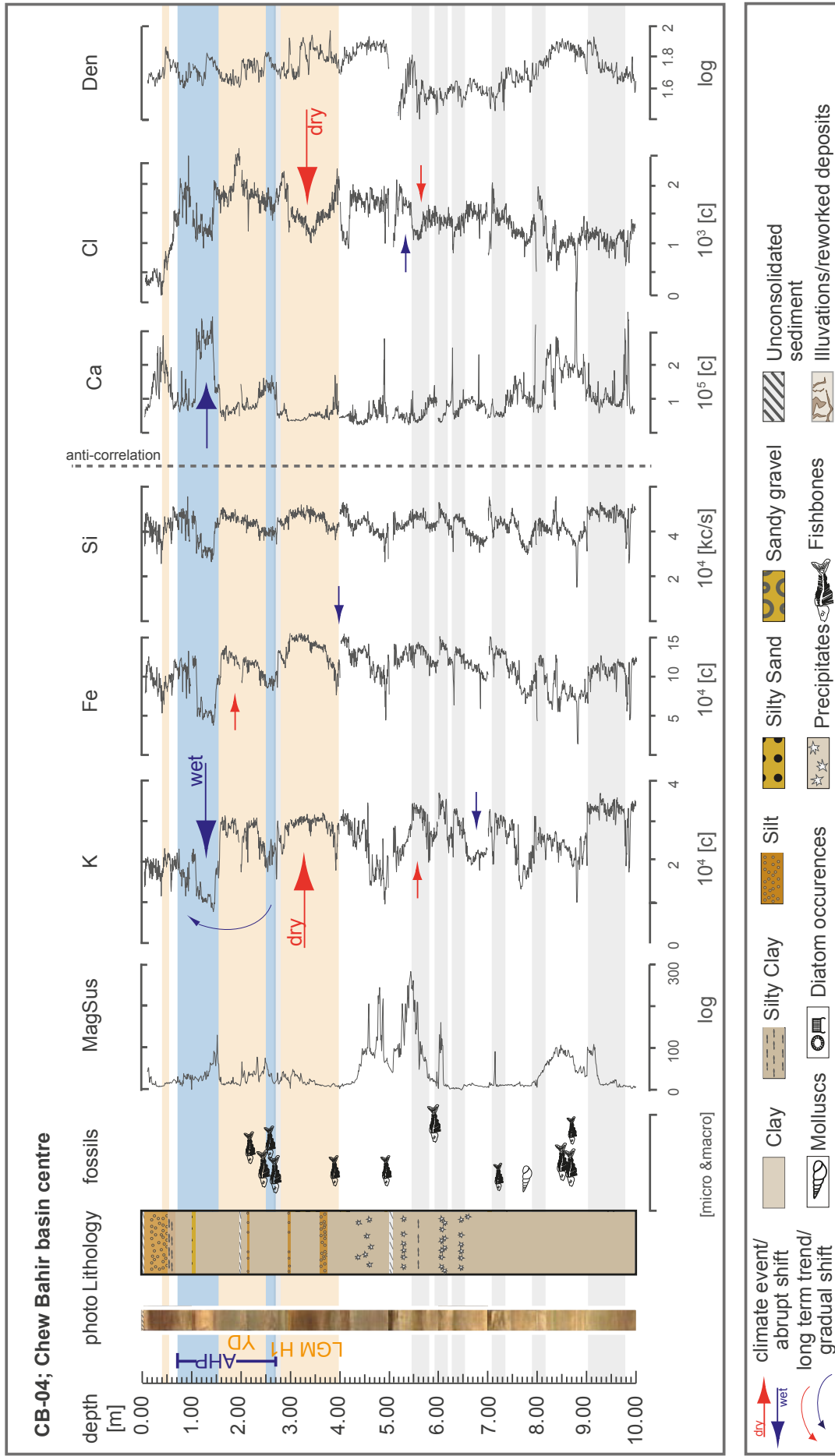


Figure 6.4 | Tuned potassium record of the Chew Bahir transect cores. All cores were tuned to the composite age model based on cal. 14C ages (grey circles).

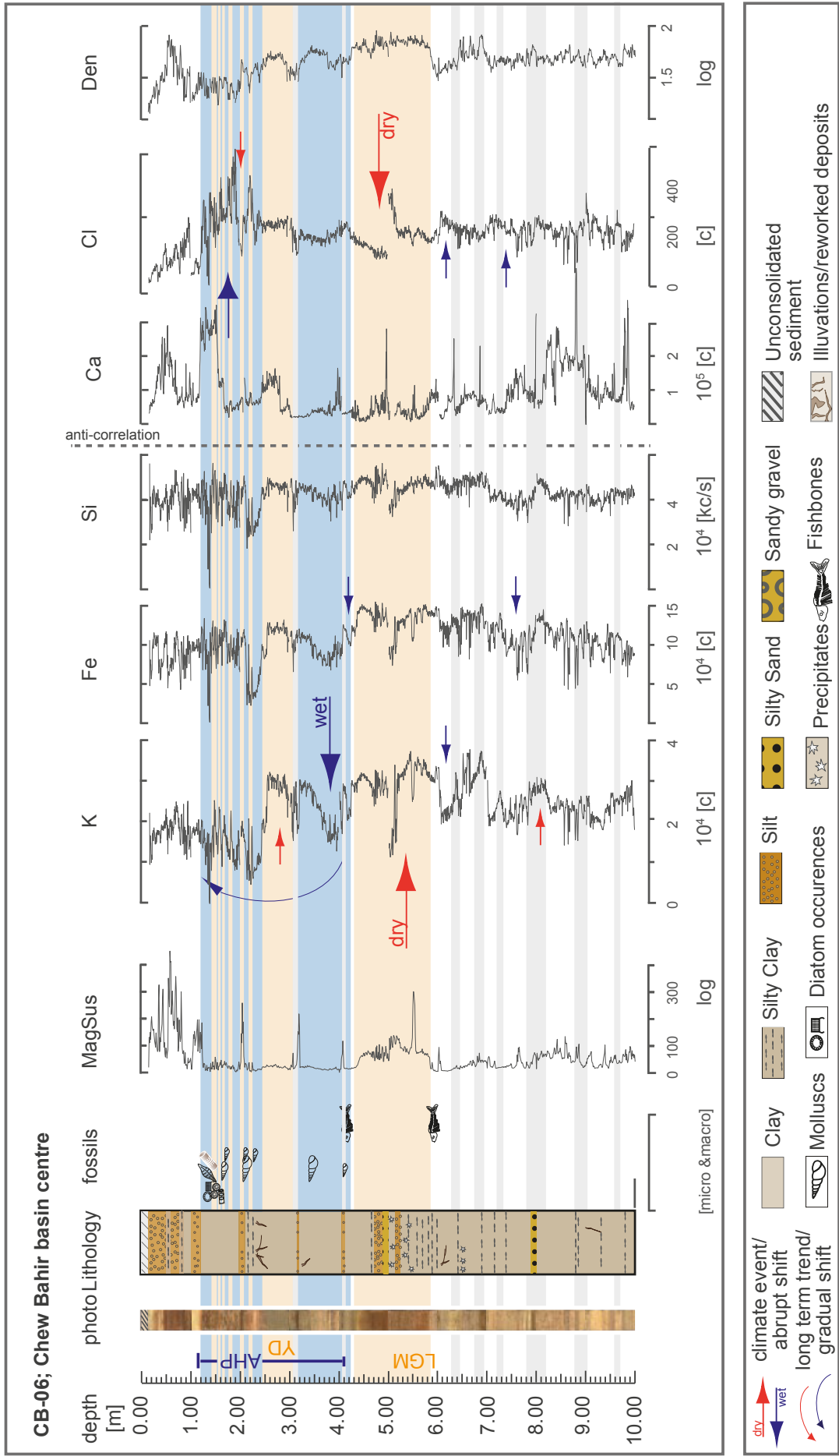
data available at the moment is crucial, to at least to approach a real deposition history, but keeping in mind the restrictions of the model which have been developed, is of key importance for the final quality of the climatic interpretation.

6.2 Results from CB-04 and CB-06

Cores CB-04 and CB-06 were both recovered from coring sites which lie within the central area of the Chew Bahir basin, and are therefore expected to show similar results to CB-05 in terms of the lithology and multiproxy analyses. Analysis and interpretation of the cores shows that each core contains characteristics that can be attributed to variations in sedimentation conditions. CB-04 is most similar to CB-05, excepted due to their proximity to one another, but contains more reworked sections especially in the core section spanning the Holocene period. CB-06 is comprised of some highly disturbed parts in the pre-LGM period, which are most likely to have been caused by bioturbation or deep dry-cracks during total desiccation, which were infilled with transported material, as shown in Figure 6.5 and the core picture. As a result, the geochemical signal of CB-06 in particular, but also of CB-04, are relatively noisy; though blurred, major cycles and transitions are apparent, (AHP, YD, mid-Holocene dry event, LGM). Both lithologies are comprised of mostly fine fractioned deposits, similar to CB-05, with a dominance of clay, intercalated by silty clay and silty layers and few sand occurrences. There is also a rich occurrence of distinct evaporation layers: evaporites, mostly calcite and up to 2 mm in diameter occur in a fine clay matrix (Fig. 6.5 and 6.6), formed due to the repeated fluctuations which led to total regression of the paleo-lake. Fish-fossils throughout the core frame transitional phases also indicate the presence of a fluctuating palaeo-lake. Characteristic oscillations between abrupt shifts towards wet conditions and longer saw-tooth shaped returns are evident in CB-04 and CB-06 (Fig. 6.5 and 6.6), indicating dry conditions in the lower parts of both cores. These oscillations reinforce the association which was made for the other cores between similar observed cycles and the high-latitude D-O warm-cold oscillations. Though a clear correlation of these fluctuations cannot be provided due to the uncertainties within the chronology, their presumed presence in all cores underlines the proposed pronounced influence of high-latitude climate control during most of MIS 3, which accounts for both the D-O cycles as well as for possibly represented H-events.



A Figure 6.5 | Sediment composition of (A) CB-04 and (B) CB-06 with selected results of geochemical and physical analysis. Red and blue arrows point out prominent moisture shifts towards arid/humid conditions. Straight arrows indicate abrupt events, crooked show gradual trends. Orange (dry) and blue (wet) bars mark interpreted climate phases, referred to in the text; grey bars show arid phases that roughly coincide with high-latitude Heinrich events (H1–H4). MagSus – Magnetic Susceptibility; LGM – Last Glacial Maximum; YD – Younger Dryas; AHP – African Human Period. 51



B Figure 6.5 | Sediment composition of (A) CB-04 and (B) CB-06 with selected results of geochemical and physical analysis. Red and blue arrows point out prominent moisture shifts towards arid/humid conditions. Straight arrows indicate abrupt events, crooked show gradual trends. Orange (dry) and blue (wet) bars mark interpreted climate phases, referred to in the text; grey bars show arid phases that roughly coincide with high-latitude Heinrich events (H1–H4). MagSus – Magnetic Susceptibility; LGM – Last Glacial Maximum; YD – Younger Dryas; AHP – African Human Period. 51



Chapter VII

Synoptic Discussion

Final discussion and synthesis of the main key themes of this work

VII Synoptic Discussion

7.1 Chew Bahir as a terrestrial climate archive

One of the main aims of this research was to test the potential of the Chew Bahir (sediments) as a terrestrial climate archive which is situated in the source region of modern man. This comprised of the determination of the basin infill, including type and age of the sediments, as well as gaining a conceptual understanding of the processes from source to sink. The analyses and interpretation of the pilot core CB-01 and the additional short cores (9–11 m) that were cored along a NW-SE transect through the basin (CB-02, CB-03, CB-04, CB-05 and CB-06) provided initial insight into the potential of Chew Bahir as a climate archive (see in detail Chapter II and III), not least in order to test whether this was a suitable site for scientific drilling in the context of longer time-scale climate reconstruction.

7.1.1 Type and character of sediment

The type and character in Chew Bahir was determined by using the full range of multi-proxy studies (as described in detail in Chapter II and III). These include geochemical, geophysical and sedimentological analyses which were applied to the entire core material and core catchers, with emphasis, that is a higher resolution and further advanced interpretation, on three cores each representing a separate position in the basin and therefore different sedimentation conditions: CB-01 at the basin margin, CB-05 at the centre of the basin and CB-03 at the transitional part. The results of CB-04 and CB-06, due to being similar to CB-05, have not been included in the in-depth discussion in the Chapters II–V, but the most important findings are briefly presented in Chapter VI. Their further interpretation is part of ongoing work.

The analysed sediments show that the deposits are not homogenous through time and thus contain the recorded signal of a highly variable environment during the late Quaternary. This is indicated by changing material composition that can already be identified visually (see also Figures in the appendix showing composition of

core picture from the core halves, made with the MSCL line-scan camera), by changing grain sizes and colours. The uppermost deposits (9–18.8 m) of the Chew Bahir basin are characterised by mostly fine materials, such as clays, silty clays and silts, intercalated by few sand layers and precipitate- (carbonate) rich horizons. Furthermore occurrences of diatoms, molluscs and fish-bones could be identified which indicate different lacustrine stages through time (Fig. 2.3, Fig. 3.3a+b, Fig. 6.5 and 6.6).

The gastropod *Melanoides tuberculata*, occurring in all cores in several distinct horizons and also individually distributed over sections of the core as complete shells and fragments, is suitable for providing carbonates for radiocarbon age determinations. Moreover, this mollusc represents a sensitive bio-indicator for a lowering water-level, as it is known to be dependent on a littoral habitat or shallow water level not deeper than 10 m, mostly < 2m (Chapter II; Foerster et al., 2012; Junginger et al., 2014). Diatoms such as the common *Aulacoseira* and *Cyclotella* occur in a few distinct horizons which are associated with fresh water lake phases, but are not preserved throughout the entire records. The absence of preserved fossil pollen or spores indicates deposition conditions that are marked by the repeated regression of the palaeo-lake, thus repeatedly exposing the deposits to the influence of oxygen.

The topmost section in all cores has been subjected to soil formation processes, which have resulted in unconsolidated material that was not available for logging and scanning measurements, the layers of which increased in size towards the cores closer to the flanks. Overall, the lithology is a finer grained material, mostly during long wet phases, ranging from fine lacustrine green–greyish clays to silty clays, whereas particularly in the cores closer to the basin margin and the alluvial fans, horizons with sand up to coarse detrital fragments seem to reflect strong rain events during general drought conditions. Additionally, reddish silts seem to correlate with a phase marked by prevailing aridity. Longer stable dry phases are expressed in finer material which appear to be connected to aeolian transport. In the lowermost sections of the pilot core several distinct



Fig. 7.1 | Profile through the Chew Bahir basin showing coring sites along the NW-SE transect and the dimension of the extensive sediment trap.

carbonate layers occur and point at the termination of a lacustrine sequence, whereas in the cores closer to the centre (CB-05, CB-04 and CB-06) precipitates can be found in the older parts of the sediment core, imbedded in clay matrix. These precipitate occurrences point at phases in which evaporation prevailed and general aridity can be deduced.

Comparing the lithology of the cores along the transect, it becomes apparent that those cores closer to the basin margin tend to contain thicker and a greater number of horizons with coarser fractions than those towards the centre, where clay significantly dominates the lithology. This generalised grain size gradient from margin to centre is derived from the proximity of CB-01 and CB-02 to the alluvial fans which potentially transport sand and gravel during strong rain events, the cores CB-04, CB-05 and CB-06 instead, representing the sites in the middle. This outlines that centre positions are rather under the influence of fluvial input and lacustrine redeposition. CB-03, in an intermediate position, is alternately controlled by lacustrine and alluvial deposition processes.

7.1.2 Datable material

Datable material in the analysed Chew Bahir deposits was identified and the chronology is found to comprise mostly of biogenic carbonates and organic sediment, which were subsequently used for radiocarbon dating. The series of calibrated ^{14}C ages are summarised in Table 3.2. In general, the cores contained datable deposits, without age reversals, apart from a few obvious outliers that have each been discussed previously in detail (Chapter 3.4.1). The determination of a reservoir effect that could be expected in East African lakes fails, however, due to a lack of sufficient parallel dating opportunities between aquatic biogenic carbonates and terrestrial-derived organic material (i.g. fossilised charcoal). Nevertheless, the influence of ^{14}C depleted runoff seems rather unlikely, considering that no consistent offset between the dated molluscs and the ages derived from organic bulk was evident. The sedimentation rate deduced from the linear relationship between the measured ages and individual depths as well as the composite depth, shows that two wet episodes with sedimentation rates around $\sim 0.5\text{--}0.7$ mm/yr are framing an interval with much lower sedimentation rates of ~ 0.1 mm/yr (values for the composite age-model). This drier interval correlates well with the overall dry climate during the LGM and the precession driven dry phase (see Chapter III). Therewith we observe a general 6–7-fold increase of the mean sedimentation per year with the change to humid conditions. Sedimentation is found to vary not only through time, but also from core

to core along the transect. The mean annual sedimentation decreases from the basin margin (CB-01) from ~ 0.7 mm/yr to ~ 0.2 mm/yr towards the basin centre (CB-05), which has implications for the timeframe covered by the cored deposits and accordingly the annual resolution provided by each mm of core: whereas ~ 45 ka BP are contained in 10 m of core, approximately the same amount of time is represented in 18.8 m in CB-01, hence resulting in a higher resolution.

The established age-depth model includes the thorough consideration of various models and statistic approaches, but is nevertheless still the most vulnerable point of all results, due to a lack of further dates to validate the currently robust but basic age-model that is based on the linear interpolation of eventually six age control points, that are deemed reliable however (Chapter 2.5.1; 4.2.1 and Chapter VI). Several more ages that were integrated to the composite age model via core correlation along carefully chosen tie points, generally support the current model, but it is questionable as whether their incorporation would improve the quality of the model. Concerning the choice of a linear model with the chronological data at hand it should be annotated, that a model based on two degrees of freedom (linear) or three to four degrees of freedom (spline) is clearly of advantage as opposed to models that have as many degrees of freedom as they have data points, plus the two parameters that can be modified within the gamma distribution, plus two more parameters that control the memory effects (memory strength and memory mean) in some models (e.g. Trauth, 2014).

The model itself is reliable, but leaves a relatively floating chronology for the last ~ 45 ka cal BP, the older parts beyond the oldest age control point are based on the extrapolation of the deduced sedimentation rates therewith meaning that CB-04 showing the conspicuous D-O cycle pattern could reach the last ~ 60 ka BP. Within this chronology that, though floating, means that we see the climatic transitions and events but the exact temporal determination of these cannot exceed a precision of a couple of hundred years with this current model. However, the resolution of the geochemical and physical dataset in combination with the sedimentation rates leads to a resolution of the climatic history of $\sim 3\text{--}12$ years, which allows us to make estimates concerning the abruptness of events and trends, but, as highlighted previously, does not enable us to determine with precision when the observed events took place.

The correlation of the cores, as described in Chapters III and VI, may represent the weak point of the interpretation, even though used all available information and

the state of the art techniques into account. The choice of tuning points is based on best knowledge about material and high-resolution geochemical data, but nevertheless several tie points are still rather ambiguous. Total confidence can never be achieved, regardless of the choice of statistical and methodological strategies, especially since the age-depth model itself remains per se an assumption for all intervals in between the age control points and their reliance. However, we learned that, without a chronology, the record will not provide climatic history. Therefore, the current correlation and thus the application of the composite age model (which was tuned to each individual core) is just one of several plausible solutions. Its validity is dependent on the stage of current knowledge and is likely to change with the integration of new data. The incorporation of the palaeomagnetic results, for instance would improve the stability of the chronology, provided that additional data would increase the confidence of the identification of the palaeomagnetic event as well as the correlation with the master core. Also current efforts to identify tephtras (that are mostly known and dated for southern Ethiopia) in the sediment cores would largely improve the confidence of the chronology and could add valuable information which are independent of the lacustrine system.

7.1.3 Development of a basic proxy-concept

A basic proxy toolbox has been established (Chapter III), that is based on the broad set of multi-proxy analyses. We postulate a distinct set of proxies to indicate dry conditions and evaluated all indicators that suggest humidity in Chew Bahir (Fig. 3.4). For dry conditions we observe K as the most reliable aridity indicator, reacting pronouncedly sensitive towards moisture increase. As its humidity-controlled counterpart we find Cl reacts sensitively towards moisture fluctuations, with chemical weathering prevailing during those humid periods. Both elements are easy soluble and have a high reactivity which makes them fast to respond to climate induced humidity alternations. Arid phases in Chew Bahir further correlate with a desiccated or strongly regressed lake, low sedimentation rates and a lower productivity of the lake, and less vegetation on the slopes. Generally a higher lithogenic fraction can be observed, as well as the occurrence of precipitates. Deposits are transported mainly via extensive alluvial fans, which run off the rift flanks. Humid phases in Chew Bahir are furthermore marked by high sedimentation rates, a higher productivity, the occurrence of fresh water diatoms and fish, and longer wet phases, which show characteristically fine grained deposits that are transported fluvially by the perennial rivers Segen and Weyto. We postulate an extensive palaeo-lake, which could reach a maxi-

mum of 50 m water depth until overflowing into Lake Turkana. Also a dense vegetation cover on the surrounding slopes is suggested. Ca could be established as a marker proxy for the onset of wet conditions as sharp Ca peaks appear towards the beginning of a wet phase. The termination, as well as the onset of a lake phase, correlating with shallow water cover, is mostly marked by the rich occurrence of the common mollusc *M. tuberculata*. The derived sediment proxies (mostly chemical and physical) are controlled by three factors: firstly, the distance to the source (proximity to the basin margin), as well as the restriction of the provenance result in the clearness of the signal in the deposits; K works as a clear marker, because it originates from a restricted source (the metamorph gneisses found in the Hammar Range) which is mostly activated under dry conditions and leads to the second factor; transport mechanisms. Naturally we find the dominance of fluvial input during wet phases, and associated vegetation cover, which, appears to play an important role as it contributes to prevent erosion of material off the flanks and stops deflation. The capacity of the alluvial fans is thus largely restricted to arid phases, with little vegetation cover and increased lateral runoff. Thirdly, the type of weathering has an important influence on the prevailing availability of material, which influences the grain size as well as the kind of chemically dissolved material. At present, little is known about the complex interplay between weathering processes and transportation processes, as the analyses within the Chew Bahir study were restricted to the interpretation of the deposited material, and the geological data which was already available from a former mapping project (Davidson, 1983). However to gain a comprehensive understanding which goes beyond the limitations that were met in this study, specialised analyses concentrating on the weathering and transportation processes as a bridge between provenance and the herein analysed deposits would be crucial.

7.1.4 Conclusions on the potential of the climate archive

In conclusion, the interpretation of the core material shows that Chew Bahir represents a suitable terrestrial climate archive to decipher the climatic history in the source region of modern man, as it provides valuable insight into a highly variable environment that is subdued to the complex East African dry-wet cycles. Even under the given constraints of the age model we identified, that the recorded changes in the sediment cores are clearly controlled by dry-wet alternations, and the detailed analyses of the core material can therefore potentially help to decipher and understand those shifts in moisture availability as well as high-latitude controlled

events. Although the results discussed here are specifically concerned with the very uppermost deposits (in relation to the assumed 5 km infill) and anything beyond that is based on assumptions and extrapolation of our initial results, we dare to deduct similar deposition conditions for dry as well as wet intervals into the longer past. As a result it is suggested that a 400 m long core from the centre of the basin could provide the much needed climatic history in the source region of modern man, reaching back at least ~500 ka BP, extrapolating the determined sedimentation rates, more likely ~750 ka BP, particularly since we know that at least within the timeframe focussed here the tropical-subtropical climate during the Quaternary was largely driven by precessional cycles, two of which we analysed and interpreted here.

7.2 Dry-wet shifts in East Africa

The second key objective of this work was furthermore the advanced understanding of East African climate variability. Initially, with only very few information at hand, deducted from other lakes in the region, the record was not anticipated to go beyond the timeframe of the AHP. However, the results show that not only the last orbital controlled dry-wet cycle was recorded in the retrieved deposits, but also the penultimate one. This allows us to hypothesise about the underlying forcing mechanisms and coupled feedback in general and with focus on the AHP in detail and therefore test highly debated hypotheses.

7.2.1 The African Humid Period

The Chew Bahir record provides important insights into timing, magnitude, synchronicity and internal variability of the last dry-wet-dry cycle. The palaeoclimatic evidence derived from the sediment cores outline the extreme environmental response to the insolation increase driven by the orbital constellation and therewith support the proposed link between insolation changes and monsoon strength already suggested by Kutzbach and Street-Perrott in 1985. Our multi-proxy analysis of the Chew Bahir cores show that during the time interval ~15–5 ka BP the basin was under the influence of pronounced humid conditions that caused the establishment of an extensive lake, surrounded by a dense vegetation cover. This is, as shown in Chapter II, III and in the synoptic discussion 7.1, most clearly indicated by the decrease in K and the increase of Cl and supported by the other chemical, physical and biological proxies. We deduct a considerable precipitation increase in the entire catchment with the onset of the AHP. Simplified, the AHP is the result of the insolation

increase in the NH for northern summer (JJA), that was caused by a precessional minimum during low eccentricity (see Chapter II and III and references therein). This insolation-controlled moisture increase via the enhancement of the monsoon strength is stated for a number of sites along the EARS. The increase in insolation caused a northwest-ward displacement of the ITCZ (Chapter 1.33). The extreme humidity observed for the AHP in large parts of East Africa has been proposed to have been furthermore enhanced by the eastward lateral shift of the Congo Air Boundary. This shift of the CAB, which transports moist air masses from the west, possibly provided additional precipitation during the present short dry season in summer (Kutzbach and Street-Perrott, 1985; Hailemichael et al., 2002; Junginger and Trauth, 2013; Junginger et al., 2014; Chapter V). Furthermore, the intensification of the West African Monsoon has been proposed as another factor to have contributed to the AHP, as the WAM is thought have weakened the African easterly jet, which transports moisture away from East Africa under regular conditions (Patricola and Cook, 2007).

7.2.2 The Magnitude of the AHP

The magnitude of the AHP, might best be demonstrated by a number of considerably enlarged lakes in East Africa as shown by Trauth et al. (2010), Junginger et al. (2014) and our Figure 2.6. Although the morphology of the basin limits the depth of palaeo-lake Chew Bahir to max. 50 m, a considerable amount of additional precipitation must have been necessary to cause the extensive basin (~2000 km²) to fill up to the this critical depth. The overflow-sill (+50 m) was repeatedly reached during the AHP. Besides this over-flow indicator, the analyses of the Chew Bahir cores could not provide clarity on the actual extend of palaeo-lake Chew Bahir during lake phases, since the proxies reflect dry-wet variations but don't allow quantitative estimates. Studies using Sr isotopes from molluscs from Chew Bahir as well as from Lake Turkana have been conducted test-wise in a collaborating research project and show that further research could help to come to a temporal assessment of overflow events. Also these studies could provide valuable information on the provenance of fresh-water in the paleo-lakes during wet phases. The identification of palaeo-shore lines during the deep-drilling campaign could also contribute to the assessment of the magnitude of the AHP and possibly of earlier wet phases. The rise of the lake level of paleo-lake Suguta in northern Kenya, to +280 m during the AHP, demonstrates clearly, which impact the AHP had on large parts of East Africa and what tremendous amounts of additional moisture this dry-wet cycle brought to the study site.

7.2.3 The synchronicity and internal variability of the AHP

Comparing the Chew Bahir record to other East African records (Fig. 2.6), indicates that Chew Bahir's response to the AHP is mostly synchronous with that of for instance Lake Naivasha, Lake Nakuru, Lake Suguta, Lake Ziway-Shala (Fig. 2.6; Junginger et al., 2014, Fig. 10) with minor leads and lags. The lateral shift of the CAB is proposed to have largely contributed to the synchronicity observed in the response of the lakes. These are located more or less along a N-S line, which is approximately parallel to the position of the CAB during the AHP and when drawn eastwards, this zone of increased moisture influx arrived along this line synchronously (Costa et al., 2014). During the AHP, the record shows a considerable amount of internal variability that is expressed in several dry episodes on different time-scales that punctuate this otherwise full humid interval. Among these are a) the local expressions of the Older Dryas, a major arid event around 14 ka BP; b) the sharply defined shift towards extreme arid conditions from 12.8–11.6 ka BP, which corresponds with the Younger Dryas; c) several smaller droughts during the Holocene on centennial time scales and d) a major aridity event around 7.8 ka BP, possibly the precursor of the high-latitude 8.2 ka event (Chapter II and III).

7.2.4 The onset and termination of the AHP

The transition in and out of this significant humid phase, receives most attention however, as a possible abruptness of both the onset and/or the termination has been claimed, based on marine records recovered off north-west Africa (deMenocal et al., 2000), whereas other records in particular one from a lacustrine archive from the Sahara (Kröpelin et al., 2008) postulate a rather gradual termination of this wet phase (Chapter II). These contrasting findings induced a decade-long debate on the possible abruptness of this transition, including strong debates on the validity of records and how far results from a marine site are applicable for other parts of the African continent. After all, the transition has far reaching implications for the transformation of the living environment of humans in the area at that time. The Chew Bahir records show a distinct abrupt onset of humid conditions around ~15 ka BP, which is evident in all cores, by a marked shift of all geochemical proxies (Figure 3.3), visible in the lithology and detectable in the MS signal (Chapter III), most strikingly in CB-03. Although the determination of the exact timing of the onset of the AHP is constrained by the age-model, the abruptness is still evident. The record suggests the establishment of full humid conditions within < 500 yrs (Chapter 3.6.1). Interestingly, Junginger et al. (2014) proposed similar results concerning the rapid change towards full humidity for paleo-lake Suguta,

with the help of constructed transgression curves for the onset of the AHP, that are based on a hydro-balance model. The response recorded in the Chew Bahir is thus highly non-linear as opposed to the gradual increase in insolation. The abruptness could be associated with the eastward shift of the CAB (see previous subchapter), due to an atmospheric pressure gradient between Asia and East Africa (Junginger and Trauth, 2013). The termination of the AHP did not follow the gradual decline of insolation values either. Instead, the observed aridification, that marks the end of the AHP, sets in at ~6.5 ka BP. Full arid conditions were not reached before ~5ka BP, which means the termination was with a 1,500 yrs-long moisture decrease of a distinct gradual character. As Trauth et al. (in press, Chapter IV) observe, a series of 20–80 year-long minor dry episodes punctuate this gradual aridification trend, which contributes to the discussion of increased instability postulated for transitions between different climatic modes, that was already initiated by Maslin (2004) and Maslin and Christensen (2007).

7.2.5 The penultimate precession cycle

The penultimate orbital driven dry-wet cycle (~46–23 ka BP) recorded in the Chew Bahir deposits, shows a far weaker response (concerning moisture increase) compared to the AHP. That this penultimate precessional cycle is also contained in the records has important implications as it provided the opportunity to compare the climatic response of two precessional cycles under different conditions: the penultimate precessional minima (insolation maxima) occurred during the glacial, which resulted in reduced atmospheric pressure gradients and a reduced level of moisture availability in general (Gasse, 2000). Corresponding, the Chew Bahir record implies a strongly buffered moisture increase during this interval of increased insolation. This emphasises, that the climatic response is not as easily predictable [reconstructable] as the calculation of insolation values implies. Instead, this underlines the complexity of the interrelationship between several climate forcing factors, that was briefly outlined in Chapter 1.4.1.

7.2.6 Climate oscillations on a 10³ timescale

Several climate events on a millennial time scale mark the Chew Bahir records (Chapter III). Most prominent are several dry-wet excursions that could represent the local expression of the well described high latitude D-O cycles, which are characterised by rapid warming and a subsequent saw-toothed shaped gradual cooling cycle (Chapter 3.6.2). Though the uncertainties of our age model hinder us from distinctly correlating these similar shaped millennial scale dry-wet cycles with specific D-O cycles, it is obvious that these distinct excursions reflect the low-latitude expression of high-latitude

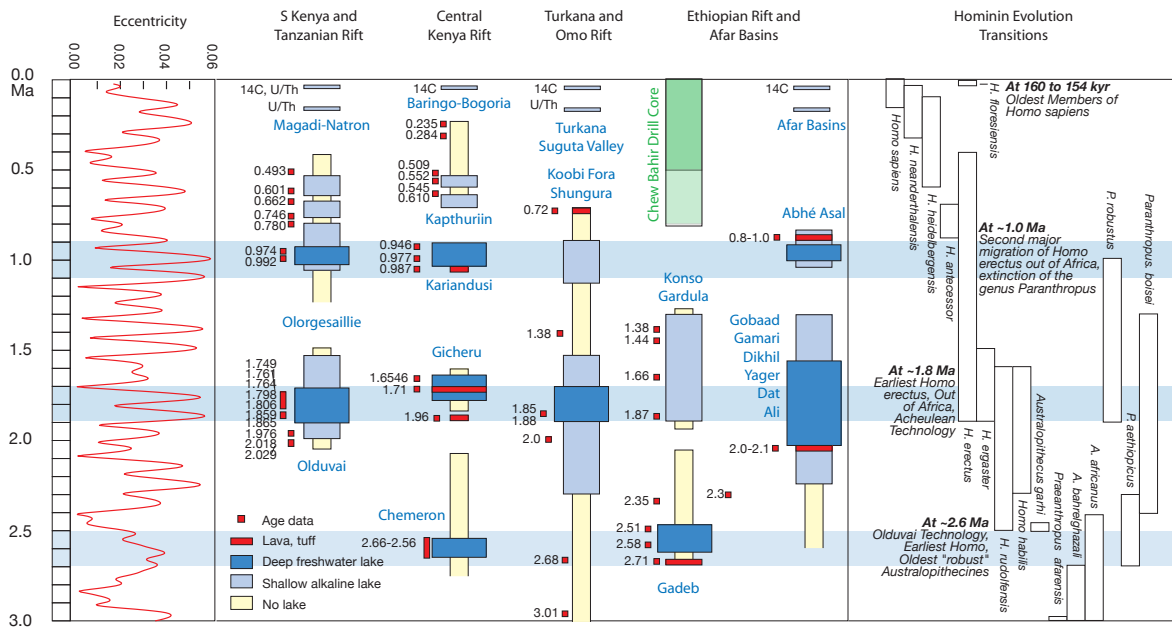


Figure 7.2 | Insolation variation, wet periods in East Africa and human evolution. The compilation of lake records is based on a large volume of literature (Olduvai, Magadi-Natron-Olorgesailie, Baringo-Bogoria, Omo-Turkana-Suguta, Ethiopian Rift and Afar), (Central Kenya Rift) (see Trauth et al. (2005) and references therein for details). The expected Chew Bahir record is marked as green box in the compilation. From Trauth and Schäbitz, 2012.

climate events. Furthermore, these cycles underline once more the sensitive teleconnection between high- and low-latitudes as well as the sensitive response of the East African climate to even minor changes in surrounding SSTs. During a confined phase during the Holocene several dry-shifts occur on a centennial scale that might have been triggered by short-term changes in solar activity as outlined in Chapter 1.3.6 and 3.6.3.

7.3 Human-climate linkages on different time scales

Discussing possible human-climate linkages on any given timescale is based on the assumption that climate plays an important role - in the evolution and dispersal of modern man, as well as for cultural innovations in the human history. As outlined in the introductory Chapter, besides being biased this assumption is natural deterministic and per se infers causalities that might overestimate the role of climatic changes. Nevertheless, the multitude of hypotheses (Chapter 1.4) surrounding this topic human-climate linkages (on long and short time scales) (Chapter IV) demonstrate how crucial reliable palaeoenvironmental data are to test those models.

7.3.1 Climate-evolution linkages

Testing hypotheses on the impact of climatic variability on the emergence of archaic and modern humans is challenging, since this requires a) certainty concerning the paleoenvironmental reconstruction covering

at least the timeframe associated with the evolution of the genus Homo (~2.6 Ma; Trauth, 2005). This would ideally involve the record which produces the climatic history is recovered from a source near to the archaeological data; b) a comprehensive understanding of the spatiotemporal dimension of newly emerging species and subspecies.

Furthermore, humans have been found to be extremely adaptable and flexible, and therefore able to buffer the response to environmentally-induced evolutionary pressure. Naturally, this makes it even more complicated to work out correlations between climatic forcing and developments in evolution. Trauth et al. (in press) suggest, as outlined in Chapter IV, that switching from stable to highly instable climatic conditions, driven by orbitally-forced insolation changes, coincides with several critical phases of hominin speciation and brain expansion. Subsequently, the instability associated with the transition between extreme wet and extreme dry climate conditions would be the key mechanisms to drive evolution instead long stable trends. This observation, though further focussed on the orbital triggering mechanism of these phases of instability, follow the basic principle of Potts' *Variability Selection Hypothesis* (1988) (Chapter 1.4.2 and Chapter 4.4). In Figure 7.2 the correlation between reconstructed wet phases and steps in human evolution are correlated and show the interval that a future Chew Bahir core would cover. The Chew Bahir record in this study (~0–60 ka BP) can not contribute to the discussion on an evolutionary time

scale, but the results shown throughout this work outline that a long core from Chew Bahir within the framework of the deep drilling initiative can considerably contribute to the current debate on climate-evolution linkages. It also became clear, that the data is much needed to advance and test the understanding of climatic variability-evolution linkages.

7.3.2 Climate-migration/expansion linkages

To determine the prevailing climatic conditions during the expansion of *Homo sapiens* beyond the limits of Eastern Africa, is a pre-condition for the discussion of whether unfavourable drought conditions compelled humans to leave their original habitat (extreme aridity as push factor; Carto et al., 2009), or whether stable wet conditions favoured the opening of migration corridors through the Sahara (Vasks et al., 2007; Castañeda et al., 2009) and into the Levant. Both scenarios are based on the assumption that the Out of Africa migration was climatically pulsed and less determined by socio-cultural factors (Chapter 1.3.6). But human agency is tied to threshold conditions (Dobres and Robb, 2000). Hence, aridity, as expressed in the megadroughts of the Late Quaternary, is limiting the freedom of choice for pre-historic humans. Archaeological evidence points to a first dispersal of *Homo sapiens* between ~130–100 ka BP (Vasks et al., 2007), though climate reconstructions from the Negev desert (Israel) point for a time window created by climatic change during the Eemian interglacial between ~140–110 ka BP, from hyper-arid to wetter conditions during which overcoming the natural barrier of the Sahara might have been possible (Vasks et al., 2007). Castañeda et al. (2009), using the expansion of C_3 vegetation in the Sahara region, limit this window of climatic favourable conditions roughly to ~120–110 ka BP, but support the premise that only a period with a significant increase in moisture could have resulting in the Sahara being a dispersal route out of Africa. Later waves of expansion (~105 ka BP) would have met unstable and drier conditions, it is assumed that after ~90 ka BP the chances to cross the Sahara would have become impossible. At least until the onset of generally warmer and wetter conditions around the start of MIS 3 (~60 ka BP; Brandt et al., 2012). This phase, however, as shown in our record, was punctuated by severe moisture fluctuation as described for the D-O cycles and H-events in Chapter III. How far proposed water courses could have contributed to create effective corridors through North-eastern Africa during ‘green Sahara’ stages through time (Drake et al., 2011; Larrasoana et al., 2013), would have important implications for the way in which modern humans could have spread globally. In addition to the timing of the climate-migration linkage debate, the magnitude and synchronicity of the climatic state is postulated to have driven migration. As demonstrated on the basis of the Chew Bahir record for younger

dry-wet shifts, insolation variations (dry-wet alternations) could have had significant varying expressions in the magnitude of moisture increase (Chapter III). During the AHP, full humid conditions were entered, and the penultimate dry-wet cycle was marked by a less prominent increase in moisture. The spatial synchronicity also plays a significant role, particularly when considering the opening or closing of possible corridors. The example of the termination of the AHP along the EARS shows how regionally sensitive the environmental response to just minor threshold constellation of different driving factors can be. How far and at which timeframes the migration in Ethiopia might have been pushed by droughts or conflicts over resources, and how far migration could also have been curiosity driven remains a question to be tested by interdisciplinary studies implementing socio-cultural dimensions and continuous and well-constrained environmental reconstruction.

7.3.3 Climate-innovation linkages

Whether climatic change spurred technological, social and economic innovation was tested on a millennial and centennial timescale within the framework of this work in Chapter V. The last 20 ka of the Chew Bahir climate record (including hypothesised intervals that are thought to have caused climatic stress situations on the biosphere (including humans)) were linked to the occupation intensity in different assumed retreat areas. On longer time scales refugia are thought to have worked as key areas of innovation, because they were intensely occupied during phases that were marked by a profound changing living environment and therefore necessitated the innovation of adaptive strategies of all kinds to survive. We were interested in testing whether a temporal threshold of changing climate had to be crossed to see the emergence of cultural innovation. Bearing the constraints of the chronology of both the climatic and archaeological record in mind, it was postulated that during the millennial-centennial scale climate shifts the time to adapt to a rapidly changing environment was not sufficiently long enough to trigger the emergence of subsistence change. A substantial re-organisation of the societal and cultural structure would have been inextricably involved (Chapter V and references within). Instead a short-term vertical migration of a highly mobile hunter-gatherer society to the moister SW highlands was proposed, during which these phases used the most efficient survival strategy to cope with the Holocene arid excursions. This concept of increased mobility during highly variable climatic conditions could represent a short-term adaptive strategy [migration], but requires at the same time technical adaptations to a new living environment and changing resources. As discussed in Chapter IV, a major climatic transition from ~106 ka BP on, towards an episode of high cli-

matic instability was documented in the lake record of Lake Naivasha. This transition, the MIS 5–4 transition, is found to coincide with increased cultural differentiation and innovations of early hunter-gatherers (chapter IV; Potts, 2013). These innovations comprised hunting techniques and foraging activities, including the production of fishing tools as well as the emergence of symbolic expressions (Potts, 2013). For the youngest example, the mid-Holocene transition, recorded in the Chew Bahir records, the adaptation of prevailing food gathering strategies from fishing to herding (Hildebrand and Grillo, 2012) is postulated to have been driven by the gradual aridification after the termination of the AHP (Chapter IV). This concept is adapted and discussed in the following chapter, acknowledging the parallel emergence of pastoralism in the Turkana area around that time interval (e.g. Garcin et al., 2012). This fits into the framework of the emergence of food-production, which was, connected by an overall restructuring of the socio-economic adaptation to a food producing community, including the re-organisation of ownership structures and the emergence of a formal leadership. At present, the chronology of the Chew Bahir record does not draw parallels between archaeological findings and climate events, and so these observations remain highly speculative and need validation through improved age control and further insights into cultural transitions in southern Ethiopia for this interval.

7.4 Conclusions and Outlook

The potential of the terrestrial climate archive Chew Bahir to provide the climatic context for key developments in human evolution, dispersal and -important for the timeframe covered herein- cultural innovation has been tested. The results of this pre-study prove that the sediment records from the uppermost deposits of the Chew Bahir basin contain a number of valuable climate proxies that provide high resolution climate reconstructions for the past ~60 ka. The Chew Bahir records show a distinct pattern of changing environmental conditions during the Late Quaternary in southern Ethiopia. These climate changes, expressed in pronounced wet-dry cycles on different timescales, can be correlated to well-known wet-dry alternations for tropical east Africa (e.g., LGM, AHP, YD). This supports the validity of the robust age-depth model that is based on six data points, that are considered as reliable though. However, the floating chronology constitutes constraints concerning the match with for instance archaeological findings, which on top also include uncertainties. The timing, magnitude and character of the reconstructed wet-dry transitions would have had important consequences for the biosphere including humans. Based on examples for the major

modes of climatic change (gradual vs. abrupt and brief vs. long), the gradual mid-Holocene transition and several pronounced abrupt droughts that punctuate the AHP, we tested hypotheses on climate-migration and climate-innovation linkages. We compared our climatic results to archaeological records, which are based on settlement activities in potential adjacent refugia.

By the time of writing a coring campaign within the framework of the CRC 806, with the aim to retrieve a 50 m long sediment record from the centre of Chew Bahir, was in progress, with 40 m already recovered. The coring site for this deep drilling campaign, close to the location of the herein analysed CB-05, was chosen on the basis of the conceptual understanding established within this work. Coring in the centre of the basin, we have to expect to find sequences that have been redeposited and disturbed during full lacustrine phases. This we trade in for a lower resolution, due to lower sedimentation rates, which offer the opportunity however to cover a wider timeframe with a shorter record. On grounds of our findings we are confident that a record from this site will enable us to retrieve the climatic history of the last ~200 ka with the 50 m record, thus hopefully providing the valuable environmental information back to the timeframe of the emergence of *Homo sapiens*. The to-be cored 400 m long sequence from Chew Bahir within the framework of the HSPDP, had to be postponed for a year in late 2013 due to logistic problems and the narrow time window created by the rainy seasons. But based on this study, this 400 m record is conservatively estimated to cover at least the last 500 ka, possibly the last 750 ka and therewith the crucial climatic and environmental changes through the critical intervals of human evolution.

The framework for the interpretation of the proxies was laid with the documentation and work of our pre-study and crucial factors to obtain a comprehensive and reliable core and core interpretation of the long records to come are clear: first of all, reliable age control is of key importance, also beyond the limits of radiocarbon dating. Besides other dating techniques, for this site tephrochronology and palaeomagnetic analyses show a high potential. Secondly, the choice of the coring site within the highly variable extensive basin, this includes besides sedimentary issues also technical and logistical matters as learned from the experience of the previous field campaigns. Thirdly, the importance of overlapping core sections, or a duplicate core. And fourth, further in-depth studies on the provenance, weathering and transport mechanisms from source to the actual deposits in the cores and a research study that investigates the -for now only hypothesised- different moisture sources and the provenance of freshwater in palaeo-lake Chew Bahir.

VIII References

[of Chapters I, VI and VII]

- Abram, N.J., Gagan, M.K., Liu, Z., Hantoro, W.S., McCulloch, M.T., Suwargadi, B.W., 2007. Seasonal characteristics of the Indian Ocean Dipole during the Holocene epoch. *Nature* 445, 299–302.
- Abram, N.J., Gagan, M.K., Cole, J.E., Hantoro, W.S., Mudelsee, M., 2008. Recent Intensification of Tropical Climate Variability in the Indian Ocean. *Nature Geoscience* 1, 849–853.
- Ambrose, S.H., 1998. Late Pleistocene human population bottlenecks, volcanic winter, and the differentiation of modern humans. *Journal of Human Evolution* 35, 115–118.
- Annamalai, H, Ping Liu, and Shang-Ping Xie, 2005. Southwest Indian Ocean SST Variability: Its Local Effect and Remote Influence on Asian Monsoons. *Journal of Climate* 18, 4150–4167.
- Armitage, S.J., Jasim, S.A., Marks, A.E., Parker, A.G., Usik, V.I., Uerpmann, H.-P., 2011. Evidence for an early expansion of modern humans into Arabia. *Science* 331, 453–457.
- Asfaw, B., Beyene, Y., Suwa, G., Walter, R. C., White, T. D., WoldeGabriel, G., Yemane, T., 1992. The earliest Acheulean from Konso-Gardula. *Nature* 360, 732–735.
- Asrat, A., Bates, R., Berger, G., Beyene, Y., Brandt, S., DeGusta, D., Duller, G., Ebinger, C., Endale, T., Hart, W.K., Hildebrand, E., Katoh, S., Kidane, T., Lamb, H., Leng, M., Lezine, A.-M., Marshall, M., Morgan, L., Pearce, N., Prave, T., Renne, P., Schäbitz, F., Strecker, M., Suwa, G., Tadesse, K., Tadesse, T., Trauth, M., Umer, M., Vogel-sang, R., White, T., WoldeGabriel, G., Zeleke, A., 2009. The Chew Bahir Drilling Project: A Plio-Pleistocene Climate Record from the Southern Ethiopian Rift, a Crucible of Human Evolution. Proposal for the ICDP-HSPDP (Hominin Sites and Palaeolakes Drilling Project), pp. 1–8.
- Awoke, H. and Hailu, F., 2004. Geology of the Yabello Area, Geological Survey of Ethiopia, Addis Ababa.
- Barker, P. and Gasse, F., 2003. New Evidence for a Reduced Water Balance in East Africa During the Last Glacial Maximum: Implication for Model-Data Comparison. *Quaternary Science Reviews* 22, 823–837.
- Barker, P.A., Talbot, M.R., Street-Perrott, F.A., Marret, F., Scourse, J., Odada, E.O., 2004. Late Quaternary variability in intertropical Africa. In: Battarbee, R.W., Gasse, F., Stickley, C.E. (Eds.), *Past Climate Variability through Europe and Africa*. Springer, Dordrecht, Netherlands, pp. 117–138.
- Basell, L.S., 2008. Middle Stone Age (MSA) site distributions in eastern Africa and their relationship to Quaternary environmental change, refugia and the evolution of *Homo sapiens*. *Quaternary Science Reviews* 27, 2484–2498.
- Benvenuti, M., Carnicelli, S., Belluomi, G., Dainelli, N., Di Grazia, S., Ferrari, G.A., Iasio, C., Sagri, M., Ventra, D., Atnafu, B., Kebede, S., 2002. The Ziway–Shala Lake Basin (Main Ethiopian Rift, Ethiopia): a Revision of Basin Evolution with Special Reference to the Late Quaternary. *Journal of African Earth Sciences* 35, 247–269.
- Berger, A., 1978. Long-Term Variations of Daily Insolation and Quaternary Climatic Changes. *Journal of Atmospheric Sciences* 35, 2362–2367.
- Berger, A. and Loutre, M.-F., 1991a. Insolation values for the climate of the last 10 million years. *Quaternary Science Reviews* 10, 297–317.
- Berger, A. and Loutre, M.-F., 1991b. Dataset Orbital Variations, 5,000,000 Years. <http://www.ncdc.noaa.gov/data-access/paleoclimatology-data/datasets/climate-forcing>, (last access: 04.03.2014).
- Berger, A., 1992. Orbital Variations and Insolation Database. IGBP PAGES/World Data Center for Paleoclimatology. Data Contribution Series # 92-007, NOAA/NGDC Paleoclimatology Program, Boulder CO, USA, <ftp://ftp.ncdc.noaa.gov/pub/data/paleo/insolation/>
- Berger, A. and Loutre, M. F., 1997. Intertropical latitudes and precessional and half-precessional cycles. *Science* 278, 1476–1478.
- Berger, A., Loutre, M. F., Melice, J.L., 2006. Equatorial insolation: from precession harmonics to eccentricity frequencies. *Clim. Past* 2, 131–136.
- Björck, S. and Wohlfarth, B., 2001. Chronostratigraphic techniques in Pleistocene research. In: Last, W. and Smol, J. (Eds.), *Developments in Paleoenvironmental research*, Vol. 1. Kluwer Academic Press, Dordrecht, 2002.
- Blaauw, M., Christen, J.A., 2011. Flexible paleoclimate age-depth models using an autoregressive gamma process. *Bayesian Analysis* 6 457–474.
- Blaauw, M. and Heegard, E. 2012. Estimation of Age-Depth Relationships. In: Birks, H.J., Lotter, A., Juggins, S., Smol, J.P. (Eds.), *Developments in Paleoenvironmental Research. Tracking Environmental Change Using Lake Sediments*. Vol. 5. ESpringer, Dordrecht, Netherlands, pp. 379–413., doi:10.1007/978-94-007-2745-8.
- Blome, M., Cohen, A., Tyron, C.A., Brooks, A.S., 2012. The environmental context for the origins of modern human diversity: A synthesis of regional variability in African climate 150,000–30,000 years ago. *Journal of Human Evolution* 62, 563–592. doi:10.1016/j.jhevol.2012.01.011.
- Bond, G., Kromer, B., Beer, J., Muscheler, R., Evans, M.N., Showers, W., Hoffmann, S., Lotti-Bond, R., Hajdas, I., Bonani, G., 1991. Persistent Solar Influence on North Atlantic Climate During the Holocene 294, 2130–2136.
- Bosworth, W., 1987. Off-axis volcanism in the Gregory rift, east Africa: Implications for models of continental rifting. *Geology*, 15, 397–400.
- Bosworth, W., 1989. Basin and Range style tectonics in East Africa. *Journal of African Earth Sciences* 8, 191–201.
- Bradley, R. S., 1999. *Paleoclimatology, Reconstructing Climates of the Quaternary*, 2nd edition. Elsevier Academic Press, San Diego, US, pp. 1–631.
- Brandt, S. A., 1986. The Upper Pleistocene and early Holocene prehistory of the Horn of Africa. *The African Archaeological Review* 4, 41–82.
- Brandt, S.A., Fisher, E.C., Hildebrand, E.A., Vogel-sang, R., Ambrose, S.H., Lesur, J., Wang, H., 2012. Early MIS 3 occupation of Mochena Borago Rockshelter, Southwest Ethiopian Highlands: Implications for Late Pleistocene archaeology, paleoenvironments and modern human dispersals, *Quaternary International* 274, 38–54.
- Broecker, W. S. and Henderson, G., 1998. The sequence of events surrounding Termination II and their implications

- for the cause of glacial-interglacial CO₂ changes. *Paleoceanography* 13, 352–364.
- Bronk Ramsey, C., 1995. Radiocarbon calibration and analysis of stratigraphy: the OxCal program, *Radiocarbon*, 36, 425–430.
- Buck, D. (Regie), 2012. Die Vermessung der Welt. Drehbuch: Buck, D., Kehlmann, D.; Warner Bros. Deutschland. DVD, 119 Min.
- Bureau of Meteorology, Australian Government, El Niño -Detailed Australian Analysis, El Niño 2009-10, webpage: www.bom.gov.au/climate/enso/enlist/ (last access: 15.01.2014).
- Camberlin, P., 1997. Rainfall anomalies in the source region of the Nile and their connection with the Indian summer monsoon. *J. Climate* 10, 1380–1392.
- Campbell, M.C. and Tishkoff, S.A., 2010. The Evolution of Human Genetic and Phenotypic Variation in Africa. *Curr Biol*. 20, R 166–R173, doi:10.1016/j.cub.2009.11.050.
- Carto, S.L., Weaver, A.J., Hetherington, R., Lam, Y. and Wiebe, E.C., 2009. Out of Africa and into an ice age: on the role of global climate change in the late Pleistocene expansion of early modern humans out of Africa, *Journal of Human Evolution* 56, 139–151.
- Castañeda, I.S., Mulitza, S., Schefuß, E., Santos, R.A.L., Damste, J.S.S. and Schouten, S., 2009. Wet phases in the Sahara/Sahel region and human expansion patterns in North Africa. *Proceedings of the National Academy of Sciences* 106, 20159–20166.
- Cavendish, H.S.H., 1889. Through Somaliland and around and South of Lake Rudolf. *The Geographical Journal* 11, 372–393. National Research Council, 2010. Understanding Climate's Influence on Human Evolution. Washington, DC: The National Academies Press.
- Charney, J. and Stone, P., 1975. Drought in the Sahara: A Biogeophysical Feedback Mechanism. *Science* 187, 434–435.
- Chorowicz, J., 2005. The East African rift system. *J. Afr. Earth Sci.* 43, 379–410.
- Claussen, M., Kubatzki, C., Brovkin, V., Ganopolski, A., Holzmann, P., Pachur, H.J., 1999. Simulation of an abrupt change in Saharan vegetation in the mid-Holocene. *Geophysical Research Letters* 26, 2037–2040.
- Cohen, A.S.: *Paleolimnology, The History and Evolution of Lake Ecosystems*, Oxford University Press, Oxford, pp. 500, 2003.
- Corti, G., 2009. Continental rift evolution: from rift initiation to incipient break-up in the Main Ethiopian Rift, East Africa. *Earth-Science Reviews* 96, 1–53.
- Costa, K., Russell, J., Konecky, B., Lamb, H.F., 2014. Isotopic reconstruction of the African Humid Period and Congo Air Boundary migration at Lake Tana, Ethiopia. *Quaternary Science Reviews* 83, 58–67.
- CRC 806, Collaborative Research Centre 806, Our Way to Europe. Culture-Environment Interaction and Human Mobility in the Late Quaternary, website, homepage: <http://www.sfb806.uni-koeln.de/> (last access: 20.03.2014).
- Dart, R., 1925. *Australopithecus africanus*: The man-ape of south Africa. *Nature* 115, 195–199.
- Dart, R., 1953. The predatory transition from ape to man. *International Review of Anthropology and Linguistics* 1, 201–218.
- Darwin, C., 1871. *The Descent of Man and Selection in Relation to Sex*. London: Murray.
- Davidson, A. and Rex, D. C., 1980. Age of volcanism and rifting in southwestern Ethiopia. *Nature* 283, 657–658.
- Davidson, A., 1983. The Omo River project: reconnaissance geology and geochemistry of parts of Ilubabor, Kefa, Gemu Gofa and Sidamo. *Ethiopian Institute of Geological Surveys Bulletin* 2, 1–89.
- deMenocal, P., 1995. Plio-Pleistocene African Climate, *Science* 270, 53–59.
- deMenocal, P., Ortiz, J., Guilderson, T., Adkins, J., Sarnthein, M., Baker, L., Yarusinsky, M., 2000. Abrupt onset and termination of the African Humid Period: rapid climate responses to gradual insolation forcing. *Quaternary Science Reviews* 19, 347–361.
- deMenocal, P., 2004. African climate change and faunal evolution during the Pliocene-Pleistocene. *Earth and Planetary Science Letters* 220, 3–24.
- Diro, G.T., Grimes, D.I.F., Black, E., O'Neill, A., Pardo-Iguzquiza, E., 2009. Evaluation of reanalysis rainfall estimates over Ethiopia. *International Journal of Climatology* 29, 67–78.
- Dobres, J. and Robb, J. (Eds.): *Agency in archaeology*, Routledge, London and New York, 2000.
- Donges JF, Donner RV, Trauth MH, Schellnhuber HJ, Kurths J, 2011. Nonlinear detection of paleoclimate-variability transitions possibly related to human evolution. *Proceedings of the National Academy of Sciences of the United States of America*, 108, 20423–20427.
- Drake, N., Blench, R., Armitage, S., Bristow, C., White, K., 2011. Ancient watercourses and biogeography of the Sahara explain the peopling of the desert. *PNAS* 108, 458–462.
- Ebinger, C.J. and Sleep, N.H., 1998. Cenozoic magmatism throughout east Africa resulting from impact of a single plume. *Nature* 395, 788–791.
- Ebinger, C.J., Yemane, T., Harding, D., Tesfaye, S., Kelley, S., Rex, D., 2000. Rift deflection, migration, and propagation: linkage of the Ethiopian and Eastern rifts, Africa. *Geological Society of America Bulletin* 112, 163–176.
- Foerster, V., Junginger, A., Langkamp, O., Gebru, T., Asrat, A., Umer, M., Lamb, H., Wennrich, V., Rethemeyer, J., Nowaczyk, N., Trauth, M. H., and Schäbitz, F., 2012. Climatic change recorded in the sediments of the Chew Bahir basin, southern Ethiopia, during the last 45,000 years, *Quaternary International* 274, 25–37.
- Foerster, V., Junginger, A., Asrat, A., Lamb, H. F., Wennrich, V., Weber, M., Rethemeyer, J., Frank, U., Brown, M.C., Trauth, M.H. and Schaebitz, F.: 46 000 years of alternating wet and dry phases on decadal to orbital timescales in the cradle of modern humans: the Chew Bahir project, southern Ethiopia, *Climate of the Past*, doi:10.5194/cpd-10-1-2014, 2014.
- Foerster, V., Vogelsang, R., Junginger, A., Asrat, A., Lamb, H. F., Schaebitz, F. and Trauth, M.H.: Environmental Change and Late Upper Palaeolithic Occupation of Southern Ethiopia, (submitted to QSR).
- Friis, I., Demissew, Sebsebe and van Breugel, P., 2001. *Atlas of the Potential Vegetation of Ethiopia*. Addis Ababa University Press. Shama Books. Addis Abebea, Ethiopia, pp. 307.

- Fu, Q., Mittnik, A., Johnson, P., Bos, K., Lari, M., Bollongino, R., Sun, C., Giemsch, L., Schmitz, R., Burger, J., Ronchitelli, A., Martini, F., Cremonesi, R., Svoboda, J., Bauer, P., Caramelli, D., S., Reich, D., Pääbo, S., Krause, J., 2013. A Revised Timescale for Human Evolution Based on Ancient Mitochondrial Genomes. *Current Biology* 23, 553–559.
- Garcin, Y., Melnick, D., Strecker, M.R., Olago, D. and Tiercelin, J.-J., 2012. East African mid-Holocene wet–dry transition recorded in palaeo-shorelines of Lake Turkana, northern Kenya Rift, *Earth and Planetary Science Letters* 331–332, 322–334.
- Gasse, F., Street, F.A., 1978. Late Quaternary lake level fluctuations and environments of the northern Rift Valley and Afar Region (Ethiopia and Djibouti). *Palaeogeography, Palaeoclimatology, Palaeoecology* 25, 145–150.
- Gasse, F., 2000. Hydrological changes in the African tropics since the Last Glacial Maximum. *Quaternary Science Reviews* 19, 189–211.
- Gasse, F., Chalié F., Vincens, A., Williams, M.A.J., Williamson, D., 2008. Climatic patterns in equatorial and southern Africa from 30,000 to 10,000 years ago reconstructed from terrestrial and near-shore proxy data. *Quaternary Science Reviews* 27, 2316–2340.
- GeoMapApp, 2014. Marine Geoscience Data System. GeoMapApp3.3.9 available at: <http://www.geomapp.org> (last access: 27.01.2014).
- GeoMappApp, after Ryan, W. B. F., Carbotte, S.M., Coplan, J. O., O'Hara, S., Melkonian, A., Arko, R., Weissel, R.A., Ferrini, V., Goodwillie, A., Nitsche, F., Bronckowski, J. Zemsky, R., 2009. Global Multi-Resolution Topography synthesis, *Geochem. Geophys. Syst.* 10, Q03014, doi:10.1029/2008GC002332.
- George, R., Rogers, N., Kelley, S., 1998. Earliest magmatism in Ethiopia: Evidence for two mantle plumes in one flood basalt province. *Geology* 26, 923–926.
- Grove, A.T., Street, F.A., Goudie, A.S., 1975. Former Lake Levels and Climatic Change in the Rift Valley of Southern Ethiopia. *The Geographical Journal* 141, 177–194.
- Gupta, A. K., Das, M. and Anderson, D.M., 2005. Solar influence on the Indian summer monsoon during the Holocene, *Geophys. Res. Lett.* 32, L17703, doi:10.1029/2005GL022685.
- Hailemichael, M., Aronson, J.L., Savin, S., Tevesz, M.J.S., Carter, J.G., 2002. $\delta^{18}\text{O}$ in mollusk shells from Pliocene Lake Hadar and modern Ethiopian lakes: Implications for history of the Ethiopian monsoon. *palaeogeogr. Palaeoclimatol. Palaeoecol.* 186, 81–99.
- Hardy, A., 1960. Was man more aquatic in the past? *New Scientist* 7, 642–645.
- Hardy, A., 1977. Was there a *Homo aquaticus*? *Zenith* 15, 4–6.
- Hassen, N., Yemane, T. and Genzebu, W., 1991. Geology of the Agere Maryam Area. Geological Survey of Ethiopia, Addis Ababa.
- Higuera, P.E., Brubaker, L.B., Anderson, P.M., Hu, F.S., Brown, T.A., 2009. Vegetation mediated the impacts of post-glacial climatic change on fire regimes in the south-central Brooks Range, Alaska. *Ecological Monographs* 79, 201–219.
- Hildebrand, E. and Grillo, K.: Early herders and monumental sites in eastern Africa: New radiocarbon dates, *Antiquity*, 86, 338–352, 2012.
- Hominin Sites and Palaeolakes Drilling Project (HSP-DP), homepage: <http://hsdpd.asu.edu/> (last access: 25.03.2014).
- Institute of Biodiversity Conservation, CBD Clearing House Mechanism of Ethiopia, website: <http://www.biodiv.be/ethiopia/biodiversity/ecosystems-ethiopia> (last access: 27.02.2014).
- IPCC, 1996. Climate Change 1995: Impacts, Adaptations and Mitigation of Climate Change, Scientific and Technical Analysis. Contribution of Working Group II to the Second Assessment Report of the Intergovernmental Panel on Climate Change. Chapter 10, Hydrology and Freshwater Ecology. Cambridge University Press.
- IPCC, 2001. Special Report on The Regional Impacts of Climate Change: An Assessment of Vulnerability. Intergovernmental Panel on Climate Change, WMO/UNEP.
- IPCC, 2007. Climate Change 2007: Synthesis Report. Contribution of Working Groups I, II and III to the Fourth Assessment Report of the Intergovernmental Panel on Climate Change. (IPCC Fourth Assessment Report). IPCC, Geneva, Switzerland.
- IPCC, 2013. Summary for Policymakers. In: Climate Change 2013: The Physical Science Basis. Contribution of Working Group I to the Fifth Assessment Report of the Intergovernmental Panel on Climate Change [Stocker, T.F., D. Qin, G.-K. Plattner, M. Tignor, S. K. Allen, J. Boschung, A. Nauels, Y. Xia, V. Bex and P.M. Midgley (Eds.)]. Cambridge University Press, Cambridge, United Kingdom and New York, NY, USA.
- IPCC, Intergovernmental Panel on Climate Change, website, homepage: <http://www.ipcc.ch/organization/> (last access: 15.02.2014).
- IRI, 2014. International Research Institute for Climate and Society, Earth Institute, Columbia University, Climate and Society Maproom available at: <http://iridl.ideo.columbia.edu/maproom/> (last access: 03.02.2014).
- Junginger, A. and Trauth, M. H., 2013. Hydrological constraints of paleo-Lake Suguta in the northern Kenya Rift during the African humid period (15–5 ka BP). *Global Planet. Change*, 111, 174–188.
- Junginger, A., Roller, S., Olaka, L. A., Trauth, M. H., 2014. The effect of solar radiation changes on water levels in paleo-Lake Suguta, Northern Kenya Rift, during late Pleistocene African Humid Period (15–5 ka BP). *Paleogeography, Paleoclimatology, Paleoecology* 396, 1–16.
- Katoh, S., Nagaoka, S., WoldeGabriel, G., Renne, P., Snow, M., Beyene, Y., Suwa, G., 2000. Chronostratigraphy and correlation of the Plio-Pleistocene tephra layers of the Konso Formation, southern Main Ethiopian Rift, Ethiopia. *QSR* 19, 1305–1317.
- Key, R. M., 1988. Geology of the Sabarei area: Degree sheets 3 and 4, with coloured 1:250000 geological map and results of geochemical exploration (Report), Ministry of Environment and Natural Resources, Mines and Geology Dept., Nairobi, Kenya.
- Kingston, J.D., 2007. Shifting Adaptive Landscapes: Progress and Challenges in Reconstructing Early Hominid Environments. *Yearbook of Physical Anthropology* 50, 20–58.
- Kröppelin, S., Verschuren, D., Lézine, A.-M., Eggermont, H., Cocquyt, C., Francus, P., Cazet, J.-P., Fagot, M., Rumes,

- B., Russell, J. M., Darius, F., Conley, D. J., Schuster, M., von Suchodoletz, H., and Engstrom, D. R., 2008. Climate-driven ecosystem succession in the Sahara: the past 6000 years, *Science*, 320, 765–768.
- Kutzbach, J. E. and Otto-Bliesner, B.L., 1982. The sensitivity of the African-Asian monsoonal climate to orbital parameter changes for 9000 years BP in a low-resolution general circulation model. *Journal of the Atmospheric Sciences* 39, 1177-1188.
- Kutzbach, J.E., Street-Perrott, F.A., 1985. Milankovitch forcing of fluctuations in the level of tropical lakes from 18 to 0 kyr BP. *Nature Geoscience* 317, 130–134.
- Kutzbach, J.E. and Liu, Z., 1997. Response of the African Monsoon to Orbital Forcing and Ocean Feedbacks in the Middle Holocene. *Science* 278, 440-443.
- Lahr, M.M. and Foley, R. 1998. Towards a Theory of Modern Human Origins: Geography, Demography, and Diversity in Recent Human Evolution. *Yearbook of Physical Anthropology* 41, 137–176.
- Larrasoana, J.C., Roberts, A.P., Rohling, E.J., 2013. Dynamics of Green Sahara Periods and Their Role in Hominin Evolution. *PLoS ONE* 8, e76514, doi:10.1371/journal.pone.0076514.
- Laskar, J., Robutel, P., Joutel, F., Gastineau, M., Correia, A.C.M., Levrard, B., 2004. A long term numerical solution for the insolation quantities of the Earth. *A&A* 428, 261-285, doi 10.1051/0004-6361:20041335.
- Last, W., and Smol, J., 2002. 1. An Introduction to Basin Analysis, Coring and Chronological techniques used in Paleolimnology. In: Last, W. and Smol, J. (Eds.), *Developments in Paleoenvironmental research*, Vol. 1. Kluwer Academic Press, Dordrecht, 2002.
- Lesur, J., Hildebrand, E.A., Abawa, G. and Guthertz, X, 2013. The advent of herding in the Horn of Africa: New data from Ethiopia, Djibouti and Somaliland, *Quaternary International*, dx.doi.org/10.1016/j.quaint.2013.11.024.
- Ludescher, J., Gozolchiani, A., Bogachev, M.I., Bunde, A., Havlin, S., Schellnhuber, H.J., 2014. Very Early Warning of Next El Nino. *PNAS* 111, 2064–2066, doi:10.1073/pnas.1323058111.
- Macdonald, R., Rogers, N.W., Fitton, J.G., Black, S., Smith, M., 2001. Plume-Lithosphere Interactions in the Generation of the Basalts of the Kenya Rift, East Africa. *Journal of Petrology* 42, 877-900.
- Marshall, F. and Hildebrand, E., 2002. Cattle before crops: The beginnings of Food Production in Africa. *Journal of World Prehistory* 16, 99–143.
- Maslin, M.A., 2004. Ecological verses Climatic Thresholds. *Science*, 306, 2197–2198.
- Maslin, M. and Christensen, B., 2007. Tectonics, orbital forcing, global climate change, and human evolution in Africa: introduction to the African paleoclimate special volume. *Journal of Human Evolution* 53, 443–464.
- Mathisen, M.E. and Vondra, C.F., 1983. Provenance of the Plio-Pleistocene sediments in the East Turkana Basin, northern Kenya. *Palaeogeography, Palaeoclimatology, Palaeoecology* 44, 141–168.
- Mellars, P., 2011. Why did modern human populations disperse from Africa ca. 60,000 years ago? A new model. *PNAS* 103, 9381–9386.
- MCageDepth, a program for chronology development in continuous sediment records, based on Monte Carlo resampling of calibrated radiocarbon dates, download from <http://code.google.com/p/mcagedepth/> (last access: 14.10.2012).
- McBrearty, S. and Brooks, A., 2000. The revolution that wasn't: a new interpretation of the origin of modern human behaviour. *Journal of Human Evolution* 39, 453–563.
- McDougall, I., Brown, F.H., Fleagle, J.G., 2005. Stratigraphic placement and age of modern humans from Kibish, Ethiopia. *Nature* 433, 733–736.
- Morgan, E., 1982. *The Aquatic Ape*. Souvenir Press, London.
- Moy, C.M., Seltzer, G.O., Rodbell, D.T., Anderson, D.M., 2002. Variability of El Niño/ Southern Oscillation activity at millennial timescales during the Holocene epoch. *Nature* 420, 162e165.
- Muller, R. A. and MacDonald, G. J., 2000. *Ice Ages and Astronomical causes*. Data Spectral Analysis and Mechanisms. Springer, London.
- Nagaoka, S., Katoh, S., WoldeGabriel, G., Sato, H., Nakaya, H., Beyene, Y., Suwa, G., 2005. Lithostratigraphy and sedimentary environments of the hominid-bearing Pliocene–Pleistocene Konso Formation in the southern Main Ethiopian Rift, Ethiopia. *Palaeogeography, Palaeoclimatology, Palaeoecology* 216, 333–357.
- National Research Council, 2010. *Understanding Climate's Influence on Human Evolution*. National Academies Press, Washington, DC.
- Neff, U., Burns, S.J., Mangini, A., Mudelsee, M., Fleitmann, D., Matter, A., 2001. Strong coherence between solar variability and the monsoon in Oman between 9 and 6 kyr ago. *Nature* 411, 290–293.
- Nicholson, S.E., 1996. A review of climate dynamics and climate variability in eastern Africa. In: Johnson, T.C., Odada, E.O. (Eds.), *The Limnology, Climatology and Paleoclimatology of the East African Lakes*. Gordon & Breach, Amsterdam, pp. 25e56.
- Nicholson, S.E., 2000. The nature of rainfall variability over Africa on time scales of decades to millennia. *Global and Planetary Change* 26, 137-158.
- Nicholson, S.E., 2001. Climatic and environmental change in Africa during the last two centuries. *Climate Research* 17, 123-144.
- Nowaczyk, N.R., Arz, H.W., Frank, U., Kind, J., Plessen, B., 2012. Dynamics of the Laschamp geomagnetic excursion from Black Sea sediments. *Earth and Planetary Science Letters* 351-352, 54-69.
- OCHA, 2011. United Nations Office for the Coordination of Humanitarian Affairs. *East Africa Drought Humanitarian Report No.3* Issued by the Sub-regional Office for Eastern Africa, Nairobi. [<http://reliefweb.int/report/burundi/eastern-africa-drought-humanitarian-report-no-3>], (last access: 19.02.2014).
- Odada, E., Olafo, D., Bugenyi, F., Kulindwa, K., Kurimumuryango, J., West, K., Ntiba, M., Wandiga, S., Aloo-Obudho, P., Achola, P., 2003. Environmental assessment of the East African Rift Valley lakes. *Aquat. Sci.* 65, 254–271.
- Olaka, L.A., Odada, E., Trauth, M.H., D., 2010. The sensitivity of East African rift lakes to climate fluctuations. *Journal of Paleolimnology* 44, 629-644.

- Oppenheimer, S., 2009. The great arc of dispersal of modern humans: Africa to Australia. *Quaternary International* 202, 2–13.
- Partridge, T.C., Lowe, J., Barker, P., Hoelzmann, P., Magri, D., Saarnisto, M., Vandenberghe, J., Street-Perrott, F., Gasse, F., 2004. *Climate Variability in Europe and Africa: a PAGES-PEP III Time Stream II Synthesis*. Springer, Dordrecht.
- Patricola, C. M. and Cook, K. H., 2007. Dynamics of the West African monsoon under mid-Holocene precessional forcing: regional climate model simulations, *J. Climate*, 20 694–716.
- Pik, R., Marty, B., Carignan, J., Yirgu, G., Ayalew, T., 2008. Timing of East African Rift development in southern Ethiopia: Implication for mantle plume activity and evolution of topography. *Geology* 36, 167–170.
- Potts, R., 1996. Evolution and Climate Variability. *Science* 273, 923.
- Potts, R., 1998. Environmental Hypotheses of Hominin Evolution. *Yearbook of Physical Anthropology* 41, 93–136.
- Potts, R., 2013. Hominin evolution in settings of strong environmental variability. *Quaternary Science Reviews* 73, 1–13.
- Reimer, P.J., Baillie, M.G.L., Bard, E., Bayliss, A., Beck, J.W., Blackwell, P.G., Bronk Ramsey, C., Buck, C.E., Burr, G.S., Edwards, R.L., Friedrich, M., Grootes, P.M., Guilderson, T.P., Hajdas, I., Heaton, T.J., Hogg, A.G., Hughen, K.A., Kaiser, K.F., Kromer, B., McCormac, F.G., Manning, S.W., Reimer, R.W., Richards, A.A., Southon, J.R., Talamo, S., Turney, C.S.M., van der Plicht, J. and Weyhenmeyer, C.E., 2009. INTCAL09 and MARINE09 radiocarbon age calibration curves, *Radiocarbon*, 51, 1111–1150.
- Reimer, P., Bard, E., Bayliss, A., Beck, J., Blackwell, P., Bronk-Ramsey, C., Buck, C., Cheng, H., Edwards, R.L., Friedrich, M., Grootes, P.M., Guilerson, T., Hafliason, H., Hajdas, I., Hatte, C., Heaton, T., Hoffmann, D., Hogg, A., Hughen, K., Kaiser, F., Kromer, B., Manning, S., Niu, M., Reimer, R., Richards, D., Scott, M., Southon, J., Staff, R., Turney, C., van der Plicht, J., 2013. INTCAL13 AND MARINE13 RADIOCARBON AGE CALIBRATION CURVES 0–50,000 YEARS CAL BP. *Radiocarbon* 55, 1869–1887.
- Renssen, H., Brovkin, V., Fichefet, T. and Goosse, H., 2006. Simulation of the Holocene climate evolution in Northern Africa: The termination of the African Humid Period. *Quat. Int.* 150, 95–102.
- Richter, J., Melles, M., Schäbitz, F., 2012a. Temporal and spatial corridors of *Homo sapiens sapiens* population dynamics during the Late Pleistocene and early Holocene. *Quaternary International* 274, 1–4.
- Richter, J., Hauck, T., Vogerlsang, R., Widlock, T., Le Tensorer, J.-M., Schmid, P., 2012b. “Contextual areas” of early *Homo sapiens* and their significance for human dispersal from Africa into Eurasia between 200 ka and 70 ka. *Quaternary International* 274, 5–24.
- Ruddiman, W., 2008. Book Review on: Hominin Environments in the East African Pliocene: An Assessment of the Faunal Evidence. *EOS Bookreview* 89, 1.
- Saji, N.H., Goswami, B.N., Vinayachandran, P.N., Yamagata, T., 1999. A dipole mode in the Indian Ocean. *Nature* 401, 360–363.
- Scheinfeldt, L. B., Soi, S., Tishkoff, S.A., 2010. Working toward a synthesis of archaeological, linguistic, and genetic data for inferring African population history. *PNAS*, doi/10.1073/pnas.1002563107, 1–8.
- Scholz, C., Johnson, T., Cohen, A., King, J., Peck, J., Overpeck, J., Talbot, M., Brwon, E., Kalindekaffe, L., Amoako, P., Lyons, R., Shanahan, M., Castaneda, I., Heil, C., Forman, S., McHargue, L., Beuning, K., Gomez, J., Pierson, J., 2007. East African megadroughts between 135 and 75 thousand years ago and bearing on early-modern human origins. *PNAS* 104, 16416–16421.
- Segele, Z.T., P.J. Lamb, 2005. Characterisation and variability of Kiremt rainy season over Ethiopia. *Meteorology and Atmospheric Physics* 89,153-180.
- Segele, Z.T., Lamb, P.J., Leslie, L.M., 2009. Seasonal-to-Interannual Variability of Ethiopia/Horn of Africa Monsoon. Part I: Associations of Wavelet-Filtered Large-Scale Atmospheric Circulation and Global Sea Surface Temperature. *Journal of Climate* 22, 3396–3421, doi:10.1175/2008JCLI2859.1.
- Seleshi, Y. and Zanke, U., 2004. Recent changes in rainfall and rainy days in Ethiopia. *International Journal of Climatology* 24, 973- 983.
- Sepulchre, P., Ramstein, G., Fluteau, F., Schuster, M., Tierce-llin, J.J., Brunet, M., 2006. Tectonic uplift and eastern Africa aridification. *Science* 313, 1419–1423.
- Shakleton, R.M., 1996. The final collision zone between East and West Gondwana: where is it? *Journal of African Earth Sciences* 23, 271–287.
- Shiferaw, A., Gebre, E., T., M., Alemayehu, W., Davidson, A., Moore Jr., J.M., Davies, J.C., 1972. *Geologic Map of the Omo River Project Area*. In: Davidson, A. (Ed.). Ethiopian Government.
- Singer, B., Guillou, H., Jicha, B., Kissel, C., Brian, B., Johnson, C., 2009. ⁴⁰Ar/³⁹Ar, K–Ar and ²³⁰Th–²³⁸U dating of the Laschamp excursion: A radioisotopic tie- point for ice core and climate chronologies. *Earth and Planetary Science Letters* 286, 80–88.
- Solanki, S. K., Usoskin, I. G., Kromer, B., Schüssler, M., Beer, J., 2004. Unusual activity of the sun during recent decades compared to the previous 11,000 years. *Nature* 431, 1084–1087.
- Soromessa, T., Teketay, D., Demissew, S., 2004. Ecological study of the vegetation in Gamo Gofa zone, southern Ethiopia. *Tropical Ecology* 45, 209-221.
- Stager, J. C., Mayewski, P. A., Meeker, L. D., 2002. Cooling cycles, Heinrich event 1, and the desiccation of Lake Victoria. *Palaeogeogr. Palaeoclimatol.* 183, 169–178.
- Stringer, C., 2003. Out of Ethiopia. *Science* 423, 692–694.
- Stuiver, M., Reimer, P.J., Reimer, R.W., 2005. CALIB 6.0html. <http://calib.org>, (last access: 15.02.2014).
- Suwa, G., Asfaw, B., Haile-Selassie, Y., White, T., Katoh, S., WoldeGabriel, G., Hart, W. K., Nakaya, H., Beyene, Y., 2007. Early Pleistocene *Homo Erectus* fossils from Konso, southern Ethiopia. *Anthropological Science* 115, 133–151.
- Telford, R.J., Heegard, E., Birks, H.J.B., 2004. All age-depth models are wrong: but how badly? *Quaternary Science Reviews* 23, 1–5.
- Tierney, J.E., Russell, J.M., Sinninghe Damsté, J.S., Huang, Y., Verschuren, D., 2011. Late Quaternary behavior of

- the East African monsoon and the importance of the Congo Air Boundary. *Quaternary Science Reviews* 30, 798–807.
- Tishkoff, S.A. and Verrelli, B.C., 2003. Patterns of Human Genetic Diversity: Implications for Human Evolutionary History and Disease. *Annu. Rev. Genomics Hum. Genet.* 4, 293–340, doi: 10.1146/annurev.genom.4.070802.110226.
- Trauth, M.H., Deino, A.L., Bergner, A.G.N., Strecker, M.R., 2003. East African climate change and orbital forcing during the last 175 kyr BP. *Earth and Planetary Science Letters* 206, 297–313.
- Trauth, M.H., Maslin, M.A., Deino, A., Strecker, M.R., 2005. Late Cenozoic Moisture History of Eastern Africa. *Science*, 309, 2051–2053.
- Trauth, M.H., Maslin, M.A., Deino, A.L., Strecker, M.R., Bergner, A.G.N., Dühnforth, M., 2007. High- and low-latitude forcing of Plio-Pleistocene East African climate and human evolution. *Journal of Human Evolution* 53, 475–486.
- Trauth, M.H., Maslin, M.A., Deino, A.L., Junginger, A., Lesoloyia, M., Odada, E.O., Olago, D.O., Olaka, L.A., Strecker, M.R., Tiedemann, R., 2010. Human evolution in a variable environment: the amplifier lakes of Eastern Africa. *Quaternary Science Reviews* 29, 2981–2988.
- Trauth, M.H., 2014. A new probabilistic technique to build an age model for complex stratigraphic sequences. *Quaternary Geochronology*, in press.
- Trauth, M. H., Bergner, A., Foerster, V., Junginger, A., Maslin, M., and Schäbitz, F., 2015. Episodes of environmental stability vs. instability in late Cenozoic lake records of eastern Africa. *J. Hum. Evolution*, in press.
- Trauth, M.H. and Schäbitz, F., 2012. The Chew Bahir Drilling Project. A Half-Million Year Climate Record from the Southern Ethiopian Rift, Crucible of Human Evolution. New proposal for a research grant to the International Continental Scientific Drilling Program Germany Priority Programme (DFG SPP 1006 ICDP), pp. 1–19.
- Umer, M. and Bonnefille, R., 1998. A late Glacial/late Holocene pollen record from a highland peat at Tamsaa, Bale Mountains, south Ethiopia. *Global and Planetary Change* 16–17, 121–129.
- Umer, M., Lamb, H.F., Bonnefille, R., Lezine, A.M., Tiercelin, J.J., Gibert, E., Cazet, J.P., Watrin, J., 2007. Late Pleistocene and Holocene Vegetation History of the Bale Mountains, Ethiopia. *Quaternary Science Reviews* 26, 2229–2246, doi:10.1016/j.quascirev.2007.05.004.2007.
- Vasko, A., Bar-Matthews, M., Ayalon, A., Matthews, A., Halicz, L., Frumkin, A., 2007. Desert speleothems reveal climatic window for African exodus of early modern humans. *Geology* 35, 831–834.
- Vrba, E.S., 1985. Environment and evolution: alternative causes of the temporal distribution of evolutionary events. *South African Journal of Sciences* 81, 229–236.
- Vrba, E.S., 1993. The pulse that produced us: two major global coolings may have prodded antelopes and humans to evolve: how did humans get that way? *Natural History* 102, 47–51.
- Wang, Y.J., Cheng, H., Edwards, R.L., He, Y., Kong, X., An, Z., Wu, J., Kelly, M.J., Dykoski, C.A., Li, X., 2005. The Holocene Asian monsoon: links to solar changes and North Atlantic climate. *Science* 308, 854–857.
- Wang, X. and Wang, C., 2014. Different Impacts of Various El Niño Events on the Indian Ocean Dipole. *Climate Dynamics* 42, 991–1005.
- Weninger, B. and Jöris, O., 2008. A 14C age calibration curve for the last 60 ka: the Greenland-Hulu U/Th timescale and its impact on understanding the Middle to Upper Paleolithic transition in Western Eurasia. *Journal of Human Evolution* 55, 772–781.
- White, F., 1983. The vegetation of Africa, a descriptive memoir to accompany the UNESCO/AETFAT/UNSO vegetation map of Africa. UNESCO, Natural Resour. Res. 20, 1–356.
- White, T.D., Asfaw, B., DeGusta, D., Gilbert, H., Richards, G.D., Suwa, G., Howell, F.C., 2003. Pleistocene Homo sapiens from Middle Awash, Ethiopia. *Nature* 423, 742–747.
- Widlok, T., Aufgebauer, A., Bradtmöller, M., Dikau, R., Hoffmann, T., Kretschmer, I., Panagiotopoulos, K., Pastors, A., Peters, R., Schäbitz, F., Schlummer, M., Solich, M., Wagner, B., Weniger, G.-C., 2012. Towards a theoretical framework for analysing integrated socio-environmental systems. *Quaternary International* 274, 259–272.
- WoldeGabriel, G., Aronson, J.L., 1987. Chow Bahir: A 'failed' rift, in Southern Ethiopia. *Geology* 15, 430–433.
- Wood, R.B. and Talling, J.F., 1988. Chemical and algal relationships in a salinity series of Ethiopian inland waters. *Hydrobiologia* 158, 29–67.
- WoldeGabriel, G., Hart, W.K., Katoh, S., Beyene, Y., Suwa, G., 2005. Correlation of Plio-Pleistocene Tephra in Ethiopian and Kenyan rift basins: Temporal calibration of geological features and hominid fossil records. *Journal of Volcanology and Geothermal Research* 147, 81–108.

IX. Summary

Climate change, as a key topic in our society, has far reaching implications for many aspects of our lives, in the past present and evermore in the future. Climatic variability and a rapidly changing environment are considered to have had a significant influence on human evolution, migration and cultural and technological innovation. However, to evaluate the impact that climatic shifts on different timescales might have had on the living conditions of prehistoric humans, an understanding and continuous reconstruction of these climatic fluctuations and their underlying driving mechanisms are essential.

This work presents results from such a high resolution (up to 3 years) lake-sediment record from the palaeo-lake Chew Bahir, a newly invested climate archive in a tectonic-bound basin in southern Ethiopia. The record was obtained from six 9–18.8 long cores along a 17 km NW-SE transect across the basin, today an extensive saline mudflat. The objective of this work is to understand and reconstruct the sensitive patterns and expressions of East Africa's highly variable climate, as the climatic context for important cultural transitions in the source region of *Homo sapiens*.

Now, the multi-proxy analyses and interpretation being the heart piece of this thesis, provide the climatic history of the past ~60 ka cal BP and show that Chew Bahir responded sensitively with pronounced shifts in moisture availability towards climatic fluctuations on millennial to centennial timescales, and to the precessional cycle.

The first part of this work concentrates on a) the reconstruction of the velocity and character of these late-Quaternary wet-dry transitions on different time scales (orbital, millennial–centennial and decadal) and b) a basic proxy concept for Chew Bahir for the last two insolation controlled wet-dry cycles. This concept comprises besides the deciphering of major intra-basin dynamics and mechanisms controlling the way from source to sink, an initial understanding of site-specific proxies: especially potassium as a sensitive indicator for aridity and chlorine as a humidity proxy. The records are based on a set of geochemical, physical and biological indicators as well as a suite of AMS radiocarbon dates. The Chew Bahir cores document a highly non-linear response to the last insolation controlled dry-wet cycle, the so-called African Humid Period (~15–5 ka BP) with a pronounced abrupt onset of humid conditions within <500 yrs and a disproportionally gradual decline of moisture availability, as compared to the decrease in insolation. Feedback mechanisms and a complex interrelationship with the monsoon circulation and the diverse topography

of the East African Rift have been suggested as possible key factors. The AHP frames a sharply defined arid phase, corresponding to the Younger Dryas chronozone (~12.8–11.6 ka BP). During the overall arid phase of MIS 3, several oscillations to wetter conditions have been recorded, that resemble the high latitude Dansgaard-Oeschger cycles. Heinrich-events are suggested to be expressed in several episodes of extreme aridity. The full humid conditions of the Holocene wet period [AHP], are punctuated by several abrupt droughts on a centennial to millennial time-scale, the termination of the AHP is though gradual, a textbook example for climatic instability during a transition. A series of 20–80 yr long droughts modulate the 1,500 yr long shift from full wet to arid conditions.

In a broader spatio-temporal context this Mid Holocene wet-dry transition in Chew Bahir is evaluated together with two other examples of a change from stable to unstable environmental conditions: the MIS 5–4 transition in the Naivasha basin (central Kenya rift) and thirdly, the Mid Pleistocene Transition in the Ologesaille basin (Southern Kenya Rift). The concept of hominin speciation, dispersal and cultural innovation being possibly influenced by this transition from stable to unstable environmental conditions is tested on the three different timescales provided by the three records.

As a contribution towards a better understanding of human-climate interaction, we compared the last 20 ka of the paleo-climate record from Chew Bahir with the settlement history of adjacent possible refugia in the Ethiopian highlands and around lake margins. Shifts in and out of favourable living conditions are deducted from the climatic history, which shows besides orbitally driven long-term transitions several short abrupt climate events. These are expressed as shifts to pronounced aridity, suggesting phases of climatic stress. Comparing the frequency of archaeological findings as a parameter for human occupation in refugia to this close-by climate record, allows us to outline how complex the interplay between humans and environment during the last 20 ka really was.

The results comprised in this work represent an important prerequisite for the ICDP "Hominid Sites and Paleolakes Drilling Project" and for the CRC-806 programme "Our Way to Europe", which aim to determine climatic and environmental context of human evolution and dispersal. The potential of this deep terrestrial climate archive has been evaluated herein and proved that the sediment deposits are suitable to provide a longer climate history, to be precise to cover with a 400 m core the climatic history of >500,000 yrs in the source region of modern humans.

IX. Zusammenfassung

Klimaveränderungen, ein Schlüsselthema unserer Gesellschaft, haben weitreichende Auswirkungen auf zahlreiche Aspekte unseres Lebens. Das betrifft Vergangenheit, Gegenwart und Zukunft. Man geht davon aus, dass Klimaschwankungen und eine sich rasch verändernde Umwelt erheblichen Einfluss hatten auf die menschliche Evolution, Wanderungsbewegungen, und kulturelle als auch technische Entwicklungen. Um den möglichen Einfluss evaluieren zu können, ist jedoch das Verständnis und die kontinuierliche Rekonstruktion dieser Fluktuationen und deren zugrundeliegenden Antriebsmechanismen Grundvoraussetzung.

Diese Arbeit stellt die Ergebnisse eines hoch auflösenden (bis 3 Jahre) Klimadatensatzes dar. Dieser basiert auf einem See-Sedimentkern aus dem Paläosee Chew Bahir. Hierbei handelt es sich um ein erst kürzlich erschlossenes Klimaarchiv das in einem tektonischen Becken in Südäthiopien liegt. Der Klimadatensatz stammt aus sechs 9–18,8m langen Kernen die entlang eines 17km Transekts quer durch das Becken, heute eine ausgedehnte Salztonebene, verlaufen. Ziel dieser Arbeit ist es, die sensiblen Muster und Formen des Klimawandels in Afrika zu entschlüsseln und detailliert zu rekonstruieren, um einen klimatischen Bezugsrahmen für maßgebliche kulturelle Entwicklungen in der Ursprungsregion des Menschen zu schaffen.

Die Multi-proxy Analysen und deren Interpretation, das Herzstück der Arbeit, stellen die Klimageschichte der letzten ~60.000 Jahre bereit und zeigen, dass Chew Bahir empfindlich auf die ausgeprägten Klimaschwankungen reagiert hat. Diese spiegeln sich in erheblichen Veränderungen des Feuchtigkeitshaushalts wider und zwar auf tausendjährigen bis hundertjährigen Zeitskalen sowie in orbitalen Zyklen.

Der erste Teil der Arbeit konzentriert sich auf a) die Rekonstruktion der Terminierung der Art und der Geschwindigkeit dieser feucht-trocken Wechsel im Spätquartär auf verschiedenen Zeitskalen (orbital, tausend- bis hundertjährig und dekadisch); b) ein grundlegendes Proxy-Konzept für Chew Bahir für die letzten zwei durch Einstrahlungsenergie gesteuerten Feucht-Trocken Zyklen. Dieses Konzept umfasst Erkenntnisse über grundlegende Dynamiken innerhalb des Beckens sowie der Mechanismen die den Weg vom Ursprung zur letztendlichen Sedimentation steuern. Außerdem wird ein erstes Verständnis der lokations-spezifischen Stellvertreterdaten konzipiert, die dazu dienen die Ergebnisse zu entschlüsseln. Insbesondere der Kalium Gehalt konnte als sensibler Indikator für Trockenheit

herausgearbeitet werden, wohingegen Chlor als ein Feuchtigkeits-Proxy etabliert werden konnte. Der Datensatz basiert auf einer Reihe geochemischer, physikalischer und biologischer Indikatoren, sowie einem Satz von AMS Radiokarbonalter. Die Chew Bahir Kerne dokumentieren eine höchst nicht-lineare Reaktion auf den letzten Insulations gesteuerten Feucht-trocken Zyklus, die so genannte Afrikanische Feuchtphase (AHP; ~15.000–5000 Jahre vor heute). Diese zeigt einen ausgesprochen abrupten Einsatz von feuchteren Bedingungen von innerhalb weniger als 500 Jahren und eine im Verhältnis zur Abnahme der Einstrahlung unverhältnismäßig graduelles Ende (~zwischen 6.5–5 ka BP). Als mögliche Schlüsselfaktoren dafür werden Rückkopplungsmechanismen und komplexe Verknüpfungen mit der Monsun Zirkulation und der hoch diversen Topographie des Ostafrikanischen Rifts angenommen. Die AHP umrahmt eine scharf definierte Trockenphase, die zeitlich mit der Jüngeren Dryas einhergeht (~12.8–11.6 ka BP). Die generell trockenen Phase des MIS 3, wird durch mehrere Oszillationen zu feuchteren Bedingungen unterbrochen. Diese zeigen eine hohe Ähnlichkeit mit den markanten Dansgaard-Oeschger Zyklen aus den höheren Breiten. Einige Umschwünge zu extremer Trockenheit könnten als Auswirkungen der so-genannten Heinrich-Ereignisse interpretiert werden.

Die voll humiden Bedingungen während der holozänen Feuchtphase [AHP], werden von mehreren abrupten Dürreperioden (10^2 – 10^3) unterbrochen. Das Ende der AHP -obwohl ausgesprochen graduell- stellt nahezu ein Lehrbuchbeispiel für klimatische Instabilität während eines Übergangs dar. Eine Reihe von 20–80 Jahre andauernder Dürren bestimmt diesen 1.500 Jahre langen Übergang von Feucht zu Trocken. Dieser Mittel-Holozäne Übergang wird dann in einem breiteren raum-zeitlichen Kontext evaluiert, zusammen mit zwei weiteren Beispielen für den Wandel von stabilen zu instabilen Umweltbedingungen: der MIS 5–4 Übergang im Naivasha Becken (zentrales Kenia Rift) und der Mittel-Pleistozäne Übergang im Ologesaille Becken (südliches Kenia Rift). Die Hypothese, dass menschliche Artenbildung, räumliche Verbreitung, und kulturelle Entwicklung möglicherweise von diesen stabil-instabil Übergängen beeinflusst sein könnte, wird getestet anhand der drei Zeitscheiben, die diese drei Klimadatensätze hergeben.

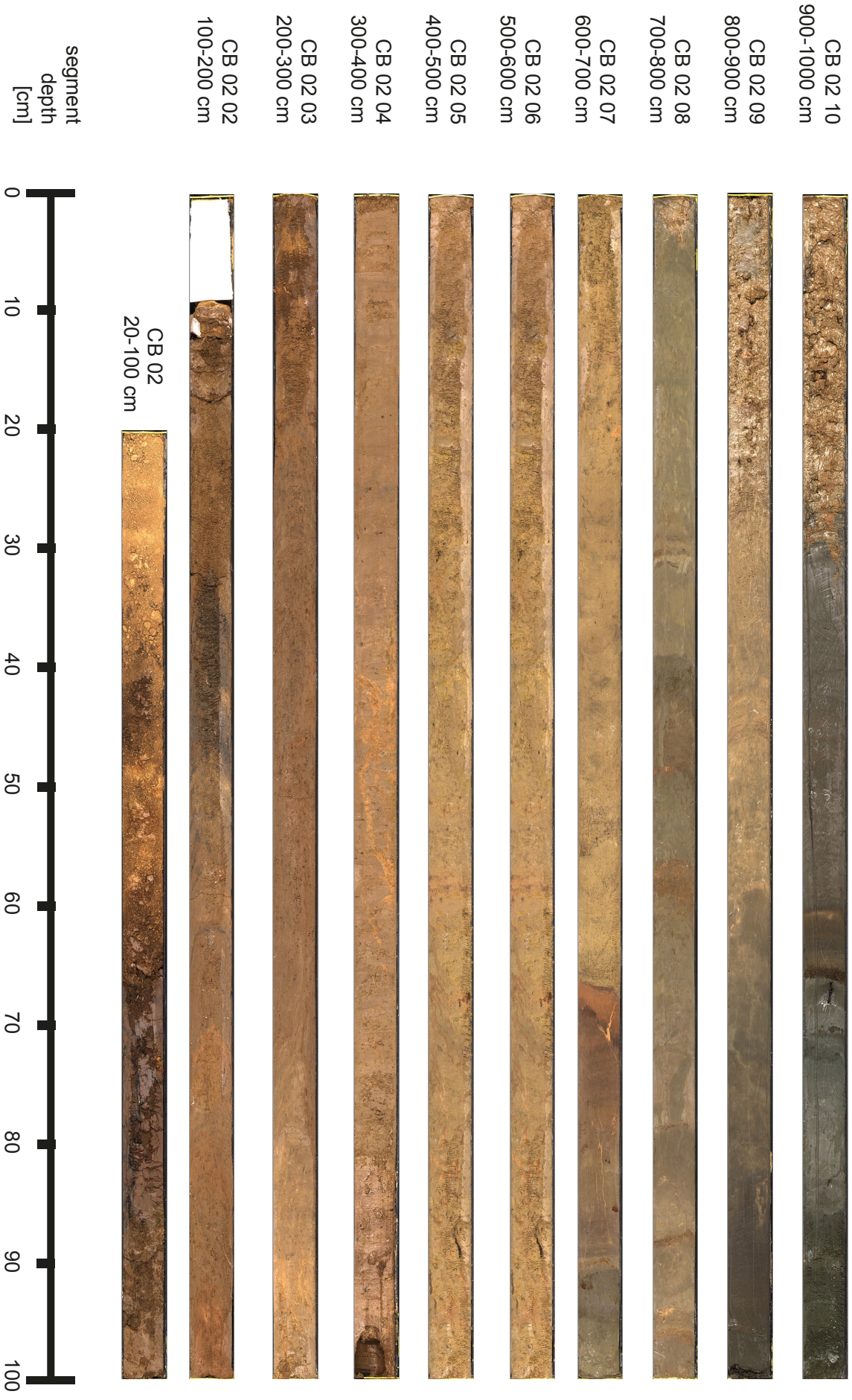
Als einen Beitrag zur Verbesserung des Verständnisses von Mensch-Klima Wechselwirkungen, haben wir einen Vergleich zwischen der Klimageschichte aus Chew Bahir (die letzten 20.000 Jahre) und der Besiedlungsgeschichte in angrenzenden Refugien unternommen. Diese Refugien werden zeitweilig für das

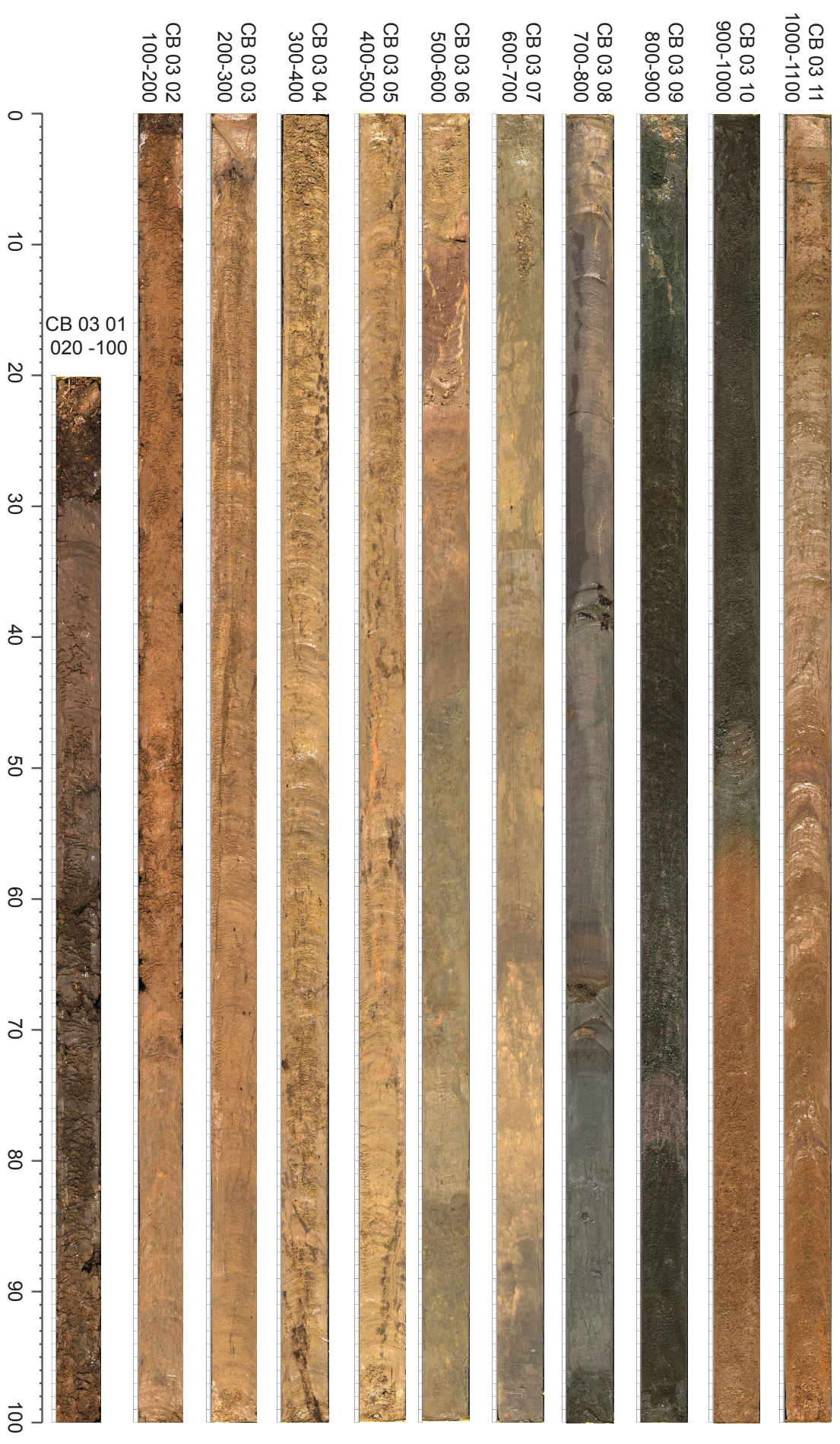
Südwestliche Hochland in Äthiopien als auch für die Randbereiche um die großen Seen angenommen.

Aus der Klimageschichte werden unterschiedliche Wechsel zwischen günstigen und ungünstigen Lebensbedingungen für den Menschen abgeleitet. Die Klimageschichte zeigt neben den orbital gesteuerten Langzeit-Wechseln auch einige kurze und äußerst abrupt auftretende Klimaereignisse. Diese letzteren sind meist Wechsel zu extremen Dürreperioden, mit denen für Menschen klimatische Stresssituationen in Verbindung gebracht werden. Der Vergleich dieser Klimaereignisse aus dem nahe gelegenen Klimaarchiv mit der Häufigkeit archäologischer Funde als Anzeiger für menschliche Besiedlung des Refugiums, ermöglicht es uns zu umreißen, wie komplex die Wechselwirkung zwischen Mensch und Umwelt während der letzten 20.000 Jahre tatsächlich einmal gewesen sein mag.

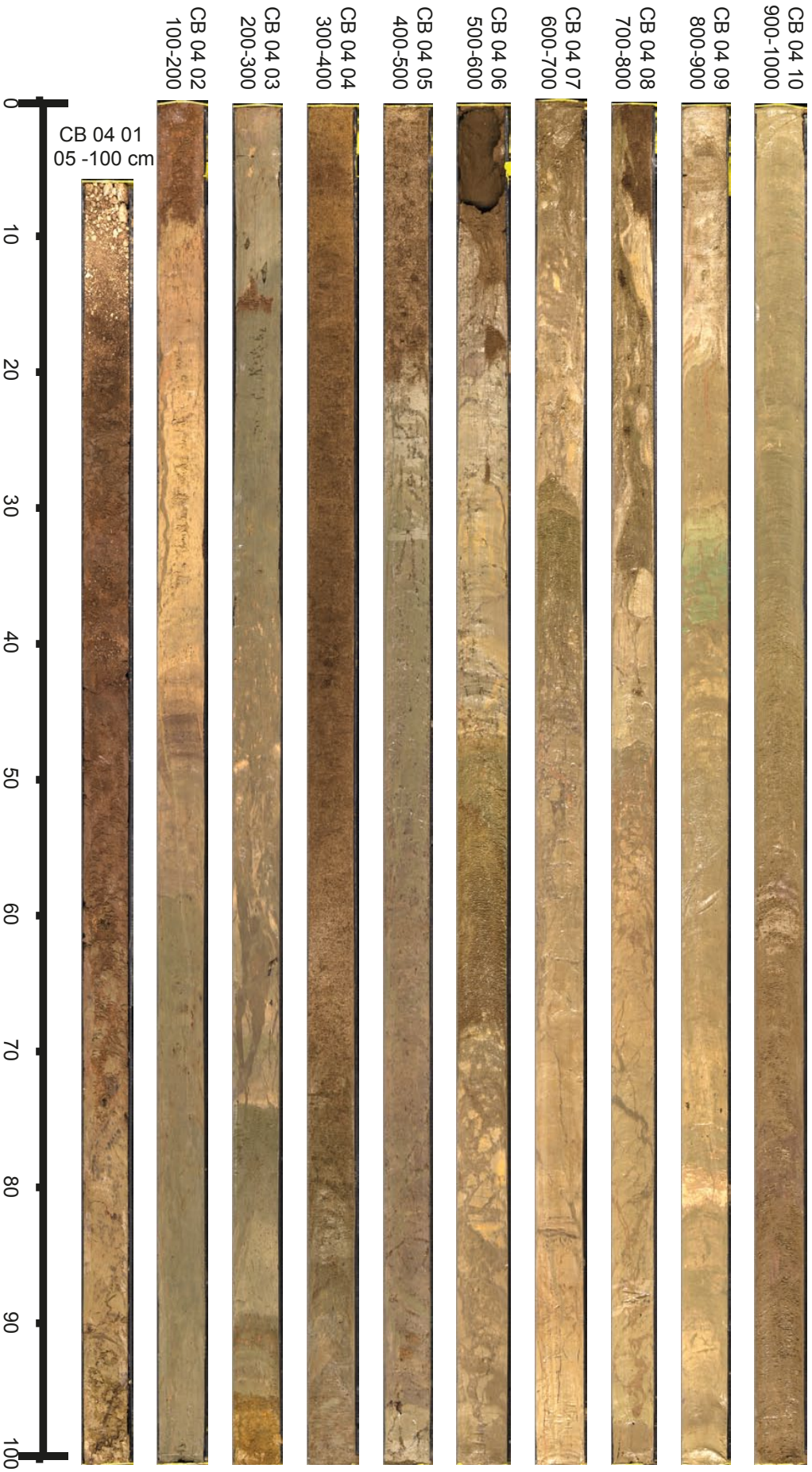
Die Ergebnisse, die in dieser Arbeit gezeigt werden, stellen eine wichtige Voraussetzung für das *“Hominid Sites and Paleolakes Drilling Project”* und den Sonderforschungsbereich 806 *“Our way to Europe”* dar. Diese Projekte wollen eben jenen klimatischen Kontext der menschlichen Evolution und Verbreitung untersuchen. Das Potential dieses tiefen terrestrischen Klimaarchivs wurde hier geprüft und die gezeigten Ergebnisse legen dar, dass die sedimentären Ablagerungen sich tatsächlich eignen um Klimageschichte auch über grössere Zeitfenster hinaus rekonstruieren zu können. Genau genommen, deuten die Ergebnisse darauf hin, dass mit einem 400 m langen Sedimentkern die Klimageschichte der letzten >500.000 Jahre in der Ursprungsregion des Menschen rekonstruiert werden könnte.

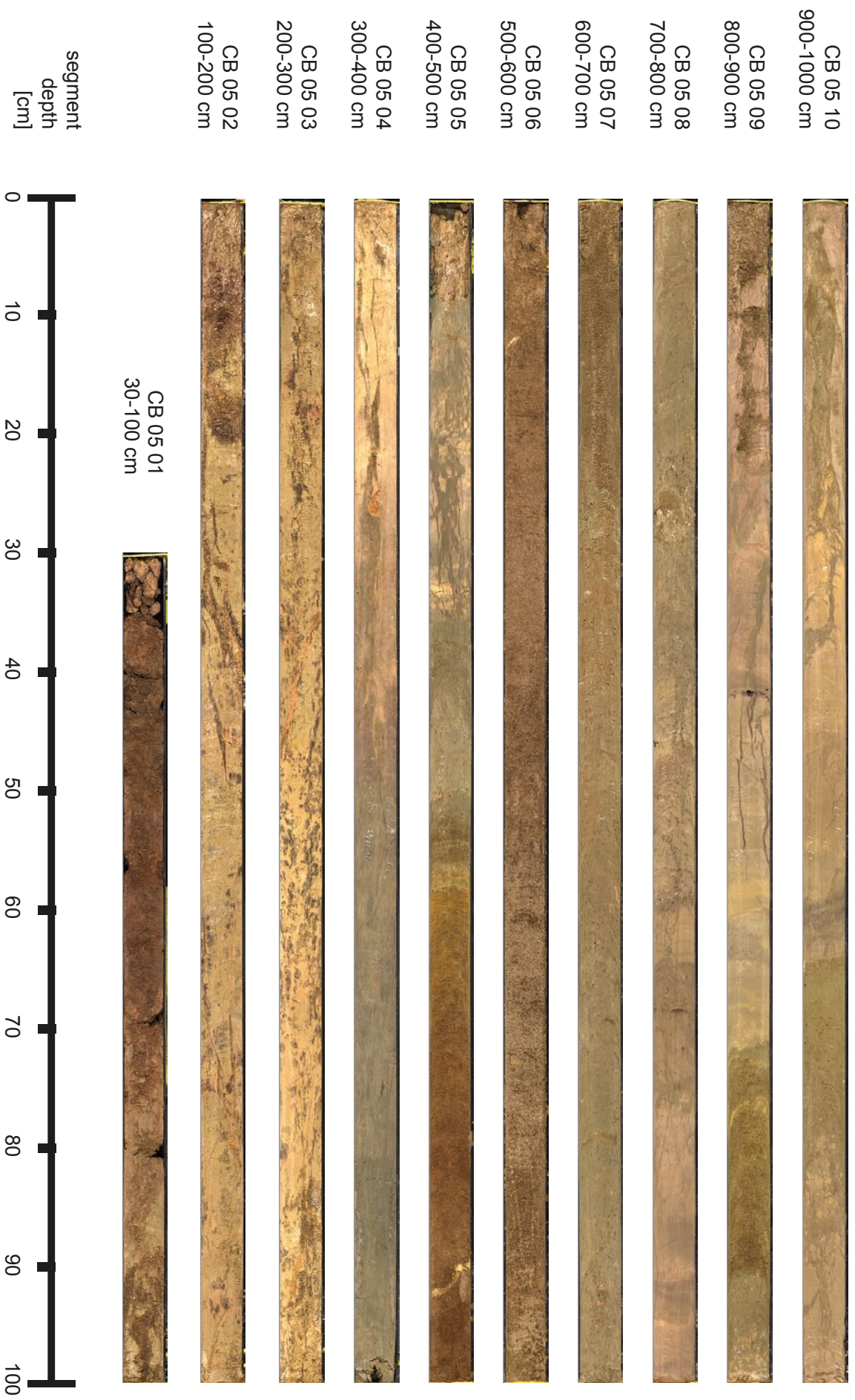
Appendix A - Line-scan photographs

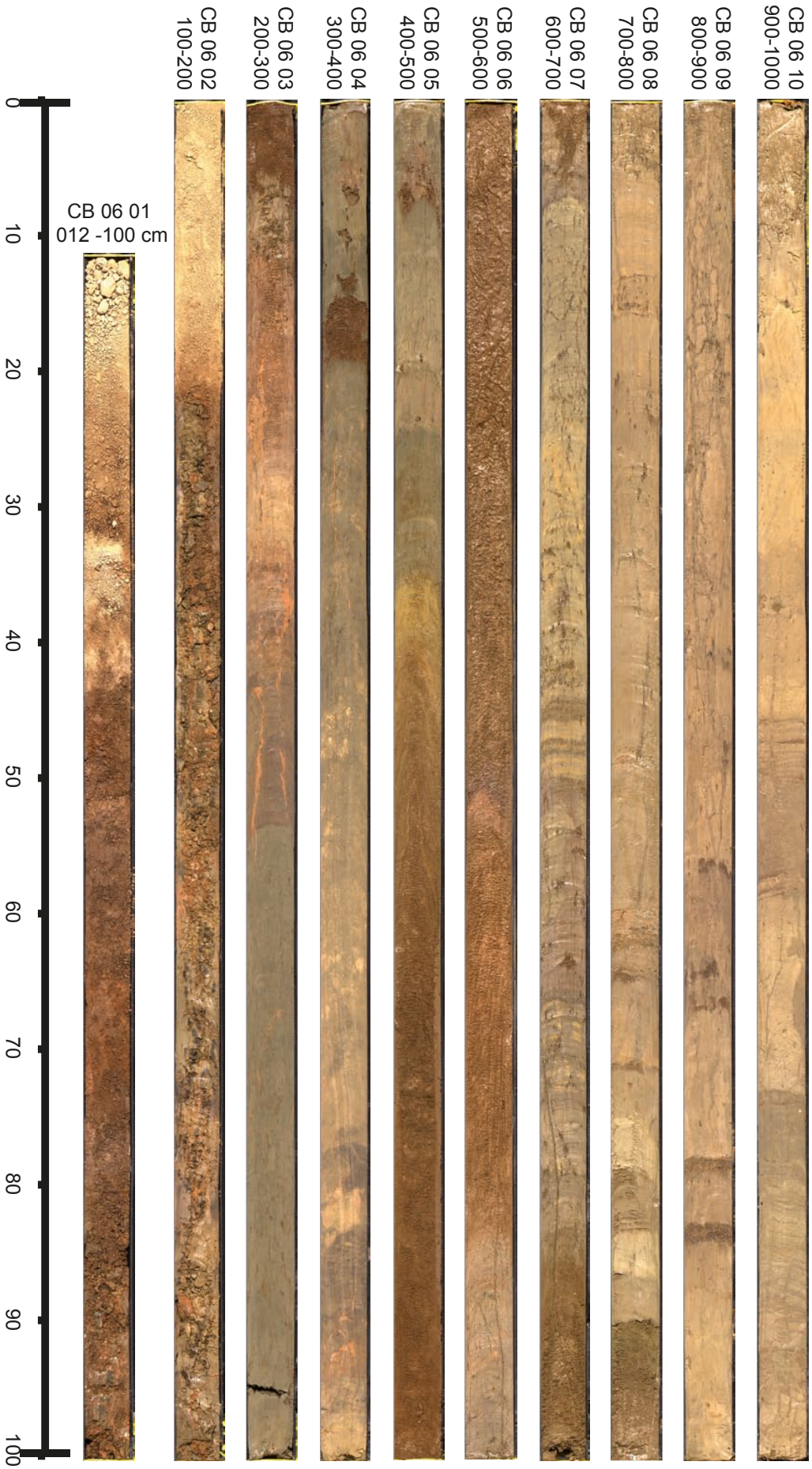




Appendix - CB-03







Appendix B Database

Geochemical and physical data of CB-01, CB-03, CB-05 will be made available to access online at the following link of the CRC 806 Database: <http://crc806db.uni-koeln.de/>

Metadata and project information are available at:

http://crc806db.uni-koeln.de/index.php?id=5&no_cache=1&tx_felogin_pi1%5Bforgot%5D=1#/datasets

◀ Figure caption Appendix A | Line-scan photographs of the cores along the NW-SE transect: CB-03, CB-02, CB-04, CB-05 and CB-06. For coring site refer to Fig.3.1. 10–11 continuous sections, covering the last ~20–60 ka BP. High resolution colour image taken by MSCLogger shows the deposited lacustrine material of the Chew Bahir cores reflecting marked changes of a highly variable environment during the late Quaternary: Lacustrine clays to silty clays, with grain size and colour changes visible, varying between green gray in clay layers to reddish brown in silt layers. The cores contain also micro- and macrofossils and profess fluctuations in sediment density.

Chapter Contributions

Chapter II: Climatic change recorded in the sediments of the Chew Bahir basin, southern Ethiopia, during the last 45,000 years.

This first publication was completely composed by Foerster with support from Junginger (EA Holocene climate fluctuations), Trauth (age modelling, correlation with global records), Schäbitz (bio proxies), Lamb (EA context) and Asrat (geology), who contributed their advise on the interpretation in their relevant field of expertise. The geochemical, biological and sedimentological dataset was developed by Foerster and was placed in the overall context of East African climate variability. Asrat and Umer paved the way for the realisation of the field campaigns. Langkamp provided the XRF raw-data within the framework of his diploma thesis and was supported by Wennrich. Nowaczyk performed the MS logging at the GFZ, Rethemeyer contributed the determination of 5 radiocarbon ages. Gebru supported the sampling party. Junginger mostly produced the figures and tables. Lamb language checked the final edition. Foerster's overall contribution to this paper accounts at least 65 %.

Chapter III: 46, 000 years of alternating wet and dry phases on decadal to orbital time-scales in the cradle of modern humans: the Chew Bahir project, southern Ethiopia*

* In the final version of this dissertation this article appears under the new title of the revised article version: **Climate flickers during the last 46,000 years in the Chew Bahir basin, Southern Ethiopia.**

The original article that represents chapter III of this dissertation (see the original article also under the doi:10.5194/ cpd-10-1-2014) was revised and updated during the review process of the paper. In this first version, published in *Climate of the Past Discussions*, the workshare was as follows: Foerster conducted all analyses that represent the underlying data base of this article: XRF, XRD, MS, MSCL, Diatom analyses, GS, development of the lithology. She evaluated and correlated all data, contributed to the development of the composite age mode and comprised all results in the manuscript. All Figures were produced by Foerster. The work was supervised by Trauth and Schäbitz, who repeatedly advised her during the development of the manuscript. She drew inferences from the results of all analyses and discussed critically the results in the context of global climate on time scales from 10^1 – 10^4 Jahren. Trauth worked intensely with Foerster on the age model, supported by Brown. Trauth developed the MATLAB script that was used to correlate and the cores and tune these to the age model (see also Chapter VI.2. Junginger contributed significantly to the interpretation of the data on precessional timescales and lead worked on the efforts of parallel dating by identifying the few charcoal particles. Brown and Frank conducted palaeomagnetic analyses and especially Frank contributed to the identification of suitable tie points. Asrat, Lamb and Schäbitz lead the field campaign that produced the core material, Foerster participated actively in the field work. Rethemeyer contributed the determination of 15 radiocarbon ages and advised on sample selection for dating. Weber lead the MSCL logging campaign and contributed initial interpretation and correlation with high latitude records.

The latest version of the article, as seen in the final version of this dissertation, was resubmitted to *Palaeogeography, Palaeoclimatology, Palaeoecology* in February 2015 and besides an altered

title comprises an additional chapter (chapter 3.5), which contains the improved in-depth understanding of geochemical processes in the Chew Bahir basin. The additional chapter was largely composed by Stroncik, together with Foerster. Overall contribution of Foerster to Chapter III exceeds 90%.

Chapter IV: Episodes of Environmental Stability vs. Instability in Late Cenozoic Lake Records of Eastern Africa.

Trauth undertook the main interpretation of all data, that is based on the re-evaluation of three records, one of these being the Chew Bahir record, that is part of chapter III. Trauth wrote the text with contributions from Bergner, Foerster, Junginger, Maslin and Schaebitz. Maslin also supported the final Discussion. These contributions were mainly related to the relevant sections: For section 4.2.1 and 4.3.1 Foerster and Schaebitz provided geochemical data and interpretation respectively that was discussed by Trauth in the overall context. The age model for Chew Bahir corresponds to the one presented in Chapter III and was developed by Trauth and Foerster. Foerster's contribution to the subchapters is 20%, and overall to Chapter IV ~5%.

Chapter V: Environmental Change and Late Upper Paleolithic Occupation of Southern Ethiopia. *

* In the final version of this dissertation this article appears under a slightly altered title: **Environmental Change and Human Occupation of Southern Ethiopia and Northern Kenya during the last 20,000 years.**

Foerster and Vogelsang undertook the main interpretation and data collection as well as the text production. Vogelsang collected all published archaeological data and thus entirely composed the archaeological dataset. Furthermore he contributed the interpretation of all data with archaeological and anthropological relevance in close collaboration with Foerster. Vogelsang's contribution is 40 %. Foerster provided the climatological background including the dataset that was used and wrote the climatological interpretation with contributions from foremost Junginger, but also Schäbitz and Trauth. Trauth initiated the idea of this work. Asrat, Lamb, Trauth, Junginger and Schäbitz contributed ideas to final manuscript, written by Vogelsang and Foerster. Foerster's overall contribution to Chapter V exceeds 50 %.

Erklärung

Ich versichere, dass ich die von mir vorgelegte Dissertation selbständig angefertigt, die benutzten Quellen und Hilfsmittel vollständig angegeben und die Stellen der Arbeit – einschließlich Tabellen, Karten und Abbildungen –, die anderen Werken im Wortlaut oder dem Sinn nach entnommen sind, in jedem Einzelfall als Entlehnung kenntlich gemacht habe; dass diese Dissertation noch keiner anderen Fakultät oder Universität zur Prüfung vorgelegen hat; dass sie – abgesehen von unten angegebenen Teilpublikationen – noch nicht veröffentlicht worden ist, sowie, dass ich eine solche Veröffentlichung vor Abschluss des Promotionsverfahrens nicht vornehmen werde.

Die Bestimmungen der Promotionsordnung sind mir bekannt. Die von mir vorgelegte Dissertation ist von Prof. Dr. Frank Schäbitz betreut worden.

Nachfolgend genannte Teilpublikationen liegen vor:

1. Foerster, V., Junginger, A., Langkamp, O., Gebru, T., Asrat, A., Umer, M., Lamb, H., Wennrich, V., Rethemeyer, J., Nowaczyk, N., Trauth, M.H., Schäbitz, F., 2012. Climatic change recorded in the sediments of the Chew Bahir basin, southern Ethiopia, during the last 45,000 years. *Quaternary International* 274, 25–37.
2. Foerster, V., Junginger, A., Asrat, A., Umer, M., Lamb, H.F., Weber, M., Rethemeyer, J., Frank, U., Brown, M.C., Trauth, M.H., Schaebitz, F., (in review). 46, 000 years of alternating wet and dry phases on decadal to orbital timescales in the cradle of modern humans: the Chew Bahir project, southern Ethiopia. *Climate of the Past, Discussions* 10, doi:10.5194/cpd-10-1-2014, 1–48.
3. Trauth, M.H., Bergner, A., Foerster, V., Junginger, A., Maslin, M., Schaebitz, F., (in review). Episodes of Environmental Stability vs. Instability in Late Cenozoic Lake Records of Eastern Africa. *Journal of Human Evolution*, 1–24.
4. Foerster, V., Vogelsang, R., Junginger, A., Asrat, A., Lamb, H.F., Trauth, M.H., Schaebitz, F., (in preparation). Environmental Change and Late Upper Paleolithic Occupation of Southern Ethiopia.

Köln, den 28.04.2015

(Verena E. Foerster)